

Genetic background of relapsing lymphoid neoplasms: comprehensive genetic characterization of primary- relapse pairs by chromosomal copy number and mutational analysis

Inauguraldissertation

zur

Erlangung der Würde eines Doktors der Philosophie

vorgelegt der

Philosophisch-Naturwissenschaftlichen Fakultät

der Universität Basel

von

Darius Juškevičius

aus Litauen

Basel, 2016

Originaldokument gespeichert auf dem Dokumentenserver der Universität Basel
edoc.unibas.ch

Genehmigt von der Philosophisch-Naturwissenschaftlichen Fakultät

auf Antrag von

Prof. Dr. Nancy Hynes

Prof. Dr. Jürg Schwaller

Prof. Dr. Alexandar Tzankov

Basel, den 23. Februar 2016

Prof. Dr. Jörg Schilber

Dekan

I dedicate this work to my wife Reda and to my parents

TABLE OF CONTENTS

SUMMARY	1
1. INTRODUCTION.....	3
1.1 B-cell development.....	3
1.1.1 Early stages of B-cell development.....	3
1.1.2 Structural organization and rearrangement of <i>IG</i> genes.....	6
1.1.3 The germinal center reaction and parafollicular activation of B-blasts	8
1.2 Diffuse large B-cell lymphoma, not otherwise specified (NOS)	15
1.2.1 Molecular pathogenesis of DLBCL	17
1.2.3 Treatment of DLBCL.....	24
1.2.4 Prognostic and predictive markers in DLBCL.....	27
1.2.5 Clinical importance and biological background of DLBCL relapses	29
1.2.6 Clonal relationship in relapsing lymphomas	31
2. AIMS.....	34
3. RESULTS.....	36
3.1 Distinct genetic evolution patterns of relapsing diffuse large B-cell lymphoma revealed by genome wide copy number aberration and targeted sequencing analysis.....	36
3.2 Extracavitary primary effusion lymphoma: clinical, morphological, phenotypic and cytogenetic characterization using nuclei enrichment technique.....	71
3.3 Follicular lymphoma transformation into histiocytic sarcoma: indications for a common neoplastic progenitor.....	86
3.4 Clinical, morphologic, phenotypic, and genetic evidence of cyclin D1-positive diffuse large B-cell lymphomas with <i>CYCLIN D1</i> gene rearrangements	90
3.5 Array CGH-based analysis of post-transplant plasmacytic hyperplasia reveals 'intact genomes' arguing against categorizing it as part of the post-transplant lymphoproliferative disease spectrum.....	100
3.6 Comprehensive phenotypic characterization of PTLTD reveals potential reliance on EBV or NF- κ B signaling instead of B-cell receptor signaling.....	104
3.7 Lenalidomide monotherapy leads to a complete remission in refractory B-cell post-transplant lymphoproliferative disorder	116
3.8 Multiparameter analysis of homogeneously R-CHOP-treated diffuse large B cell lymphomas identifies CD5 and FOXP1 as relevant prognostic biomarkers: report of the prospective SAKK 38/07	121
4. DISCUSSION	133
4.1 Clonally-unrelated relapses of DLBCL.....	133
4.2 DLBCL relapses occur via two distinct genetic evolution patterns	134
4.3 Identification of genetic drivers of DLBCL relapse.....	140

4.4 Branching evolution and hematopoietic plasticity of follicular lymphoma relapse and its transformation to histiocytic sarcoma	143
4.5. Sorting of FFPE-tissue derived tumor nuclei enables genetic investigation of rare cancer cell populations	145
GENERAL CONCLUSION	147
REFERENCES.....	149
LIST OF ABBREVIATIONS	160
CURRICULUM VITAE	162
ACKNOWLEDGEMENTS	164

SUMMARY

Diffuse large B-cell lymphoma (DLBCL) is the most frequent tumor of the lymphoid system. Standard first line therapy is successful in the majority of cases, however about 30% of DLBCL are either refractory to it or relapse after a period of remission. Therapy options for such patients are very limited and disease outcomes are often unfavorable. Recent years of research have considerably advanced our understanding of molecular processes that drive lymphomagenesis of primary DLBCL. However, due to lack of focused studies, knowledge on the genetic basis of DLBCL relapse remains scarce. It is largely unknown how tumors evolve under treatment, which genetic events lead to recurrence, how resistance emerges and whether relapses can be reliably predicted at the timepoint of initial diagnosis.

We sought to address these questions by comprehensive genetic analysis of two retrospective DLBCL cohorts. One consisted of paired primary and relapse samples from 20 relapsing DLBCL cases, another of 11 non-relapsing primary DLBCL samples. We performed histological characterization, investigated genome-wide DNA copy number aberrations and most common nucleotide-level alterations, and tested clonal relationships between paired tumors of the same patient. Our study provided important novel findings and strengthened some previous observations.

Clonally-unrelated DLBCL relapses were previously equivocally documented by demonstration of distinct immunoglobulin gene (*IG*) rearrangements between the first and the second lymphoma occurrence. We support this observation and provide high quality evidence showing not only distinct *IG* rearrangements, but also lack of unifying genetic alterations throughout the whole tumors' genomes of clonally-unrelated relapses. Therefore we propose to call such manifestations second *de novo* DLBCL occurring in the same individual.

Genetic evolution of DLBCL at relapse is largely unexplored except of a single study, but much is assumed from results and conclusions in other lymphoid neoplasms. Analysis of the dynamics of shared and private alterations in paired tumors suggested existence of at least two distinct patterns of genome evolution at relapse. About one third of investigated clonally-related cases followed an early-divergent/branching pattern of a relapse, characterized by a small number of shared mutations between the two occurrences and a large number of primary tumor-specific alterations. The rest of the cases relapsed via a late-divergent/linear pattern. They were characterized by sharing most mutations between the respective primaries and relapses and very small numbers, if any, of primary tumor-specific genetic alterations.

The identification of precise genetic drivers and prognostic factors of relapse is challenged by an extreme heterogeneity of DLBCL. Together with the small sample sizes of analyzed collectives, this is probably the main reason why there is only a limited overlap in findings between studies, addressing this issue up to date. Our analysis identified two genes, *KMT2D* and *MEF2B*, which recurrently gained additional mutations at relapse. Further, we identified recurrently shared alterations of *CD79B*, *KMT2D*, *MYD88*, *PIM1*, which represented early drivers of lymphomagenesis. Finally, comparing genetic data between relapsing and non-relapsing DLBCL cohorts we identified group-specific DNA lesions (recurrent gains of 10p15.3-13 containing *GATA3* and *PRKCQ* in primary relapsing DLBCL and mutations of *SOCS1* and *RELN* in non-relapsing DLBCL). The prognostic power of them could be further investigated in dedicated large-scale studies.

We are committed in further analyzing paired lymphoma samples, also in difficult settings, as demonstrated by two small-scale studies included in this dissertation. We developed and applied a technique to enrich rare lymphoma cells from formalin-fixed paraffin-embedded tissues. It enables meaningful genetic analysis of relapses in lymphoid neoplasms, such as classical Hodgkin lymphoma, which are important but understudied, due to their research-limiting morphological properties.

1. INTRODUCTION

1.1 B-cell development

1.1.1 Early stages of B-cell development

B-lymphocytes (B-cells) are a population of cells expressing clonally diverse cell surface immunoglobulin (Ig) receptors, which recognize specific antigens. B-cells develop from the hematopoietic precursor cells that reside in the bone marrow. Their development involves multiple stages beginning with the emergence of lineage in the primary lymphoid tissue (e.g. fetal liver, adult bone marrow) and continuing with functional maturation in secondary lymphoid organs (the spleen, lymph nodes, Peyer's patches, mucosal tissues etc.). B-cells terminally differentiate into either memory cells, which can initiate a secondary immune response or into non-proliferating plasma cells. The functional endpoint of B-cell development is the production of antigen-specific antibodies¹ (Figure 1).

During embryogenesis, bone marrow is seeded by the hematopoietic stem cells from the developing fetal liver. It provides complex and dynamic microenvironment, or niche, required for the development of hematopoietic cells. A crucial role hereby play different types of bone marrow stromal cells that support B-cell differentiation in two major ways: first, by expressing specific types of adhesion molecules they assure physical localization of developing B-cells to the appropriate bone marrow compartments; second, they secrete cytokines that transfer key signals for B-cell differentiation².

Early bone marrow-dependent stages of B-cell development are structured around the rearrangements of immunoglobulin genes (*IG*). These early B-cell precursors also have a characteristic pattern of expressed surface markers and activated transcription factors. The expression of the B-lineage marker CD45D and increased amount of the transcription factor EBF1 marks the entrance of the developing lymphoid cell into the **pre-pro B-cell** stage³. At this stage EBF1 binds to the immunoglobulin heavy chain (*IGH*) gene and prepare it for D to J_H recombination. Also, its expression is required for the later initiation of CD79A and CD79B production. Both of these molecules are essential components of the B-cell receptor (BCR)⁴.

D to J_H recombination is completed in the early **pro-B cell** stage. At this stage, activated by the binding of EBF1 to its promoter, the expression of *PAX5* starts. *PAX5* is a key B-cell transcription factor that is present in all B-cells throughout all subsequent developmental

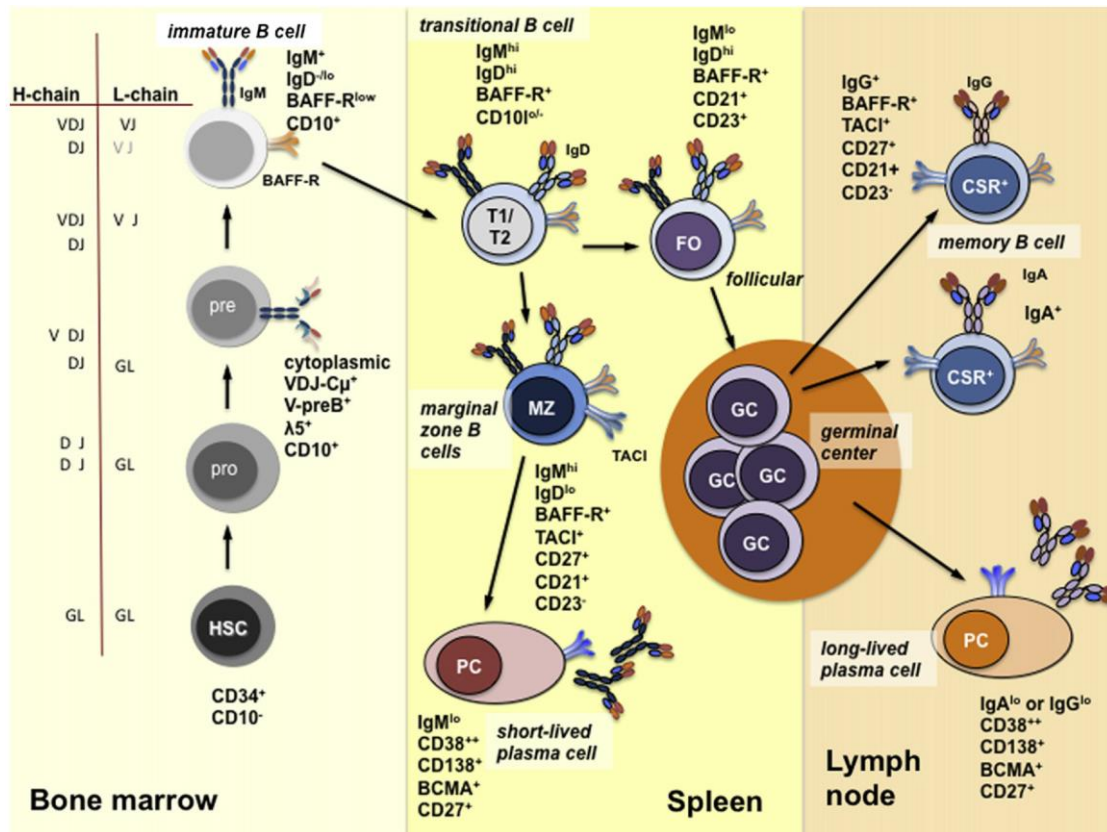


Figure 1. Development of B-cells is a step-wise process that occurs in multiple distinct organism sites. Early stages take place in bone marrow where progenitor cells commit to a B-cell lineage, rearrange their immunoglobulin genes and start expressing a B-cell receptor. Immature B-cells migrate to the spleen to become transitional cells, which give rise to either naïve follicular B-cells or marginal zone B-cells. Follicular B-cells can form germinal centers and differentiate into memory B-cells or plasma cells. Adapted from ref¹⁰.

stages until differentiation into plasma cells⁵. It is experimentally proven, that PAX5 is essential for the V to DJ_H recombination since mice lacking PAX5 are unable to complete the second stage of *IG* heavy chain rearrangement⁶. Also, during the pro-B cell stage CD79A/B are produced and PAX5 initiates the expression of the surface marker CD19, which itself is another essential component of the BCR and a widely used diagnostic marker for the B-cell lineage⁵. Furthermore, PAX5 is of paramount importance to the B-cells and is required for the full commitment of the hematopoietic progenitor cells to the B-cell fate, probably due to its ability to suppress expression of *NOTCH1*^{7,8}.

VDJ_H rearrangement is completed at the end of the pro-B cell stage and the expression of the pre-B cell receptor (pre-BCR) marks the entry to the **early pre-B-cell** developmental stage. Pre-BCR is composed of freshly rearranged *IGH* and surrogate light chain components VpreB and λ 5. Pre-BCR signaling downregulates RAG1/2 enzymes and prevent further *IGH* rearrangements. The second *IGH* allele is suppressed due to allelic exclusion. Cells that fail to display a pre-BCR at this stage undergo controlled cell death by apoptosis, representing the

first checkpoint in the B-cell development. Cells that successfully pass the first checkpoint undergo several rounds of proliferation before continuing with the rearrangement of the *IG* light chain genes. This leads to a possibility of several B-cell clones with identical *IGH* rearrangements but distinctly rearranged light chains.

After successful proliferation the pre-BCR receptor is lost and this marks the entry to the **late pre-B-cell stage**. At this stage the expression of RAG1/2 is reactivated and the cells prepare for light-chain gene rearrangement. First κ light chain genes are rearranged. If rearrangements are non-productive, λ light chain alleles are rearranged⁹. After successful rearrangement the IgM receptor is displayed on the surface of B-cell. IgM expression is characteristic to the immature B-cells.

Immature B-cells are tested for their reactivity against self-antigens in the bone marrow. Cells, which show self-reactivity, either undergo apoptosis (a process called clonal depletion) or editing of the *IG*. Non-reactive immature B cells leave the bone marrow and circulate to the spleen where they emerge as transitional 1 (T1) cells. Here T1 cells are once more tested for their reactivity against self-antigens present in the spleen. Again, self-reactive cells undergo apoptosis or edit their rearranged heavy- or light-chain genes. After this stage non-reactive cells enter spleen follicles where mRNA splicing is activated. Due to splicing B-cells start expressing IgD as a part of BCR, thus decreasing the amount of surface IgM receptors¹⁰.

Besides the BCR signaling, the survival of B-cells in the periphery is dependent on signaling by the B-cell activator of the TNF- α family (BAFF). The BAFF receptor (BAFF-R) is first expressed at the end of the immature B-cell stage¹¹. BAFF signaling promotes the expression of anti-apoptotic molecules such as BCL-2 and BCL-xl, providing survival signals to T1, T2 and mature B-cells. Also BAFF is involved in non-canonical NF- κ B activation^{12,13}. In mice, knockout of *Baff-r* or *Baff* results in decreased mature B-cell counts and weakened immune response – a phenotype, which can be reversed by overexpression of *Bcl-2*¹⁴.

Fully mature B cells that leave the spleen and recirculate between blood and lymphoid follicles in the lymphoid organs are called follicular B-2 cells. They express high levels of IgD and moderate levels of IgM and are ready to be activated if encountering foreign antigens fitting to their BCR. T2 cells also give rise to marginal zone B cells that are located in the outer regions of the white pulp of the spleen¹. Recirculating follicular B-cells constitute the majority of mature B-cells and are the relevant type in the context of the majority of B-cell lymphomas, therefore further description of the B-cell maturation will be focused on them.

1.1.2 Structural organization and rearrangement of *IG* genes.

Immunoglobulins (Ig) are formed by four separate polypeptides: two identical heavy chains and two identical light chains. Those polypeptides are coded by separate loci within the human genome. Heavy chain gene locus is located on chromosome (chr) 14, while the λ and κ light chain genes loci are located on chr 22 and chr 2, respectively. Germline *IG* have a unique multigene structure, which needs to be rearranged before production of functional Ig is possible. Such rearrangement process is restricted to B-cells in humans. Similar processes take place to rearrange receptor genes in T cells. The multigene structure is the source of profound variation that gives a potential for large numbers of combinations and therefore diverse specificity of the Ig¹⁵.

The organization of light and heavy chain genes is very similar. The light chain locus consists of variable (V) genes, joining (J) genes and constant (C) genes. Heavy chain genes additionally have a diversity (D) region between V and J segments. The number of genes in each cluster differs (Figure 2). V genes are separated into families based on their sequence similarity. If similarity of two genes is lower than 80%, those genes belong to different V gene family¹⁶. V genes are always located at the 5' end of each *IG* locus. While a typical V gene is about 300 bp long, they are interspersed by non-coding DNA sequences.

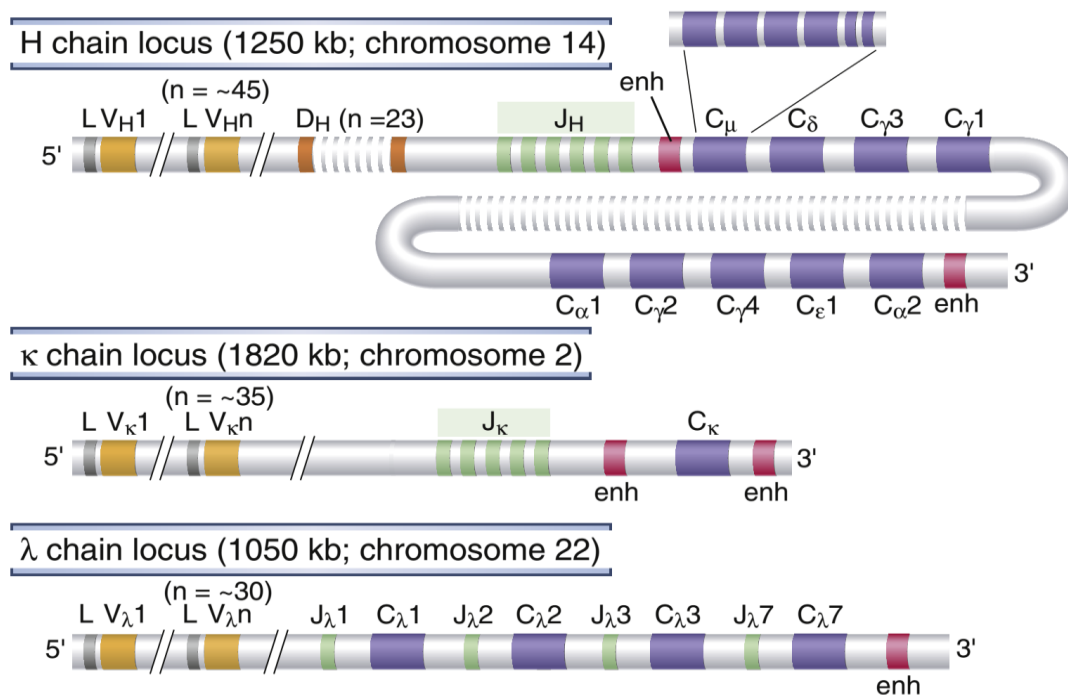


Figure 2. Schematic representation of human *IG* loci. The scale of the boxes is approximate. Only functional genes are shown. Non-coding sequences are displayed in gray. Note that joining (J) regions in lambda light chain are located between the constant regions. enh – enhancer; L – leader exon; Adapted from ref¹⁵.

Consequently, one V cluster can be as long as 200 kb in a germline genome. Upstream of each V cluster there is a leader exon, which encodes a leader peptide required for Ig translation and its import into the endoplasmic reticulum. 5' to each leader peptide lies a V gene promoter, which is required for transcription¹⁵.

3' to the V genes are several J segments. They are typically 30 to 50 bp long, separated from each other by non-coding sequences. D segments are located in between V and J segments. Constant (C) genes lie 3' to the J segments. In the *IGL* locus, the C gene consists of only one exon, while in the *IGH*, C genes typically have five or six exons.

Non-coding sequences neighboring and within the *IG* loci play an important role in regulation of recombination and gene expression. These sequences contain repressors, enhancers, switch regions and recognition motifs that are essential for successful recombination and later transcription of the gene¹⁵.

During B-cell development, *IG* can potentially undergo two types of rearrangements: V(D)J recombination and class switch recombination (CSR)¹. Only the former is essential for *IG* transcription and expression of functional Ig. CSR is shortly addressed later in the chapter concerning germinal center reaction.

During the V(D)J recombination the 3' end of one *D* gene is brought to the 5' end of one *J* gene. This stage is called DJ joining. Then in a similar manner the 3' end of one of the *V* genes is ligated to the 5' end of the *DJ* cluster, resulting in complete *VDJ* construct¹⁷. The light chain is rearranged in the same way, except there is only one stage i.e. VJ joining. Mechanistically, rearrangement is made possible by an availability of specific non-coding DNA sequences called recombination signal sequences (RSS). RSS are very conserved blocks of 7 (heptamers) and 9 (nonamers) nucleotides that occur upstream and downstream of *V*, *D* and *J* genes. They also include less conserved spacers of either 12 or 23 bp. The specific distribution pattern of these elements allows precise excision and joining of the target sequences¹⁶. The best understood enzymes that are involved in the recombination process are called recombination-activating genes 1 and 2 (RAG1 and RAG2)¹⁸. They recognize the RSS sequences and induce DNA strand breaks at specific sites. End processing and joining is performed with the help of additional protein complex including Artemis, DNA ligase IV, Terminal deoxynucleotidyl transferase (TdT) and other components of non-homologous end joining machinery. Of these, the expression of RAG1/2 and TdT is restricted only to lymphoid cells¹⁵.

1.1.3 The germinal center reaction and parafollicular activation of B-blasts

Germinal centers (GC) were first discovered in 1884 by Dr. Walter Flemming. He described them as transient and distinct micro-anatomical structures in secondary lymphoid organs that contain dividing cells¹⁹. GC form after antigen- and T-cell-dependent B-cell activation and their main function is the affinity maturation of the BCR. This involves dynamic processes of dedicated structure formation, intra- and intercellular signaling, positive and negative selection, cell death, migration and differentiation (Figure 3).

Circulating naïve B-cells express chemokine receptor CXCR5 and are attracted to the lymphoid follicles by follicular dendritic cells (FDC) that express the ligand chemokine CXCL13²⁰. There B-cells encounter, by means of their BCR, foreign peptide antigens either in a soluble form (antigens under 70kDa) or bound on the membranes of antigen-presenting cells (macrophages, T-cells, dendritic cells)²¹. Then BCR-antigen complexes are internalized,

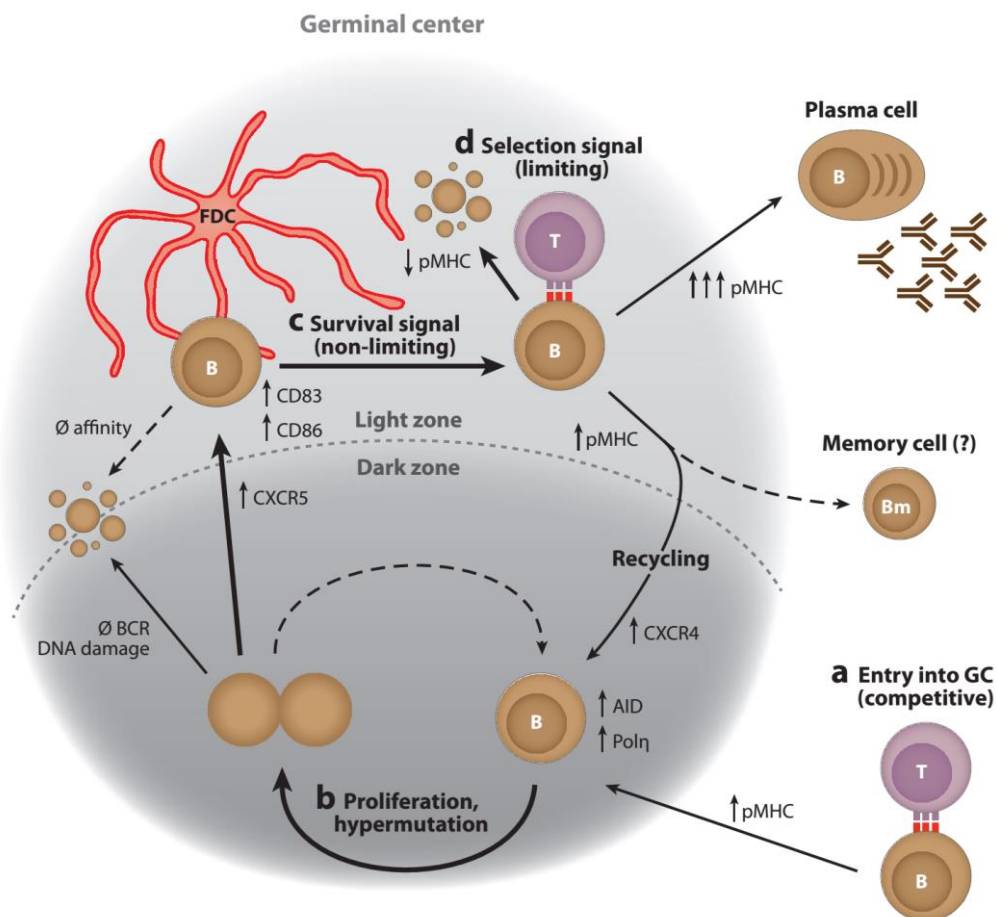


Figure 3. Germinal centers consist of two functional compartments: the dark zone and the light zone. In the dark zone B-cells (centroblasts) undergo intense proliferation and somatic hypermutation. Then they migrate as centrocytes to the light zone, where affinity of the B-cell receptor is tested and class switch recombination occurs. B-cells can recycle multiple times between dark and light zones until enough receptor specificity is achieved. Besides B-cells, follicular dendritic cells and follicular helper T-cells are essential for the germinal center reaction. Adapted from ref²⁸.

processed and displayed on a major histocompatibility complex (MHC) class II (MHC-II) molecule on the surface of the B-cell. Following antigen recognition by BCR, a specific chemokine receptor CCR7 is upregulated, which guides B-cells outside the follicle to a T zone where T cells express the CCR7 ligands CCL19 and CCL21. There the MHC-bound antigen is recognized by a specific T-cell receptor (TCR) and bidirectional activation between the respective B- and T-cells takes place^{22,23}. Crucial for B-cell activation is the contact between the CD40 receptor on the B-cell with its ligand CD154, which is membrane-bound on the surface of the T-cell²⁴. This contact provides strong activation and proliferation signals for the B-cell. Mice with disabled interaction between CD40 and CD154 do not develop GC²⁵. This effect is also manifested in humans because mutations in *CD154* lead to abolished CD40 signaling and X chromosome-linked immunodeficiency with so called hyper-IgM syndrome^{26,27}. Additional stimulation for B-cells is achieved via secretion of IL-2, IL-4 and IL-5 by activated T-cells. T-cell-dependent activation, according to the favored hypothesis²⁸, is competitive: only limited numbers of CD4+ T-cells are available in the parafollicular space and only those B-cells that display relatively strong affinity towards the antigen, and consequently display more MHC-II-antigen complexes, are allowed to enter follicles and form GC. Other B-cells, whose BCR binds the respective antigen with low affinity undergo alternative destinies, e.g. apoptosis due to low BCR signal and lack of T-cell stimulation²⁹ or differentiation into GC independent long-lived (extrafollicularly/parafollicularly activated and matured) plasma cells secreting low-specificity IgM antibodies³⁰.

Following activation, B-cells transform into centroblasts, migrate to the center of the follicle, and start fast proliferation. The duration of centroblasts' cell cycle range between 6 and 12 hours and they are therefore the fastest proliferating human cells^{22,31,32}. Centroblasts uniformly have a low cytoplasm-to-nucleus ratio, therefore the area where they are located appears darker under a light microscope and was termed the dark zone (DZ) of GC¹⁹. Centroblasts are maintained in the DZ due to their relatively high levels of CXCR4. This chemokine receptor is activated by its ligand CXCL12 expressed by locally present stromal cells³³. Prior to the formation of GC, the centers of follicles are mostly occupied by recirculating naïve B-cells. Intensely proliferating centroblasts push them out to the periphery of the follicle where they form a compartment called B-cell mantle²².

Additionally to intense proliferation, GC is the site of a process called somatic hypermutation (SHM). During SHM the Ig variable region (IgV) of the rearranged *IG* genes is modified³⁴. This process is heavily dependent on the activity of an enzyme called activation-induced deaminase (AID), which performs targeted deamination of deoxycytidine³⁵. Deamination

leads to a formation of a U:G mispair. The type of lesion introduced to the DNA strand following deamination largely depends on the way in which the mispair is identified, processed and resolved³⁶. One major pathway is the mutation recognition by the DNA base excision repair machinery. Then the uracil base is excised by uracil-DNA-glycosylase (UNG) and the abasic site is filled randomly with one of the four possible DNA bases leading to a potential transition or transversion³⁷. Alternatively, U:G mismatch can be processed by DNA mismatch repair mechanism involving the mismatch repair enzymes MutS protein homolog 2 (MSH2) and MSH6. As a result of this pathway A:T pairs in place of C:G are formed³⁸. SHM introduce DNA lesions at approximate rate of 10^{-3} mutations per base per generation. SHM is related to DNA strand breaks and the majority of alterations produced are point mutations³⁹. However, duplications and deletions were also reported⁴⁰. Most mutations are concentrated to the complementarity-determining regions (CDR) of IgV as well as on coding and regulatory regions 2kb downstream of the transcription initiation site (Figure 4)³⁶.

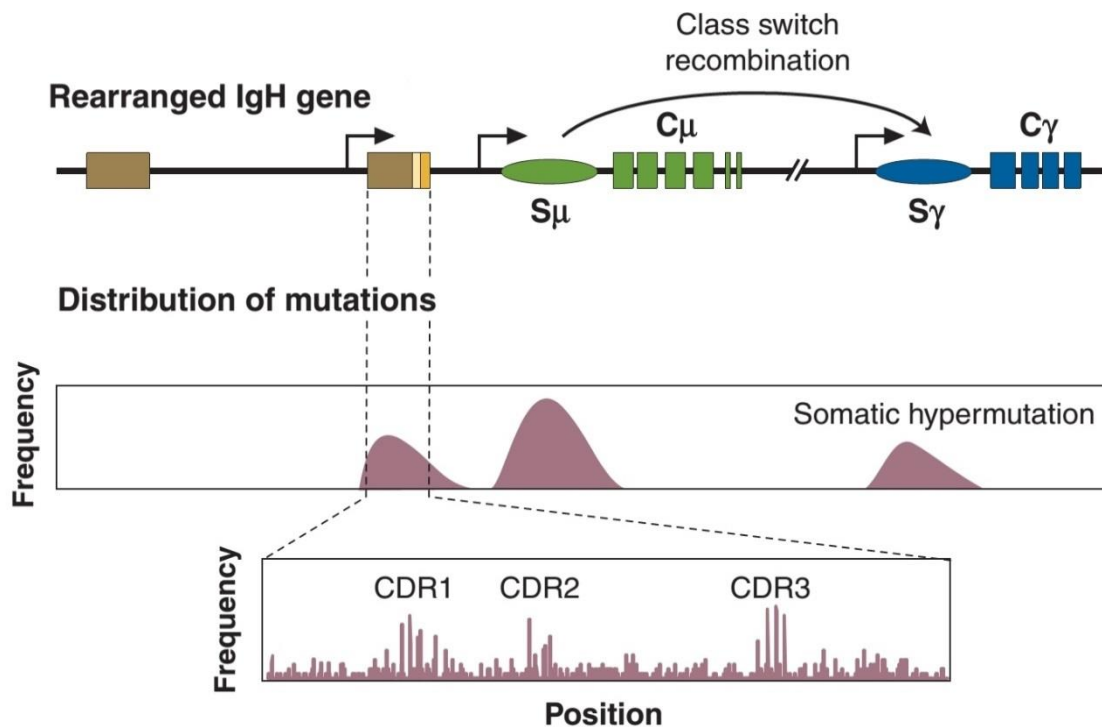


Figure 4. Localization of somatic hypermutation in the immunoglobulin gene (*IG*). DNA lesions are concentrated to complementarity determining regions within the variable sequences as well as in the switch regions of the heavy chains. C – constant region; CDR – complementarity determining region; S – switch sequences; Adapted from ref³⁶.

Following several rounds of proliferation and SHM, centroblasts leave the DZ of the GC and migrate to the light zone (LZ) composed of B-cells called centrocytes in a dense mesh of FDC²⁸. This migration is enabled by the increased expression of a chemokine receptor CXCR5 by DZ B-cells, which then guides them towards LZ where the concentration of CXCL13 is higher.³³ Transition of centroblast to centrocytes is marked by upregulation of

CD83 and CD86 levels. These two markers are used to distinguish these two cell types in FACS experiments⁴¹. Centrocytes test the effects of recent mutagenesis in the DZ by binding the antigen presented on the immune complexes of the FDC. This interaction is not competitive, meaning that potentially every B-cell that make its way to the LZ interacts with FDC⁴². If the BCR of that cell has lost its affinity due to SHM, the cell undergoes apoptosis, due to lack of survival signals from the BCR. If BCR recognizes the respective antigen, it is again internalized into the B-cell, processed and displayed on the plasma membrane with a MHCII molecule. Similar to the initial activation, B-cells then competitively seek contact with T-cells for signals determining their further fate. T-cells are able to discriminate B-cells according to the amount of MHCII-antigen complexes presented, favoring those, which display more^{43,44}. This, combined with the limited counts of T-cells in the LZ, proves that B-cells have to compete for T-cell interaction.

It has been shown that affinity maturation in GC is not a one-way process. The fraction of centrocytes that show strong but insufficient affinity for antigen migrate back to the DZ to undergo additional rounds of SHM and proliferation. This migratory pattern is termed cyclic re-entry⁴⁵.

Additionally, the LZ is thought to be the main site of class (isotype) switch recombination (CSR). The mechanism of CSR is relatively well known. Here as in SHM, an important role is played by AID, which helps to induce double stranded DNA breaks within donor and acceptor switch domains⁴⁶. The DNA between these breaks is removed and the resulting ends are ligated by non-homologous end joining^{15,47}. Naïve B-cells have potential to switch to any isotype and to change their antibody-coding heavy chain from μ to either ϵ , α or γ . Induction of CSR can be T-cell-dependent and independent. Besides the major role of CD40 in induction⁴⁸, signaling by BAFF-R, cyclophillin-ligand interactor (TACI) and inducible T-cell co-stimulator (ICOS) has also been demonstrated^{49,50}. The combination of cytokines and costimulatory signals determine the class of the resulting Ig after switching. For example stimulation by interferon gamma (INF- γ) results in production of IgG, while IL-4 induces switching to IgE. Anatomical sites also matter: B-cells located in mucosal tissues switch predominantly to IgA, which is most effective against microbes attempting to penetrate through epithelia. Different classes of antibodies have distinct effector functions and are involved in defense against different types of infectious agents. Therefore, CSR is an important step in diversification of B-cell antibody repertoire.

After centrocytes complete BCR affinity maturation and class switching, they migrate outside the LZ and differentiate either into plasma cells or into memory B-cells. As will be explained

later, processes in the GC are prone to errors and can generate significant numbers of DNA lesions affecting tumor suppressors and oncogenes. These GC reaction-specific lesions contribute significantly to pathogenesis of B-cell lymphomas.

Regulatory networks of germinal center reaction.

Initiation of the GC, transit between functional zones, exit and differentiation are regulated by a complex intracellular and humoral signaling systems. Major players in these processes have been identified and include PAX5, BCL-6, NF- κ B, C-MYC and BLIMP1 (Figure 5). The knowledge about the precise mechanism of action is lacking for some of these molecules, but their role has been proven by functional experiments *in vivo* and *in vitro*^{51,52}.

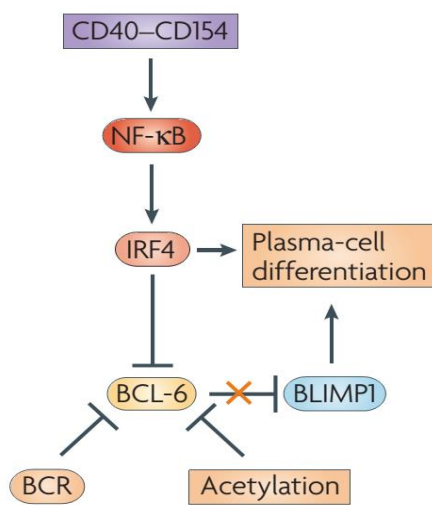


Figure 5. Inhibition of BCL-6 and plasma cell differentiation. BCL-6 is downregulated in centrocytes following activating contact with helper T-cells, which is transduced via NF- κ B and BCR signaling as well as protein acetylation. Repression of BCL-6 lifts the inhibition of BLIMP1 and leads to plasma cell differentiation. Adapted from³⁴

BCL-6 is acknowledged as one of the most important transcriptional regulators of the GC reaction. Its expression is initiated by successful B-cell activation, as well as by the activity of interferon-regulatory factor 8 (IRF8) and MEF2B. Upon activation, BCL-6 can bind its own promoter to negatively regulate its transcriptional levels⁵³. Primarily BCL-6 acts as transcriptional repressor. It binds specific DNA motifs and recruits histone deacetylases (HDAC) directly or through interactions with other co-factors. HDAC deacetylate histones in target loci to render them inaccessible for DNA transcription. BCL-6 is strongly expressed in centroblasts and, to a lesser extent, in centrocytes. It has multiple roles in the GC reaction. First, it provides tolerance to the high level of DNA damage occurring in centroblasts and centrocytes during SHM and CSR, respectively. It has been shown

that BCL-6 represses transcription of *TP53* and *CDKN1A* and rescues cells from apoptosis and cell cycle arrest^{54,55}. Second, BCL-6 prevents premature B-cell activation by T-cells by downregulating *STAT1*, *CD69* and *CD80*^{56,57}. This mechanism ensures that B-cells do not leave GC too early when sufficient BCR affinity is not yet achieved. Third, BCL-6 inhibits premature differentiation of GC B-cells into plasma cells, by repressing *PRDM1*, encoding a master regulator of plasma cell differentiation BLIMP1, and IRF4^{58,59}. Fourth, it induces the expression of AID by inhibiting expression of two microRNAs, miR-155 and miR-361, which

negatively regulate AID⁶⁰. BCL-6 is downregulated following strong and definitive T-cell-dependent B-cell activation in the LZ. This permits differentiation of centrocytes into plasmablasts or memory-B cells⁶¹. Adding to its importance, BCL-6 also acts as regulator of transcriptional program in GC T-cells⁶².

IRF8 is expressed in centroblasts but not in centrocytes during the GC reaction. It positively regulates BCL-6 and AID⁶³. Furthermore, it binds PU.1 to maintain the expression of PAX5. Knock-out of both IRF8 and PU.1 leads to premature plasma cell differentiation in the GC⁶⁴.

C-MYC is upregulated for a short period during GC initiation. Later its expression is transcriptionally suppressed in the DZ by BCL-6 but reactivated again in the small subset of centrocytes in the light zone that eventually re-enter the DZ⁶⁵. The exact effects of MYC activation in the GC are not clear but it is believed that it stimulates metabolism, DNA replication and telomerase function⁶⁶.

NF- κ B signaling is absent in centroblasts but it is indirectly activated in centrocytes following strong stimulation by BCR, CD40, BAFF and cytokines and signaling by MAPK, PI3K and toll-like receptors⁵¹. Besides other important effects, NF- κ B activates IRF4 (MUM1p) to promote plasma cell differentiation⁶⁷.

PAX5 is a crucial transcription factor for B-cell identity maintenance. Its expression starts early in B-cell development upon the definite commitment of precursors to the lymphoid lineage at the pro-B stage, and continues throughout the mature B-cell phase as well as during the GC reaction. It binds a plethora of DNA sites and acts as both initiator and repressor of transcription. It regulates the expression of BCR components (IGH, CD79A), and other molecules that define B-cell identity (CD19, CD21, BLK, IRF4, IRF8)⁵. It also represses lineage-inappropriate markers such as FLT3, CD28, NOTCH1 and others⁸. Downregulation of PAX5 is essential for centrocyte differentiation into Ig-secreting plasma cell. On the other hand, its expression is maintained in memory B-cells³⁴.

IRF4 is expressed at low levels during GC initiation where it induces the expression of BCL-6 and AID. During the late stages of GC reaction IRF4 is strongly upregulated in centrocytes following elevated BCR signaling and activation of NF- κ B. Then it represses BCL-6 and stimulates the expression of BLIMP1^{52,64}.

BLIMP1, coded by *PRDMI*, is essential for differentiation of B-cell into a plasma cell and its expression is restricted to the latter cell type. It is activated by IRF4 in late GC. During commitment to plasma cell, BLIMP1 represses PAX5, BCL-6 and C-MYC, which are responsible for B-cell and especially for B-cell GC phenotype. It also activates *XPB1*, which is important, but not essential regulator of plasma cell differentiation⁶⁸. XPB1 induces the

development of the endoplasmic reticulum and accommodates cells for secretion of large quantities of proteins⁶⁹.

1.2 Diffuse large B-cell lymphoma, not otherwise specified (NOS)

Diffuse large B cell lymphoma (DLBCL) is an aggressive form of B-cell lymphoma, which accounts for 30% of all newly diagnosed lymphomas worldwide⁷⁰. The median age of occurrence is between 60 and 70 years, but it can also arise in young adults and children. DLBCL is slightly more frequent in males than in females^{71,72}. It can affect nodal and extranodal sites. The most frequent extranodal locations are the gastrointestinal tract, the bones, testes, spleen and Waldeyer's ring. Predominantly DLBCL is a *de novo* disease, but it can also manifest as transformations from other more indolent lymphoid neoplasms such as follicular lymphomas, marginal zone lymphomas and chronic lymphocytic leukemias (the latter is called Richter's transformation). DLBCL is a very heterogeneous disease, which has distinct morphological, phenotypic, molecular and clinical characteristics. Some of those characteristics have been used as a basis for a numerous different classifications (see Table 1)⁷².

<p>Diffuse large B-cell lymphoma, not otherwise specified (NOS)</p> <ul style="list-style-type: none"> Common morphologic variants <ul style="list-style-type: none"> Centroblastic Immunoblastic Anaplastic Rare morphologic variants Molecular subgroups <ul style="list-style-type: none"> Germinal centre B-cell-like (GCB) Activated B-cell-like (ABC) Immunohistochemical subgroups <ul style="list-style-type: none"> CD5-positive DLBCL Germinal centre B-cell-like (GCB) Non-germinal centre B-cell-like (non-GCB) <p>Diffuse large B-cell lymphoma subtypes</p> <ul style="list-style-type: none"> T-cell/histiocyte-rich large B-cell lymphoma Primary DLBCL of the CNS Primary cutaneous DLBCL, leg type EBV positive DLBCL of the elderly <p>Other lymphomas of large B cells</p> <ul style="list-style-type: none"> Primary mediastinal (thymic) large B-cell lymphoma Intravascular large B-cell lymphoma DLBCL associated with chronic inflammation Lymphomatoid granulomatosis ALK-positive LBCL Plasmablastic lymphoma Large B-cell lymphoma arising in HHV8-associated multicentric Castlemann disease Primary effusion lymphoma <p>Borderline cases</p> <ul style="list-style-type: none"> B-cell lymphoma, unclassifiable, with features intermediate between diffuse large B-cell lymphoma and Burkitt lymphoma B-cell lymphoma, unclassifiable, with features intermediate between diffuse large B-cell lymphoma and classical Hodgkin lymphoma

Table 1. Categorization of DLBC in the 4th edition of WHO classification of hematopoietic and lymphoid tissues⁷². ALK, anaplastic lymphoma receptor kinase; CNS, central nervous system; EBV, Epstein-Barr virus; HHV8 human herpes virus 8.

Gene expression and genetic studies revealed several molecular subtypes of DLBCL: the germinal-center B-cell (GCB) subtype, the activated B-cell (ABC) subtype and the primary mediastinal large B-cell lymphoma (PMBCL) subtype⁷³⁻⁷⁵. However, 10-15% of DLBCL cases cannot be classified into any of these categories. The three DLBCL subtypes are thought to derive from distinct B-cell developmental phases as their gene expression profiles match closely with the gene expression profiles of their healthy counterparts. Thus, the cell of origin (COO) concept has emerged. It has been shown that gene expression profile of GCB-DLBCL closely matches with a profile of healthy GC B-cells. Moreover, GCB-DLBCL frequently express BCL-6, CD10, GCET1, HGAL and LMO2 and have highly mutated *IG* genes, which are all properties of GC B-cells. In contrast, the transcriptional signature of ABC-DLBCL matches best with the one of post-GC B-cells or plasmablasts; they more frequently express IRF4, FoxP1, CD44 and lack CD10 as well as GCET1. PMBCL originates from a rare thymic B-cell and is morphologically (clear cells, compartmentalizing fibrosis), phenotypically (CD23+, CD30+, p63+), molecularly (*JAK2* and *PDL1* locus gains, *C-REL* locus gains, *PTPN1*, *STAT6* and *SOCS1* mutations) and clinically clearly distinguishable from the other two subtypes.

Some authors argue that the COO concept can be misleading, because it gives an impression that lymphomagenesis start at a defined stated phase of B-cell development. In reality, however, the actual initiating events could potentially occur at an earlier stage of B-cell development, but allow further development up until the stage where additional genetic aberrations impose a differentiation block. Thus, COO would represent not the actual normal counterpart, but the stage at which differentiation block occurred⁷⁶. Several findings support this line of reasoning. For example, the t(14;18) translocation involving the *BCL2* oncogene and the *IGH* gene is clearly a pathogenic event and is frequently found in GCB type of DLBCL. However, it is known that this translocation occurs due to aberrant *V(D)J* rearrangement during the pre-B phase of B-cell development - a far earlier stage than a GC centroblast, which is the hypothesized normal counterpart of GCB-DLBCL⁷⁷. Additionally, it is known that malignant cells of ABC type of DLBCL most frequently express IgM⁷⁸. Again, this is contradictory to a suggested understanding that ABC-DLBCL develop from post-GC plasmablast, since isotype switch occurs in the light zone centrocytes prior to plasmacytic differentiation⁷⁹.

Although COO classification was produced by genome-wide gene expression profiling, numerous additional techniques were shown to closely reproduce the initial findings. These include immunohistochemical and transcriptional profiling algorithms of a selected subset of markers, classification according to Ig expression and others⁸⁰⁻⁸³. These approaches not only

replicated the results of COO classification by assigning DLBCL cases to the same subtype, but also showed that the distinguished categories differ in many additional aspects and thus proved the relevance of the initial findings. These endeavors were mainly pursued due to notion that COO classification has not only biological but also prognostic^{74,84} and therapeutic^{85,86} significance. There was and still is a need of a quick, robust but simple method to reliably classify new DLBCL cases.

1.2.1 Molecular pathogenesis of DLBCL

As all cancers, DLBCL is an uncontrolled accumulation of cells due to numerous genetic lesions – amplifications, deletions, translocations and point mutations – that change cell's regulatory circuits either by activating pro-oncogenic pathways or by inactivating mechanisms that keep cell's growth in check. In addition to common oncogenic processes, DLBCL employ B-cell-specific physiological mechanisms to generate additional lesions. It has been proven that aberrant somatic hypermutation (ASHM), defects in RAG1/2-mediated *IG* rearrangement and error-prone CSR can cause additional lymphoma-specific lesions^{87–89}. These lesions are even more likely because cells have an increased tolerance to DNA damage and higher threshold for apoptosis throughout a GC reaction⁵⁴.

During the last five years revolutionary DNA sequencing technologies allowed sequencing of several hundred full DLBCL genomes or exomes^{90–93}. These sequencing studies have confirmed some previously known mutations in established drivers of lymphomagenesis, but, more importantly, identified new recurrent mutations in genes, whose role in DLBCL was not yet recognized. Coupled with functional studies on many of these newly identified genes, a more comprehensive picture of the genetic landscape of DLBCL has emerged. Despite rather complex genomes and relatively high mutational rate (on average 50-100 DNA lesions per genome), most of mutations converge on several cellular pathways indicating their key role in lymphomagenesis⁷⁶. Some of these pathways are common for all subtypes of DLBCL showing their common origin from a developing B-cell. Others are characteristic only to one particular subtype in accordance to differences in molecular classification and clinical characteristics (Figure 6).

Alterations common for all subtypes

At least three different cellular processes were found to be consistently affected in all subtypes of DLBCL. These include epigenetic maintenance of normal chromatin state,

regulation of BCL-6 transcription and cell control by the immune system. Mechanisms of deregulation are ambiguous as multiple components of the same pathway can be deregulated resulting in same or similar outcome.

Genetic lesions in chromatin modifiers

CREBBP, *EP300* and *KMT2D* are the most frequently mutated genes in all subtypes of DLBCL that affect chromatin remodeling⁹⁴. *CREBBP* and *EP300* are two acetyltransferases that acetylate both histone and non-histone protein residues and in this way alter the activity of numerous DNA-binding transcription factors. They are mutated in approximately 40% of DLBCL^{95,96}. Predominantly, all these mutations are inactivating, but occur only in one of the two alleles, suggesting that the function of these proteins is dose-dependent. It has been shown, that lack of function of both *CREBBP* and *EP300* impairs acetylation of *BCL-6* and *TP53* and disrupts their normal functions.

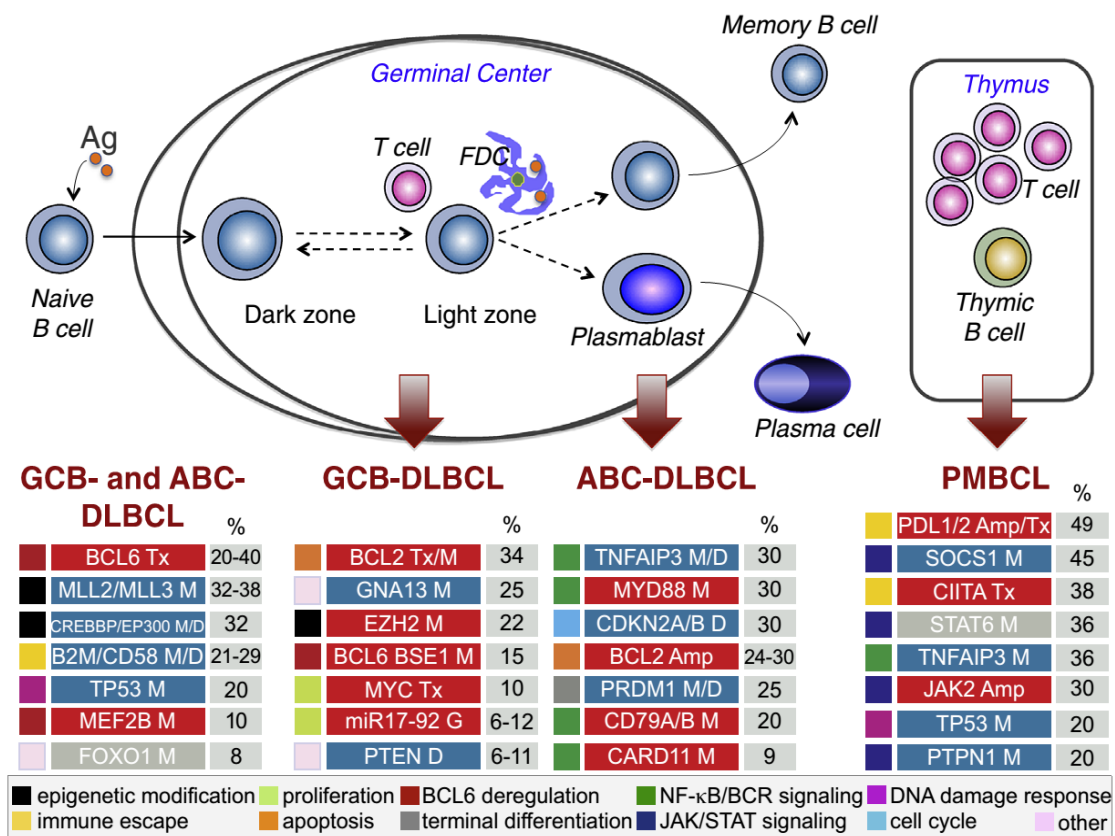


Figure 6. Genetic lesions in DLBCL. Germinal center reaction and its relation to different subtypes of DLBCL pathogenesis is schematically represented. Below, the most frequent genetic alterations are shown with nearby squares color-coded according to the affected cellular process. Blue - loss of function; red - gain of function. FDC – follicular dendritic cell. Adapted from ⁹⁴

KMT2D codes for a methyltransferase that methylates lysine at the 4th position of histone 3 (H3K4). It is mutated in at least 30% of DLBCL. Most of mutations are inactivating, and present in both alleles, suggesting the importance of total *KMT2D* loss for lymphomagenesis.

Despite high mutational frequency, the precise effects of KMT2D abrogation are currently unknown. Animal experiments showed diminished global H3K4 methylation in GC cells and increase of GC B-cell count. Moreover, ablation of *Kmt2d* in mice that overexpress Bcl-2 led to increased incidence of GC-derived lymphoma. It is therefore suggested that KMT2D acts as a tumor suppressor. Its early loss might promote lymphomagenesis by modification of the broad epigenetic landscape of the cancer precursor B-cells⁹⁷.

Deregulation of BCL-6

The lymphomagenic potential of BCL-6 deregulation has been demonstrated in mouse models⁹⁸. Constantly active BCL-6 renders cells resistant to apoptosis, tolerant to a genetic stress and blocks further differentiation by stable inhibition of *PRDM1*⁶¹. Approximately 50% of DLBCL, more frequently ABC-DLBCL, have direct or indirect deregulation of this oncogene. One of the best described mechanism of direct deregulation are translocations (observable in 30% of DLBCL, 25% GCB-DLBCL, 40% ABC-DLBCL), which put the intact coding part of *BCL-6* under the control of differentially regulated promoters. In such case *BCL-6* loses its normal transcriptional regulation and is not silenced at the end of the GC reaction⁹⁹. Additionally, the 5' end of *BCL-6* is recurrently affected by point mutations, which, most likely, are the result of an ASHM. These lesions can have a double effect: first, they might disrupt auto-regulatory mechanisms of *BCL-6* by which it can downregulate its own expression⁵³; second, they can impair binding of IRF4, which normally repress BCL-6 following activation by CD40¹⁰⁰. Indirectly, BCL-6 is deregulated by decreased activity of EP300 and CREBBP. Furthermore, 10-15% of DLBCL harbor activating mutations in the *MEF2B* transcription factor - a positive regulator of BCL-6. Finally, 4% of DLBCL cases have loss-of-function mutations/deletions of *FBXO11* that impair proteosomal degradation of the BCL-6 protein⁶¹.

Immune escape

More than 60% of DLBCL lack expression of MHC class I (MHCI) molecules on the cell surface. Lacking MHCI, lymphoma cells are “invisible” for both cytotoxic T-lymphocyte- and natural killer cell-mediated immune surveillance. In about 30% of cases this defect is attributed to disruptive mutations of the *B2M* gene, which codes for beta-2-microglobulin - a key subunit of MHCI complexes⁹⁰. Additionally, MHCI expression can be lost due to either frequent deletions of the *HLA-A*, *HLA-B* and *HLA-C* loci, which are especially frequent in DLBCL of the central nervous system, or by defect transport of the B2M protein to the cell

surface. In 21% of cases loss-of-function mutations affect the *CD58* gene, which encodes a protein necessary for natural killer- and T-cell-mediated cell responses¹⁰¹.

Other genes that are frequently affected in all types of DLBCL are *TP53* and *FOXO1*. *FOXO1* is a transcription factor that act as a tumor suppressor downstream of PI3K/AKT signaling pathway. About 9% of DLBCL bear mutations in the 5' end of the *FOXO1* gene. They deregulate its translocation to the nucleus and binding to its transcriptional targets¹⁰². These mutations are likely to occur due to ASHM. The *TP53* gene is directly inactivated by damaging point mutations/deletions in about 25% of DLBCL, abolishing its anti-tumor activities^{91,103}.

Lesions associated with GCB-DLBCL

Best characterized GCB-DLBCL-specific genetic aberrations are chromosomal translocations involving *C-MYC* (most frequently t(8;14)) and *BCL-2* (most frequently t(14;18)). They are detected in ~10 and ~30% of GCB-DLBCL, respectively and result in elevated expression of the involved proteins. These lesions are thought to at least partially override the BCL-6-mediated suppression of *C-MYC* and *BCL-2*, to promote cellular growth and grant resistance to apoptosis^{104,105}.

Recently, the histone methyltransferase *EZH2* was associated with GCB-DLBCL pathogenesis. A gain-of-function *EZH2* mutation targeting the Y641(N) hotspot was detected in ~20% of cases¹⁰⁶. Normally, *EZH2* effectively converts unmethylated lysine 27 of histone

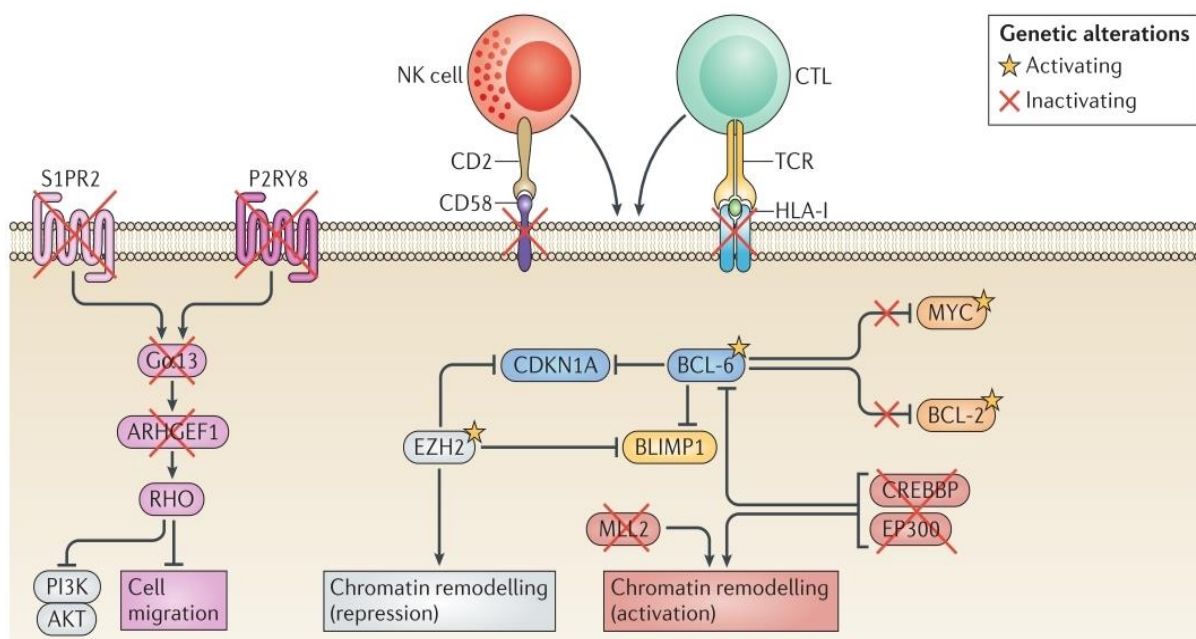


Figure 7. Schematic representation of events involved in GCB-DLBCL pathogenesis. Adapted from⁵¹.

3 (H3K27) to a mono-methylated state. Mutations in *EZH2* change this efficiency and increase the conversion of K27 to a tri-methylated state¹⁰⁷. Tri-methylated lysine residue represses transcription of targeted DNA regions. Among targets of aberrant EZH2-mediated transcriptional repression are *PRDM1*, *IRF4* and *CDKN1A*. In mouse model hypermethylation of H3K27 results in B-cell differentiation blockade, GC hyperplasia and lymphomagenesis¹⁰⁸. Around 30% of GCB-DLBCL have a disrupted $G\alpha 13$ pathway that is responsible for growth and localization of GC B-cells. This disruption is associated with mutations in sphingosine-1-phosphate receptor-2 (*SIPR2*), guanine nucleotide binding protein alpha 13 (*GNA13*), RHO guanine nucleotide exchange factor 1 (*ARHGEF1*) and purinergic receptor P2Y (*P2RY8*)¹⁰⁹. Normally GC B-cells remain strictly within the lymphoid organs and do not recirculate. Mutations in *GNA13* and *ARHGEF1* cause dissemination of GC B-cells to lymph fluid and blood. This effect was not achieved by *SIPR2* mutations. However, *SIPR2* alterations led to GC-type lymphoma formation in mice¹¹⁰. Taken together, these findings reveal a mechanism by which lymphoma cells can leave their tissue of origin and spread to distant sites. Amplification and overexpression of miR-17-92 occurs in 12.5% of GCB-DLBCL¹¹¹. The expression of this microRNA is controlled by a complex transcriptional network containing oncogenes and tumor suppressors. Its upregulation is caused by a coordinated activity of transcription factors C-MYC and E2F¹¹². On the other hand it is downregulated by p53 under hypoxic conditions¹¹³. The active transcription of miR-17-92 is thought to downregulate *PTEN*, *CDKN1A* and *BIM*, which allows tumor cells to escape senescence and to grow more rapidly^{114,115}. Mice with transgenic overexpression of miR-17-92 cluster develop lymphoproliferative disease¹¹⁶. In addition to silencing by miR-17-92, *PTEN* is lost due to deletions in 6 to 55% of GCB-DLBCL cases^{111,117}.

Genetic lesions associated with ABC-DLBCL

Mutations detected in ABC-DLBCL are thought to promote lymphomagenesis by two main mechanisms: activation of NF- κ B transcription factor signaling and preventing of terminal differentiation. Additionally, specific types of BCR displayed on the surface of ABC-DLBCL cells contribute to their phenotype and behavior. IgM expression is atypical for post GC B-cells, since class switch happens during the GC reaction. However, the majority of ABC-DLBCL have a native *IG* heavy chain genes and therefore produce BCR that contains IgM. The heavy chain of IgM has a shorter intracellular domain compared to other class-switched Ig, such as IgG. Because of that it delivers qualitatively different signals to the cell: IgM provides signals associated with cellular proliferation and survival, whereas IgG produces

strong ERK, MAPK and calcium responses that promote B-cell differentiation into plasma cell^{118,119}.

Chronic signaling of NF-κB

NF-κB transcriptional family consists of five family members: p65, c-Rel, RelB, p105/p50 and p100/p52. In the resting state they are bound by their specific inhibitors and sequestered in the cytoplasm. Activation by an upstream signaling removes this inhibition, NF-κB transcription factors form heterodimers and translocate to the nucleus where they elicit their functions by binding multiple DNA targets¹²⁰. The activation can be achieved either via classical (canonical) or alternative (non-canonical) pathways. Canonical activation pathway is by far the most important one in the context of ABC-DLBCL⁷⁶. NF-κB signaling is transiently active during B-cell activation and differentiation. It controls a broad range of cellular processes such as immune and stress responses, apoptosis, proliferation, differentiation and development¹²⁰. However, in ABC-DLBCL NF-κB signaling is chronically active and drives lymphomagenesis by aberrant expression of cyclin D1, cyclin D2, BCL-2, C-MYC, IL-2, IL-6 and others^{121–123}. Mice with chronic NF-κB activation develop B-cell and plasma cell hyperplasia and additional inactivation of BLIMP1 leads to formation of lymphomas reminiscent of ABC-DLBCL¹²⁴. Inhibition of NF-κB signaling kills ABC-DLBCL cells¹²⁵. Constitutive activation is achieved by multiple mechanisms such as chronic BCR signaling, *MYD88* mutations (see later) and disruption of negative regulation circuits (Figure 8).

Chronic BCR signaling

Survival and development of B-cells is dependent on their ability to display functional BCR. Upon antigen encounter, BCR forms clusters in the plasma membrane bringing multiple BCR in a close physical proximity. This facilitates Src-family kinase-mediated phosphorylation of tyrosine residues on the immunoreceptor signaling motif (ITAM) domains of CD79A and CD79B. These phosphorylated residues provide binding sites for SH2 domains of the spleen tyrosine kinase (SYK). It induces a broad signaling cascade that engages the NF-κB, PI3K, MAPK, RAS and other signaling pathways¹²⁶.

It is known that even in the absence of cognate antigens naïve B-cells depend on signals from BCR. These signals are termed tonic BCR signaling¹²⁷. In contrast, ABC-DLBCL cells often have BCR clustered on the membrane surface indicative of chronic active signaling. This chronic signaling can potentially be attributed to BCR activation by self antigens¹²⁸. Additionally, more than 20% of ABC-DLBCL cases bear mutations in the ITAM domains of

CD79A and *CD79B*. These mutations are thought to circumvent negative feedback regulation loops (prevention of receptor endocytosis and/or suppression of LYN kinase activity), thus maintaining chronically active BCR signaling. Knock-down of CD79 adaptors leads to apoptosis of specifically ABC-DLBCL cell lines¹²⁹.

In around 9% of ABC-DLBCL activation of BCR-like signaling and consequent NF- κ B activation is caused by mutations in the caspase recruitment domain-containing protein 11 (*CARD11*) gene^{92,130}. *CARD11* is a multi-domain signaling adapter, which translocates to the inner side of plasma membrane upon phosphorylation by the upstream components of the BCR signaling pathway. It then interacts with BCL10 and MALT1 and forms a so-called CBM complex¹³¹. The active CBM complex eventually facilitates degradation of the NF- κ B inhibitor complex (I κ B) and allows transcription factors to enter the nucleus. Mutations in the coiled-coil domain render permanent activation of *CARD11* and abrogate the need of phosphorylation. This results in BCR-independent activation of NF- κ B¹³².

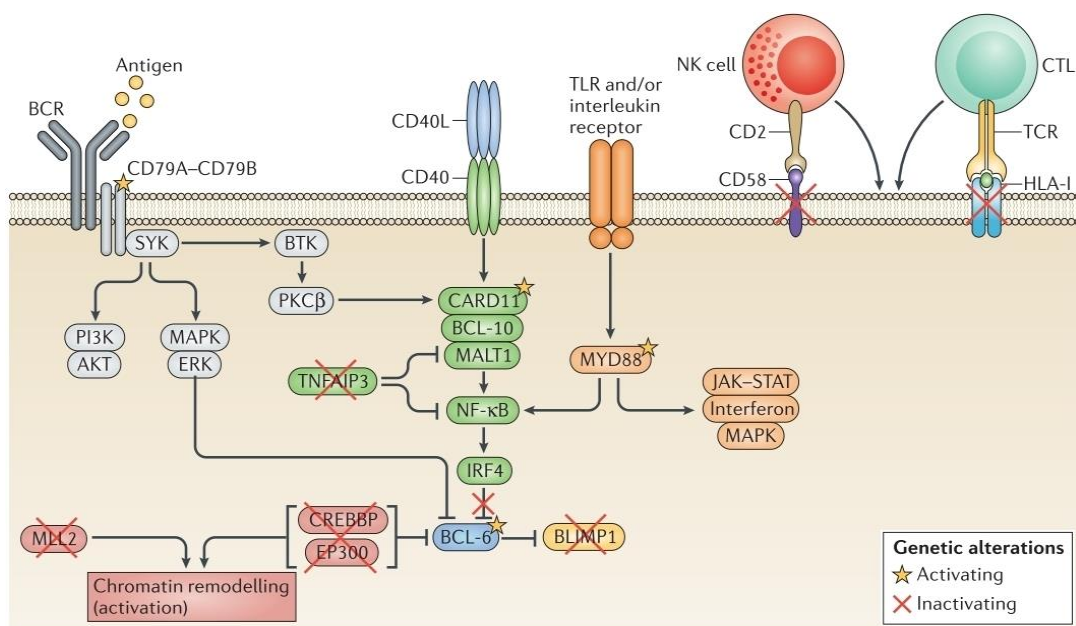


Figure 8. Schematic representation of pathways deregulated in ABC-DLBCL. Adapted from⁵¹.

Mutations of *MYD88*

Approximately 30% of ABC-DLBCL patients harbor mutations in the gene encoding myeloid differentiation primary response protein 88 (*MYD88*). Although several different mutations have been described, the most frequent mutation cause a L265P amino acid change in the intracellular Toll/IL-1 receptor domain (TIR) of this adaptor molecule. This mutation allows *MYD88* to spontaneously assemble a complex containing of IRAK4 and IRAK1, which leads to activation of NF- κ B. Mutations in *MYD88* can also cause JAK/STAT3 transcriptional

responses^{133,134}. Genetic and functional data shows, that *MYD88* mutations cooperate with chronic active BCR signaling to induce NF- κ B and promote lymphomagenesis. These lesions are overlapping in a significant share of ABC-DLBCL cases. Moreover, simultaneous inactivation of *MYD88* and *CD79A* results in higher toxicity for lymphoma cells than abrogation of any of these molecules alone¹³³.

Disruption of negative regulation of NF- κ B

In addition to a wide range of activators, NF- κ B has also several repressors, which downregulate its transcriptional response after the physiologic goals of signaling are completed. These negative regulators act as tumor suppressors and are recurrently targeted by inactivating mutations in ABC-DLBCL. One of such regulators is a deubiquitinating enzyme A20 encoded by *TNFAIP3* gene. It is involved in termination of toll-like receptor induced NF- κ B signaling. A20 exerts its activity by post-transcriptional modification of several members of NF- κ B pathway, targeting them for proteosomal degradation. Both alleles of *TNFAIP3* are inactivated by truncating mutations/deletions in 30% of ABC-DLBCL cases¹³⁵. These mutations cause prolonged NF- κ B responses leading to active proliferation and resistance to apoptosis. In mice, knock-down of *TNFAIP3* leads to spontaneous inflammation and inability to terminate toll-like receptor -dependent activation of NF- κ B¹³⁶.

Blocking of plasma cell differentiation

Blocking of differentiation in ABC-DLBCL occurs via multiple mechanisms, all of which eventually converge to the master regulator of plasma cell development BLIMP1. First, *PRDM1* gene encoding BLIMP1 is lost due to bi-allelic truncating mutations/deletions in ~25% of cases. Second, *PRDM1* can be constitutively suppressed by aberrantly active BCL-6. Finally, it is recently discovered that ~25% of ABC-DLBCL have gain-of-function mutations in *SPIB*¹¹¹. This gene encodes a transcription factor, which directly binds IRF4 and disrupts an IRF4-mediated induction of *PRDM1* expression^{137,138}. The profound impact of BLIMP1 to lymphomagenesis is demonstrated by experiments showing that mice lacking *PRDM1* develop NF- κ B-dependent lymphomas, reminiscent of ABC-DLBCL^{124,139}

1.2.3 Treatment of DLBCL

DLBCL is an aggressive disease but it can be successfully treated and cured in >50% of all cases, even in advanced stages. Currently the treatment of choice is a multi-agent

chemotherapy regimen consisting of cyclophosphamide, hydroxydaunorubicin, oncovin and prednisone combined with a chimeric monoclonal antibody against the CD20 receptor, Rituximab (R-CHOP)¹⁴⁰. Prior to introduction of Rituximab, CHOP alone was used for treatment. The first large clinical study comparing treatment outcomes of CHOP vs R-CHOP came out in 2002. It reported approximately 15% improvement in complete remission, 2-year event free survival (EFS) and 10-year overall survival (OS)¹⁴¹. These results were confirmed by additional studies on various different patient cohorts^{142,143}. There have been attempts to develop and test additional chemotherapy regimens for treatment of DLBCL and they had some success. For example, a dose-adjusted treatment with etoposide, doxorubicin, cyclophosphamide, vincristine, prednisone and rituximab (DA-EPOCH-R) showed high efficiency against PMBCL⁸⁶ and is probably more efficient in ABC-DLBCL.

The standard salvage treatment for patients who fail to respond to the initial therapy or recur after a period of complete remission is high-dose chemotherapy supported with autologous stem cell transplantation (ASCT). However success rates are poor¹⁴⁴.

Molecular subgroups of DLBCL respond differently to standard therapy. Nearly 100% of PMBCL can be cured with R-CHOP or DA-EPOCH-R. In a clinical study of 69 patients with previously untreated DLBCL, for the group of GCB-DLBCL a 100% 5-year progression free survival (PFS) was reported, but for ABC-DLBCL the PFS was only 69%¹⁴⁵. This shows, that the majority of patients who relapse, have the latter type of lymphoma.

The recent directions of improving outcomes for DLBCL patients has been undoubtedly related to the plethora of new genetic information that has been acquired about this group of tumors during the last decade. The presumption is that if one can find out what the drivers of lymphomagenesis are in each individual tumor and understand the principles by which they promote cancer formation, selective interference with their signaling circuits can be exercised and the benefits that tumor cells are gaining from them can be abolished. This is the idea of precision medicine. To that direction, a lot of different compounds have been developed which interfere with nearly every driver molecule and signaling circuit described in the previous section (Figure 9)¹⁴⁰. Many of them showed efficacy in killing DLBCL cells *in vitro*, some entered clinical trials and some have already been successfully used for treating patients with relapsed or refractory DLBCL.

Arguably, the most successful of them was PCI-32765 termed ibrutinib. Ibrutinib acts upon and irreversibly inhibits Bruton's tyrosine kinase (BTK) - a signaling kinase, which transduces signals coming from BCR to activate the NF- κ B pathway. It acts downstream of BCR, but upstream of CARD11. Consequently, ibrutinib is effective against tumors with

chronic BCR activation e.g. due to self-antigens or *CD79A* and *CD79B* mutations. It is completely inefficient against tumors with mutations in coiled-coil domain of *CARD11*, or tumors with altered *MYD88*^{129,146}. Interestingly, ibrutinib is effective against tumors with both *CD79B* and *MYD88* mutations, probably because of cooperation of these two alterations in lymphomagenesis¹³³. In recent phase I/II clinical trial 37% of relapsed/refractory ABC-DLBCL patients responded positively to treatment with ibrutinib showing benefits in PFS and OS¹⁴⁷. In the same study only one patient with GCB-DLBCL responded. Ibrutinib showed a

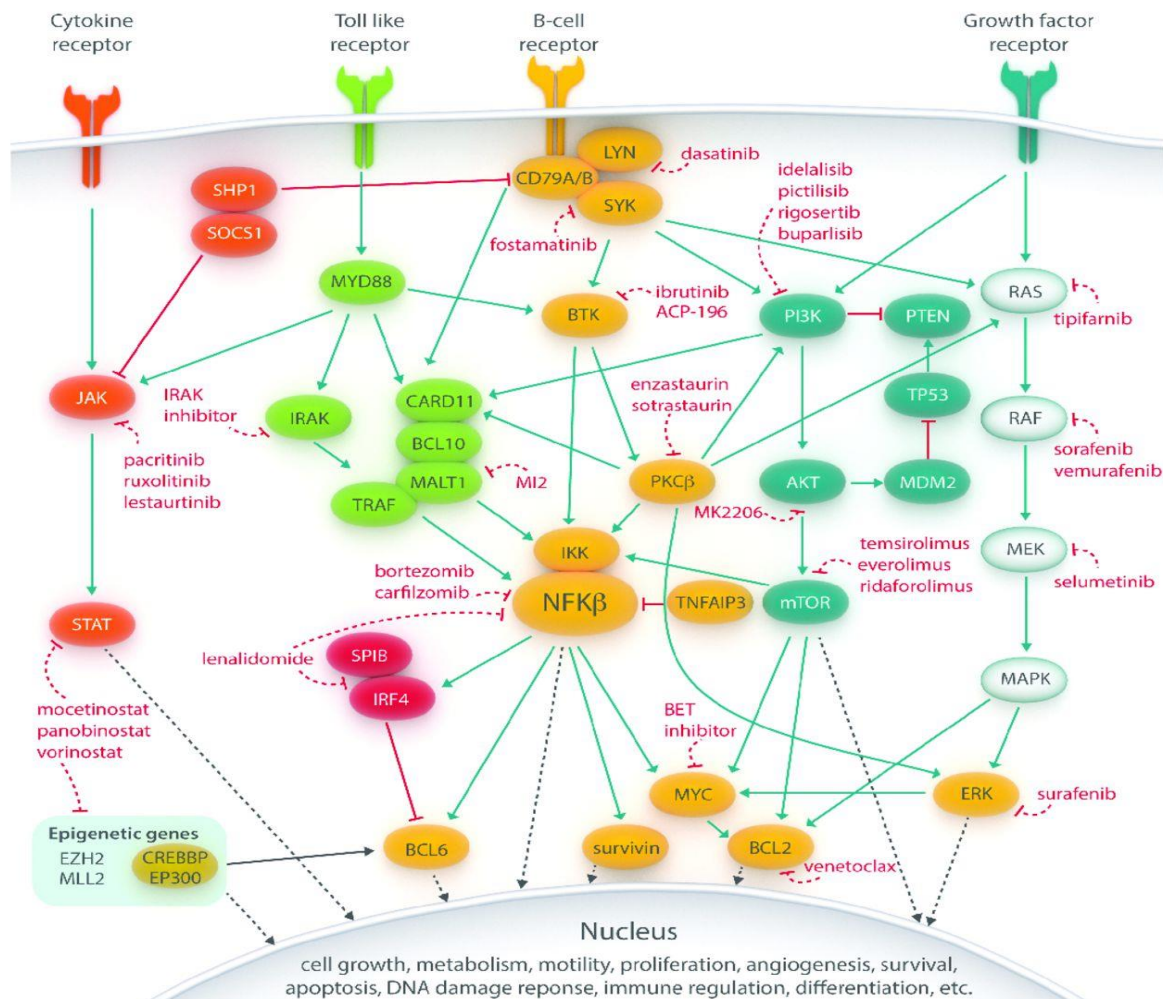


Figure 9. Signaling pathways in DLBCL and compounds that are used for their inhibition. Note that one signaling pathway can be inhibited by multiple agents at different levels, potentially precluding the development of resistance. Adapted from²⁵⁸.

good tolerance and manageable side effects, so further the efficacy of this targeted treatment will be tested in a phase III clinical trial only on ABC-DLBCL patients¹⁴⁷.

In addition to targeted single molecule inhibitors, lenalidomide has shown some good potential in managing relapsed/refractory DLBCL, especially ABC-DLBCL. It is an immunomodulatory drug, which has a direct anti-neoplastic activity. By targeting tumor microenvironment it induces blocking of tumor cell proliferation and angiogenesis as well as stimulation of T-cell- and natural killer cell-mediated immune responses^{148–150}. Lenalidomide

also downregulates the expression of IRF4 leading to increased IFN- β production¹⁴⁶. Different regimens are being tested, ranging from lenalidomide monotherapy to its combination with Rituximab or even complex combinations with multiple chemotherapy agents¹⁵¹. A recent clinical trial reported a 30% response rate to lenalidomide treatment in refractory/resistant DLBCL¹⁵². Another study showed the predominant effect of single lenalidomide therapy against relapsed/refractory ABC-DLBCL. The overall response rate in this subtype was 52.9% as compared to only 8.7% in GCB-DLBCL ($p=0.006$). Despite this, there was no difference in OS between the two subtypes¹⁵³.

To conclude, currently satisfactory treatment results of DLBCL are expected to improve following the entrance of variety of single molecule inhibitors to clinical use. In particular, management of relapsed/refractory DLBCL has to be improved. This can be achieved by identification and efficient simultaneous targeting of multiple cellular pathways (or even several components of the same pathway, to increase efficiency) on which the survival and growth of tumor cells depend.

1.2.4 Prognostic and predictive markers in DLBCL

A key requirement for a successful individualized DLBCL therapy is the availability of prognostic and particularly predictive biomarkers. Such biomarkers should provide reliable information on the likely clinical course of newly diagnosed tumors (prognostic value) as well as identify patients, who would profit the most from available treatments (predictive value).

The international prognostic factor (IPI) is a prognostic factor based on biological and clinical parameters, such as age, stage of disease, level of serum lactate dehydrogenase, performance status and sites of involvement. It was introduced in 1993 and separated DLBCL patients into 4 distinct groups, which had a 5-year OS ranging from 26 to 73%¹⁵⁴. The IPI was revised after introduction of Rituximab to therapy regimens. Although it maintained its prognostic value, the range of outcomes narrowed substantially, and the high-risk patients cannot be identified reliably^{155,156}. Besides IPI other clinical prognostic factors have been proposed. They include tumor size, gender, presence of tumor involvement of the bone marrow, serum level of free chains and others¹⁵⁷⁻¹⁶⁰.

The molecular classification of DLBCL by gene expression profiling also has a prognostic value. The 3-year PFS is lower in ABC-DLBCL compared to GCB-DLBCL (40% vs 75%, $p<0.001$)⁸⁴. However, gene expression profiling of fresh or fresh-frozen tumors by microarrays is not practical in diagnostic setting because it requires fresh or fresh-frozen tumor material, lengthy and time consuming laboratory procedures. Therefore,

immunohistochemical algorithms as well as alternative methods for transcriptional profiling of subset of genes were developed, which allow satisfactory allocation of DLBCL cases to either of molecular subtypes^{82,83}. In addition to its prognostic value, molecular subtyping also provides information about likely genetic alterations that drive tumor formation. This information can be used to target aberrant cellular circuits in a personalized manner.

The presence of concurrent translocations of *C-MYC* and *BCL-2* is one of the strongest negative prognostic markers in DLBCL. Such tumors are termed “double-hit” lymphomas and have an extremely poor outcome with median survival of approximately 8 months when treated with standard R-CHOP therapy¹⁶¹. This suggests that all new patients who are diagnosed with DLBCL containing both of these genetic lesions should be treated with more aggressive alternative regimens¹⁶¹. Although translocations of *BCL-2* and *C-MYC* often lead to protein overexpression, detection by genetic rather than immunohistochemical methods is preferred¹⁶².

Similarly to clinical markers, evaluation of prognostic and predictive biomarkers by immunohistochemistry (IHC) is technologically and economically feasible. Additionally, inherent to this technology is that it measures the amount of protein, which is an end product and a potential determinant of oncogenic effects. This is not the case in, for example, transcriptional profiling. Therefore the use of many IHC-based biomarkers was proposed. Most important ones include such molecules as MUM1p, BCL-2, BCL-6, FOXP1, C-MYC, CD10 and CD5. They can be used either as single markers or in combinations attempting to create a functional prognostic model^{163–166}. However, IHC suffers from relatively poor reproducibility, which is dependent on the use of different procedures, inconsistent cut-offs and subjective scoring. There has been efforts to reduce these drawbacks and to standardize IHC marker evaluation^{167,168}.

The positron emission tomography with computed tomography imaging (PET/CT) is routinely used to locate sites of lymphoma involvement at DLBCL diagnosis. It has also been shown that the presence of identifiable tumor masses at the end of the standard treatment is associated with worse PFS and OS. A consolidation radiotherapy is suggested for such patients to increase chances of sustainable remissions^{169,170}.

Most DLBCL relapses occur within two years after initial diagnosis. Event-free status of minimum 24 months after the initial diagnosis is regarded as one of the strongest predictors of a long term survival. Patients, who do not have a relapse during the next two years following diagnosis have an excellent prognosis with OS similar to that of age- and sex- matched general population¹⁷¹.

Currently no effective predictive markers in DLBCL are available. One potential candidate is

the presence of *MYD88* gene mutations, which predict a poor response to ibrutinib in relapsed/refractory DLBCL. However, it is not yet a standard treatment. Additionally, molecular subtype seems to predict treatment efficacy of bortezomib and ibrutinib as both are more potent against ABC-DLBCL⁸⁶.

1.2.5 Clinical importance and biological background of DLBCL relapses

Current treatment options provide favorable outcomes to large part of DLBCL patients who either enter a long-time clinical remission or are cured. However, ~30% of patients who fail the initial therapy either because of resistance to the treatment (~10%) or due to especially early relapse (~20%) have a dismal prognosis and often succumb to disease^{143,172}. Moreover, the addition of Rituximab to a first-line regimen, yet bringing a high advantage to the long term outcome of all DLBCL patients, resulted in significantly inferior outcomes after secondary treatment¹⁷³. As mentioned earlier, the treatment of choice for such patients are more aggressive chemotherapy regimens and ASCT¹⁷⁴. However, this treatment is associated with risks of lethal infections and severe toxicity. Only ~50% of patients can sustain such an intense approach; others are not eligible due to advanced age or comorbidities.

Besides double rearrangements of *BCL-2* and *MYC* there are no reliable prognostic markers to identify patients with unfavorable outcome¹⁷¹. Even the high-risk category identified by IPI has ~50% chance of cure and provides no rationale for deviating from the standard first line R-CHOP treatment. Therefore, refractory/relapsed DLBCL present a yet unmet challenge in terms of understanding the underlying biological mechanisms, identifying prognostic markers that would identify these patients before starting treatment and, most importantly, developing effective treatments capable of curing more patients.

The majority of recurrences happen during the first 3 years after initial therapy. However, ~10% of patients relapse >5 years after the first diagnosis. It is hypothesized, that resistance/relapse occurs either due to intrinsic tumor heterogeneity or as a consequence of ongoing genomic tumor evolution under the selective pressure of therapy, or both. Initial genetic heterogeneity of the tumor can confer propensity to relapse due to present subclonal population(s), which have a pre-developed resistance to treatment and which can outgrow following extermination of the dominant clone¹⁷⁵. On the other hand, genomic tumor evolution can occur after treatment if the initial clone was not completely eradicated. This evolution can potentially be driven by genetic instability caused by DNA alkylating and intercalating agents present in the chemotherapy regimen (cyclophosphamide and

hydroxydaunorubicine in CHOP) and consolidated by selective pressures exerted by the treatment like immunosuppression/immune escape¹⁷⁶.

The genetic and biological mechanisms of therapy resistance and relapses are just started to be uncovered. Up to date as little as 3 dedicated studies have addressed the genetic background of DLBCL relapses^{175,177,178}. All three studies combined, 66 exomes of relapsed/refractory DLBCL were analyzed, among them there were 7 matched primary-relapse pairs. The remaining samples were either single refractory/relapse cases or matched relapse/normal pairs. Each study reported somewhat different results concerning potential drivers of DLBCL relapse. This can be attributed to relatively small study cohorts, which are far from saturating and comprehensively representing the full spectrum of such a heterogeneous disease like DLBCL. Direct comparison of matched diagnostic and relapse samples provides several advantages: first, it allows studying only genetic alterations that occurred specifically at relapse; second, it allows identification of patient-specific shared somatic mutations, which represent early drivers in tumorigenesis; third, it allows investigating tumor evolution at a genome scale.

Deep-sequencing of *IGH* rearrangements in 14 primary-relapse pairs identified two patterns of tumor evolution: 1) in an early-divergent pattern, *IGH* locus of primary and relapse tumors had the same *V(D)J* rearrangement but significant differences in the SHM profiles; they clustered into two distinct groups indicating that populations bearing those rearrangements separated early and evolved independently; 2) in a late-divergent pattern, *IGH* sequences clustered to the same group as there were minimal differences in the SHM profiles; this suggests that these tumors separated late and didn't acquire many tumor-specific alterations. Similar evolution patterns were also discovered in DLBCL that arose as transformation from a follicular lymphoma^{179,180}.

In search of possible genetic drivers of relapse, several commonly mutated genes and pathways were identified. Jiang et al. suggested that DLBCL relapses might be driven by mutations in immune surveillance genes. Exome-sequencing revealed relapse-specific alterations in either *CD58* or *B2M* or both in 5 out of 7 investigated pairs¹⁷⁵. Another study reported *B2M* and *CD58* mutations enriched in relapses of PMBCL-DLBCL and ABC-DLBCL, respectively¹⁷⁷.

Alterations in the JAK-STAT pathway components were also reported. *STAT6* bore mutations of D419 residue in ~40% of relapsed/refractory DLBCL. Mutational status correlated well with the expression of phosphorylated *STAT6* levels in affected tumors, indicating, that these lesions were activating¹⁷⁸. Additionally, inactivating mutations in *SOCS1*, a negative regulator

of JAK-STAT pathway, were also frequently detected, predominantly in PMBCL subtype of DLBCL¹⁷⁷.

Alterations in *NFKBIE* and *NFKBIZ* have not previously been reported in the context of *de novo* DLBCL pathogenesis. These two genes encode IκBε and IκBζ, respectively - two inhibitors of NF-κB pathway. They were mutated at a combined frequency of 18% within the studied relapsed/refractory DLBCL cohort¹⁷⁸. Given the important role of NF-κB pathway in lymphomagenesis, it is likely that these mutations could provide an alternative NF-κB activation mechanism for tumor cells¹⁸¹.

In some cases relapse-specific alterations could be detected at a very low frequency in diagnostic DLBCL biopsies, suggesting the presence of minor therapy-resistant clone in the primary tumor. Selection at relapse was observed by increased allelic frequency of the mutation. However, these findings were not confirmed by all reports so remains controversial. Other frequently reported genes in these studies included *TP53*, *KMT2D*, *PIM*, *MLL3*, *EZH2*, *FOXO1*, *MYD88*, *CCND3*, *FAS*, *FOXP1*, *GNA13*, *CARD11* and others. However, due to inherent limitations (lack of paired primary-relapse samples), the relapse-specific nature of these mutations is uncertain, especially given the fact that many of them are known to be related with the molecular pathogenesis of *de novo* DLBCL.

1.2.6 Clonal relationship in relapsing lymphomas

Second and subsequent occurrences of lymphoid neoplasms in the same patient after a period of complete remission are traditionally regarded as clonally-related outgrowths of the primary tumor. Since an acquired tumor resistance is expected, more aggressive second line treatment strategies are applied in such instances. However, the concept of clonally-related relapses has been challenged by multiple studies, showing that a significant percentage of secondary occurrences represent a second clonally unrelated neoplasm.

In the biggest published study on DLBCL clonality so far, 13 pairs of DLBCL relapsing 4 years or later after initial diagnosis were investigated. Authors reported 3 cases (23%) in which clonal relationship could not be confirmed. However, the methodology employed did not allow unambiguous demonstration of lack of clonal relationship either¹⁸². In a smaller study all 5 (100%) DLBCL relapses, which localized to the central nervous system, were found to be unrelated to the initial tumors (4 DLBCL, 1 mantle cell lymphoma)¹⁸³. The most recent report found 2(20%) clonally-unrelated relapses within the paired cohort of 10 DLBCL cases¹⁸⁴.

Lack of clonal relationship has also been associated with morphological transformations of more indolent lymphoid neoplasms. For example ~22% of DLBCL relapses emerging as Richter's transformations had distinct *IGH* rearrangements^{185,186}. Also, approximately 20% of classical Hodgkin lymphoma relapses represent *de novo* lymphoid neoplasms¹⁸⁷.

The occurrence of a second clonally-unrelated lymphoid neoplasm suggests the existence of risk factors, which can predispose patients to acquire a second tumor the same diagnostic category. These can include inborn genetic properties, viral infections, immune suppression and exogenous exposure to mutagens¹⁸⁸. Additionally, it has recently been discovered that somatic mutations of tumor suppressors and oncogenes with high allelic frequencies and even with high clonal load are present in the hematopoietic systems of otherwise healthy mid-aged and elderly patients¹⁸⁹. While implications of this phenomenon are not yet clear, it is possible that such mutations can predispose multiple and recurrent but clonally independent tumor formation in individuals who carry them.

Clonally-unrelated relapses also have clinical implications: as they effectively are *de novo* neoplasms, high-dose second line therapies might not be the most suitable option for such patients. Instead, the use of a conventional first line therapies could be justified but this has to be evaluated by specifically designed prospective clinical trials¹⁸⁸.

Techniques for clonality testing

Since B-cell lymphomas originate from different stages of developing B-cells, as clonal outgrowths of lymphocytes, they have a physiologically occurring clonality marker in the form of uniquely rearranged *IG* genes. Indeed, this feature has been exploited in research as well as in clinical setting, where confirmation of clonal lymphoid proliferation is sometimes an important component of a conclusive clinical diagnosis⁷². Thus, many different strategies were detected to assay genetic rearrangements between primary and subsequent occurrences. They include early analysis by Southern blotting, PCR-based techniques of locus amplification and fragment length comparison as well as recently introduced scanning of rearrangement spectrum by high-throughput sequence analysis¹⁹⁰.

The multiplex PCR approach that was introduced almost two decades ago remains the golden standard for clonality testing. By this technique standardized sets of consensus PCR primers are used to amplify different regions of the *IGH* and *IGL* loci. Then lengths of the generated amplicons are investigated by a preferred method (usually based on capillary electrophoresis). The assumption is that that clonally-related cases will have the same *V(D)J* rearrangements and thus identical fragment lengths, while in clonally-unrelated cases these lengths will be

different. In ambiguous cases, generated amplicons can be analyzed by sequencing the amplicons directly or after cloning and selection of individual plasmids. The multiplex PCR method is still preferred because of its high sensitivity, specificity, ability to analyze DNA from fresh- as well as formalin-fixed tissue DNA samples and relatively low price.

Next generation sequencing (NGS) techniques have recently been successfully applied also for clonality testing^{191–193}. Additional to advantages offered by the massive parallel sequencing approach and depending on the target enrichment techniques used, NGS can provide sequence information not only of a major clone, but also many secondary clones, including those, which represent healthy B-cell populations. This allows observing frequency dynamics of distinct subpopulations between multiple, particularly timely-separated samples. The NGS approach is also more sensitive, making it useful for minimal residual disease monitoring¹⁹⁴. Although it is currently not yet widespread, it is likely that within next 5 years its use will dramatically increase.

Clonal relationship between two different tumors can also be determined by studying other tumor-specific somatic events. For example, the presence of the same translocation with identical breakpoints can be used as an evidence for clonal relationship. However, tumors often acquire recurrent genetic alterations that affect same targets therefore the reliability of clonal relationship estimation depends on the number of different genetic loci interrogated. Genome-wide techniques such as array comparative genomic hybridization (aCGH) and whole exome or genome sequencing are suitable for this purpose^{195–198}. Due to lack of other clonality markers the latter two techniques are most frequently used in demonstrating clonal relationships between two distinct solid tumors or a primary solid tumor and its (probable) metastasis. In lymphomas, aCGH and NGS was mostly used to determine clonal relationships between synchronous composite tumors and connection between primary indolent and aggressive transformed disease^{199,200}.

2. AIMS

2.1 To test the existence of clonally-unrelated recurrences and to investigate the genetic evolution of relapses in DLBCL

Despite multiple demonstrations of clonally-unrelated relapses in lymphoid neoplasms, second DLBCL occurrence in the same patient is still generally regarded as a direct outgrowth of the primary tumor. As shown in other entities, clonal relationship or lack of it might have a prognostic value as well as a clinical importance. Therefore we aimed to test the existence of clonally-unrelated DLBCL relapses by investigating chromosomal copy number aberrations and nucleotide-level somatic alterations in paired primary and relapse DLBCL samples.

The availability of paired samples also allowed tracking of tumor genetic progression. Recent findings in carcinomas as well as in other lymphoid neoplasms, such as follicular and mantle cell lymphoma, suggested branching mode of evolution in some cases. We wanted to extend these findings to DLBCL and test whether similar relapse patterns are characteristic to this heterogeneous lymphoid neoplasm.

2.2 To identify recurrently occurring genetic alterations associated with relapsing as well as non-relapsing DLBCL

Despite relatively successful first line R-CHOP treatment, 30-40% of DLBCL patients relapse or are refractory to initial therapy. Such patients have limited treatment options and generally unfavorable outcomes. Currently, the understanding of the molecular basis of DLBCL relapse is scarce. Only a few studies on paired primary-relapse/refractory DLBCL samples attempted to pinpoint the potential molecular drivers of the process. We therefore aimed to identify recurrent genetic lesions that happen at the transition between primary and relapse hoping to identify genetic culprits of recurrences. Furthermore, we included a cohort of primary non-relapsing DLBCL and contrasted their genetic profiles to these of relapsing DLBCL in order to identify potential markers, which would be useful in predicting at diagnosis whether tumor has or hasn't the propensity to relapse.

2.3 To develop and to apply a technique for rare cell nuclei enrichment from archival formalin-fixed paraffin-embedded (FFPE) tissues by flow sorting and to enable comprehensive genetic analysis on the enriched sorted populations

Prerequisite for the precise use of most of the genome-assaying techniques is that cells-of-interest would constitute a significant part of the investigated sample. However, the biology of certain human malignancies, such as classical Hodgkin lymphoma, T-cell/histiocyte rich B-cell lymphoma and others does not fulfill this criterion. Additionally, such diseases are often rare. This means that samples are very limited and are often present only in a form of FFPE tissue blocks left-over after a diagnostic histological processing.

Throughout the duration of my PhD studies I have been developing protocols that would allow efficient marker-based enrichment of FFPE tissue-derived nuclei by fluorescence-associated cell sorting (FACS) technique. In this work I present two papers where this technique was practically applied. The first study investigated copy number aberrations in LANA1-of-HHV8-enriched nuclei from two cases of primary effusion lymphoma. In the second study, MUM1-positive plasma cells were sorted to investigate genomic complexity of early post-transplant lymphoproliferative disorders.

3. RESULTS

3.1 Distinct genetic evolution patterns of relapsing diffuse large B-cell lymphoma revealed by genome wide copy number aberration and targeted sequencing analysis.

Juskevicius D., Lorber T., Gsponer J., Perrina V., Ruiz C., Dirnhofer S., Tzankov A.

-Research article-
Currently under revision in *Leukemia*, 2016

Contribution: I performed the experiments, analyzed the data and wrote the manuscript

Abstract

Recurrences of diffuse large B-cell lymphomas (DLBCL) result in significant morbidity and mortality, but their underlying genetic and biological mechanisms are unclear. Clonal relationship so far is mostly addressed by the investigation of immunoglobulin (*IG*) rearrangements, therefore lacking deeper insights into genome-wide lymphoma evolution. We studied mutations and copy number aberrations in 20 paired relapsing and 11 non-relapsing DLBCL samples to test the clonal relationship between primaries and relapses, to track tumors' genetic evolution and to investigate the genetic background of DLBCL relapses. Three clonally-unrelated DLBCL recurrences were identified (15%), in which tumors showed no shared genetic characteristics. Also, two different patterns of genetic evolution were detected: (1) early-divergent/branching evolution from a common progenitor in 6 patients (30%), and (2) late-divergent/linear progression of relapses in 11 patients (65%). Analysis of recurrent genetic events identified early drivers of lymphomagenesis (*KMT2D*, *MYD88*, *CD78B* and *PIM1*). The most frequent relapse-specific events were additional mutations in *KMT2D* and *MEF2B*. Comparison of alterations between non-relapsing and relapsing DLBCL identified recurrent group-specific genetic events. Non-relapsing DLBCL had recurrent deletions of *CYP7B1* and mutations of *SOCS1* and *RELN*. Recurrent gains of 10p15.3-p13 in relapsing lymphomas containing *PRKCQ* and *GATA3* were associated with a potential to relapse.

Introduction

Diffuse large B-cell lymphoma (DLBCL) is the most common lymphoid neoplasm worldwide. While the majority of patients can be cured by existing therapeutic regimens, still about 30-40% relapse or are refractory to standard treatment. A DLBCL relapse is defined as appearance of new lesions after achieving complete remission for at least three months, and is linked to significantly increased morbidity and mortality¹. Standard treatment of such patients consists of high-dose chemotherapy with autologous stem cell transplantation (HDT-ASCT)², and the 3-year overall survival is only about 50%³.

Relapses of lymphoid neoplasms, even after long-lasting clinical remission, are generally regarded as direct outgrowths of the primary tumor⁴⁻⁶, although rare clonally-unrelated relapses have been documented⁷⁻¹⁰. Such unrelated recurrences point to an increased general risk for patients developing a second *de novo* neoplasm of the same diagnostic category, and raises the question of potential predisposition factors in these types of relapses. Clinically, the choice of the most effective treatment is complicated in such instances, i.e. HDT-ASCT or a standard primary regimen^{4,7}.

The gold standard for determination of a clonal relationship is analysis of immunoglobulin (*IG*) *V(D)J* gene rearrangement, which is unique for mature B-cells and is stably transferred to daughter cells during the process of clonal expansion¹¹. Clonal relationship can also be determined at the genomic level by genome-wide approaches such as array-comparative genomic hybridization (aCGH) and deep sequencing¹²⁻¹⁴.

Despite being a major cause of morbidity and mortality in DLBCL, genetic mechanisms of DLBCL relapse remain poorly characterized due to the paucity of sequential paired primary-relapse samples. The potential of paired sample analyses to identify key genetic events in tumor evolution are evident from a study of DLBCL pairs by deep exome and *IGH* sequencing as well as studies addressing transformation of follicular lymphoma (FL) to DLBCL. These studies have shown recurrent alterations of *REL*, *MYC*, *PIMI1*, *CDKN2A* and *B2M*, suggesting a functional importance^{12,15-18}.

In this study, we performed comprehensive characterization of 20 paired relapsing- and 11 non-relapsing DLBCL samples and demonstrated clonally-unrelated relapses at the genomic level as well as two distinct genetic evolution patterns in clonally-related DLBCL relapses. Finally, we observed recurrent shared mutations suggesting early drivers of lymphomagenesis and recurrent group-specific genetic aberrations in non-relapsing and relapsing primary DLBCL, which might be linked to recurrences and treatment susceptibility, respectively.

Materials and Methods

See supplementary information for the description of additional materials and methods.

Samples

Lymphoma samples were from the archive of the Institute of Pathology at the University Hospital Basel, Switzerland. In the relapsing cohort primary and relapse materials of patients diagnosed with DLBCL recurrences (n=20 pairs) after periods of complete remission were included. The non-relapsing cohort (n=11) consisted of well-preserved diagnostic biopsies of patients who had a single occurrence of DLBCL and were relapse-free for at least 7 years. Formalin-fixed, paraffin-embedded (FFPE) and fresh frozen (FF) (if available) tissues were used (see Table S1). A previously reported historic DLBCL cohort of over 250 cases brought into tissue microarrays was used to evaluate GATA3 overexpression¹⁹. Retrieval of tissue and data were performed according to regulations of the local institutional review boards and data safety laws. The study was approved by the Ethics Committee of North-Western and Central Switzerland (EKNZ 2014-252).

aCGH data analysis

aCGH data were assessed with a series of QC metrics and subsequently analyzed using Agilent Genomic Workbench v.7.0 software with the aberration detection algorithm ADM2²⁰. Using derivative log₂ spread ratio as the primary quality assessment criterion and manual inspection, microarrays were separated into multiple subgroups for which different ADM2 threshold values were applied. Subsequently, cumulative probe-based aberration frequency data was exported for each sample set (primaries of relapsing DLBCL, relapses, primaries of non-relapsing DLBCL) and further processed by a custom workflow programmed in R (<http://www.r-project.org/>).

Variant calling and filtering

Library construction and sequencing was successful in 19 of 20 (95%) relapsing DLBCL pairs and 11 (100%) non-relapsing DLBCL samples. Mutation identification was performed by the Variant caller plug-in IonTorrent software suite v4.4 using low stringency parameters, listed in Table S2. Variants were annotated with IonReporter software using Variant annotation workflow v4.4. Depth of coverage, coverage uniformity and number of variants called are summarized in Table S1. At the initial quality filtering, variants with Phred-based quality score <50, strand bias >0.75, and number of variant-supporting reads <10 were discarded from the analysis. Depending on the analysis application, different filtering workflows were used at the final variant filtering stage as depicted in Figure S1. Only exonic non-synonymous mutations were considered for the identification of recurrent mutations, while synonymous and non-exonic variants were additionally included for tumor evolution analysis. Pairs in which sequencing quality was low in one or both samples due to poor coverage uniformity (<70%) or exceptionally large mutation numbers (more than two standard deviations) were excluded from the evolutionary analysis and used only for identification of shared recurrent mutations.

Evolutionary analysis

Lack of relationship was established when paired samples contained distinct *IG* chain rearrangements and/or no common chromosomal aberrations with identical breakpoints in all 22 autosomes and the X chromosome. Clonal relationship was established when paired samples contained the same *IG* rearrangement and at least one chromosomal aberration with an identical breakpoint. The presence of shared mutations was not considered evidence of clonal relationship due to the lack of appropriate germline controls, but mutations were used for evolutionary distance estimation. Tumor evolution via a common progenitor was assumed in clonally-related cases when at least one homozygous or heterozygous deletion with a unique breakpoint was detected in the primary tumor, but was not present in the paired relapse sample. Evolutionary distance from a common progenitor was calculated using the adapted Jaccard's formula for distance calculation between asymmetric binary attributes: $d = \frac{q}{p+q}$; here, q is the count of unique genetic alterations in primary or relapse tumor, and p is the count of shared genetic alterations²¹. The distance (d) can result in values between 0 and 1. In this application, $d = 0$ implies that there are no private alterations (no progression from the common progenitor), while $d = 1$ implies the lack of shared genetic events between tumors, and thus maximal distance.

Statistical analysis

Descriptive statistics were used to characterize samples in both cohorts. Two-tailed Fisher's exact test, Chi-square and Mann-Whitney U tests were utilized where appropriate to determine distribution differences between groups and to calculate the statistical significance of the differential recurrent aberrations between groups of samples. The Kaplan-Meier method was used to evaluate overall survival of DLBCL patients grouped by GATA3 expression. All statistical calculations were performed with MS Excel 2013, SPSS 22 or R statistical package. Statistical significance threshold of $p < 0.05$ was assumed in all analyses.

Results

Relapsing DLBCL show more advanced tumor stages and stronger BCL2 expression

Available clinical and pathological characteristics of the patient cohorts are summarized in Table 1, Figure 1 and Figure S2. Therapy information was retrieved for 27 of 31 patients. First line therapy with curative intent was administered in all but one patient and consisted of CHOP (n=1) or R-CHOP (n=25) with (n=4) or without irradiation (n=23). Depending on the risk factors, intrathecal chemotherapy was administered in 9 patients (4 who relapsed and 5 who did not). Median age at initial diagnosis was 66.5 years for the relapsing DLBCL cohort and 74 years for the non-relapsing cohort ($p>0.05$); the former cohort presented with more advanced disease stages ($p=0.029$).

Of the classifiable samples (n=18) in the relapsing DLBCL cohort, 12 primary tumors were of non-germinal center B cell-like (non-GCB) and 6 of GCB origin (Figure 1 and Table S3). In the non-relapsing DLBCL cohort, 10 of 11 cases could be classified, 5 of GCB origin and 5 non-GCB (see supplementary results for information on cell of origin changes at relapse and Figure S2).

Primaries of relapsing DLBCL expressed higher levels of BCL2 than non-relapsing (median positivity $80\% \pm 29$ vs $35\% \pm 29$, $p=0.027$). When positivity was evaluated by applying the cut-off value of $70\%^{22}$, this difference remained significant (positive 14/19 vs 2/10, $p=0.008$). No significant differences in expression of C-MYC, BCL6 or MIB1 were observed between the cohorts (Table S3).

Clonally-unrelated DLBCL relapses

Analysis of genetic data within the individual pairs of primary and relapsed DLBCL identified clonally-unrelated recurrences and two different evolution patterns among clonally-related DLBCL relapses (Figure 1). Interestingly, intra-tumoral heterogeneity was evident in multiple instances both at the primary and relapse stages (Figure S3).

Clonally-unrelated relapses were detected in 3 patients (cases 1, 15 and 17). Primary and relapse tumors in these pairs showed no shared chromosomal aberrations. Even when certain chromosomal loci were aberrant in both samples, breakpoint regions never matched (Figure 2A). Targeted sequencing revealed no shared single nucleotide mutations in cases 1 and 17, but 2 shared single nucleotide variants in *EP300* and *CD79A* in sample 15. As expected, from the evolutionary point of view, clonally-unrelated tumors showed maximal dissimilarity as there were no or very few genetic events in common between primary lymphoma and relapse (Figure 3A). Lack of clonal relationship in cases 1 and 15 was additionally confirmed by fragment size and sequence analysis of the rearranged *IG* genes (Figure 2B and Figure S4). However, attempts to amplify *IG* rearrangement regions in sample 17 were unsuccessful, likely due to heterozygous deletions of the *IGH* locus in both primary and relapse tumors and the deletion of the *IGK* locus in the primary tumor. Compared to other relapses (see later), clonally-unrelated relapses tend to occur latest after initial lymphoma presentation. Times to relapse were 103, 32 and 81 months (median 81 months) in cases 1, 15 and 17, respectively.

Two patterns of clonally-related DLBCL relapse

The first genetic pattern within the group of clonally-related relapses, *early-divergent/branching evolution from a common progenitor*, was detected in 6 cases. In addition to shared aberrations with identical breakpoints between primary and relapse, primary tumors had CNA, most importantly homozygous and heterozygous deletions, which were not present in the subsequent relapse samples (Figure 2C). Taking into account mutations detected by targeted NGS, most (5/6) of the primary tumors characterized by this pattern showed larger genetic distances from the putative common progenitor than that seen in the relapses (Figure 3B and Figure S5A), suggesting that the divergence of primary and relapse tumor clones occurred early. This is also supported by the longer median time to relapse, in this cohort 54 months (range 18-141 months), compared to relapses with late-divergent evolution (see later). Clonal relationships in all 6 cases were confirmed by detection of identical *IGH* rearrangements and presence of shared single nucleotide mutations (median 5, range 1-23).

The second and the most frequent relapse pattern (detected in 11 cases), *late-divergent/linear evolution with or without progression*, most closely reflects the current concept of DLBCL recurrence. In cases characterized by this pattern, primary tumors had no private CNA compared to relapses (Figure 2D), yet a limited degree of divergence was evidenced by small numbers of private single nucleotide mutations in primary tumors. Nevertheless, these private mutations yielded only a minimal genetic distance from the putative common progenitor population, which was, in all cases, smaller than the genetic distance from the common progenitor to relapse (Figure 3C and Figure S5B). At relapse, the majority of cases (9/11) showed increased numbers of genetic alterations despite the fact that the median time to relapse was shortest in this group (17 months, range 8-53 months).

Recurrent genetic alterations in relapsing and non-relapsing DLBCL

The most frequent CNA in primaries of both relapsing and non-relapsing DLBCL were heterozygous deletions of chromosome 6q (affecting *PRDMI*) in 16 of 31 (52%) cases as well as gains of large parts of chromosome 7 and 18, 10/31 (32%) and 12/31 (39%) cases, respectively. The most frequently mutated gene overall was *KMT2D*, which harbored mutations in 10/16 (63%) of clonally-related relapsing DLBCL and 5/11 (46%) of non-relapsing DLBCL cases. Mutations were scattered across many exons of this gene without hotspot. Other frequently-mutated genes included *CD79B*, *BTG1* and *PIMI* (Figure 4 and Table S4).

Losses of 6q22.31-q22.33 and gains of chromosome 7 were the most frequent CNA occurring early in the progenitor cell population before divergence. Mutations of *KMT2D* (7/16), *CD79B* (5/16), *MYD88* (4/16) and *PIMI* (4/16) were shared in clonally-related tumor pairs, suggesting that they occurred early and were drivers of lymphomagenesis. Of note, mutations in the latter three genes were restricted to DLBCL of non-GCB cell of origin and were concurrent in 3 tumors.

Most of the tumors acquired multiple chromosomal gains and losses at relapse, but no recurrent CNA could be identified. Mutations in *KMT2D* were the most frequent relapse-specific sequence

alteration, occurring in 7 of 16 (44%) evaluated relapses. The second most frequently mutated gene at relapse was *MEF2B*, affecting 3 of 16 cases (19%).

Comparison of CNA between primaries of relapsing DLBCL and non-relapsing DLBCL identified several differentially aberrant regions (Figure 5 and Table 2). Predominantly, DNA copy gains emerged that were more frequently observed in non-relapsing DLBCL, the most significant of which were amplifications in the short arm of chromosome 2, spanning and continuing downstream of the lymphoma oncogene *C-REL*. Other gains affected parts of chromosomes 6, 9, 13, 14, 19 and 22, and were also more prevalent in the non-relapsing DLBCL cohort. These alterations affected a total of 553 protein-coding genes, 14 of which were included in the COSMIC cancer gene census list.

The only recurrent CNA characteristic to primaries of relapsing DLBCL was a gain in 10p15.3-p13, which contained more than 70 protein-coding genes including GATA binding protein 3 (*GATA3*) and protein kinase C-theta (*PRKCQ*). To test the prognostic significance of *GATA3* overexpression in DLBCL 23 of the study cases with sufficient material and a well-characterized historic DLBCL microarray of 250 evaluable cases was immunohistochemically examined (see Supplementary results and Figure S6 and S7). A reliable anti-*PRKCQ* antibody for immunohistochemistry is currently not available.

The only recurrent differential copy number loss between relapsing and non-relapsing DLBCL primaries was a heterozygous deletion of 8q12.3, affecting cytochrome 7 beta polypeptide 1 gene (*CYP7B1*), which was found exclusively in the non-relapsing group. At the nucleotide level, two genes, *RELN* and *SOCS1*, were found to be mutated in 3 of 11 non-relapsing DLBCL cases, but were not affected in any of the relapsing DLBCL ($p=0.052$).

Discussion

First presentations and subsequent recurrences of lymphomas are generally regarded as direct outgrowths of the primary tumor clone^{4,6}. However, cases of clonally-unrelated relapses have been documented in indolent and aggressive lymphoma transformations^{5,23}, as well as in Hodgkin and composite lymphomas^{9,24,25}. Reports on unrelated relapses of DLBCL are scarce. One study found two equivocally unrelated recurrences within a group of 13 late-relapsing DLBCL⁴, and another reported five late central nervous system relapses of DLBCL unrelated to the respective primaries²⁶. These studies relied on multiplex PCR-based determination of clonal relationship, a technique that, while robust in addressing clonal relationship, is based on the analysis of a single or a few genetic loci, providing no insight into the underlying genetic composition of the respective diseases. Array-CGH microarrays have been previously used to establish relationship between multiple lesions or primaries and metastases in solid tumors^{13,27,28}. Here, we demonstrate that this approach can also be successfully applied to analysis of paired lymphoma samples. PCR-based clonality analysis combined with genome-wide copy number arrays and targeted massive parallel sequencing unequivocally proved the existence of clonally-unrelated DLBCL recurrences and exposed the profound genetic composition differences between primary and relapse tumors. Moreover, our approach advantageously clarified clonal relationship in instances where *V(D)J* rearrangements could not be amplified or interpreted, as in our case 17.

In agreement with other reports, clonally unrelated relapses in our study occurred after relatively long intervals from the initial DLBCL diagnosis, thus being considered late (32 months) or very late (81, 103 months). The reasons for a second “*de novo*” appearance of DLBCL in the same patient are unclear, but could be related to continuous exogenous hazards, genetic predisposition, treatment-induced DNA damage, acquired mutations in the (hemato-)lymphopoietic stem cell pool or prolonged immunosuppression. The presence of clonal somatic mutations at low frequency in non-malignant hematopoietic cells is a recently described phenomenon²⁹. One of the clonally-unrelated cases in our cohort (case 15) showed the presence of two mutations, an inactivating nonsense mutation in *EP300* and a missense mutation in *CD79A*, in both primary and relapse tumors, which were otherwise genetically distinct with different *IGH* rearrangement and EBV status (EBV+ primary, EBV- relapse). Thus, it is possible that these two mutations were inherent to a putative B-lymphopoietic progenitor cell pool and increased the chance of this patient developing a second lymphoid malignancy. Additionally, the patient’s clinical history of immunosuppression due to solid organ transplantation suggests a second risk factor, i.e. immunosuppression. Lack of clonal relationship (i.e. second *de novo* DLBCL and not a progress of the initial DLBCL) may have played a role in the remarkably successful treatment of the relapse tumor with lenalidomide monotherapy, after which the patient achieved lasting clinical remission³⁰. Also notable in this context is the clinical history of patient 17, diagnosed with primary testicular DLBCL followed 81 months later by an unrelated DLBCL of the central nervous system. Interestingly, both lymphomas occurred at immuno-privileged sites, supporting possible underlying immune deregulatory mechanisms or immunogenetic defects as unifying risk factors. Importantly, clonally-unrelated DLBCL recurrences in the same patient and demonstration of their different genetic constitutions raise a question of immediate clinical impact, i.e. whether adjusted treatment regimens could be applied. Theoretically, standard first-line treatments might be efficient for such patients, thus abrogating the adverse side effects of high-dose myeloablative chemotherapy with the need of ASCT. However, given the rarity of unrelated relapses and the significant therapeutic consequences therefrom, this subject requires assessment on a selected, large-scale cohort of clinical samples.

The existence of two different patterns of clonally-related DLBCL relapses in our study resonates well with other findings from genomic studies on paired transformed FL and relapsing DLBCL cohorts. Pasqualucci et al. reported divergent evolution from a common progenitor as the more frequent mode, occurring in 10 cases, while linear progression was detected in only 2 instances¹⁷. Okosun et al. found that all transformed FL evolved from either rich (n=8) or sparse (n=2) ancestral common progenitor clones¹⁸. Likewise, by sequencing rearranged *V(D)J* junctions of paired primary and relapse DLBCL samples, Jiang et al. identified early- and late-divergent patterns of clonal evolution¹². All three studies observed shared mutations between clonal populations of primaries and recurrences, indicating a common clonal origin, whereas other mutations were unique for each manifestation. This is analogous to our identification of shared chromosomal aberrations with identical breakpoints and unique CNA in primary tumors that were not detectable in the subsequent relapse samples in the 6 divergent/branching evolution pairs. The 11 pairs that appeared to follow a more linear evolution path by CNA analysis, but had low number of single nucleotide mutations, are reminiscent of the “rich common progenitor” or “late-divergent categories” described in the latter two studies. These relapse patterns are

characterized by evolutionary late separation of subclones from a common progenitor and, therefore, bear minor genetic distances between the respective manifestations.

We hypothesized that genetic factors are present in the primary DLBCL tumors that determine whether the tumor will or will not recur. To test this hypothesis, we compared CNA and mutational data between primary relapsing and primary non-relapsing DLBCL cohorts and identified genetic events that occurred more frequently in one or the other group. Surprisingly, the majority of recurrent genomic aberrations were detected in the non-relapsing cohort. Differentially amplified regions in this group contained oncogenes (*FLT3*, *PDGFB*, *MKL1*) as well as tumor suppressors (*RBI*, *BRCA2*, *STK11*, *EP300*). The precise significance of these genes in the context of successful treatment response needs additional investigation. The only recurrent differentially-deleted region was 8q12.3 in non-relapsing lymphomas; it contained a single gene, *CYP7B1*, which encodes a multi-functional protein of cytochrome P450 family that primarily acts as steroid hydroxylase and is directly implicated in bile acid synthesis³¹ and steroid metabolism³². Its genetic defects are linked to severe liver insufficiency in newborns and adult neuropathies³³. Interestingly, prednisone, a steroid drug and a component of the CHOP regimen, has been suggested as a metabolic substrate of *CYP7B1*^{34,35}. Moreover, vincristine and doxorubicin, two other components of CHOP, are known to be catabolized and thus inactivated by the P450 complex. Taken together, loss of *CYP7B1* might increase sensitivity to CHOP and partially explain why this recurrent chromosomal deletion is present in the non-relapsing DLBCL group.

In our study, *SOCS1* mutations were exclusive to the non-relapsing cases. It has been shown that truncating mutations in tumor-suppressor *SOCS1* are prognostic for a favorable DLBCL outcome³⁶. Indeed, 2 of 3 affected cases had nonsense mutations truncating the *SOCS1* protein, and the third case had missense mutation in the kinase inhibitory domain (KIR), which is required for binding Janus kinases and suppressing their activity. We did not find any known associations between *RELN* mutations and decreased propensity to relapse.

Paired DLBCL exome sequencing study reported that mutations within histone modifiers are potential driver mutations in DLBCL¹², a finding we partially confirm by identification of *KMT2D* as the most commonly mutated gene in both primary and relapse tumors in our cohort. Additionally, our data indicate that the *MYD88* L265P mutation, the *CD79B* Y197C mutation and *PIMI* mutations are early events in DLBCL genetic evolution that are shared in clonally-related tumor pairs, suggesting they played a driver role in lymphomagenesis.

Numerous studies already addressed the negative prognostic value of *BCL2* expression in DLBCL²² [and references therein]. The significant differences in *BCL2* expression between primaries of relapsing and non-relapsing DLBCL observed in our cohort corroborate these observations, reappraising the negative prognostic importance of *BCL2* in DLBCL.

In conclusion, genome-wide CNA profiling and targeted sequence analysis of paired primary and relapse DLBCL samples reliably demonstrates, for the first time, the existence of clonally-unrelated DLBCL recurrences at the genomic level. Further, our results show that genetic evolution of DLBCL at relapse occurs through early or late divergence from a common progenitor clone. Finally, we demonstrate differentially aberrant regions between primary

relapsing and non-relapsing DLBCL containing genes that are potentially involved in sensitivity to treatment as well as propensity to relapse potential.

Acknowledgements

The study was supported by Krebsliga beider Basel and Stiftung zur Krebsbekämpfung Zürich.

Authorship contributions

D.J. performed the research, analyzed and interpreted data and wrote the manuscript; J.G., C.R. and T.L. analyzed data and revised the manuscript; V.P. contributed to sequencing analysis; S.D. performed histological and immunohistochemical analysis, revised the manuscript; A.T. conceived and designed the study, performed histological and immunohistochemical analysis, analyzed and interpreted data, revised the manuscript.

Disclosure of Conflicts of Interest

There are no relevant conflicts of interest to disclose.

Data depositing

The chromosomal copy number aberration data reported in this paper has been deposited at the National Center for Biotechnology Information Gene Expression Omnibus (accession no. GSE65720). The targeted sequencing data has been deposited to Sequence Read Archive (SRA) accession no. (pending).

References

- 1 Friedberg JW. Relapsed/Refractory Diffuse Large B-Cell Lymphoma. *ASH Educ Progr B* 2011; **2011**: 498–505.
- 2 Philip T, Guglielmi C, Hagenbeek A, Somers R, Van der Lelie H, Bron D, *et al.* Autologous bone marrow transplantation as compared with salvage chemotherapy in relapses of chemotherapy-sensitive non-Hodgkin's lymphoma. *N Engl J Med* 1995; **333**: 1540–5.
- 3 Gisselbrecht C, Glass B, Mounier N, Singh Gill D, Linch DC, Trneny M, *et al.* Salvage regimens with autologous transplantation for relapsed large B-cell lymphoma in the rituximab era. *J Clin Oncol* 2010; **28**: 4184–90.
- 4 de Jong D, Glas AM, Boerrigter L, Hermus M-C, Dalesio O, Willemse E, *et al.* Very late relapse in diffuse large B-cell lymphoma represents clonally related disease and is marked by germinal center cell features. *Blood* 2003; **102**: 324–7.
- 5 Geurts-Giele WRR, Wolvers-Tettero ILM, Dinjens WNM, Lam KH, Langerak AW. Successive B-Cell Lymphomas Mostly Reflect Recurrences Rather Than Unrelated Primary Lymphomas. *Am J Clin Pathol* 2013; **140**: 114–26.
- 6 Shioyama Y, Nakamura K, Kunitake N, Kimura M, Terashima H, Masuda K. Relapsed non-Hodgkin's lymphoma: detection and treatment. *Radiat Med* 2000; **18**: 369–75.
- 7 Libra M, De Re V, Gloghini A, Navolanic PM, Carbone A, Boiocchi M. Second primary lymphoma or recurrence: a dilemma solved by VDJ rearrangement analysis. *Leuk Lymphoma* 2004; **45**: 1539–43.
- 8 Nishiuchi R, Yoshino T, Teramoto N, Sakuma I, Hayashi K, Nakamura S, *et al.* Clonal analysis by polymerase chain reaction of B-cell lymphoma with late relapse: a report of five cases. *Cancer* 1996; **77**: 757–62.
- 9 Obermann EC, Mueller N, Ruffle A, Menter T, Mueller-Garamvoelgyi E, Cathomas G, *et al.* Clonal relationship of classical hodgkin lymphoma and its recurrences. *Clin Cancer Res* 2011; **17**: 5268–74.
- 10 Siddiqi IN, Ailawadhi S, Huang Q, Shibata RK, Kang H, Shibata D. Deep sequencing reveals lack of a clonal relationship between a metachronous classical hodgkin and diffuse large B-cell lymphoma. *Clin Lymphoma Myeloma Leuk* 2014; **14**: e87–93.
- 11 Cobb RM, Oestreich KJ, Osipovich OA, Oltz EM. Accessibility control of V(D)J recombination. *Adv Immunol* 2006; **91**: 45–109.
- 12 Jiang Y, Redmond D, Nie K, Eng KW, Clozel T, Martin P, *et al.* Deep-sequencing reveals clonal evolution patterns and mutation events associated with relapse in B-cell lymphomas. *Genome Biol* 2014; **15**: 432.
- 13 Torres L, Ribeiro FR, Pandis N, Andersen JA, Heim S, Teixeira MR. Intratumor genomic heterogeneity in breast cancer with clonal divergence between primary carcinomas and lymph node metastases. *Breast Cancer Res Treat* 2007; **102**: 143–55.
- 14 Ostrovnaya I, Olshen AB, Seshan VE, Orlow I, Albertson DG, Begg CB. A metastasis or a second independent cancer? Evaluating the clonal origin of tumors using array copy number data. *Stat Med* 2010; **29**: 1608–21.
- 15 Davies AJ, Rosenwald A, Wright G, Lee A, Last KW, Weisenburger DD, *et al.* Transformation of follicular lymphoma to diffuse large B-cell lymphoma proceeds by distinct oncogenic mechanisms. *Br J Haematol* 2007; **136**: 286–93.
- 16 Kwiecinska A, Ichimura K, Berglund M, Dinets A, Sulaiman L, Collins VP, *et al.* Amplification of 2p as a genomic marker for transformation in lymphoma. *Genes Chromosomes Cancer* 2014; **53**: 750–68.
- 17 Pasqualucci L, Khiabani H, Fangazio M, Vasishtha M, Messina M, Holmes AB, *et al.* Genetics of follicular lymphoma transformation. *Cell Rep* 2014; **6**: 130–40.
- 18 Okosun J, Bödör C, Wang J, Araf S, Yang C-Y, Pan C, *et al.* Integrated genomic analysis identifies recurrent mutations and evolution patterns driving the initiation and progression of follicular lymphoma. *Nat Genet* 2014; **46**: 176–81.
- 19 Nagel S, Hirschmann P, Dirnhofer S, Günthert U, Tzankov A. Coexpression of CD44 variant isoforms and receptor for hyaluronic acid-mediated motility (RHAMM, CD168) is an International Prognostic Index and C-MYC gene status-independent predictor of poor outcome in diffuse large B-cell lymphomas. *Exp Hematol* 2010; **38**: 38–45.
- 20 Lipson D, Aumann Y, Ben-Dor A, Linial N, Yakhini Z. Efficient calculation of interval scores for DNA copy number data analysis. *J Comput Biol* 2006; **13**: 215–28.
- 21 Finch H. Comparison of Distance Measures in Cluster Analysis with Dichotomous Data. *J Data Sci* 2005; **3**: 85–100.
- 22 Visco C, Tzankov A, Xu-Monette ZY, Miranda RN, Tai YC, Li Y, *et al.* Patients with diffuse large B-cell lymphoma of germinal center origin with BCL2 translocations have poor outcome, irrespective of MYC status: a report from an International DLBCL rituximab-CHOP Consortium Program Study. *Haematologica* 2013; **98**: 255–63.
- 23 Mao Z, Quintanilla-Martinez L, Raffeld M, Richter M, Krugmann J, Burek C, *et al.* IgVH mutational status

- and clonality analysis of Richter's transformation: diffuse large B-cell lymphoma and Hodgkin lymphoma in association with B-cell chronic lymphocytic leukemia (B-CLL) represent 2 different pathways of disease evolution. *Am J Surg Pathol* 2007; **31**: 1605–14.
- 24 Ganzel C, Pogrebjisky G, Krichevsky S, Neuman T, Yehuda D Ben. Separate diagnoses of Hodgkin lymphoma and non-Hodgkin lymphoma in an individual patient might not signify a common clonal origin. *Exp Hematol* 2012; **40**. doi:10.1016/j.exphem.2012.05.009.
- 25 Libra M, De Re V, Gasparotto D, Gloghini A, Marzotto A, Milan I, *et al.* Differentiation between non-Hodgkin's lymphoma recurrence and second primary lymphoma by VDJ rearrangement analysis. *Br J Haematol* 2002; **118**: 809–12.
- 26 Lossos A, Ashhab Y, Sverdlin E, Amir G, Ben-Yehuda D, Siegal T. Late-delayed cerebral involvement in systemic non-hodgkin lymphoma: A second primary tumor or a tardy recurrence? *Cancer* 2004; **101**: 1843–9.
- 27 Wa C V, DeVries S, Chen YY, Waldman FM, Hwang ES. Clinical application of array-based comparative genomic hybridization to define the relationship between multiple synchronous tumors. *Mod Pathol* 2005; **18**: 591–7.
- 28 Waldman FM, DeVries S, Chew KL, Moore DH, Kerlikowske K, Ljung BM. Chromosomal alterations in ductal carcinomas in situ and their in situ recurrences. *J Natl Cancer Inst* 2000; **92**: 313–20.
- 29 Steensma DP, Bejar R, Jaiswal S, Lindsley RC, Sekeres MA, Hasserjian RP, *et al.* Clonal hematopoiesis of indeterminate potential and its distinction from myelodysplastic syndromes. *Blood* 2015; **126**: 9–16.
- 30 Läubli H, Tzankov A, Juskevicius D, Degen L, Rochlitz C, Stenner-Liewen F. Lenalidomide monotherapy leads to a complete remission in refractory B-cell post-transplant lymphoproliferative disorder. *Leuk Lymphoma* 2015; : 1–11.
- 31 Rose KA, Stapleton G, Dott K, Kieny MP, Best R, Schwarz M, *et al.* Cyp7b, a novel brain cytochrome P450, catalyzes the synthesis of neurosteroids 7alpha-hydroxy dehydroepiandrosterone and 7alpha-hydroxy pregnenolone. *Proc Natl Acad Sci U S A* 1997; **94**: 4925–30.
- 32 Kim S-B, Chalbot S, Pompon D, Jo D-H, Morfin R. The human cytochrome P4507B1: catalytic activity studies. *J Steroid Biochem Mol Biol* 2004; **92**: 383–9.
- 33 Tsaousidou MK, Ouahchi K, Warner TT, Yang Y, Simpson MA, Laing NG, *et al.* Sequence alterations within CYP7B1 implicate defective cholesterol homeostasis in motor-neuron degeneration. *Am J Hum Genet* 2008; **82**: 510–5.
- 34 Nation RL, Evans AM, Milne RW. Pharmacokinetic drug interactions with phenytoin (Part I). *Clin Pharmacokinet* 1990; **18**: 37–60.
- 35 Jeng S, Chanchairujira T, Jusko W, Steiner R. Prednisone metabolism in recipients of kidney or liver transplants and in lung recipients receiving ketoconazole. *Transplantation* 2003; **75**: 792–5.
- 36 Schif B, Lennerz JK, Kohler CW, Kreuz M, Bentink S, Melzner I, *et al.* SOCS1 Mutation Subtypes Predict Divergent Outcomes in Diffuse Large B-Cell Lymphoma (DLBCL) Patients. *Oncotarget*. 2012; **4**: 35–47.

Figures

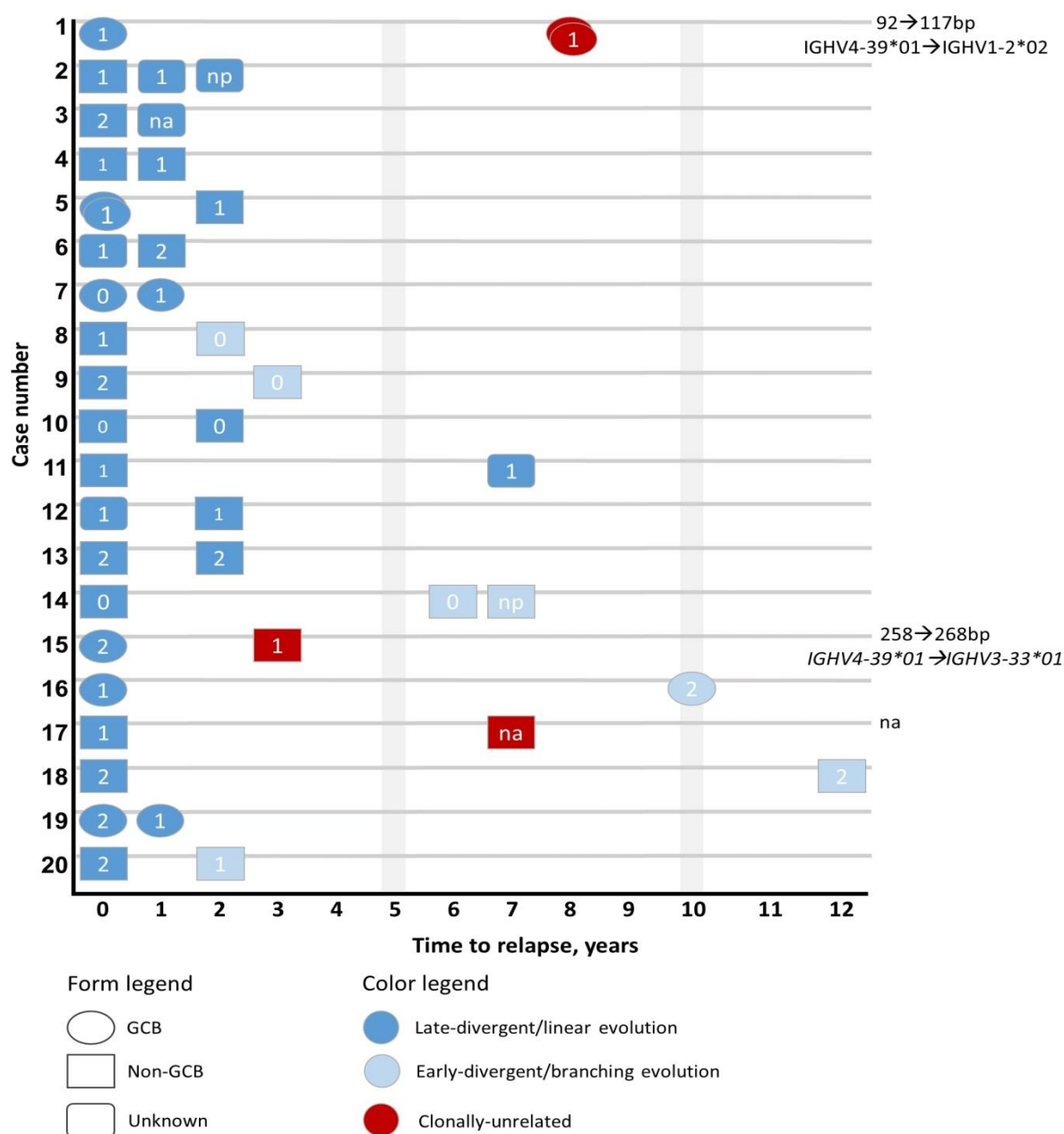


Figure 1

Figure 1. Disease history overview of the relapsing DLBCL cohort. Cell of origin is represented by symbol shape and clonal relationship by color. Numbers centering the symbols represent respective C-MYC and BCL2 co-expression double-hit scores. Stacked symbols (cases 1 and 5) represent two parts of the same tumor profiled by aCGH where intratumoral heterogeneity was detected (see Figure S3). At the right side, sizes of the amplified IGH rearrangement products are indicated for clonally unrelated cases. Abbreviations: na – not accessed; np – not processed.

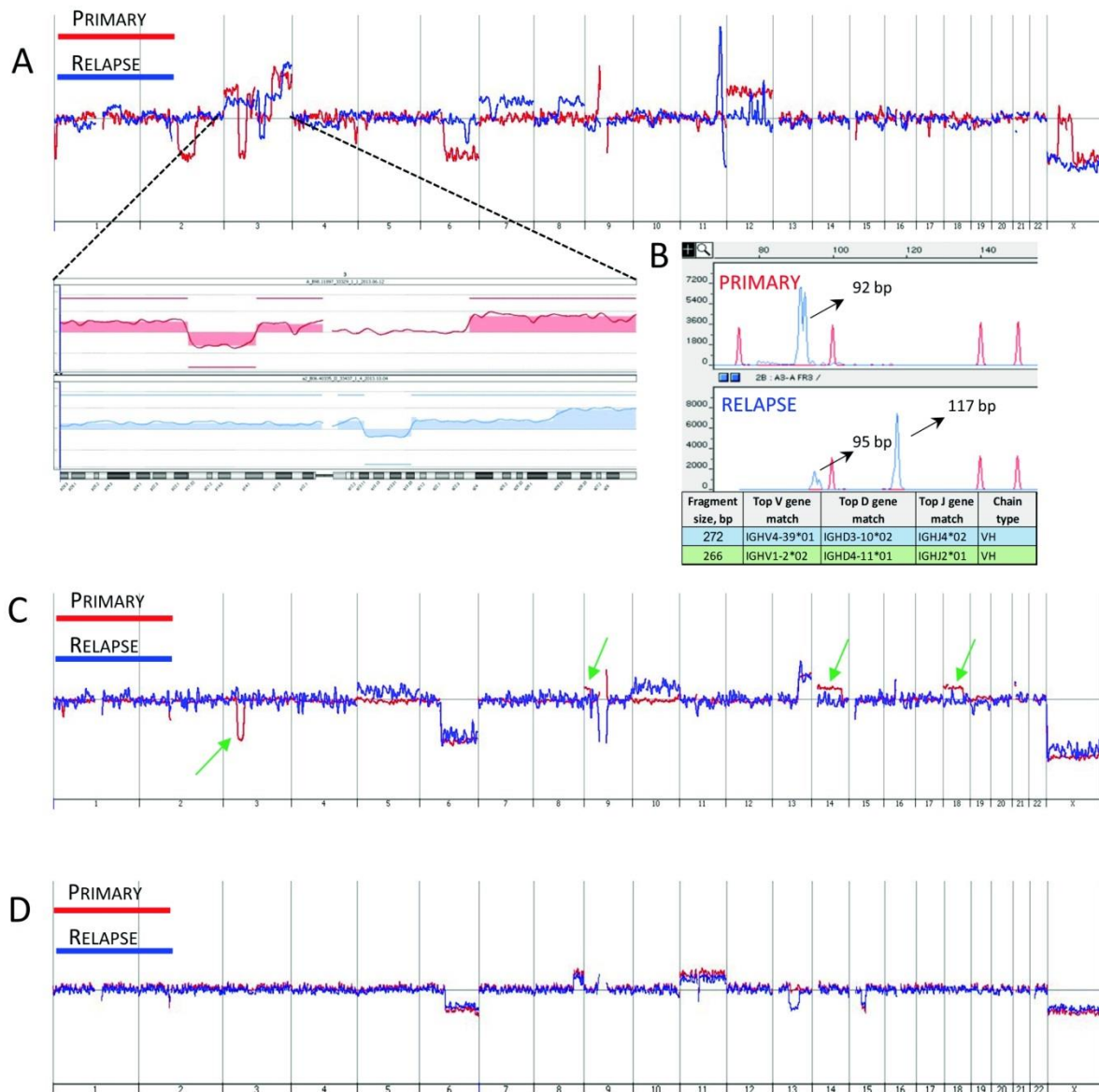


Figure 2. Different modes of DLBCL relapse. **A.** A genome-overview plot of a clonally unrelated pair (case 1) is shown. Genome position is represented on the abscissa and the \log_2 ratio on the ordinate. Moving average of the primary (red) and the relapse (blue) is plotted. Regions above and below the \log_2 ratio value of 0 represent gain or loss of DNA, respectively. None of the aberrations match between primary and relapse tumors. For example, chromosome 3 is highly aberrant (magnified, color tint represent the start and end of the aberrant region) in both cases, but breakpoints of gains and losses do not match. **B.** Amplified FR3 and FR2 region of *IGH V(D)J* rearrangements show distinct sizes between both DLBCL occurrences and FR2 sequences align to different families of *IG* variable genes. **C.** An example of a clonally-related DLBCL pair (case 8), in which primary and relapse tumors emerged through early-divergent/branching evolution from a common progenitor cell clone. Both tumors share some chromosomal aberrations (chromosomes 6, 13, 21) confirming their shared origin, but aberrations unique to the primary tumor (green arrows) suggest separation and independent evolution of the tumor-initiating clones. **D.** An example of a clonally-related DLBCL pair (case 4) in which the relapse emerged through late-divergent/linear evolution from the common progenitor population tumor but gained some additional chromosomal aberrations. * -not called by the CNA detection algorithm.

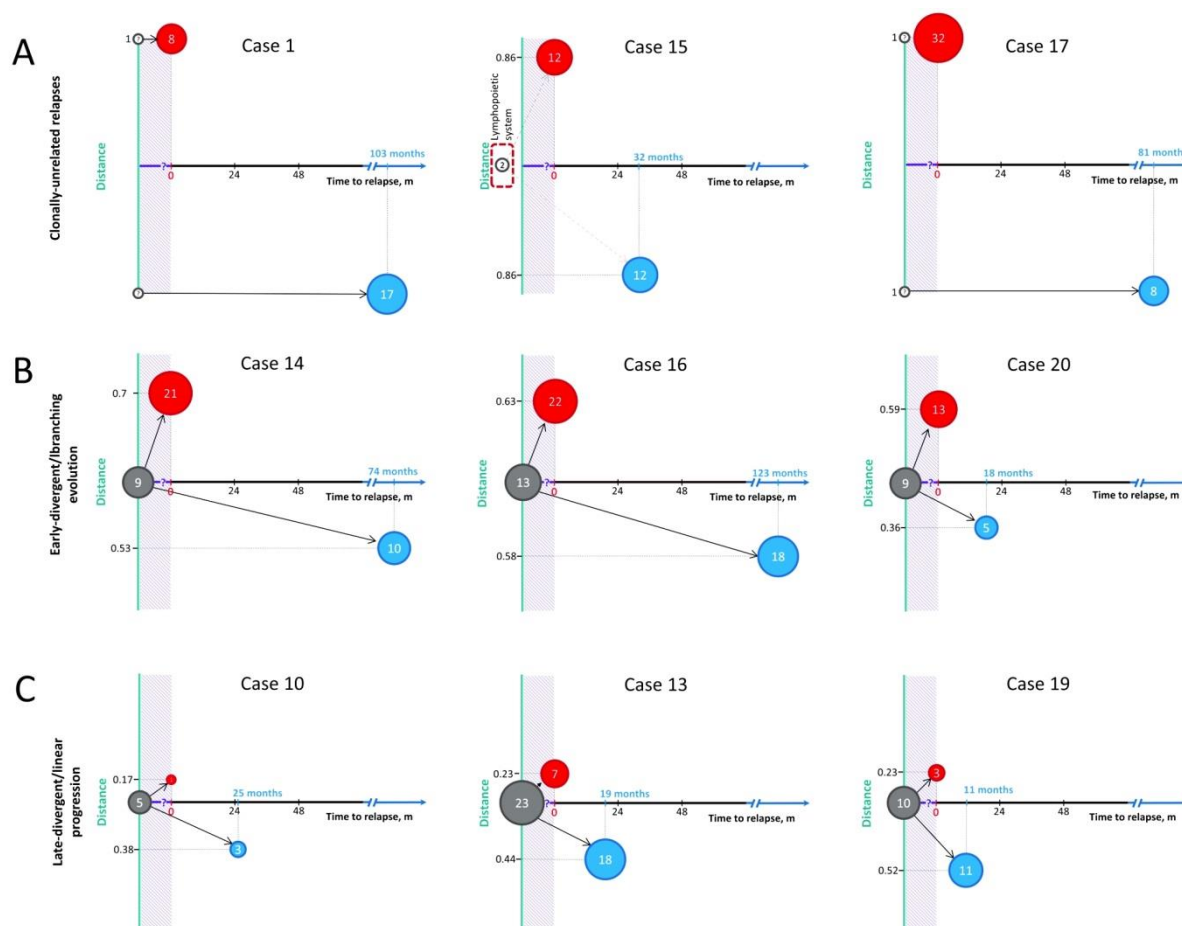


Figure 3. Genetic evolution patterns in relapsing DLBCL. **A.** Schematic representation of clonally-unrelated DNA relapses showing few or lack of unifying genetic alterations and a maximal genetic distance from one another. **B.** Primary tumors belonging to the early-divergent/branching pattern of DLBCL recurrence have high numbers of private genetic alterations and, therefore, large genetic distance from the putative common progenitor. In these cases relapses are genetically less distant to the common progenitor than primaries. **C.** In the late-divergent evolutionary pattern, primary tumors are genetically very close to the putative common progenitor, while relapses show higher divergence.

Numbers inside circles represent a combined count of mutations and copy number aberrations in the respective population. Circle sizes are scaled according to the number of genetic alterations. Dashed purple area symbolizes the time from putative divergence of populations to occurrence of primary lymphoma, which is unknown. Red – genetic alterations unique to primary tumor. Blue – genetic alterations unique to relapse. Grey circle – putative common progenitor. The genetic distance from the common progenitor is plotted on the y axis; at the top of the x axis for the primary tumor, at the bottom for the relapse.

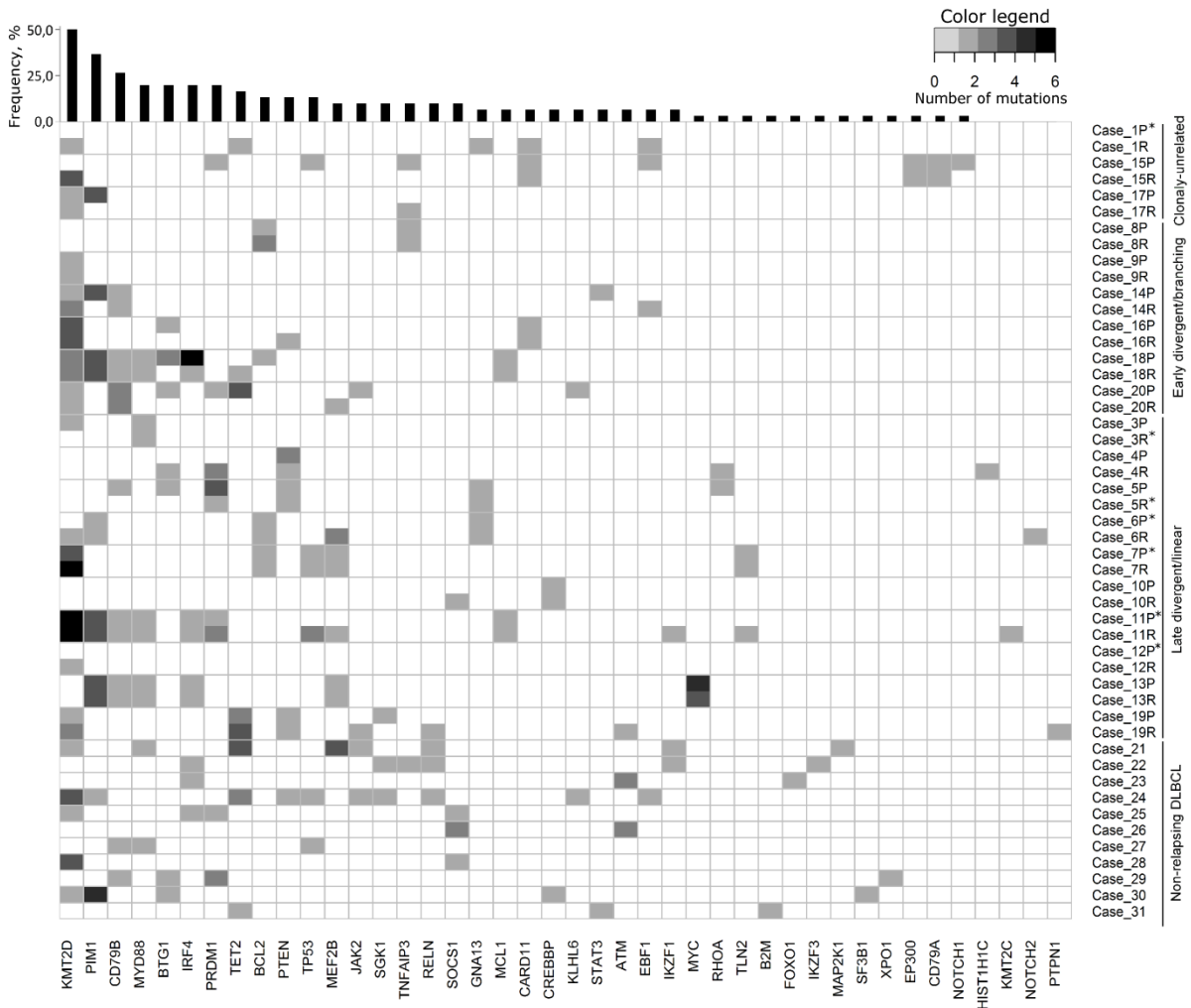


Figure 4. Non-synonymous variants in studied DLBCL cases

A heatmap plot of all non-synonymous variants that were detected by targeted NGS. Genes are ordered left-to-right according to the decreasing number of mutations observed. * – samples in relapsing DLBCL cohort, which were evaluated only for shared mutations due to sub-optimal sequencing quality.

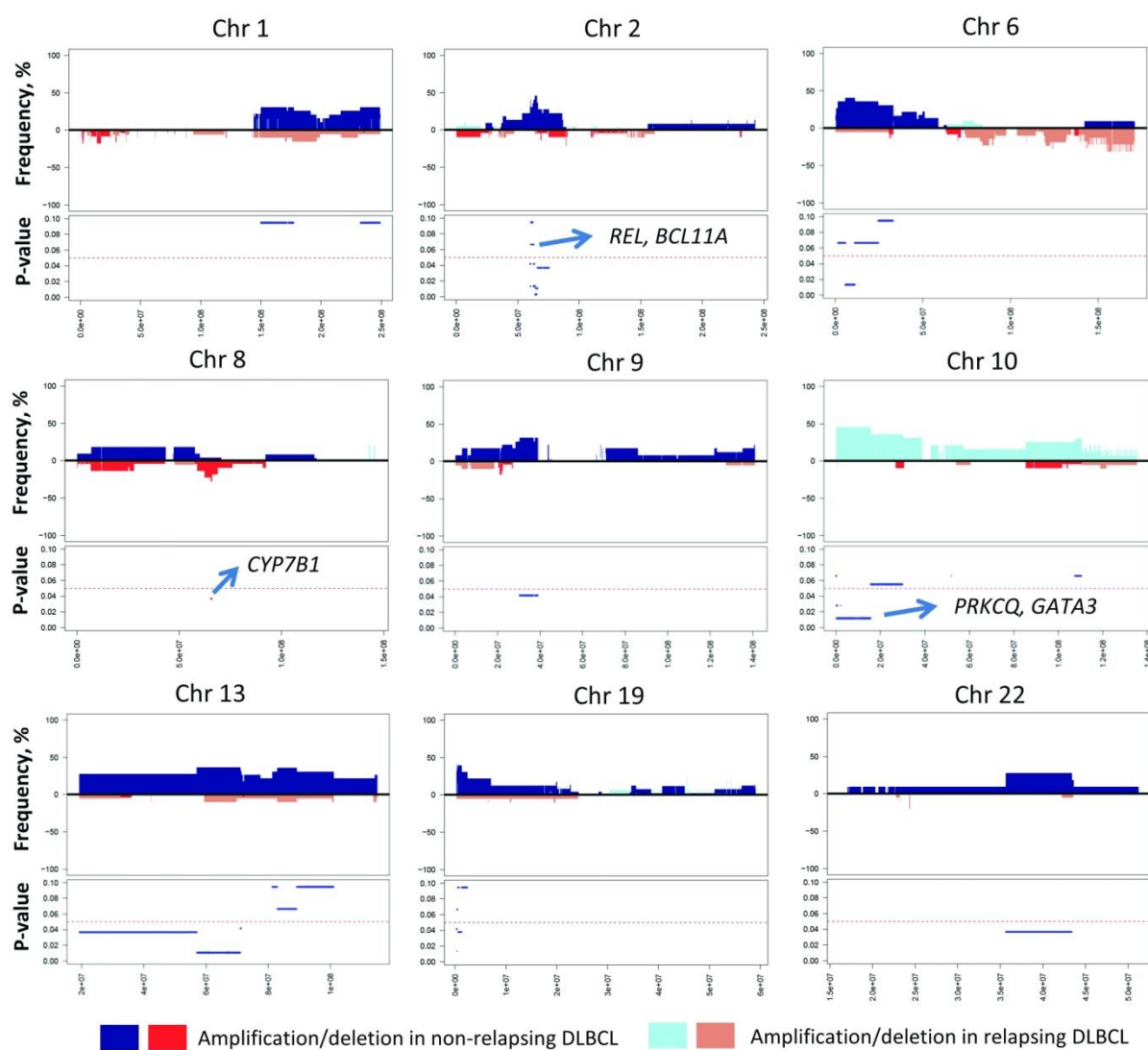


Figure 5. Differential comparison of chromosomal copy number aberrations between primary relapsing (n=20) and non-relapsing (n=11) DLBCL. The upper part of each graph plots the frequency of aberrations (%; amplification in positive, deletion in negative scale) against the chromosomal position (base pairs). In the bottom panel, p-values are plotted. Dark colors represent aberrations more frequently detected in the non-relapsing set of DLBCL, while light colors represent aberrations characteristic of the relapsing set of DLBCL. Genes affected in regions with p-value < 0.1 are listed in Table S5.

Table 1. Clinical characteristics of the study cohorts

Nr	Gender	Age, y	Stage	Primary location	Follow-up, m	Therapy	Time to relapse, m	Relapse location	Dead
Relapsing cohort									
1	F	71	NA	Bronchus	104	NA	103	Soft tissue	1
2	M	62	NA	Lymph node	27	6x R-CHOP	11	Lymph node	1
3	M	72	IIIA	Lymph node	12	6x R-CHOP	9	Stomach	1
4	M	80	IVA	Lymph node	19	6x R-CHOP	8	Lymph node	1
5	M	61	IVA	Lymph node	27	6x R-CHOP+2x R-mono, ITH, irradiation	26	Duodenum	1
6	F	81	IIA	Lymph node	6	6x R-CHOP, irradiation	10	Lymph node	NA
7	F	74	IIB	Upper abdomen	41	Palliative 5x R+gemcitabine	17	Muscle	1
8	M	37	IIA	Soft tissue upper arm	32	6x CHOP, irradiation	19	Bone	NA
9	M	49	IIIA	Lymph node	51	6x R-CHOP	33	Brain	1
10	F	77	IVB	Lymph node	25	6x R-CHOP, ITH	25	Lymph node	NA
11	M	75	IVB	Lymph node	124	8x CHOP, ITH	53	Chest wall	1
12	F	29	IIIB	Lymph node	116	8x R-CHOP	18	Lymph node	0
13	F	56	IV	Lymph node	74	6x R-CHOP, ITH	19	Lymph node	NA
14	M	71	IIA	Lymph node	84	6x R-CHOP	74	Lymph node	0
15	F	42	NA	Lymph node	39	6x R-CHOP+2x R-mono	32	Small intestine	0
16	M	50	NA	Lymph node	126	NA	123	Soft tissue	0
17	M	42	IIA	Testicle	147	8x R-CHOP, ITH	81	Brain	0
18	M	71	NA	Eye ball	141	NA	141	Lymph node	0
19	F	90	NA	Lymph node	11	NA	11	Omentum	0
20	F	31	IIA	Lymph node	19	6x R-CHOP	18	Lymph node	0
Non-relapsing cohort									
21	F	64	IVB	Colon	119	8x R-CHOP, ITH	NA	NA	0
22	F	83	IVB	Lymph node	67	6x R-CHOP	NA	NA	0
23	M	74	IIIA	Lymph node	116	6x R-CHOP	NA	NA	0
24	M	84	IIIA	Intranasal	51	6x 80% R-CHOP, ITH	NA	NA	0
25	M	83	IA	Tounge	78	6x R-CHOP	NA	NA	0
26	M	65	IV	Lymph node	115	8x R-CHOP, ITH	NA	NA	0
27	M	36	IIA	Maxillary sinus	118	6x R-CHOP, ITH	NA	NA	0
28	F	57	IA	Vaginal mucosa	99	6x R-CHOP	NA	NA	0
29	M	53	IA	Lymph node	107	6x R-CHOP	NA	NA	0
30	M	84	IA	Lymph node	71	3x R-CHOP, irradiation	NA	NA	0
31	M	84	IA	Lymph node	78	6x 80% R-CHOP	NA	NA	0

Abbreviations: 1-dead; 0-alive; CHOP-cyclophosphamide, hydroxydaunorubicin, oncovin, prednisone; F-female; ITH-intrathecal chemotherapy; M-male; m-months; NA-not available; R-Rituximab; y-years.

Table 2. Differentially aberrant chromosomal regions between relapsing and non-relapsing DLBCL

Chromosome	Start	Stop	Cytoband	p-value	Cancer census gene*	CNA in relapsing DLBCL	CNA in non-relapsing DLBCL
Non-relapsing DLBCL							
Amplifications						0/20	5/11
chr2	64050753	65340372	p14-15	0.0027		0/20	4/11
chr2	64119395	66009092	p14	0.0105		0/20	4/11
chr13	57093042	71055517	q21.1-21.33	0.0105		0/20	4/11
chr14	19376761	20397731	p11.2	0.0105		0/20	4/11
chr2	62790398	64031168	p15	0.0132		1/20	5/11
chr6	5793643	11076650	p25.1-24.2	0.0132		1/20	5/11
chr2	65994717	75189618	p14-12	0.0367	<i>DCTN1</i>	0/20	3/11
chr13	19752698	57073684	q11.2-21.1	0.0367	<i>BRCA2, LHFP, CDX2, LCP1, RB1, FLT3</i>	0/20	3/11
chr22	35653033	43386781	q12.3-13.2	0.0367	<i>MKL1, PDGFB, MYH9, EP300</i>	0/20	3/11
chr19	578539	1272710	p13.3	0.0377	<i>STK11</i>	3/20	6/11
chr2	59987586	63605603	p15	0.0416		1/20	4/11
chr9	30321407	39058117	p21.1-13.1	0.0416	<i>FANCG</i>	1/20	4/11
chr13	71081217	71324117	q21.33	0.0416		1/20	4/11
chr19	275924	335170	p13.3	0.0416		1/20	4/11
Deletions							
chr8	65579491	66023718	q12.3	0.03671		0/20	3/11
Relapsing DLBCL							
Amplifications							
chr10	269756	838046	p15.3-13	0.0116	<i>GATA3</i>	9/20	0/11

*<http://cancer.sanger.ac.uk/cancergenome/projects/cosmic/> accessed in September, 2015

Supplementary information

Supplementary methods

Immunohistochemistry

Immunohistochemistry (IHC) was performed on serial tissue sections using an automated immunostainer Benchmark XT (Ventana/Roche, Tucson, AZ, USA) with a biotin-streptavidin-peroxidase detection system according to manufacturer's protocols. All primary antibody clones, incubation- and antigen retrieval conditions as well as cut-off values used to determine tissue positivity are summarized in Table S6. Cell of origin (COO) classification was done according to the so-called Tally algorithm¹.

Assessment of *IGH* rearrangements

A PCR-based assay for *IG V(D)J* rearrangements was performed with consensus FR2 and FR3 as well as J primers, as previously published². Examination of the PCR products was carried out with the high resolution fragment length analyzer ABI 310 (Applied Biosystems, Foster City, CA, USA). Rearrangements were evaluated primarily by interpretation of the fragment lengths of products amplified with the FR3 primers. If this result was inconclusive, Biomed-2 primers targeting the FR2 region and/or *kappa light chain*-gene rearrangements were used (Invivoscribe Technologies, San Diego, CA, USA). Clonal rearrangements were defined as prominent, single-sized amplification products within the expected size range. Fragments suggesting clonally-unrelated recurrences were cloned into pGEM-T (Promega, Madison, WI, USA) plasmids and Sanger-sequenced to unequivocally confirm different clonal origin. Sequences were analyzed with the IgBLAST tool³.

DNA extraction

H&E- and CD20-stained sections of FFPE blocks or FF tissues were reviewed by A.T. to evaluate tumor content. Only tissues with >70% tumor content were used. Depending on the distribution of tumor cells, 25µm-thick sections were cut or punches were taken from the tumor-rich tissue areas. Prior to overnight Proteinase K digestion, paraffin sections were deparaffinized and rehydrated by serial xylene and ethanol washes, respectively. Genomic DNA (gDNA) was extracted by automation using Maxwell® 16 FFPE plus LEV DNA Purification Kit (Promega, Madison, WI, USA). gDNA from samples with extremely scarce tumor material was isolated by the phenol-chloroform extraction as described previously⁴. Yields were quantified by the Qubit assay (Life Technologies, Eugene, OR, USA).

Array-CGH

At least 100ng of gDNA from each sample and 500ng of commercial 46 XX reference gDNA (Promega, Southampton, UK) were used. Reference gDNA was heat-fragmented at 95°C for 35 minutes. FFPE tissue-derived gDNA needed no additional digestion. Sample DNA extracted from FF tissues was heat-fragmented to 400-600 bp in average. DNA fragmentation was evaluated by gel electrophoresis and subsequent image analysis with the ImageJ software (<http://imagej.nih.gov/ij/index.html>, version 1.48). Samples and references were labeled with Cy-5 dUTP and Cy-3 dUTP, respectively, using the BioPrime aCGH genomic labeling system (Invitrogen, Carlsbad, CA, USA). Success of labelling was evaluated by the Nanodrop assay (Thermo Fischer Scientific, Waltham, MA, USA) before mixing and hybridization to 180k CGH arrays (Agilent Technologies, Santa Clara, CA, USA) for 24 hours in a rotating oven at 65°C. All microarray slides were scanned with an Agilent 2565C DNA scanner and the images were processed with Agilent Feature Extraction 10.7 using default settings.

Targeted NGS

Target enrichment panel was designed to include genes and their hotspots that are most frequently mutated B-cell lymphoid neoplasms according to the COSMIC database (release v70) and manual overview of the literature. 68 genes were included (Table S7). The designed panel comprised of 933 amplicons in 4 primer pools (234 amplicons/pool in average). Mean primer length was 110bp (range 64-137bp) making it suitable to amplify targets in the fragmented archival FFPE tissue-derived gDNA. Target amplification, library construction and sequencing were carried out according to recommendations of the manufacturer (Thermo Fisher Scientific, Carlsbad, CA, USA). Shortly, 10ng of FF or 15ng of FFPE DNA quantified by Qubit was used for target amplification in each primer pool. 17 and 20 PCR cycles were used for FF and FFPE DNA, respectively. Then amplicons from pools 1-3 and pools 2-4 were combined, primer sequences were digested and barcoded adaptors were ligated. Bead enrichment and chip loading was performed with an automated IonChef instrument. Libraries of 4 samples were combined and sequenced in one IonTorrent 318v2 chip with IonPGM sequencer.

Supplementary results

Retention and change of cell of origin (COO) in DLBCL relapses

Within 15 pairs, to which the Tally algorithm¹ could be reliably applied in both primary and relapse, COO change was documented in 2 cases (case 5 and case 15). In both cases, transition occurred from GCB-like to non-GCB-like phenotype.

Case 15 was a clonally unrelated DLBCL relapse in which this “switch” is likely explainable by the independent cellular origin of the respective tumor occurrences.

None of the cases with *early-divergent/branching pattern* of relapses showed a COO change at relapse; all but one primary tumor belonging to this category had a non-GCB COO.

In the group with *late-divergent/linear pattern* of relapses 3/11 cases were of GCB COO, one of them (case 5) relapsed as a non-GCB DLBCL 27 months later. The changed COO in this case might be on the one hand related to micro-environmentally induced or progression-related gene expression pattern changes respecting *LMO2* (80% positive tumor cells in the primary vs 20% in the relapse) and *FOXP1* (90% positive tumor cells in the relapse vs 25% in the primary) since the primary was diagnosed on an affected lymph node, while the relapse affected the duodenum 26 months later. On the other hand, and more probably, it might simply reflect the genuine insufficiency of immunohistochemical algorithms for error-free COO determination⁵.

Expression frequency and prognostic significance of GATA3 in DLBCL

Altogether 23 of the study cases could be analyzed. Of the 16 relapsing DLBCL, 3 (19%) expressed GATA3 compared to 1 of the 7 non-relapsing DLBCL (14%). The expression pattern was nuclear, weaker compared to tumor-infiltrating small T-cells, and present in 10 to 90% of tumor cells. There was no clear correlation between GATA3 expression and amplifications 10p14-15.

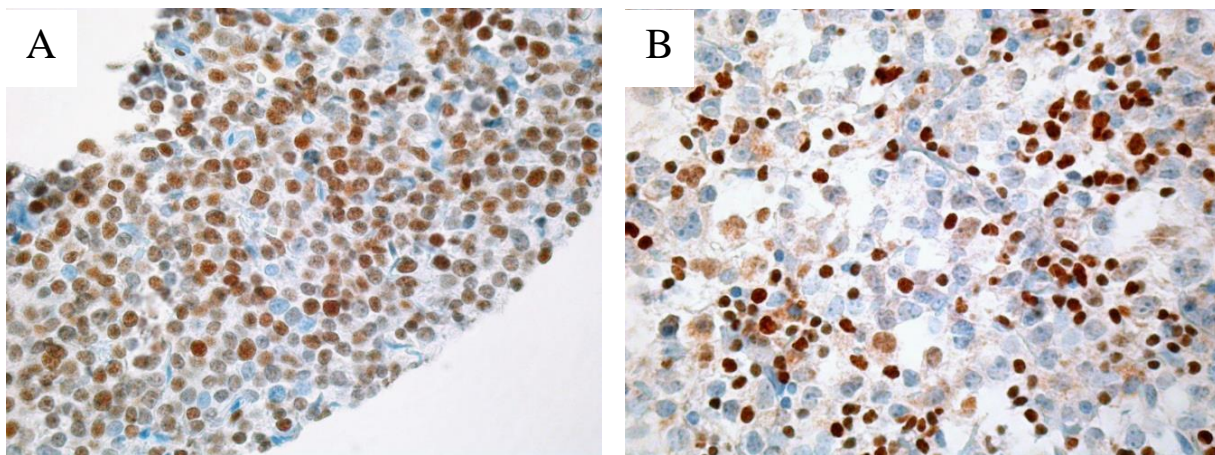


Figure S6. GATA3-positive DLBCL. A. DLBCL expressing GATA3 in 90% of the tumor cells. B. DLBCL showing weak expression (weaker than the small tumor-infiltrating T-cells) of GATA3 in 15% of the large tumor cell nuclei.

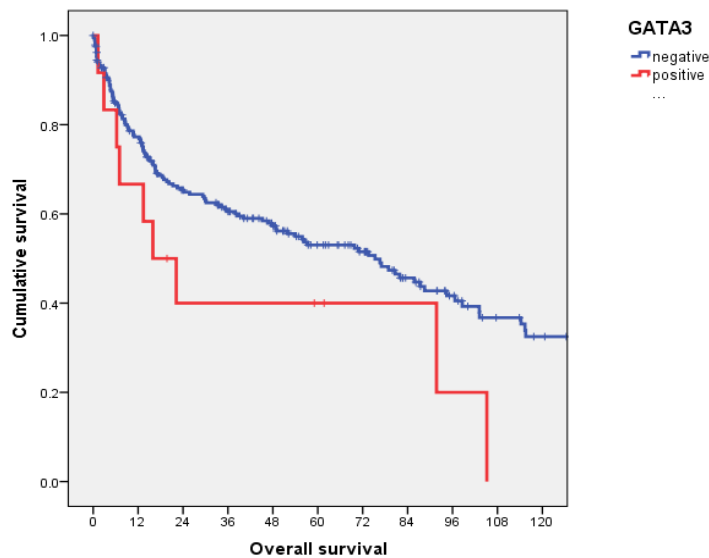


Figure S7. Survival of GATA3-positive and GATA3-negative DLBCL patients. Among 250 eligible arrayed cases⁶, only 12 DLBCL (5%) expressed GATA3. There were 128 adverse events in the 238 GATA3-negative patients (54%) compared to 9 of 12 (75%) in the GATA3-positive subgroup. Although the survival curves drifted apart, no significant outcome difference was suggested ($p=0.091$).

The observed rare expression of GATA3 and lack of correlation to 10p14-15 amplifications as well as lack of significant prognostic impact in DLBCL, despite significantly more frequent 10p14-15 amplifications in primaries of relapsing DLBCL, is likely explainable by one limitation of aCGH, i.e. that gains of genetic material do not directly or indisputably imply increased expression of genes located in the affected regions.

Supplementary tables

Table S1. NGS quality parameters and case allocation for the analysis application

Case Nr.	PRIMARY			RELAPSE			For evolution analysis	For recurrent mutation analysis
	Mean coverage	Coverage uniformity	Variants called*	Mean coverage	Coverage uniformity	Variants called*		
1	2819	47	1775	2331	82	60	NO	YES
2	-	-	-	-	-	-	-	-
3	2712	95	49	1215	82	2139	NO	YES
4	1283	94	87	1581	87	68	YES	YES
5	834	95	87	1636	46	117	NO	YES
6	566	77	1616	1182	94	158	NO	YES
7	1330	91	2137	1366	94	446	NO	YES
8	1042	91	71	825	90	302	YES	YES
9	603	95	80	830	93	286	YES	YES
10	979	96	50	879	90	105	YES	YES
11	997	92	1287	850	88	932	NO	YES
12	818	90	2014	1297	94	72	NO	YES
13	689	96	105	1065	96	51	YES	YES
14	1121	95	114	1419	94	67	YES	YES
15	821	95	161	1233	94	84	YES	YES
16	844	95	107	848	95	85	YES	YES
17	945	94	223	1164	94	86	YES	YES
18	635	95	133	1011	96	83	YES	YES
19	910	96	96	673	94	181	YES	YES
20	709	95	131	1125	96	59	YES	YES
21	549	95	74	-	-	-	NO	YES
22	794	93	153	-	-	-	NO	YES
23	1100	95	94	-	-	-	NO	YES
24	1681	90	76	-	-	-	NO	YES
25	1255	99	122	-	-	-	NO	YES
26	887	95	140	-	-	-	NO	YES
27	954	95	70	-	-	-	NO	YES
28	1149	94	97	-	-	-	NO	YES
29	1300	95	96	-	-	-	NO	YES
30	1300	94	102	-	-	-	NO	YES
31	1141	94	101	-	-	-	NO	YES

*number of variants called by the variant caller, before manual filtering

Red – samples with poor sub-optimal sequencing quality

Blue – fresh-frozen samples

Table S2. Torrent variant caller parameters used for the initial identification of variants.

Parameter	Value
snp_min_allele_freq	0.02
snp_strand_bias	0.95
hotspot_min_coverage	6
snp_strand_bias_pval	0.01
position_bias	0.75
hotspot_min_allele_freq	0.01
snp_min_variant_score	6
mnp_min_variant_score	15
hotspot_strand_bias	0.95
hp_max_length	8
filter_insertion_predictions	0.2
indel_min_variant_score	6
indel_min_coverage	15
heavy_tailed	3
outlier_probability	0.005
position_bias_ref_fraction	0.05
indel_strand_bias_pval	1
data_quality_stringency	6.5
snp_min_cov_each_strand	0
indel_as_hpindel	0
mnp_strand_bias	0.95
mnp_strand_bias_pval	1
hotspot_strand_bias_pval	1
hotspot_min_variant_score	6
hotspot_min_cov_each_strand	2
do_mnp_realignment	1

Table S3. Detailed immunophenotypic characteristics of the studied cases

Relapsing		CD10	GCET	LMO2	BCL6	MUM1	FOXP1	MIB1	BCL2	C-MYC	GATA3	COO
1	P	NA	+(dim)	+	NA	-	-	NA	NA	+(40%)	NA	GCB
	R	+(100%)	+(90%)	+(100%)	+(80%)	-(25%)	+(90%)	NA	-(0%)	+(40%)	NA	GCB
2	P	-	-	-	NA	-(40%)	+(90%)	NA	+(70%)	-(10%)	-	non-GCB
	R	NA	NA	NA	NA	NA	NA	NA	NA	-(30%)	NA	NA
3	P	-	-	-(10%)	+(50%)	-(60%)	+(80%)	90%	+(90%)	+(90%)	-	non-GCB
	R	NA	NA	NA	NA	NA	NA	NA	NA	-(20%)	NA	NA
4	P	-	-	-(20%)	+(40%)	-(25%)	+(90%)	75%	+(100%)	-(5%)	NA	non-GCB
	R	NA	NA	-	NA	NA	+(90%)	NA	+(90%)	NA	NA	non-GCB
5	P	-	-	+(80%)	+(80%)	-	-(25%)	80%	+(80%)	-(20%)	NA	GCB
	R	-	-	-(20%)	+(60%)	-(30%)	+(90%)	95%	+(100%)	-(15%)	NA	non-GCB
6	P	-	NA	NA	NA	NA	NA	80%	+(100%)	NA	NA	na
	R	-	-	-	-(2%)	+(75%)	+(85%)	95%	+(100%)	+(40%)	NA	non-GCB
7	P	+	-	NA	+(65%)	-	-	80%	-(10%)	NA	NA	GCB
	R	+	-	+(70%)	+(30%)	-	-(5%)	55%	-(15%)	+(40%)	NA	GCB
8	P	-	+	+(40%)	NA	-(40%)	+(80%)	65%	+(100%)	-(15%)	-	non-GCB
	R	-	-	+(35%)	+(100%)	-(15%)	+(70%)	70%	-(10%)	-(35%)	NA	non-GCB
9	P	-	-	+(70%)	+(30%)	-(50%)	+(80%)	90%	+(80%)	+(40%)	-	non-GCB
	R	-	-	-	+(30%)	-(25%)	+(50%)	70%	-(50%)	-(25%)	NA	non-GCB
10	P	-	+	+(70%)	-(15%)	-(50%)	+(75%)	70%	-(15%)	-(15%)	NA	non-GCB
	R	-(15%)	-	+(70%)	+(30%)	-(60%)	+(60%)	60%	-(10%)	-(15%)	NA	non-GCB
11	P	-	+	-(20%)	+(60%)	+(80%)	+(90%)	70%	+(100%)	NA	-	non-GCB
	R	NA	NA	NA	-(25%)	NA	NA	90%	NA	+(60%)	NA	NA
12	P	-	-	NA	-(1%)	NA	NA	70%	-(40%)	-(5%)	NA	na
	R	-	-	-	-(25%)	-(10%)	+(50%)	80%	+(70%)	-(10%)	NA	non-GCB
13	P	-	-	-	+(90%)	-(60%)	+(100%)	90%	+(90%)	+(90%)	-	non-GCB
	R	+(80%)	-	-	+(80%)	+(90%)	+(100%)	90%	+(100%)	+(90%)	NA	non-GCB
14	P	-	-(20%)	+(70%)	+(40%)	+(80%)	+(80%)	70%	-(40%)	-(15%)	+	non-GCB
	R	-	-	-	+(60%)	+(70%)	+(60%)	85%	-(40%)	-(15%)	NA	non-GCB
15	P	-	-	+(40-50%)	-(5%)	-(30%)	-(15%)	90%	+(80%)	+(50%)	+	GCB
	R	-	-	+(40%)	-(5%)	-(15%)	+(65%)	70%	NA	+(40%)	NA	non-GCB
16	P	+(90%)	-	+(50%)	+(80%)	+(90%)	+(70%)	70%	+(90%)	-(20%)	NA	GCB
	R	+(100%)	+(100%)	+(70%)	+(90%)	-	+(80%)	90%	+(70%)	+(70%)	NA	GCB
17	P	-	-	+(70%)	+(100%)	+(100%)	+(100%)	85%	-(50%)	+(60%)	-	non - GCB
	R	-	-	+(90%)	+(50%)	-(50%)	+(85%)	95%	NA	NA	NA	non-GCB
18	P	-	-	-	-(20%)	+(100%)	+(100%)	95%	+(100%)	+(60%)	-	non-GCB
	R	+(80%)	-	-	+(70%)	-	+(60%)	90%	+(100%)	+(100%)	NA	non-GCB
19	P	-	+(90%)	+(100%)	+(90%)	-(25%)	+(60%)	90%	+(70%)	+(40%)	+	GCB
	R	-	+(90%)	+(80%)	+(50%)	-(30%)	+(70%)	NA	-(10%)	-(25%)	NA	GCB

20	P	-	-	-	+(75%)	+(70%)	+(80%)	75%	+(100%)	+(60%)	NA	non-GCB
	R	-	-	-	+(60%)	+(100%)	+(100%)	80%	+(60%)	-(30%)	NA	non-GCB
Total	P	2/19(11%)	5/19(26%)	10/17(59%)	12/16(75%)	6/18 (33%)	14/18(78%)	80%	14/19(74%)*	9/17(52%)	3/11(27%)	
	R	4/16(25%)	3/16(19%)	8/17(47%)	13/17(76%)	4/16(25%)	16/17(94%)	81%	8/15(53%)	8/18(44%)	NA	
Non-relapsing		CD10	GCET	LMO2	BCL6	MUM1	FOXP1	MIB1	BCL2	C-MYC	GATA3	COO
21		-	-(30%)	+(100%)	+(50%)	-(60%)	+(80%)	90%	-(10%)	-(30%)	-	non - GCB
22		-	-(20%)	+(100%)	+(90%)	+(70%)	+(80%)	90%	-(40%)	-(50%)	-	non - GCB
23		-	-	+(70%)	+(45%)	-(30%)	+(70%)	70%	-(60%)	-(20%)	-	non - GCB
24		-	NA	NA	+(30%)	-(60%)	NA	NA	+(100%)	NA	-	NA
25		+	NA	-	+	+(80%)	+(70%)	60%	-(30%)	-(25%)	NA	GCB
26		-	-	-(15%)	-dim(20%)	+(70%)	+(75%)	80%	-(40%)	+(70%)	-	non - GCB
27		-	-	-	+(30%)	+(70%)	+(90%)	50%	+(90%)	-(30%)	-	non - GCB
28		NA	+(80%)	+	NA	-	-(15%)	NA	NA	-(40%)	NA	GCB
29		-(15%)	-	+(100%)	+(70%)	-(30%)	-	75%	-(25%)	-(40%)	+	GCB
30		+	+	+	+(100%)	-	-	90%	-(30%)	+(65%)	NA	GCB
31		+dim	-(40%)	+(100%)	+(80%)	-(15%)	+(50%)	NA	-(25%)	-(40%)	NA	GCB
Total		2/10(20%)	2/9(22%)	7/10(70%)	9/10(90%)	4/11(36%)	7/10(70%)	77%	2/10(20%)*	2/10(20%)	1/7(14%)	

Abbreviations: COO – cell of origin; dim – weak positivity; GCB – germinal center B cell-like; NA – not analyzed or not applicable; P – primary, R – relapse

Table S6. Antibodies used, conditions applied for immunohistochemistry and cut-off scores for evaluation

	BCL2	BCL6	CD10	C-MYC	FOXP1	GATA3	GCET	LMO2	MIB1	MUM1
Clone name	SP66	GI191E/A8	SP67	Y69	SP133	L50-823	RAM341	1A9-1	Mib-1	MEQ-43
Antigen retrieval time*	16'	32'	24'	92'	16'	32'	32'	32'	24'	24'
Incubation time	12'	28'	16'	16'	12'	32'	20'	16'	16'	16'
Cut-off	70%	30%	20%	40%	50%	any	60%	30%	NA	70%

*Antigen retrieval was performed in CC1 buffer (Ventana/Roche)

Table S7. Genes included into the custom lymphoma NGS panel

All exons		Hotspots only				
<i>TP53</i>	<i>GNA13</i>	<i>MYD88</i>	<i>KRAS</i>	<i>PIK3CA</i>	<i>STAT6</i>	<i>DNMT3A</i>
<i>CDKN2A</i>	<i>HIST1H1C</i>	<i>EZH2</i>	<i>CARD11</i>	<i>PIK3CD</i>	<i>PTPN11</i>	<i>CALR</i>
<i>IKZF1</i>	<i>MEF2B</i>	<i>NOTCH1</i>	<i>CREBBP</i>	<i>PIK3R1</i>	<i>IRF4</i>	<i>RHOA</i>
<i>KMT2D</i>	<i>PIM1</i>	<i>SF3B1</i>	<i>IDH2</i>	<i>MTOR</i>	<i>BCL10</i>	<i>SGK1</i>
<i>TNFAIP3</i>	<i>PAX5</i>	<i>CD79B</i>	<i>IDH1</i>	<i>EP300</i>	<i>IKZF3</i>	<i>KLHL6</i>
<i>ATM</i>	<i>PTPN1</i>	<i>BRAF</i>	<i>BCL6</i>	<i>MLL3</i>	<i>MCL1</i>	<i>XPO1</i>
<i>B2M</i>	<i>PTEN</i>	<i>JAK2</i>	<i>FBXW7</i>	<i>RELN</i>	<i>BCL2L11</i>	<i>CCND1</i>
<i>BCL2</i>	<i>EBF1</i>	<i>KIT</i>	<i>STAT3</i>	<i>TET2</i>	<i>MAP2K1</i>	<i>JAK3</i>
<i>PRDM1</i>	<i>MYC</i>	<i>NOTCH2</i>	<i>CD79A</i>	<i>TLN2</i>	<i>U2AF1</i>	
<i>BTG1</i>	<i>SOCS1</i>	<i>NRAS</i>	<i>CELSR2</i>	<i>FOXO1</i>	<i>FLT3</i>	

Supplementary figures

Tumor genetic evolution analysis	Recurrent mutation analysis	
	Relapsing DLBCL	Non-relapsing DLBCL
CG>TA mutations in FFPE samples with VAF<10%	CG>TA transitions in FFPE samples with VAF<10%	CG>TA transitions in FFPE samples with VAF<10%
Shared variants that are included in dbSNP database	Shared variants that are included in dbSNP database	Variants that are included in dbSNP database
All shared variants with VAF >95% in regions not affected by deletions	All shared variants with VAF >95% in regions not affected by deletions	All variants with VAF >95% in regions not affected by deletions
All variants of cases 1, 3, 5, 6, 7, 11, 12	All CG<TA transitions in the primaries of cases 1, 6,7, 11, 12 and the relapse of case 3	Variants in non-exonic regions
False-positive variants in homopolymeric regions after manual review	Variants with VAF<10% in the primaries of cases 1, 6,7, 11, 12 and the relapse of case 3	Synonymous variants
	Variants in non-exonic regions	False-positive variants in homopolymeric regions after manual review
	Synonymous variants	
	False-positive variants in homopolymeric regions after manual review	

Figure S1. Criteria for variant exclusion for different analysis applications

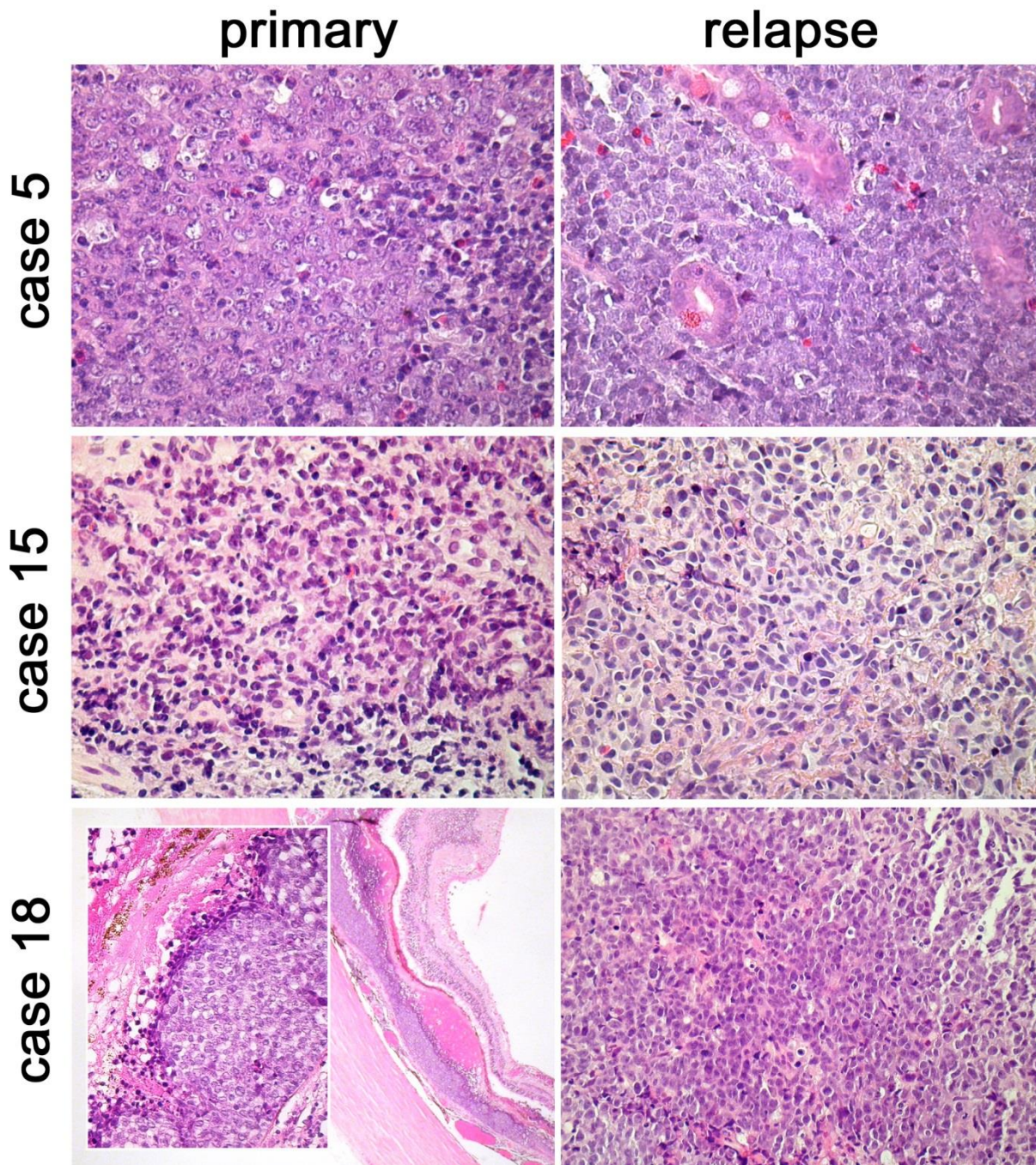


Figure S2. Morphology of primary and relapse pairs of DLBCL. Case 5 was diagnosed with nodal DLBCL with pleomorphic centroblastic morphology, LMO2+ and FOXP1dim, and relapsed 2 years later as a clonally related centroblastic DLCBL in the intestine, LMO2dim and FOXP1+, with linear genomic evolution and cell of origin (COO) “switch” (for reasons of COO switch see Supplementary description on Retention and change of cell of origin in DLBCL relapses). Case 15 was diagnosed with nodal DLBCL with centroblastic morphology, EBV+, in the setting of liver transplantation, i.e. monomorphic post-transplant lymphoproliferative disorder (PTLD) and its intestinal “relapse” turned out being a clonally unrelated and EBV- second monomorphic PLTD. Case 18 was diagnosed with DLBCL of the eye ball (subretinal spread) with centroblastic morphology and relapsed 12 years later as a clonally related centroblastic DLCBL in a cervical lymph node with branching genomic evolution, retaining its COO. Note that based on morphological analysis, COO and time to relapse, no conclusions on clonal kinships and genomic progression can be drawn.

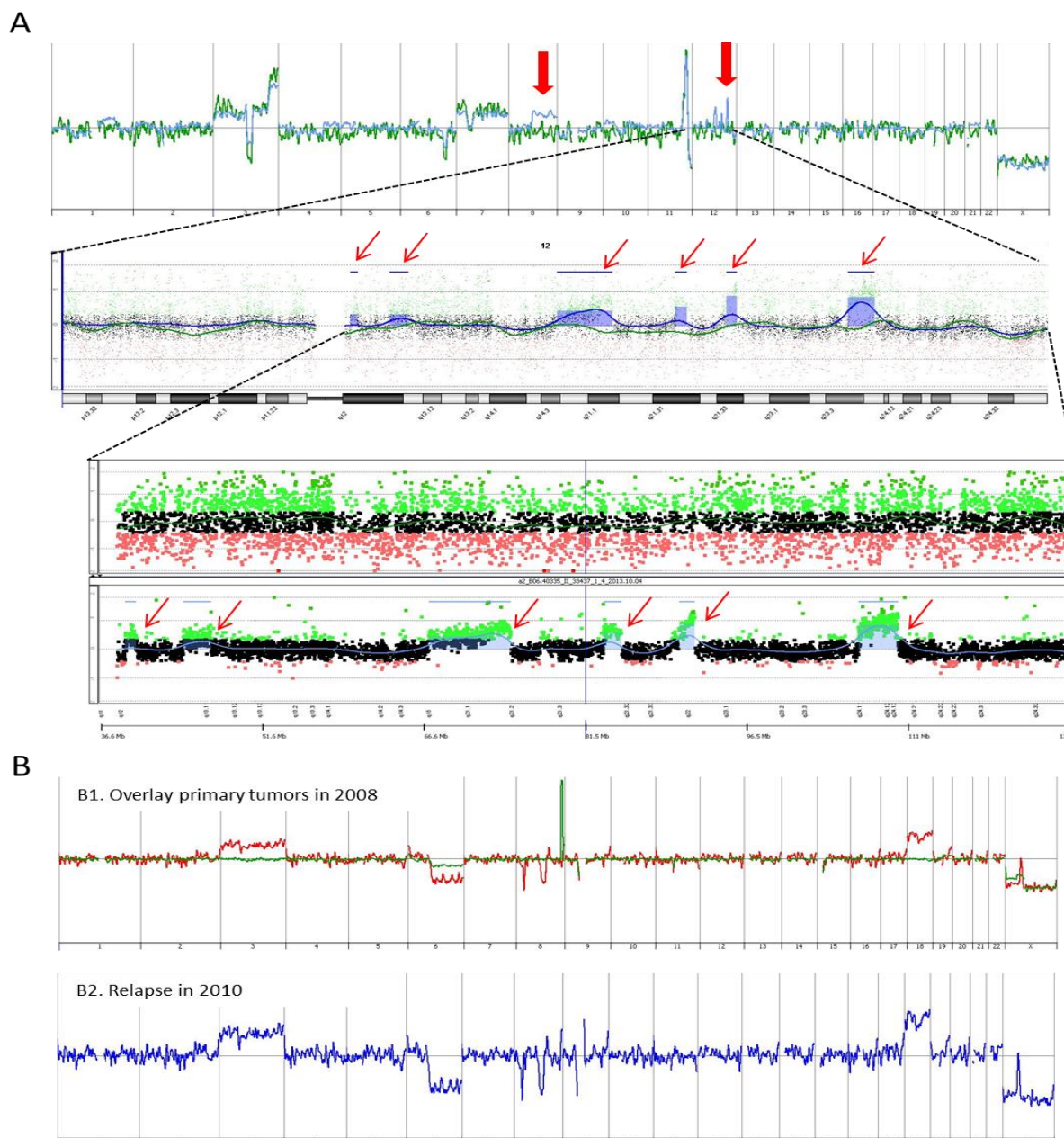


Figure S3. Evidence of intra-tumoral genetic heterogeneity in relapsing DLBCL. A. Two adjacent parts of the relapse tumor of case 1 were profiled. While the majority of chromosomal copy number aberrations match between the two tumor parts, one of them bears additional gains at 8q and focal amplifications at 12q. **B.** Similarly, two parts of the primary tumor of case 5 were profiled (B1). While parts of the same biopsy shared a heterozygous deletion 6q, there were also private aberrations of chromosomes 3, 8, 18 and X. The subsequent clonally related relapse (B2) evidently originated from one of the tumor subpopulations and not from the other.

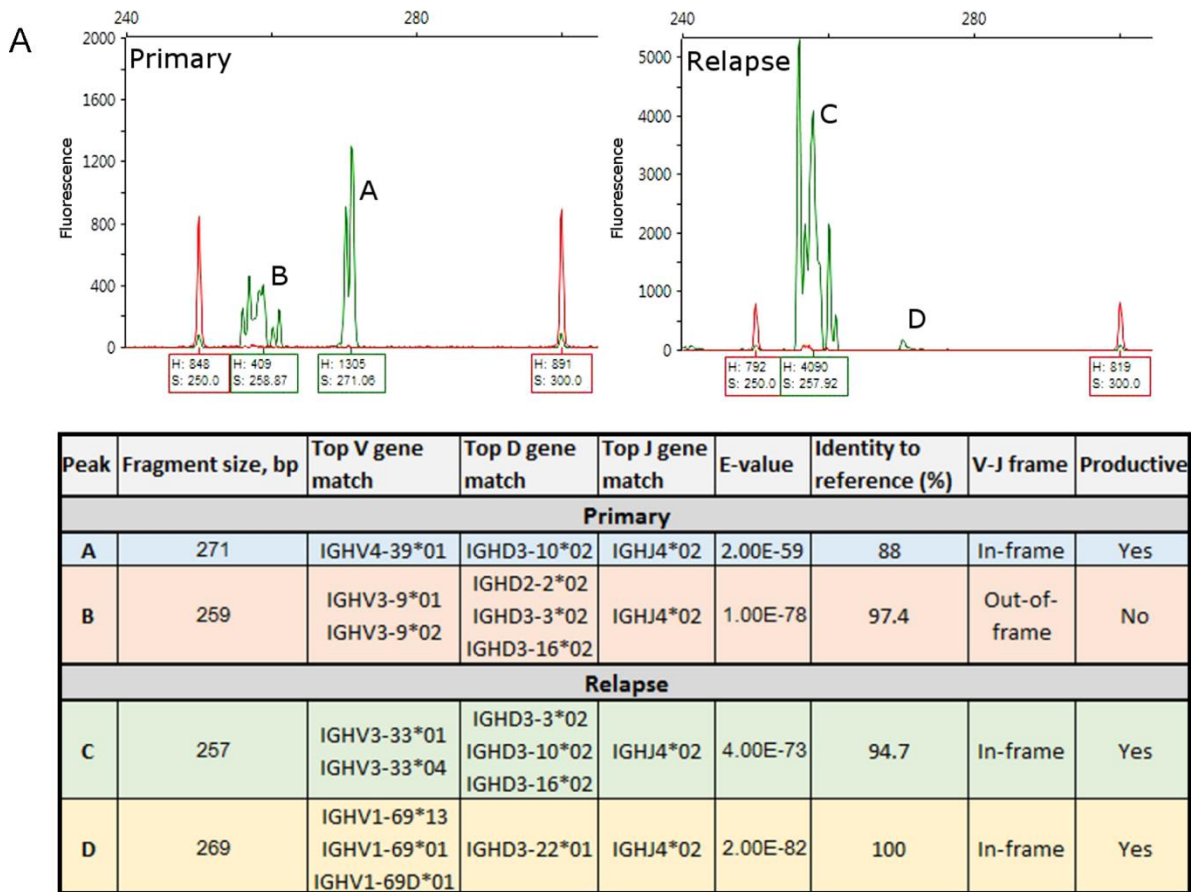


Figure S4. Analysis of immunoglobulin gene rearrangements in case 15. The primary tumor showed an oligo-clonal pattern as two fragments of different sizes were amplified. Sequencing analysis showed that one of these rearrangements (peak B 259bp) was non-productive, suggesting that it represented the second *IG* allele of the dominant lymphoma clone. At relapse, one dominant rearrangement was amplified (peak C). Although its size was close to that of the non-productive rearrangement of the primary tumor, sequencing analysis showed the usage of different variable genes. These data suggest different clonal origin of the primary and relapse occurrences. A minor peak (peak D) at relapse was detected at a size close to the productive rearrangement in the primary tumor. However, again variable gene sequences did not match and the latter gene also lacked somatic hypermutations. It is likely that this rearrangement represents part of the non-malignant B-cell gene pool.

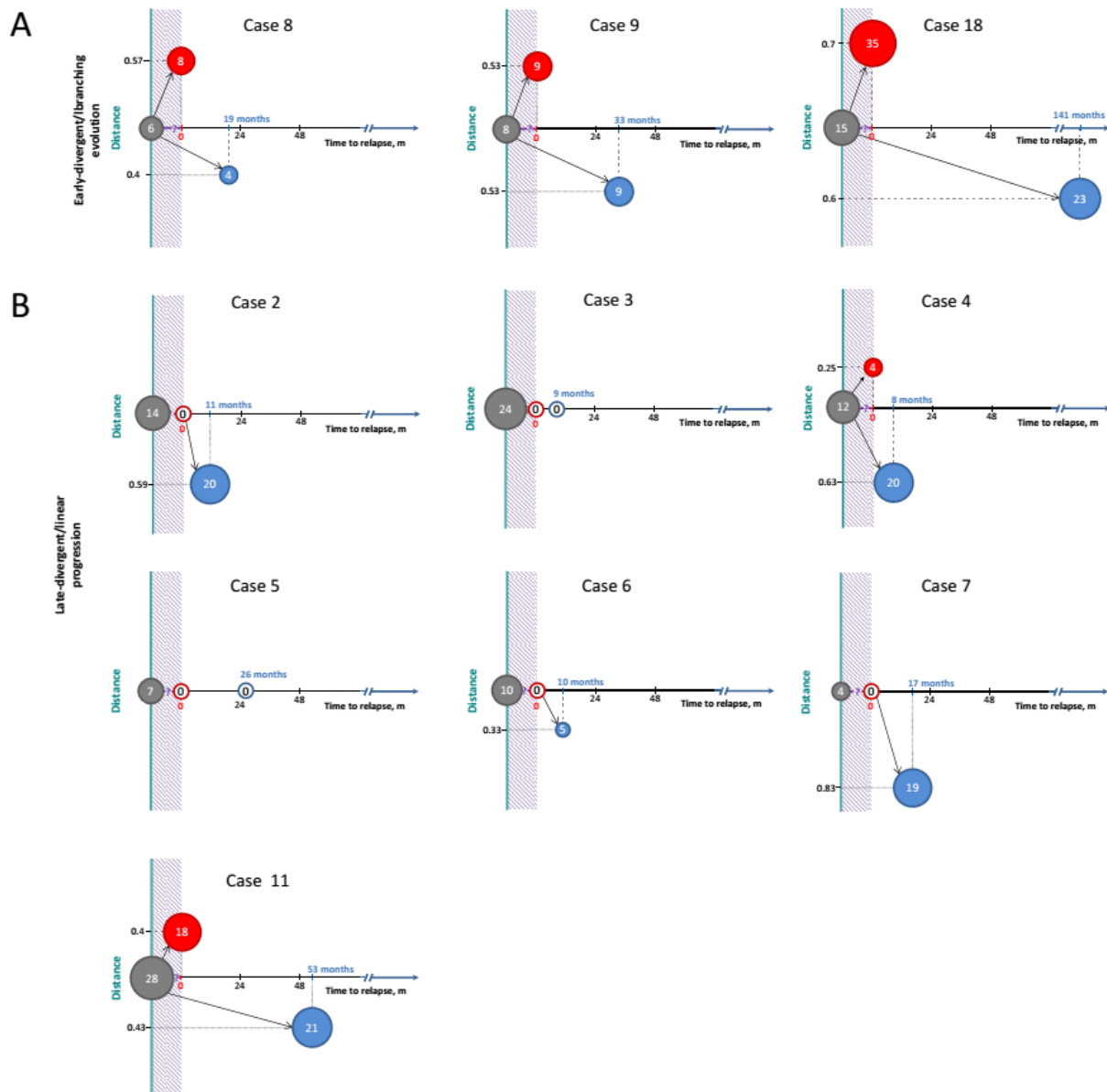


Figure S5. Genetic evolution patterns in relapsing DLBCL continued from Figure 3. Distance plots of cases with early-divergent/branching (A) and late-divergent evolutionary pattern (B). Numbers inside circles represent a combined count of mutations and copy number aberrations in the respective population. Circle sizes are scaled according to the number of genetic alterations. Dashed purple area symbolizes the time from putative divergence of populations till occurrence of primary lymphoma, which is unknown. Red – genetic alterations unique to primary tumor. Blue – genetic alterations unique to relapse. Grey circle – putative common progenitor. The “genetic distance” from the common progenitor is plotted on the y axis; at the top of the x axis for the primary tumor, at the bottom – for the relapse.

Supplementary references

1. Meyer PN, Fu K, Greiner TC, Smith LM, Delabie J, Gascoyne RD, *et al.* Immunohistochemical methods for predicting cell of origin and survival in patients with diffuse large B-cell lymphoma treated with rituximab. *J Clin Oncol* 2011; **29**: 200–7.
2. Meier VS, Ruffe A, Gudat F. Simultaneous evaluation of T- and B-cell clonality, t(11;14) and t(14;18), in a single reaction by a four-color multiplex polymerase chain reaction assay and automated high-resolution fragment analysis: a method for the rapid molecular diagnosis of lympho. *Am J Pathol* 2001; **159**: 2031–43.
3. Ye J, Ma N, Madden TL, Ostell JM. IgBLAST: an immunoglobulin variable domain sequence analysis tool. *Nucleic Acids Res* 2013; **41**: W34–40.
4. Juskevicius D, Ruiz C, Dirnhofer S, Tzankov A. Clinical, morphologic, phenotypic, and genetic evidence of cyclin D1-positive diffuse large B-cell lymphomas with CYCLIN D1 gene rearrangements. *Am J Surg Pathol* 2014; **38**: 719–27.
5. Gutierrez-Garcia G, Cardesa-Salzmann T, Climent F, Gonzalez-Barca E, Mercadal S, Mate JL, *et al.* Gene-expression profiling and not immunophenotypic algorithms predicts prognosis in patients with diffuse large B-cell lymphoma treated with immunochemotherapy. *Blood* 2011; **117**: 4836–43.
6. Nagel S, Hirschmann P, Dirnhofer S, Günthert U, Tzankov A. Coexpression of CD44 variant isoforms and receptor for hyaluronic acid-mediated motility (RHAMM, CD168) is an International Prognostic Index and C-MYC gene status-independent predictor of poor outcome in diffuse large B-cell lymphomas. *Exp Hematol* 2010; **38**: 38–45.

3.2 Extracavitary primary effusion lymphoma: clinical, morphological, phenotypic and cytogenetic characterization using nuclei enrichment technique.

Juskevicius D., Dietsche T., Lorber T., Ruffle A., Ruiz C., Mickys U., Krasniqi F., Dirnhofer S., Tzankov A.

-Research article-
Published in *Histopathology*, 2014

Contribution: I developed a FFPE nuclei-enrichment technique, performed the experiments, analyzed data, prepared figures and wrote the manuscript



Extracavitary primary effusion lymphoma: clinical, morphological, phenotypic and cytogenetic characterization using nuclei enrichment technique

Darius Juskevicius,¹ Tanja Dietsche,¹ Thomas Lorber,¹ Alexander Ruffe,¹ Christian Ruiz,¹ Ugnius Mickys,² Fatime Krasniqi,³ Stephan Dirnhofer¹ & Alexandar Tzankov¹

¹Institute of Pathology, University Hospital, Basel, Switzerland, ²Vilnius University Hospital Santariskiu Clinics, Vilnius, Lithuania, and ³Department of Oncology, University Hospital, Basel, Switzerland

Date of submission 20 March 2014

Accepted for publication 11 June 2014

Published online Article Accepted 3 July 2014

Juskevicius D, Dietsche T, Lorber T, Ruffe A, Ruiz C, Mickys U, Krasniqi F, Dirnhofer S & Tzankov A (2014) *Histopathology*

Extracavitary primary effusion lymphoma: clinical, morphological, phenotypic and cytogenetic characterization using nuclei enrichment technique

Abstract: Aims: Primary effusion lymphoma (PEL) is a rare form of aggressive B-cell lymphoma, which typically manifests as malignant effusion in the body cavities. However, extracavitary solid variants are also described. The aim of this study was to investigate copy number aberrations in two cases of solid PEL at their first occurrences and relapse by applying a newly developed methodology of tumour nuclei enrichment.

Methods and results: Using histological and genetic techniques, a novel protocol for tumour nuclei enrichment by flow sorting and array-comparative genomic hybridization, we characterized two cases of extracavitary PEL, one of which later relapsed as effusion. Both primary tumours were positive for HHV8

and EBV, confined to lymph nodes, and aberrantly expressed CD3, yet displaying clonal immunoglobulin gene rearrangements indicating B-cell origin. Cytogenetic characterization of primary tumours revealed modest number of aberrations, partially overlapping with previously reported affected loci. The effusional relapse in case 1 was cytogenetically related to the primary tumour but showed dramatic increase of chromosomal instability.

Conclusions: We for the first time demonstrate a cytogenetic relationship between solid and effusional presentations of PEL. Moreover, we provide an indirect evidence of multiple malignant clones, which gave rise to clonally-related, yet karyotypically different relapsing lymphoma manifestations.

Keywords: array comparative genomic hybridization, EBV, extracavitary primary effusion lymphoma, flow sorting, HHV8, HIV, large B-cell lymphoma

Introduction

Primary effusion lymphoma (PEL) is a HHV8-associated B-cell lymphoma, which predominantly occurs in HIV infected individuals. It is believed that immunosuppression is a prerequisite for PEL development. Apart from AIDS, it has also been reported in other

immunodeficiency conditions such as iatrogenic immunosuppression, rare cases of advanced cancer and liver cirrhosis, as well as in elderly patients.^{1–4}

Though originating from B cells, PEL usually lacks pan-B-cell markers such as CD19, CD20 and CD79a. Surface or cytoplasmic immunoglobulin (Ig) expression is rarely detected as well. Neoplastic PEL cells have monoclonal immunoglobulin gene (IG) gene rearrangements and show evidence of post-germinal centre origin by the presence of somatic hypermutations of the IG genes and in the noncoding *BCL6* region.⁵

Address for correspondence: A Tzankov, Institute of Pathology, University Hospital Basel, Schoenbeinstrasse 40, Basel CH-4031, Switzerland. e-mail: alexandar.tzankov@usb.ch

© 2014 John Wiley & Sons Ltd.

Interestingly, translocations affecting the *BCL1*, *BCL2*, *C-MYC* and *BCL6* genes, which are commonly observable in other aggressive B-cell lymphomas, are consistently absent in PEL.^{6,7} Classic PEL show a specific plasmablastic gene expression profile, which further separates it from other AIDS-related lymphomas as well as lymphomas occurring in immunocompetent patients.^{8,9}

Primary effusion lymphoma typically presents as a serous effusion in body cavities.^{5,6} However, occasionally patients with PEL develop secondary solid tumour masses¹⁰ or initially diagnosed solid tumours are followed by serous effusions in the body cavities.¹¹ Importantly, the spectrum of clinical presentation is further expanded by the identification of solid tumours compatible with the diagnosis of PEL, which are not associated with serous effusions prior, during or after the extracavitary manifestation.^{12,13}

Such extracavitary variants show similar morphology, immunophenotype, genotype, and HHV8 viral status to classic PEL and are referred as solid PEL.⁵ This subtype of PEL is usually encountered in lymph nodes but can also involve the skin, lung, gastrointestinal tract and central nervous system. The solid variant of PEL can be difficult to diagnose because of the unexpected extracavitary presentation and the unusual immunophenotype that can be 'null cell', with aberrant expression of pan-T-cell markers or show only limited evidence of B-cell differentiation.¹⁴ HHV8 infection is a defining property of PEL, whereas co-infection with EBV is found in 90% of extracavitary cases. Thus, double positivity for HHV8 and EBV often serves as decisive criterion to make a correct diagnosis. HHV8 is believed to play an important role in the pathogenesis of all PEL variants, whereas EBV is mostly regarded as opportunistic infection in this context.¹⁵

The study of Chadburn *et al.*¹⁶ demonstrated a better survival of solid PEL patients compared to classic PEL, the median survival being 11 and 3 months, respectively. Lack of highly active antiretroviral therapy (HAART) before PEL diagnosis is regarded as strongest predictor of poor outcome in the population of HIV-positive patients.^{17,18}

Cytogenetic studies of classic PEL revealed complex genotypes with both recurrent and non-recurrent genetic aberrations.^{19–22} More than one cytogenetically related neoplastic cell clone was identified in the majority of samples, giving evidence of karyotypic evolution.²³ Very limited numbers of studies with cytogenetic data on extracavitary PEL have been published. In the present study we used sorted nuclei populations of two solid PEL cases, one in a HIV-positive patient, relapsing as classic PEL (effusion), and one in a HIV-negative patient, who suffered from EBV-associated

gastric carcinoma, to study genetic abnormalities at presentation and relapse of this distinct lymphoma by array comparative genomic hybridization (aCGH).

Materials and methods

PATIENT SAMPLES

Formalin-fixed, paraffin-embedded (FFPE), lymph node biopsies were used. The sample of one of the patients was retrieved from the archive of the Institute of Pathology, University Hospital Basel, Basel, Switzerland and the sample of the other patient was obtained from Vilnius University Hospital Santariskiu Clinics, Vilnius, Lithuania. Retrieval of tissue and data were according to the regulations of the local institutional review boards and data safety laws.

IMMUNOHISTOCHEMISTRY

Immunohistochemistry was performed on serial tissue sections using an automated immunostainer Benchmark XT (Ventana/Roche, Tucson, AZ, USA) with a biotin-streptavidin peroxidase detection system according to manufacturer's protocols. For antigen retrieval, tissue sections were immersed and microwaved in Cell Conditioning Solution (CC1; Ventana/Roche). All primary antibody clone names, antibody incubation times and antigen retrieval conditions are summarized in Table 1.

FLUORESCENCE *IN SITU* HYBRIDIZATION

Fluorescence *in situ* hybridization (FISH) was performed on paraffin sections according to the manufacturer's instructions (Abbott, Abbott Park, IL, USA) to test the samples for structural and numeric aberrations involving *BCL2*, *BCL6* and *C-MYC*. Additional probes were used to confirm selected cytogenetic aberrations detected in both cases by aCGH. These are listed together with the cytogenetic positions of the aberrations in Table 2.

IN SITU HYBRIDIZATION OF EBV EARLY RNA

In situ hybridization for EBV early RNA (EBER) was carried out according to the manufacturer's protocol (ref. 800-2842; Ventana/Roche).

MULTIPLEX PCR ASSAY

Polymerase chain reaction (PCR) assay for *IGH* gene rearrangement was performed with consensus FR1

Table 1. Immunophenotypes of the reported extracavitary PEL cases

Marker	Case 1	Relapse case1	Case 2	Clone name	Antigen retrieval, min*
CD2	–	–	–	<i>MRQ-11</i>	16
CD3	+cyt	+cyt	+	<i>2GV6</i>	16
CD4	+	–	–	<i>SP35</i>	16
CD8	–	–	–	<i>SP57</i>	16
CD15	–	–	–	<i>MMA</i>	16
CD19	–	–	–	<i>LE-CD19</i>	16
CD30	–	–	–	<i>Ber-H2</i>	32
CD45	+dim	+dim	+dim	<i>LCA</i>	24
CD79a	–	–	+/-	<i>SP18</i>	24
CD38	+	+	+	<i>SP149</i>	16
CD138	+	+	–	<i>B-A38</i>	24
EMA	+	+	–	<i>E29</i>	8
HHV-8	+	+	+	<i>13B10</i>	16
Kappa	–	–	–	<i>poly</i>	8
Lambda	–	+	+	<i>poly</i>	8
IgM	–	**	+	<i>poly</i>	8
IgG	–	**	–	<i>poly</i>	8
IgA	–	**	–	<i>poly</i>	8
ALK1	–	–	–	<i>ALK01</i>	16
CD56	–	–	–	<i>123C3</i>	16
TIA-1	–	–	–	<i>TIA-1</i>	24
Pax-5	–	–	–	<i>SP34</i>	16
CD23	–	–	+	<i>SP23</i>	16
BCL2	–	–	+dim	<i>SP66</i>	16
GranB	–	–	–	<i>poly</i>	16
CD44S	–	+dim	–	<i>SP37</i>	8
C-MYC	–	–	–	<i>Y69</i>	92
EBER	+	+	+	<i>na</i>	na

*Antigen retrieval was performed in CC1 buffer, using Benchmark XT automated stainer.

**Because of interference with the ascitic fluid, the immunoglobulin heavy chain stainings were not evaluable.

and FR3 as well as J primers as previously published.²⁴ Examination of the PCR products was carried out with the high resolution fragment length analysis system (ABI 310 Genetic Analyzer; Applied

Biosystems, Foster City, CA, USA). Clonal rearrangements were defined as prominent, single-sized amplification products in a suitable size range as determined by specific assay.

Table 2. FISH probes used for confirmation of aberrations detected by aCGH

Figure 2	Aberrant region by aCGH	Probe name	Company
Case 1			
A	2p25.1-p23.3	ZytoLight [®] SPEC NMYC/2q11 Dual Color Probe	ZytoVision*
B	16q12.1-q24.2	Vysis LSI IGH/MAF Dual Color Dual Fusion Probe	Abbott Molecular*
C	18q21.1-q22.3	Vysis LSI IGH/MALT1 Dual Color Dual Fusion Probe	Abbott Molecular
Case2			
D	Trisomy 7	ZytoLight [®] SPEC EGFR/CEN 7 Dual Color Probe	ZytoVision
E	6q23.3-q27	ZytoLight [®] SPEC ESR1/CEN 6 Dual Color Probe	ZytoVision

*ZytoVision, Bremerhaven, Germany; Abbott Molecular, Des Plaines, IL, USA.

NUCLEI EXTRACTION, STAINING AND SORTING

Nuclei extraction was done based on a procedure previously described,^{25–27} with major modifications. Prior to sorting, excess paraffin was removed with a scalpel from either side of the FFPE tissue block to reduce accumulation of debris during the sorting process. To reduce the sectioned nuclei amount in the sample, 55 µm-thick sections were microtome cut and placed into individual 2 ml microcentrifuge tubes. Then the tissue scrolls were washed three times with 1 ml xylene for 5 min to remove the remaining paraffin. Each sample was rehydrated in sequential ethanol washes (100% 2 × 5 min, then 95%, 70%, 50%, and 30%) and washed two times in 1 ml of citrate buffer pH 6.0. A 1 ml aliquot of citrate buffer pH 6.0 was added to the samples and incubated at 85°C for 30 min to facilitate the removal of protein cross-links present in the FFPE tissue and to facilitate later enzymatic digestion. Samples were then cooled to room temperature for 5 min, followed by addition of 300 ml phosphate-buffered saline (PBS) pH 7.4 and gentle centrifugation for 2 min at 3.6 *g*. The supernatant was carefully removed and the pellet washed three times with 1 ml PBS pH 7.4/0.5 mM CaCl₂ to remove the remaining citrate. Each sample was then digested overnight (10–17 h) in 1 ml of a freshly prepared enzymatic cocktail containing 10 units/ml of collagenase type 3, 80 units/ml of purified collagenase, and 100 units/ml of hyaluronidase in PBS pH 7.4/0.5 mM CaCl₂ buffer. Each enzyme was rehydrated with PBS pH 7.4/0.5 mM CaCl₂ buffer then stored at –20°C prior to addition to the cocktail mixture. Following overnight digestion, samples were centrifuged for 5 min at 1500 *g*, then pellets were resuspended in 500 ml of PBS pH 7.4/10% fetal calf serum (FCS) and passed through a 25-G needle 10–20 times. The samples were filtered

through a 35 mm mesh and collected into a clean 1.5 ml microcentrifuge tube. The mesh was rinsed with an additional 500 ml of PBS pH 7.4/10%FCS and placed for 30 min at room temperature to block the possible unspecific binding sites. Samples were again centrifuged for 5 min at 1500 *g* and the pellets were resuspended in 500 ml of PBS pH 7.4/5 mM EDTA/1% FCS. Nuclei were then split into staining and appropriate control tubes. Mouse monoclonal antibody against HHV8 latency-associated nuclear antigen (LANA1) protein (clone 13B10; Cell Marque, Rocklin, CA, USA) was added to the staining tube diluted 1:200 (0.01 µg/ml) and incubated overnight (8–12 h) at +4°C. Following incubation the sample was washed twice with 1 ml PBS pH 7.4/5 mM EDTA/1% FCS and biotinylated secondary anti-mouse antibody (Vector Laboratories, Burlingame, CA, USA) diluted 1:200 was added and incubated for 30 min at room temperature. Again the sample was washed and streptavidin-conjugated Alexa647 (Jackson Immuno Research Laboratories, West Grove, PA, USA) was added to complete the three-level marker specific staining of the FFPE tissue-derived nuclei. After the final washing step with 1 ml PBS pH 7.4/5 mM EDTA/1% FCS the pellets were resuspended in NST buffer containing 10 µg/ml of 4',6-diamidino-2-phenylindole (DAPI) to later enable ploidy determination and nuclei discrimination from the debris. The samples were transferred to 5 ml polypropylene round-bottom tubes and kept on ice in the dark until used. Sample analysis and sorting was performed with Influx cytometer (Becton-Dickinson, San Jose, CA, USA). Gating strategy was used to eliminate aggregates, as well as damaged or fragmented nuclei (DAPI negative, left to G₁ peak). PEL nuclei were gated and sorted based on the positive staining by the anti-LANA1 monoclonal antibody achieved by signal amplification with streptavidin-coupled fluorochrome.

Sorted nuclei populations were mounted on microscope slides and stained with hematoxylin for morphological evaluation and purity estimation.

DNA EXTRACTION AND WHOLE GENOME AMPLIFICATION

Genomic DNA (gDNA) was extracted using phenol-chloroform according to standard procedures.²⁸ The sorted nuclei were suspended in 180 µl buffer ATL and 20 µl proteinase K (Qiagen, Valencia, CA, USA) and digested overnight (8–12 h) at 56°C until completely lysed. One micro litre (10 mg/ml) of RNase A (Thermo Scientific, Vilnius, Lithuania) was added to the samples and incubated for 10 min at 37°C to digest all intrinsic RNA. Phase Lock Gel Light (5Prime, Hamburg, Germany) was used to separate aqueous and organic phases after the addition of phenol-chloroform-isoamyl alcohol (25:24:1) mixture, and isopropanol was used for protein denaturation and DNA precipitation. Precipitated DNA was washed twice with 70% ethanol, and eluted in 20 µl of nuclease-free water. Extracted gDNA was subjected to whole genome amplification according to protocol provided by the manufacturer (Sigma Cor., Cream Ridge, NJ, USA). Amplified DNA was quantified using Nanodrop system (Thermo Fischer Scientific, Waltham, MA, USA).

ARRAY COMPARATIVE GENOMIC HYBRIDIZATION

Array comparative genomic hybridization with Agilent SurePrint G3 CGH 180k arrays was performed according to protocol provided by the manufacturer and as previously described.²⁹ Commercial 46 XX gDNA (Promega, Southampton, UK) was amplified with the GenomePlex WGA2 kit, digested to the appropriate size and used for hybridization.

Results

CASE REPORTS

Case 1 is a 51 year old male patient, known to be HIV-positive since 1992, who presented in October 2011 with B symptoms, including fever, night sweats and weight loss (10 kg in 4 weeks) as well as generalized lymphadenopathy (mediastinal, hilar, axillary, retroperitoneal, mesenteric, left paraaortic, maximum diameter 34 mm) and splenomegaly (24 cm). Excisional biopsy of the right axillary lymph node was performed and diagnosis of anaplastic/plasmablastic lymphoma double positive for HHV8 and EBV corre-

sponding to extracavitary PEL was rendered. The patient was treated with steroid shock therapy (5 days prednisone 100 mg/day) and six cycles of R-CHOP. In January 2012 clinical remission was confirmed by positron emission tomography (PET) and computer tomography (CT). Maintenance rituximab mono-therapy was applied. In September 2013 the patient came back with deteriorating general condition. Lymphoma manifested as malignant effusion in the abdominal cavity. Ascitic fluid was aspirated and malignant cells were investigated, morphologically and immunophenotypically fitting well to a relapse of the previously diagnosed extracavitary PEL. There was no evidence of nodal involvement by PET-CT scan. Bone marrow biopsy showed no lymphoma infiltration. This relapse was successfully treated with salvage therapy consisting of two cycles of ACVBP regimen, which led to clinical remission. In January 2014 autologous hematopoietic stem cell transplantation was performed after BEAM conditioning. Engraftment was successful and the patient is still alive 32 months after initial diagnosis.

Case 2 is a 63 years male, who presented in April 2010 with weakness, anaemia and thrombocytopenia and was treated by blood transfusions. In August 2010 the patient complained of epigastric pain, weight loss (20 kg in 6 months) and generalized lymphadenopathy (bilateral neck, supraclavicular, mediastinal, axillar, paraaortic, maximum diameter 18 mm). Gastric endoscopy revealed exophytic subcardial tumour, which turned out to be a poorly differentiated EBV-associated adenocarcinoma. Axillar lymph node biopsy was taken and peripheral T-cell lymphoma (PTCL) was diagnosed erroneously, mainly due to CD3 positivity. In October 2010 radical gastrectomy with lymphadenectomy was performed, on which the prior diagnosis of PTCL was revised and new diagnosis of extracavitary PEL was established. Treatment with six cycles of R-CHOP 14 protocol was administered. CT scan performed in November 2010 confirmed clinical remission with diminished right neck lymphadenopathy and stable mediastinal, axillar and paraaortal lymphadenopathy. 50 months after initial diagnosis, the patient is alive without any signs of disease and with slight anaemia.

MORPHOLOGY AND IMMUNOPHENOTYPE

Histological examination of the axillar lymph node in case 1 revealed architectural lymph node effacement and multifocal infiltration by very large, anaplastic, monstrous, dis-cohesive cells with eccentrically located immunoblast-like nuclei displaying

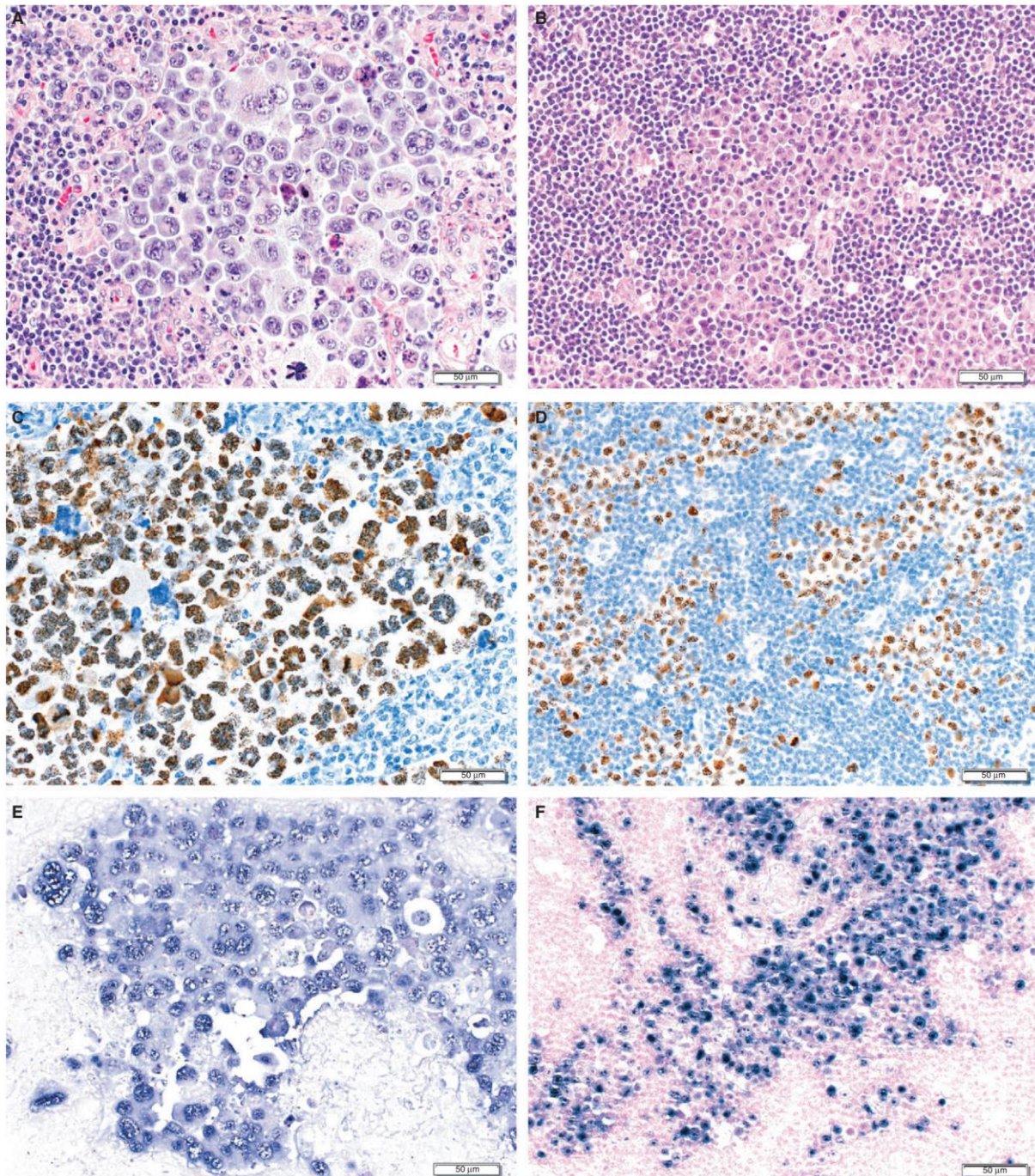


Figure 1. H&E staining of tissue sections demonstrating the morphology of tumour nuclei in case 1 (A) and case 2 (B). Tumour cells were co-infected with HHV8 (C, D) and EBV (E, F) in case 1 and case 2, respectively.

multiple atypical mitoses (Figure 1A). Full phenotypic details are provided in Table 1. Immunohistochemistry for LANA1 antigen and *in situ*

hybridization for EBER confirmed double-infection of the tumour cells by HHV8 and EBV, respectively (Figure 1C,E).

Morphologic examination of the biopsy of case 2 showed lymphoepithelioma-like lymph node effacement by medium-sized, dis-cohesive cells with eccentrically located immunoblast-like nuclei (Figure 1B). As in case 1, the tumour cells of case 2 were infected by HHV8 and EBV (Figure 1D,F). Phenotypic details are provided in Table 1.

FISH AND GENETIC ANALYSIS

Fluorescence *in situ* hybridization analysis was performed on both cases with probes detecting numerical and structural aberrations of *C-MYC*, *BCL-2* and *BCL-6* genes. No aberrations were detected. Available FISH probes verified selected deletions and amplifications detected by aCGH in the primary tumours of both cases (Figure 2 and Table 2). Monoclonal *IGH* gene rearrangements were detected in both cases, thus confirming their B lineage derivation. Rearranged fragment sizes of join (J) and variable (V) *IGH* regions were identical between the primary occurrence and the relapse of case 1, suggesting a common clonal origin of these two presentations.

SORTING OF MALIGNANT PEL CELL NUCLEI

In order to perform a meaningful genetic copy number aberration analysis by aCGH we developed a novel technique, which enables sorting and thereby enrichment of tumour cell nuclei derived from the archived FFPE tissues based on their expression of specific nuclear markers (Figure 3). FFPE tissues were dissociated by enzymatic digestion and mechanical

force to yield intact nuclei suspension. Treated nuclei retain their antigenicity and therefore can be labelled with antigen-specific monoclonal antibodies. We stained the extracted nuclei of both cases using a monoclonal antibody against viral LANA1 protein to separate malignant tumour cells nuclei from the non-malignant microenvironment, the latter accounting for $\geq 90\%$ of nuclei counts in the affected lymph nodes of both cases. In parallel, nuclei were stained with DAPI, which enabled ploidy analysis additionally assisting discrimination between intact nuclei and debris. Based on the flow cytometric analysis, there were 1.8% and 3.6% of malignant nuclei in the biopsies from case 1 and case 2, respectively. LANA1-positive nuclei were properly gated and sorted, yielding $\sim 18\,000$ and ~ 8000 of tumour nuclei in case 1 and case 2, respectively. The purity of the sorts as determined by subsequent direct morphological examination was $>90\%$.

ACGH ANALYSIS

Multiple chromosomal aberrations were detected by aCGH involving some previously reported cancer genes and also uncovering novel aberrations (Figure 4). In the primary tumour of case 1 there was a trisomy of chromosome 20, amplifications of chromosomal regions 2p25.1-p23.3 and 4p16.3-p15.1, while 4q32.2-q35.2, 12q22, 16q12.1-q24.2, 18q21.1-q22.3 regions were heterozygously deleted. The single homozygous deletion was located in Xq26.3-q28. Case 2 exhibited trisomies of chromosomes 5 and 7 as well as gain of the long arm of chromosome 15.

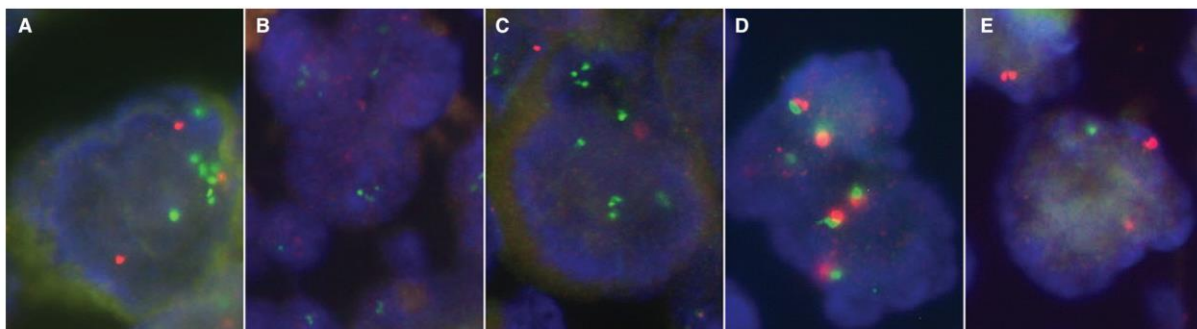


Figure 2. Available FISH probes were used to confirm chromosomal aberrations in the primary tumours of extracavitary PEL. (A) Gain of 2p25.1-p23.3 confirmed by a hybridization probe detecting *N-MYC* amplifications. Green signal – *N-MYC*; red signal – centromere 2. (B) Loss of 16q12.1-q24.2 confirmed by hybridization with *IGH/MAF* fusion probes. One copy of *MAF* at 16q22 (red signal) is lacking in the depicted nuclei. (C) Deletion of 18q21.1-q22.3 in case 1 confirmed by hybridization with probes detecting *IGH* (on chromosome 14) and *MALT1* (on chromosome 18). Red signals, representing *MALT1* at 18q21, are missing in the depicted cell nuclei. (D) three green and three red signals representing centromere 7 and the *EGFR* gene are visible, confirming trisomy 7 in case 2. (E) Loss of the 6q23.3-q27 is confirmed by the loss of one copy of *ESR1* at 6q25.1 (green signal) as compared to centromere 6 (red signal).

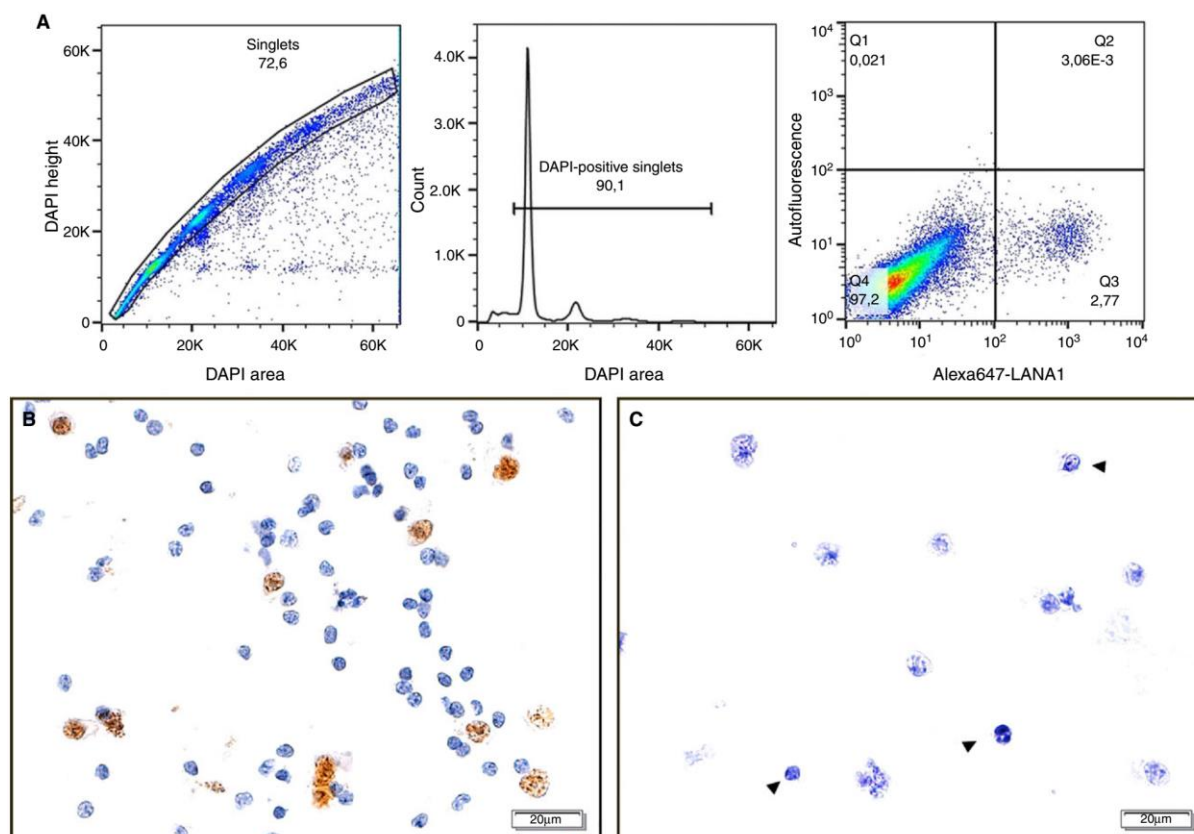


Figure 3. Labeling, analysis and sorting of nuclei extracted from the archived FFPE tissue. (A) Throughout the gating procedure (left-to-right) first the single nuclei are selected (nuclei aggregates have higher pulse area values, therefore appear below the singlet population), then debris is discriminated based on no or weaker staining with DAPI, and finally LANA1-positive population is identified (Q3). (B) Specific LANA1 antibody binding after nuclei extraction procedure confirmed by the conventional DAB-based staining. (C) Hematoxylin staining of sorted nuclei show >90% enrichment. Impurities, likely represented by HHV8-infected plasma cell nuclei are marked with arrowheads.

The single deletion was a heterozygous loss of 6q23.3-q27. On relapse, effusion cells of case 1 showed profound number of genetic aberrations scattered along the whole genome and affecting most of the chromosomes. The predominant aberration type was amplification (24 segments), eight segments were heterozygously and 1 segment homozygously deleted. Detailed information on chromosomal copy number aberrations is listed in Table 3. Chromosomal aberration analysis supported clonal relationship between the primary occurrence and relapse, which was also observable by *IGH* fragment length analysis in case 1. Both lymphoma presentations had common aberrations, namely overlapping amplifications in the short arms of chromosomes 2 and 4 as well as deletions in the chromosomes 16 and X. However, some deletions, which were present in the primary tumour, were not detectable in the relapse. For example, a

deleted stretch of Xq26.3-q28 in the primary tumour was much shorter in the relapse affecting only cytoband q27.3.

Discussion

In the present study we performed a comprehensive characterization of two extracavitary PEL, one of which later relapsed as a clonally related malignant effusion with clear genetic progression. Both primary cases were positive for HHV8 and EBV, while HIV infection in case 1 and preceding gastric carcinoma in case 2 were the expected reasons of immunodeficiency in the patients.

It is usually required that tissues contain at least 70% of tumour cells for meaningful genetic copy number aberration detection by aCGH.³⁰ Many cases of extracavitary PEL do not meet this criterion, and

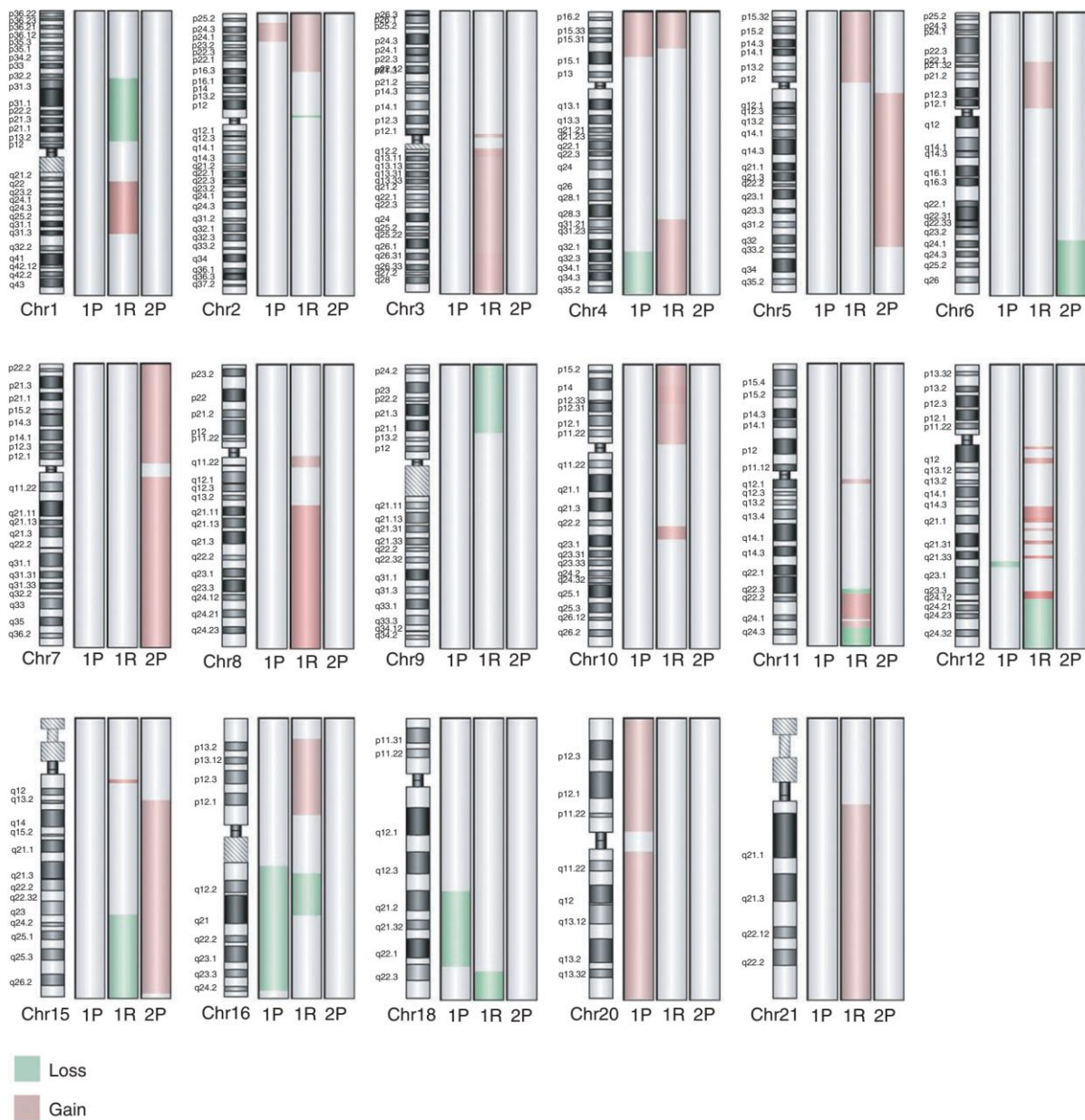


Figure 4. Chromosomal aberrations discovered in PEL cases. Aberrations are represented as coloured bars next to the ideogram and ordered from left to right as follows: primary tumour of case 1 (1P); relapse of case 1 (1R); primary tumour in case 2 (2P). Gains are marked in red, losses in green. Only the chromosomes bearing aberrations are shown.

this is one of the most important reasons why cytogenetic array-based information on this form of PEL, as well as in other tumours with low tumour cell content, is scarce. Our newly developed protocol allows extraction and staining of the FFPE tissue-derived cell nuclei based on the expression of specific nuclear protein markers, like LANA1. Although some fragmenta-

tion occurs during the preparation process of every sample, formalin fixation greatly improves the stability of extracted nuclei. Additional unspecific DNA staining with DAPI helps to discriminate between intact nuclei and debris as well as to determine ploidy of the selected populations. Stained nuclei can be enriched by fluorescence-activated cell sorting to

Table 3. Cytogenetic aberrations detected in PEL

Cytogenetic position	Start position	End position	Aberration size, MB
Case 1, primary			
Gains			
2p25.1-p23.3	8 992 704	25 841 368	16.8
4p16.3-p15.1	259 110	30 793 523	30.5
20p13-p11.21	394 577	25 492 224	25.1
20q11.21-q13.33	29 991 221	62 771 602	32.8
Losses			
4q32.2-q35.2	161 869 551	190 330 166	28.5
12q22	92 844 489	95 857 876	3.0
16q12.1-q24.2	47 630 320	87 874 092	40.2
18q21.1-q22.3	47 917 616	68 735 099	20.8
Xq26.3-q28	136 957 262	148 997 203	12.0
Case 2, primary			
Gains			
5q11.2-q33.1	53 249 259	150 925 466	97.7
7p22.3-p11.2	83 325	55 712 859	55.6
7q11.21-q36.3	64 021 202	159 118 566	95.1
15q13.2-q26.3	30 366 065	100 632 516	70.3
Losses			
6q23.3-q27	138 011 005	170 667 507	32.7
Case 1, relapse			
Gains			
1q21.2-q31.3	149 821 661	195 851 574	46.0
2p25.3-p16.3	42 444	50 992 291	50.9
3p12.1-p11.1	86 842 657	89 571 521	2.7
3q11.2-q29	96 539 898	197 845 254	101.3
4p16.3-p15.2	170 345	24 947 730	24.8
4q31.1-q35.2	140 351 759	190 747 622	50.4
5p15.33-p12	52 186	45 872 828	45.8
6p22.1-p11.2	30 271 385	58 686 125	28.4
8q11.1-q11.23	47 738 809	53 199 721	5.5
8q13.3-q24.3	72 830 487	146 294 098	73.5
10p15.3-p11.1	606 329	38 408 609	37.8
10q22.2-q23.1	77 358 301	83 730 120	6.4

Table 3. (Continued)

Cytogenetic position	Start position	End position	Aberration size, MB
11q11-q12.1	55 377 910	57 944 627	2.6
11q22.3-q24.1	110 053 514	122 203 724	12.2
11q24.1-q24.2	122 984 714	126 249 225	3.3
12q12	39 233 709	40 315 362	1.1
12q12-q13.11	44 560 942	47 128 337	2.6
12q14.3-q21.1	67 217 645	74 764 376	7.5
12q21.1	72 539 532	74 764 376	2.2
12q21.2	77 471 668	78 866 337	1.4
12q21.31	83 327 343	84 942 888	1.6
12q21.33	90 244 129	91 684 042	1.4
12q23.3-q24.11	106 821 112	110 421 465	3.6
15q11.2	22 558 697	24 005 549	1.4
16p13.3-p11.2	7 116 145	31 612 749	24.5
21q11.2-q22.3	14 771 770	48 021 818	33.3
Losses			
1p32.1-p13.2	59 828 119	115 276 698	55.4
9p24.3-p13.3	266 045	33 919 215	33.7
11q22.3	107 614 650	110 038 638	2.4
11q24.2-q25	126 278 836	134 927 114	8.6
12q24.11-q24.33	110 493 895	133 779 076	23.3
15q23-q26.3	72 051 934	102 388 476	30.3
16q12.1-q21	50 060 259	63 601 861	13.5
18q22.3-q23	70 049 344	77 862 723	7.8
Xq27.3	143 485 415	144 325 002	0.8

achieve the desired purity. Additional markers, if known, could theoretically be applied for isolation of different tumour microclones. However, since such markers are currently lacking for PEL, our approach utilizing LANA1 allowed specific tumour cell nuclei enrichment encompassing all tumour cells and, thus, all potential microclones. Previously, similar approaches have been described to separate tumour from stroma in cancers of epithelial origin.^{26,31} We further refined this approach and showed for the first time that enrichment of rare tumour populations is possible based on staining for less abundant intra-

nuclear proteins such as transcription factors or viral proteins. This method can be potentially established for a wide spectrum of nuclear marks to enrich populations of interest and allow investigation of entities where the malignant cell proportion is a concern and which were previously not accessible for genome-wide aberration analysis.

Copy number aberration profiling of both primary tumours of this study revealed relatively simple karyotypes: only four amplifications and five deletions and four amplifications and one deletion were detected in case 1 and case 2, respectively. Typically,

amplifications were gains of one additional DNA copy in the affected loci and deletions were always heterozygous. In contrast, the relapse of case 1 exhibited an extremely complex karyotype with deletions and amplifications scattering all over the genome and affecting nearly all chromosomes. Previous cytogenetic studies of primary PEL and PEL cell lines have identified recurrent aberrations in this entity, which include gains of 1q, trisomies of chromosomes 7 and 8, frequent gains of regions 12q, 19p, 20q as well as losses of 4q, 11q25 and 14q32.^{19–23} However, none of the studies have focused their attention to extracavitary manifestation of PEL. Luan *et al.* reported cytogenetic data on four out of nine investigated extracavitary PEL cases. Although the reasons for exclusion of five cases from the cytogenetic analysis were not detailed, based on our experience we believe that it might have been due to little amount of available material or to the low percentage of tumour cells in the affected tissues. On the four available cases Luan *et al.* showed that there was no significant copy number aberrations difference between solid and classic manifestations of PEL, except for gains of 11q12–13 and 13q, which were somewhat more frequent in solid PEL. We could not detect the latter two aberrations in the presently reported cases, but some of the gains and losses clearly overlapped with the recurrently affected regions in classic PEL. For example, the primary tumour of case 1 had deletion of the distal region of 4q and amplification of 20q, and the relapse showed characteristic high-level focal amplifications of 12q. Case 2 had trisomy of chromosome 7, which is reportedly detectable in 50–58% of PEL cases. So far at least four genes have been suggested as playing a role in pathogenesis of PEL on the basis of them being frequently amplified or deleted in this entity. Our data confirm the high-level amplification of 12q24.1 in the relapse of case 1 containing the Coronin 1C (*CORO1C*) and Selectin P ligand (*SELPLG*) genes. Additionally, WW domain containing oxidoreductase (*WWOX*) was found heterozygously deleted in the primary tumour of case 1, while the fourth reported candidate, fragile histidine triad (*FHIT*), was not affected in any case.

In addition, we for the first time demonstrate (cyto)genetically a direct clonal relationship and a genomic progression of a solid and an effusion manifestation of PEL in the same patient. Despite the fact that the primary and relapse were separated by almost 2 years, they clearly had overlapping chromosomal copy number aberrations and displayed the same *IGH* rearrangement. Importantly, not all deletions

observed in the primary tumour were present in the relapse. This suggests the existence of multiple malignant clones which, after branching from a putative chemoresistant tumour stem cell underwent an independent genetic evolution. In line with our observation, the existence of multiple cytogenetically related abnormal clones as an evidence of clonal evolution in classic PEL has been previously noticed.²³

Extracavitary manifestation is the main difference separating classic PEL and solid PEL. Solid tumour masses, as in the presently reported cases, are most often nodal, although alternative locations have been observed and include the chest wall, skin, atrium, gastrointestinal tract and others.^{16,32,33} A study of Chadburn *et al.* concluded that the only identifiable difference between immunophenotypes of classic and solid PEL was that the latter more often expressed B cell-associated antigens and Ig. However, this observation was not confirmed by a more recent and more comprehensive study.¹³ Instead Pan *et al.* reported the most significant differences being the expression of CD45 and CD3. The former was less frequently expressed in solid PEL compared to classic PEL (74% versus 94%), whereas the opposite was true for the latter (23% and 6%, respectively). Less significant but still notable was the higher expression of CD138 and CD30 in extracavitary PEL. In accordance to these data, both our cases were positive for CD3 and only weakly positive for CD45. Interestingly, only case 2 showed surface Ig light and heavy chain expression, although genes were rearranged in both cases.

Primary effusion lymphoma is an aggressive tumour with median survival ranging from 1.5 to 6 months and 1 year overall survival rate of 39.3%. Extracavitary PEL has a better median survival of 11 months.^{16,18} Both of our patients are still alive 32 and 50 months after initial diagnosis and probably belong to the sub-set of PEL patients with relatively favourable outcome.^{16,34,35} From the clinical point of view case 1 could be regarded as a more conventional manifestation. It affected a patient with a long-standing history of HIV infection and the disease course was more aggressive as it relapsed with life-threatening malignant effusion. His outcome was still favourable possibly due to adequate treatment, well-managed HIV infection and relatively young age of the patient. On the other hand, case 2 is more unconventional, arising in the context of EBV-associated gastric carcinoma, which was also the only likely cause of immunosuppression. EBV-associated gastric tumours predominantly arise in men, with no evident age dependence and even geographical distribution pattern, suggesting that a risk from lifestyle or

occupational factors may exist.³⁶ Apart from the general cancer-attributable immunosuppression, EBV-infection in our case was the only unifying feature between extracavitary PEL and gastric carcinoma. Importantly, EBV is 1000–10 000 times more effectively transmitted to epithelial cells via direct cell-to-cell contact with infected B-lymphocytes than via cell-free infection pathway. This suggests that probably EBV first spread into the B-cell pool prior to involvement of the gastric epithelia. However, the timing of co-infection with HHV8 in the B-cells remains unknown. It can be speculated that co-infection occurred at the time of decreased immunocompetence caused by the gastric tumour. No presence of HHV8-infected lymphocytes was observable in the gastric carcinoma. The favourable disease course of the PEL in this patient might be, in addition to its chemosensitivity to R-CHOP, related to the restored immune function after gastrectomy.

In conclusion, we present a comprehensive characterization of two PEL cases manifesting as solid tumour masses in the lymph nodes, one of which relapsed as malignant effusion 2 years later. A newly developed protocol allowed us to enrich tumour nuclei from FFPE tissue from ~1–4% to >90%, and enabled us to perform reliable molecular analyses demonstrating the feasibility of this approach for further molecular studies of tumours with low malignant cell counts.

Acknowledgements

The research was supported by the 'Krebsliga beider Basel'.

Author contributions

Darius Juskevičius: developed nuclei sorting technique, performed the experiments and wrote the manuscript; Tanja Dietche: performed nuclei sorting and data analysis; Thomas Lorber, Alexander Ruffe: developed nuclei sorting technique and contributed to data analysis; Christian Ruiz: contributed essential reagents and tools, critically revised the manuscript and contributed to data analysis; Ugnius Mickys: contributed patient samples, evaluated immunohistochemical stainings, critically revised manuscript; Fatime Kraniqi: contributed clinical data, critically revised the manuscript; Stephan Dirnhofer: evaluated immunohistochemical stainings, critically revised the manuscript; Alexandar Tzankov: designed the research study, eval-

uated immunohistochemical stainings, analyzed the data, wrote and critically revised the manuscript.

Ethics committee approval

Ref. Nr. 92/12; Ethikkommission beider Basel; 17.04.2012.

Conflict of interests

The authors have no conflicts of interest to disclose.

References

1. Jones D, Ballesta ME, Kaye KM *et al.* Primary-effusion lymphoma and Kaposi's sarcoma in a cardiac-transplant recipient. *N. Engl. J. Med.* 1998; **339**: 444–449.
2. Kapelushnik J, Ariad S, Benharroch D *et al.* Post renal transplantation human herpesvirus 8-associated lymphoproliferative disorder and Kaposi's sarcoma. *Br. J. Haematol.* 2001; **113**: 425–428.
3. Makis W, Stern J. Hepatitis C-related primary effusion lymphoma of the pleura and peritoneum, imaged with F-18 FDG PET/CT. *Clin. Nucl. Med.* 2010; **35**: 797–799.
4. Yiakoumis X, Pangalis GA, Kyrtsonis MC *et al.* Primary effusion lymphoma in two HIV-negative patients successfully treated with pleurodesis as first-line therapy. *Anticancer Res.* 2010; **30**: 271–276.
5. Swerdlow SH, Campo E, Harris NL *et al.* *WHO classification of tumours of haematopoietic and lymphoid tissues*, 4th ed. Lyon: IARC Press, 2008; 260–262.
6. Nador RG, Cesarman E, Chadburn A *et al.* Primary effusion lymphoma: a distinct clinicopathologic entity associated with the Kaposi's sarcoma-associated herpes virus. *Blood* 1996; **88**: 645–656.
7. Cesarman E, Chang Y, Moore PS, Said JW, Knowles DM. Kaposi's sarcoma-associated herpesvirus-like DNA sequences in AIDS-related body-cavity-based lymphomas. *N. Engl. J. Med.* 1995; **332**: 1186–1191.
8. Jenner RG, Maillard K, Cattini N *et al.* Kaposi's sarcoma-associated herpesvirus-infected primary effusion lymphoma has a plasma cell gene expression profile. *Proc. Natl Acad. Sci. USA* 2003; **100**: 10399–10404.
9. Klein U, Ghoghini A, Gaidano G *et al.* Gene expression profile analysis of AIDS-related primary effusion lymphoma (PEL) suggests a plasmablastic derivation and identifies PEL-specific transcripts. *Blood* 2003; **101**: 4115–4121.
10. Huang Q, Chang KL, Gaal K, Arber DA. Primary effusion lymphoma with subsequent development of a small bowel mass in an HIV-seropositive patient: a case report and literature review. *Am. J. Surg. Pathol.* 2002; **26**: 1363–1367.
11. DePond W, Said JW, Tasaka T *et al.* Kaposi's sarcoma-associated herpesvirus and human herpesvirus 8 (KSHV/HHV8)-associated lymphoma of the bowel. Report of two cases in HIV-positive men with secondary effusion lymphomas. *Am. J. Surg. Pathol.* 1997; **21**: 719–724.
12. Costes V, Faumont N, Cesarman E *et al.* Human herpesvirus-8-associated lymphoma of the bowel in human immunodeficiency virus-infected patients. *Am. J. Surg. Pathol.* 1997; **21**: 719–724.

- ciency virus-positive patients without history of primary effusion lymphoma. *Hum. Pathol.* 2002; **33**: 846–849.
13. Pan ZG, Zhang QY, Lu ZB et al. Extracavitary KSHV-associated large B-Cell lymphoma: a distinct entity or a subtype of primary effusion lymphoma? Study of 9 cases and review of an additional 43 cases. *Am. J. Surg. Pathol.* 2012; **36**: 1129–1140.
 14. Kim Y, Leventaki V, Bhajee F, Jackson CC, Medeiros LJ, Vega F. Extracavitary/solid variant of primary effusion lymphoma. *Ann. Diagn. Pathol.* 2012; **16**: 441–446.
 15. Carbone A, Cesarman E, Spina M, Ghoghini A, Schulz TF. HIV-associated lymphomas and gamma-herpesviruses. *Blood* 2009; **113**: 1213–1224.
 16. Chadburn A, Hyjek E, Mathew S, Cesarman E, Said J, Knowles DM. KSHV-positive solid lymphomas represent an extra-cavitary variant of primary effusion lymphoma. *Am. J. Surg. Pathol.* 2004; **28**: 1401–1416.
 17. Simonelli C, Spina M, Cinelli R et al. Clinical features and outcome of primary effusion lymphoma in HIV-infected patients: a single-institution study. *J. Clin. Oncol.* 2003; **21**: 3948–3954.
 18. Boulanger E, Gerard L, Gabarre J et al. Prognostic factors and outcome of human herpesvirus 8-associated primary effusion lymphoma in patients with AIDS. *J. Clin. Oncol.* 2005; **23**: 4372–4380.
 19. Luan SL, Boulanger E, Ye H et al. Primary effusion lymphoma: genomic profiling revealed amplification of SELPLG and CORO1C encoding for proteins important for cell migration. *J. Pathol.* 2010; **222**: 166–179.
 20. Roy D, Sin SH, Damania B, Dittmer DP. Tumor suppressor genes FHIT and WWOX are deleted in primary effusion lymphoma (PEL) cell lines. *Blood* 2011; **118**: 32–39.
 21. Mullaney BP, Ng VL, Herndier BG, McGrath MS, Pallavicini MG. Comparative genomic analyses of primary effusion lymphoma. *Arch. Pathol. Lab. Med.* 2000; **124**: 824–826.
 22. Nair P, Pan H, Stallings RL, Gao SJ. Recurrent genomic imbalances in primary effusion lymphomas. *Cancer Genet. Cytogenet.* 2006; **171**: 119–121.
 23. Wilson KS, McKenna RW, Kroft SH, Dawson DB, Ansari Q, Schneider NR. Primary effusion lymphomas exhibit complex and recurrent cytogenetic abnormalities. *Br. J. Haematol.* 2002; **116**: 113–121.
 24. Meier VS, Ruffe A, Gudat F. Simultaneous evaluation of T- and B-cell clonality, t(11;14) and t(14;18), in a single reaction by a four-color multiplex polymerase chain reaction assay and automated high-resolution fragment analysis: a method for the rapid molecular diagnosis of lymphoproliferative disorders applicable to fresh frozen and formalin-fixed, paraffin-embedded tissues, blood, and bone marrow aspirates. *Am. J. Pathol.* 2001; **159**: 2031–2043.
 25. Barrett MT, Lenkiewicz E, Evers L et al. Clonal evolution and therapeutic resistance in solid tumors. *Front. Pharmacol.* 2013; **4**: 1–15.
 26. Holley T, Lenkiewicz E, Evers L et al. Deep clonal profiling of formalin fixed paraffin embedded clinical samples. *PLoS One* 2012; **7**: e50586.
 27. Ruiz C, Lenkiewicz E, Evers L et al. Advancing a clinically relevant perspective of the clonal nature of cancer. *Proc. Natl Acad. Sci. USA* 2011; **108**: 12054–12059.
 28. Sambrook J, Fritsch EF, Maniatis T. *Molecular cloning: a laboratory manual*. New York: Cold Spring Harbor Laboratory, 1989; 47–54.
 29. Juskevičius D, Ruiz C, Dirnhofer S, Tzankov A. Clinical, morphologic, phenotypic, and genetic evidence of cyclin D1-positive diffuse large B-cell lymphomas with CYCLIN D1 gene rearrangements. *Am. J. Surg. Pathol.* 2014; **38**: 719–727.
 30. Johnson NA, Hamoudi RA, Ichimura K et al. Application of array CGH on archival formalin-fixed paraffin-embedded tissues including small numbers of microdissected cells. *Lab. Invest.* 2006; **86**: 968–978.
 31. Corver WE, ter Haar NT. High-resolution multiparameter DNA flow cytometry for the detection and sorting of tumor and stromal subpopulations from paraffin-embedded tissues. *Curr. Protoc. Cytom.* 2009; **6**: 6–27.
 32. Marak CP, Ponea AM, Shim C, Shaheen S, Guddati AK. Extracavitary manifestation of primary effusion lymphoma as a right atrial mass. *Case Rep. Oncol.* 2013; **6**: 114–118.
 33. Deloose ST, Smit LA, Pals FT, Kersten MJ, van Noesel CJ, Pals ST. High incidence of Kaposi sarcoma-associated herpesvirus infection in HIV-related solid immunoblastic/plasmablastic diffuse large B-cell lymphoma. *Leukemia* 2005; **19**: 851–855.
 34. D'Antonio A, Boscaino A, Addesso M, Piris MA, Nappi O. KSHV- and EBV-associated germinotropic lymphoproliferative disorder: a rare lymphoproliferative disease of HIV patient with plasmablastic morphology, indolent course and favourable response to therapy. *Leuk. Lymphoma* 2007; **48**: 1444–1447.
 35. Kumode T, Ohyama Y, Kawauchi M et al. Clinical importance of human herpes virus-8 and human immunodeficiency virus infection in primary effusion lymphoma. *Leuk. Lymphoma* 2013; **54**: 1947–1952.
 36. Iizasa H, Nanbo A, Nishikawa J, Jinushi M, Yoshiyama H. Epstein-Barr Virus (EBV)-associated gastric carcinoma. *Viruses* 2012; **4**: 3420–3439.

3.3 Follicular lymphoma transformation into histiocytic sarcoma: indications for a common neoplastic progenitor

Brunner P., Ruffe A., Dirnhofer S., Lohri A., Willi N., Cathomas G., Tzankov A., **Juskevicius D.**

-Letter to the editor-
Published in *Leukemia*, 2014

Contribution: I performed genetic characterization of the case, analyzed data, prepared figures and wrote major parts of the manuscript

Follicular lymphoma transformation into histiocytic sarcoma: indications for a common neoplastic progenitor

Leukemia (2014) **28**, 1937–1940; doi:10.1038/leu.2014.167

Histiocytic sarcomas are rare, poorly differentiated neoplasms with histiocytic phenotype.¹ The 2001 World Health Organization (WHO) classification of hematopoietic and lymphoid tissues depended on the absence of clonal B- or T-cell receptor rearrangements to establish a diagnosis of histiocytic sarcoma.² Nevertheless, some unequivocal cases of histiocytic sarcomas with immunoglobulin heavy chain (*IgH*) gene rearrangements have been described.³ Consequently, the current WHO classification of 2008 no longer excludes cases with *IgH* or T-cell receptor (*TCR*) gene rearrangements, but classifies them as examples of transdifferentiation from one hematopoietic cell lineage to another.¹ However, the process of transformation remains to be delineated. Three models are currently being considered to explain it: (1) direct transdifferentiation; (2) dedifferentiation followed by re-differentiation; and (3) evolution from a common progenitor.^{4–7} Here we provide evidence of a common neoplastic

progenitor clone in a patient who had a longstanding history of follicular lymphoma (FL), which later on transformed into histiocytic sarcoma.

A 75-year-old female was diagnosed with FL grade II in March 2007. Computed tomographic evaluation revealed diffusely enlarged lymph nodes on both sides of the diaphragm and splenomegaly. A bone marrow biopsy showed 80% infiltration by the FL. According to the FL international prognostic index, the patient was classified into the high-risk group and received five cycles of R-CHOP (rituximab, cyclophosphamide, hydroxydaunorubicin, oncovin, prednisone) therapy with two additional cycles of rituximab. In January 2008, complete remission was confirmed by clinical, radiological and laboratory findings. In April 2009, the patient relapsed and treatment with rituximab and bendamustine was initiated. Again, complete remission was achieved as assessed by positron emission tomography/computed tomography scan and bone marrow histology. In March 2011 second recurrence occurred, documented by lymph node biopsy. There was no evidence of transformation, and the patient received prednisone

Accepted article preview online 21 May 2014; advance online publication, 13 June 2014

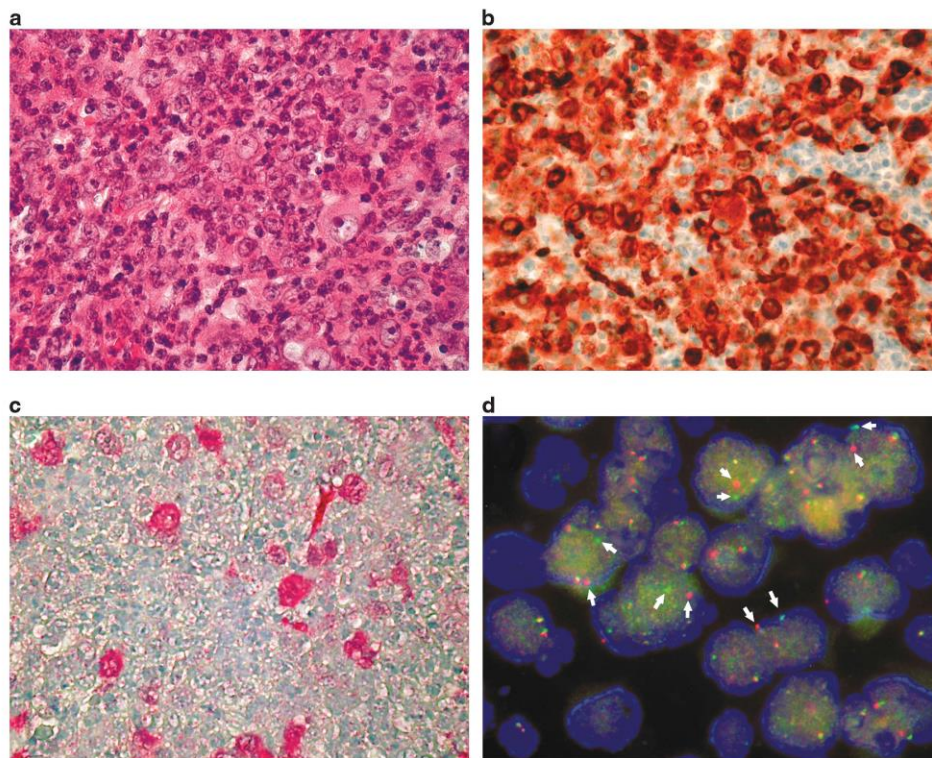


Figure 1. Histiocytic sarcoma (**a**, hematoxylin and eosin, $\times 360$) showing positivity for CD163 (**b**) and weak and patchy expression of S100 (**c**) as well as *BCL2* gene rearrangement with separated green and red signals per the applied fluorescent *in situ* hybridization break-apart probe. Separated signals are marked by arrows (**d**).

and ofatumumab treatments followed by combined therapy with chlorambucil, prednisone, cladribine and rituximab. However, no response was observed. A treatment attempt with lenalidomide was terminated due to adverse effects. In September 2012, radiation therapy with a total of 4 Gy of the left axillary and inguinal region was performed due to symptomatic lymph node enlargement. A resected lymph node at this time showed infiltration of the known FL without evidence of transformation. In February 2013 the patient presented with rapidly enlarging cervical lymphadenopathy and deterioration of her general condition. Imaging studies revealed necrotic cervical lymph nodes, and a diagnostic lymph node excision resulted in the integrative diagnosis of histiocytic sarcoma. In April 2013, the patient died due to progressive disease and decreasing general condition.

Microscopic evaluation of the biopsy from April 2013 revealed diffuse infiltration of non-cohesive large pleomorphic cells (25–40 μm) with extensive effacement of the underlying lymph node architecture (Figure 1a). The neoplastic cells were round to oval in shape with abundant pinkish cytoplasm, eccentrically located large vesicular nuclei and big nucleoli. Immunohistochemically, the cells were negative for B- and T-cell markers. Markers for follicular dendritic cells (CD21, CD23 and CD35), Langerhans cells (CD1a and Langerin) and plasmacytoid dendritic cells (CD123 and TCL1) were also negative. However, the tumor cells strongly stained for CD163 and CD4, and showed weak and patchy positivity for CD45, S100 and CD43 (Figures 1b and c). Staining for CD68 was negative. The morphology and immunoprofile were consistent with the diagnosis of a histiocytic sarcoma.

Fluorescent *in situ* hybridization analysis with a break-apart probe revealed *BCL2* gene rearrangements in 70% and 80% of the cells of FL (assessed on the diagnostic biopsy from 2007) and histiocytic sarcoma, respectively (Figure 1d). PCR assay showed fused *IGH-BCL2* amplicons of 260 bp in both entities. Their identity was confirmed by sequencing. Furthermore, identical clonal *IGH* gene rearrangements were detected in the primary FL and the histiocytic sarcoma. Taken together, this evidence shows B-cell lineage derivation of the transformed histiocytic cells and also a common clonal origin of the two malignancies.

In addition, using Agilent SurePrint microarrays (Agilent Technologies, Santa Clara, CA, USA) with median 13 kb resolution, array-comparative genomic hybridization (aCGH) was performed from the formalin-fixed paraffin-embedded tissue samples of initial diagnosis, second recurrence and persistence of FL, as well as at the time of transformation into histiocytic sarcoma (Figure 2). Surprisingly, the histiocytic sarcoma had no detectable copy number aberrations. Searching for possible driver mutations *BRAF*, *NRAS*, *KRAS* and *TP53* genes were sequenced, but showed no sequence alterations. Conversely, FL exhibited a substantial number of chromosomal aberrations in the primary and relapse occurrences. The availability of sequential FL samples allowed tracking of tumor genetic evolution at progression. Some aberrations were common to all investigated time points, suggesting a common progenitor and linear mode of evolution (Figure 2, set A). Only the primary FL tumor showed intratumoral heterogeneity as calculated from log₂ ratio imbalances in the aCGH data. Two heterozygous deletions, affecting 4p15.2-p14 and 6q23.3-q24.1 (Figure 2, set B), had a median log₂ ratio higher by

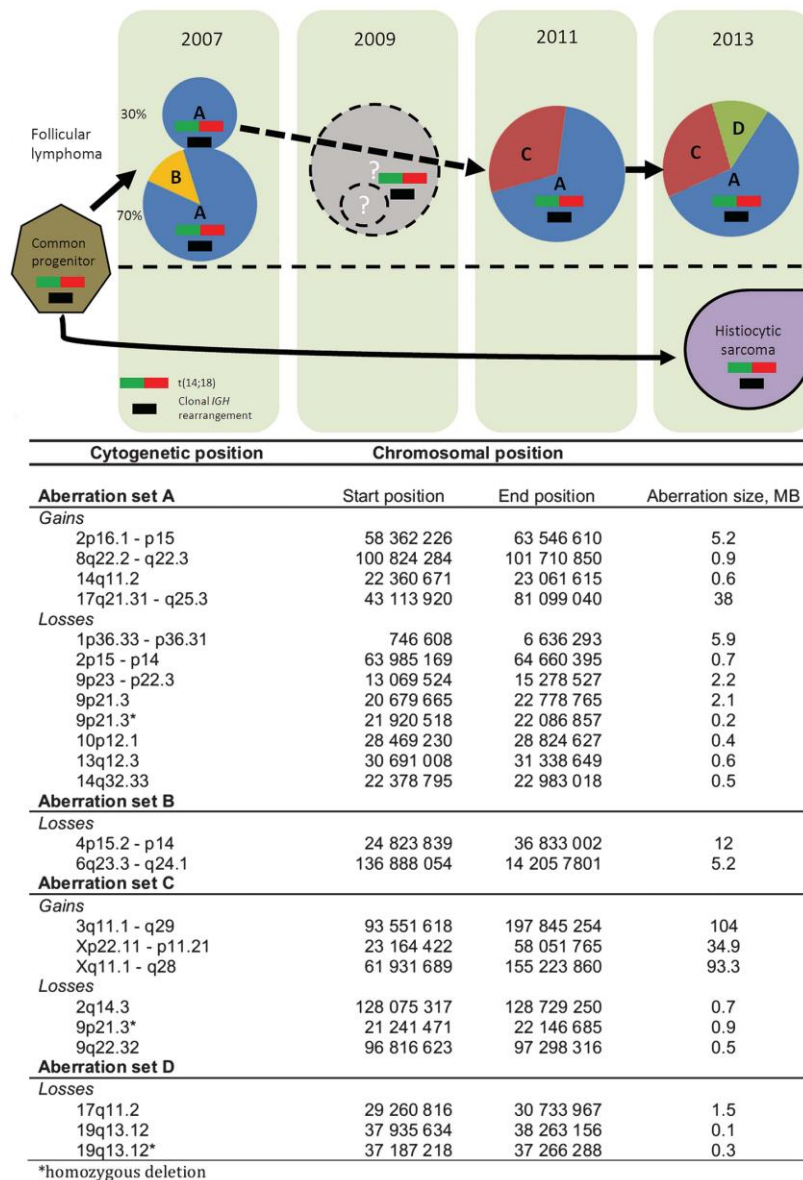


Figure 2. Copy number aberrations detected by aCGH and proposed tumor evolution model. Shared clonal *IGH* rearrangement and t(14;18) are the only common genetic events unifying both types of tumors. The primary FL detected in 2007 had at least two subpopulations: the first constituted about 30% of the tumor and bore aberrations of set A; the second constituted 70% of the tumor and bore aberrations from sets A and B. The relapse in 2009 was not biopsied. Aberrations from set B were absent in the two subsequent recurrences, indicating extermination of this subpopulation by the treatment. Additional aberrations were gained at the relapses in 2011 (set C) and 2013 (set D). The histiocytic sarcoma had no detectable chromosomal imbalances. Section sizes in the circular diagrams represent the number of aberrant genomic segments. Letter codes indicate aberration sets from the below table.

0.34 compared with other deletions, indicating the presence of these two aberrations in about 70% of the tumor cells. Importantly, these two specific deletions were not detected in the subsequent relapses. The tumor gained additional aberrations at the third and fourth relapse (Figure 2, sets C and D, respectively). No intratumoral heterogeneity was evident from the aCGH data in these tumors.

Previously, Feldman *et al.* demonstrated a clonal relationship between histiocytic sarcomas and neoplastic B cells in cases arising in the background of FL. They reported eight cases of FL transforming to histiocytic cell sarcomas with the presence of t(14;18) and identical *IGH* gene rearrangements between two entities. These investigators proposed a model of transdifferentiation from B-cell into histiocytic lineage, a thesis

reinforced by the observation that histiocytic and dendritic cell tumors lacked PAX5 expression and showed upregulation of CEBP-beta and PU.1.⁴

The second proposed model postulates dedifferentiation of neoplastic B cells followed by re-differentiation into different lineages.⁷ Again, PAX5 is thought to play a central role in this process, as decreased expression of PAX5 drives B-cell dedifferentiation into uncommitted precursors⁸ and differentiation into mature and functional T cells.⁹

In the present case, tumor cells of the histiocytic sarcoma showed clonal IGH rearrangement identical to that in FL and presence of t(14;18), indicating a clonal relationship between the two entities. Notably, the neoplastic cells of FL stained positively for PAX5, but no staining was observed in the histiocytic sarcoma.

Until now there are no published molecular cytogenetic data on histiocytic sarcomas evolving in the background of indolent B-cell lymphomas. Relationships between preceding indolent lymphomas and subsequent histiocytic sarcomas are grounded solely on common clonal IGH rearrangements or characteristic chromosomal translocations. Lost expression of tumor suppressors PTEN (5/10 cases studied) and p16INK4A (4/10 cases studied) due to deletion or promoter hypermethylation have been shown in human histiocytic sarcomas.¹⁰ Another study found the chronic lymphocytic leukemia-typical deletions in 13q and 17p in one case of histiocytic sarcoma occurring synchronously with chronic lymphocytic leukemia bearing del17p.¹¹ Surprisingly, whereas the presently investigated FL exhibited profound gains and losses of genetic material on aCGH, no aberrations were detected in the histiocytic sarcoma. This is an important finding because it shows, at least in our case, that histiocytic sarcoma could not have developed from the malignant FL cells either by direct transdifferentiation or by dedifferentiation, as the genetic aberrations in the FL component, especially genomic losses, are irreversible. Instead, our result fits best to the third and least favored model of a common progenitor clone giving rise to both neoplasms. IGH rearrangement and its faulty product, chromosomal translocations, occur relatively early in B-cell maturation during the pro-B and pre-B developmental stages.¹² It has been long known that pro-B cells retain plasticity and can be induced to differentiate into different lineages such as dendritic cells.¹³ Moreover, murine pre-B-1 cells already bearing D-J rearranged IGH genes can differentiate in the absence of PAX5 into various hematopoietic cell types, including macrophages.¹⁴ These findings support our proposed model of neoplastic evolution (Figure 2): An early putative pre-neoplastic B-cell clone characterized by clonal IGH rearrangement and t(14;18) developed in the bone marrow and initially gave rise to a FL that underwent a clonal evolution, accumulating genetic aberrations as it progressed. Later, possibly triggered by treatments targeting the FL, the pre-neoplastic B-cell clone differentiated along the myeloid lineage into a neoplastic population of histiocytes.

The availability of the unique set of samples from our case study, including primary tumor and those of two relapses, allowed us to closely document the evolution of FL. It has recently been demonstrated that intratumoral heterogeneity can be detected in different lymphoma entities by evaluating log2 ratio imbalances in the aCGH data.¹⁵ Previously, Schmid *et al.* found subclonal heterogeneity in two FL *in situ* and one FL with partial involvement.¹⁶ In line with these findings, we detected at least two different subpopulations in the primary FL. According to our proposed model, one of these subpopulations was exterminated by the treatment, whereas the other survived and gave rise to the subsequent clonally related relapses. Tumor cells followed linear path of evolution, gaining additional copy number aberrations at each relapse.

In summary, we provide further evidence for transformation of indolent B-cell lymphomas into aggressive histiocytic and dendritic cell sarcomas with molecular data on genetic tumor evolution. Our observations point toward the existence of a

putative common progenitor B-cell clone bearing IGH rearrangements and t(14;18) with the propensity to divergently differentiate into histiocytic and dendritic cell sarcoma. The previously favored hypothesis of direct low-grade lymphoma 'transdifferentiation' into histiocytic and dendritic cell sarcoma is not supported by the genetic microdissection of our studied case.

CONFLICT OF INTEREST

The authors declare no conflict of interest.

ACKNOWLEDGEMENTS

This work was supported by the Krebsliga beider Basel and Stiftung zur Krebsbekämpfung Zürich.

P Brunner¹, A Ruffe², S Dirnhofer², A Lohri³, N Willi¹, G Cathomas¹, A Tzankov^{2,4} and D Juskevicius^{2,4}

¹Institute of Pathology, Kantonsspital Baselland, Liestal, Switzerland;

²Institute of Pathology, University Hospital of Basel, Basel, Switzerland and

³Oncology/Hematology, Medical University Clinic, Kantonsspital, Liestal, Switzerland

E-mail: alexandar.tzankov@usb.ch

⁴These authors contributed equally to this work.

REFERENCES

- 1 Swerdlow SH, Campo E, Harris NL, Jaffe ES, Pileri SA, Stein H *et al.* WHO Classification of Tumours of Haematopoietic and Lymphoid Tissues. 4th edn. (IARC Press: Lyon, 2008).
- 2 Jaffe ES, Harris NL, Stein H, Vardiman J. WHO Classification of Tumours of Haematopoietic and Lymphoid Tissues. 3rd edn. (IARC Press: Lyon, France, 2001).
- 3 Vos JA, Abbondanzo SL, Barekman CL, Andriko JW, Miettinen M, Aguilera NS. Histiocytic sarcoma: a study of five cases including the histiocyte marker CD163. *Mod Pathol* 2005; **18**: 693–704.
- 4 Feldman AL, Arber DA, Pittaluga S, Martinez A, Burke JS, Raffeld M *et al.* Clonally related follicular lymphomas and histiocytic/dendritic cell sarcomas: evidence for transdifferentiation of the follicular lymphoma clone. *Blood* 2008; **111**: 5433–5439.
- 5 Wang E, Hutchinson CB, Huang Q, Sebastian S, Rehder C, Kanaly A *et al.* Histiocytic sarcoma arising in indolent small B-cell lymphoma: report of two cases with molecular/genetic evidence suggestive of a 'transdifferentiation' during the clonal evolution. *Leuk Lymphoma* 2010; **51**: 802–812.
- 6 Zeng W, Meck J, Cheson BD, Ozdemirli M. Histiocytic sarcoma transdifferentiated from follicular lymphoma presenting as a cutaneous tumor. *J Cut Pathol* 2011; **38**: 999–1003.
- 7 Takahashi E, Nakamura S. Histiocytic sarcoma: an updated literature review based on the 2008 WHO classification. *J Clin Exp Hematol* 2013; **53**: 1–8.
- 8 Cobaleda C, Schebesta A, Delogu A, Busslinger M. Pax5: the guardian of B cell identity and function. *Nat Immunol* 2007; **8**: 463–470.
- 9 Cobaleda C, Jochum W, Busslinger M. Conversion of mature B cells into T cells by dedifferentiation to uncommitted progenitors. *Nature* 2007; **449**: 473–477.
- 10 Carrasco DR, Fenton T, Sukhdeo K, Protopopova M, Enos M, You MJ *et al.* The PTEN and INK4A/ARF tumor suppressors maintain myeloid lymphoid homeostasis and cooperate to constrain histiocytic sarcoma development in humans. *Cancer Cell* 2006; **9**: 379–390.
- 11 Shao H, Xi L, Raffeld M, Feldman AL, Ketterling RP, Knudson R *et al.* Clonally related histiocytic/dendritic cell sarcoma and chronic lymphocytic leukemia/small lymphocytic lymphoma: a study of seven cases. *Mod Pathol* 2011; **24**: 1421–1432.
- 12 LeBien TW, Tedder TF. B lymphocytes: how they develop and function. *Blood* 2008; **112**: 1570–1580.
- 13 Björck P, Kincade PW. CD19+ pro-B cells can give rise to dendritic cells in vitro. *J Immunol* 1998; **161**: 5795–5799.
- 14 Rolink AG. B-cell development and pre-B-1 cell plasticity in vitro. *Methods Mol Biol* 2004; **271**: 271–281.
- 15 Umino A, Nakagawa M, Utsunomiya A, Tsukasaki K, Taira N, Katayama N *et al.* Clonal evolution of adult T-cell leukemia/lymphoma takes place in the lymph nodes. *Blood* 2011; **117**: 5473–5478.
- 16 Schmidt J, Salaverria I, Haake A, Bonzheim I, Adam P, Montes-Moreno S *et al.* Increasing genomic and epigenomic complexity in the clonal evolution from in situ to manifest t(14;18)-positive follicular lymphoma. *Leukemia* 2013; **28**: 1103–1112.

3.4 Clinical, morphologic, phenotypic, and genetic evidence of cyclin D1-positive diffuse large B-cell lymphomas with CYCLIN D1 gene rearrangements

Juskevicius D., Ruiz, C., Dirnhofer S., Tzankov A.

-Research article-

Published in *American Journal of Surgical Pathology*, 2014

Contribution: I performed the experiments, analyzed the data and wrote the manuscript

Clinical, Morphologic, Phenotypic, and Genetic Evidence of Cyclin D1-positive Diffuse Large B-cell Lymphomas With *CYCLIN D1* Gene Rearrangements

Darius Juskevicius, MSc, Christian Ruiz, PhD, Stephan Dirnhofer, MD, and Alexandar Tzankov, MD

Abstract: Overexpression of cyclin D1 in diffuse large B-cell lymphomas (DLBCLs) is observable in about 5% of cases and is linked to gains of additional *CYCLIN D1* gene copies or deregulation at the mRNA level. All cyclin D1-positive DLBCL cases reported so far lack the canonical t(11;14)(q13;q32) translocation that is a genetic hallmark and the primary cause of cyclin D1 overexpression in mantle cell lymphoma (MCL). Using standard histologic and genetic techniques, complemented with genome-wide aberration analysis by array comparative genomic hybridization, we characterized 2 exceptional cases of blastoid B-cell lymphomas with cyclin D1 overexpression, both bearing genetic rearrangements in the *CYCLIN D1* gene locus. One of them had a t(11;14)(q13;q32) translocation and featured morphology, immunophenotype, and genetic copy number aberrations typical of DLBCL. The second case had a complex t(4;11;14) translocation, but the other features were intermediate between DLBCL and MCL and did not allow unambiguous classification in any of the current diagnostic lymphoma categories. On the basis of these findings, we conclude that detection of t(11;14) should not preclude a diagnosis of cyclin D1-positive DLBCL when all other parameters are in agreement with such a diagnosis. Moreover, a yet unacknowledged diagnostic “gray zone” may exist between DLBCL and MCL.

Key Words: cyclin D1, diffuse large B-cell lymphoma, mantle cell lymphoma, gray zone lymphoma, t(11; 14)

(*Am J Surg Pathol* 2014;38:719–727)

Cyclin D1 is encoded by the *CYCLIN D1* (*CCND1*) gene, which is located on the long arm of chromosome 11 and is a member of the cyclin protein family involved in cell cycle regulation, more precisely in G₁-S transition, thus perpetuating cell proliferation.^{1,2}

Overexpression of cyclin D1 protein is implicated in several types of human cancer. Among hematopoietic and

lymphoid tumors, it is found to be overexpressed in > 90% of mantle cell lymphomas (MCLs),³ about 40% of plasma cell myelomas,⁴ and in a significant proportion of hairy cell leukemias.^{5,6} Aberrant expression of *CCND1* in the majority of MCL and plasma cell myeloma patients is attributed to t(11;14)(q13;q32) chromosomal translocation, which juxtaposes the immunoglobulin heavy chain (*IGH*) gene to the *CCND1* gene.⁷ In hairy cell leukemia translocations involving *CCND1* are rarely detected, and overexpression is thought to occur due to gains of additional gene copies or deregulation at the mRNA level.^{4,8} The latter mechanism is the least described and remains quite speculative.

Diffuse large B-cell lymphomas (DLBCLs) are aggressive B-cell neoplasms with heterogenous morphology, phenotype, and genetic features.⁹ Cyclin D1 overexpression is considered a rare feature in this entity. Initial studies failed to demonstrate cyclin D1 positivity in large cohorts of DLBCL,^{10,11} and several recent studies found its overexpression in 1.5% to 15% of cases.^{12–14} All cyclin D1-positive DLBCLs reported so far were negative for t(11;14)(q13;q32) and often showed a distinct immunophenotype (CD5⁻, SOX11⁻, CD10⁻, MUM1⁺, BCL6⁺), distinguishing them from the blastoid or pleomorphic variants of MCL.

Here, we report 2 lymphoma patients with overexpression of cyclin D1 and translocations that affected *CCND1*. On the basis of their morphologic and immunophenotypic characteristics as well as genetic copy number aberrations, we classified them as cyclin D1-positive DLBCL and cyclin D1-positive aggressive B-cell lymphoma with features intermediate between DLBCL and MCL, thus challenging the dogma that detection of t(11;14) translocation precludes diagnosis of DLBCL and suggesting a new “gray zone” (the term “gray zone lymphoma” is being used in its general sense here, and further in this paper it refers to lymphoid tumors that cannot be assigned to a defined lymphoma entity because of morphologic, clinical, or genetic reasons) within the diagnostic category of DLBCL.

MATERIALS AND METHODS

Patient Samples

Formalin-fixed, paraffin-embedded lymph node biopsies from the Institute of Pathology, University Hospital

From the Institute of Pathology, University Hospital, Basel, Switzerland. Conflicts of Interest and Source of Funding: Supported by “Krebsliga Beider Basel” foundation. The authors have disclosed that they have no significant relationships with, or financial interest in, any commercial companies pertaining to this article.

Correspondence: Alexandar Tzankov, MD, Institute of Pathology, University Hospital, Schoenbeinstrasse 40, Basel CH-4031, Switzerland (e-mail: alexandar.tzankov@usb.ch).

Copyright © 2013 by Lippincott Williams & Wilkins

Basel, were used. Retrieval of tissue and data were according to the regulations of the local institutional review boards and data safety laws.

Immunohistochemistry

Immunohistochemistry was performed on serial tissue sections using an automated immunostainer Benchmark XT (Ventana/Roche) with a biotin-streptavidin peroxidase detection system according to the manufacturer's protocols. For antigen retrieval, tissue sections were immersed and microwaved in Cell Conditioning Solution (CC1; Ventana/Roche). All primary antibody clone names, antibody incubation times, and antigen retrieval conditions are summarized in Table 1.

In Situ Hybridization of Epstein-Barr Virus Early RNA

In situ hybridization for Epstein-Barr virus-encoded early RNA (EBER) was carried out on deparaffinized and dehydrated sections. Chromogen-labeled oligonucleotides (Ventana; ref. 800-2842) complementary to portions of the EBER transcripts, were used according to the manufacturer's protocol (Ventana/Roche).

Fluorescence In Situ Hybridization

Fluorescence in situ hybridization (FISH) was performed on paraffin sections according to the manufacturer's instructions (Abbott, Abbott Park, IL). The status of *CCND1* was evaluated by Vysis LSI *CCND1* dual-color break-apart probe and Vysis LSI *IGH/CCND1* XT dual-color fusion probe. In addition, in situ hybridization probes from Vysis of *MYC* and *BCL2* were used to confirm the integrity of these genes. ZytoLight SPEC p16/CEP9 dual-color probe (ZytoVision, Bremen, Germany) was used to confirm the deletion of *CDKN2A* on 9p21.3, also following the manufacturer's instructions.

DNA Extraction

Genomic DNA (gDNA) was extracted using phenol-chloroform according to standard procedures.¹⁵ Briefly, two 30- μ m-thick formalin-fixed, paraffin-embedded block sections were deparaffinized with xylene and rehydrated by descending ethanol series (100% 5 min

\times 2, 95%, 70%, 50%, and 30% ethanol). The tissue was kept overnight at 38°C in 1 M sodium thiocyanate solution to remove DNA cross-linking due to formalin fixation, and thereafter suspended in 270 μ L buffer ATL and 30 μ L proteinase K (Qiagen, Valencia, CA) and digested for about 20 hours at 56°C until completely lysed. To the samples 1 μ L (10 mg/mL) of RNase A (Fermentas, Vilnius, Lithuania) was added and incubated for 10 minutes at 37°C to digest all intrinsic RNA. Phase Lock Gel Light (5Prime, Germany) was used to separate aqueous and organic phases after the addition of phenol-chloroform-isoamyl alcohol (25:24:1) mixture, and isopropanol was used for protein denaturation and DNA precipitation. Precipitated DNA was washed twice with 70% ethanol and eluted in 50 μ L of nuclease-free water. The quality of extracted gDNA was evaluated by Bioanalyzer (Agilent Technologies) and polymerase chain reaction (PCR) product size-based assay developed in our laboratory. The sample was regarded suitable for subsequent analysis by array comparative genomic hybridization (aCGH) if amplification of at least 300 bp amplicon was detected. Extracted gDNA was quantified using the Nanodrop system (Thermo Fischer Scientific, Wilmington, DE).

Multiplex PCR Assay

PCR assays for t(11;14) and *IgH* gene rearrangement were performed utilizing consensus FR1 and FR3 as well as J primers and primers specific for the major translocation cluster upstream to the *CCND1* gene on chromosome 11, as previously published.¹⁶ Examination of the PCR products was carried out with the high-resolution fragment length analysis system (ABI 310 Genetic Analyzer; Applied Biosystems). Clonal rearrangements and/or translocation fusion products were defined as prominent, single-sized amplification products.

Array Comparative Genomic Hybridization

For each hybridization, 500 ng of gDNA from each sample and a commercial 46 XX reference (Promega, UK) was used. Reference gDNA was digested with DNase I (Ambion), whereas sample gDNA needed no additional digestion. Samples and references were labeled with Cy-5 dUTP and Cy-3 dUTP, respectively, using a

TABLE 1. Immunophenotype of the Studied Cases and Conditions Used for Immunohistochemical Stainings

Clone name	Cyclin													
	BCL2	BCL6	CD5	CD10	CD20	D1	FOXP1	GCET	LMO2	MIB1	MUM1	p27	SOX11	CD138
SP66	GI191E/A8	SP19	SP67	L26	SP4-R	SP133	RAM341	1A9-1	Mib-1	MEQ-43	SX53G8	Polyclonal	Ventana 760-4248	
Antigen retrieval*/incubation time (min)	16/12	32/28	24/12	24/16	24/16	16/16	16/12	32/20	32/16	24/16	24/16	16/12	24/16	24/16
Case 1	-	+ dim (80%)	-	-	+	+	+	-	+ dim (60%)	+	+	+	-	-
Case 2	+	-	-	-	+	+	+	-	-	+	+	+	-	-
	(40%)				(100%)	(100%)	(100%)			(85%)	(40%)	(60%)		

Values in parentheses indicate percentage of tumour cells.

*Antigen retrieval was performed with CC1 buffer (Ventana/Roche).

BioPrime aCGH genomic labeling system (Invitrogen). All labeling reactions were assessed using a Nanodrop assay (Thermo Fischer Scientific) before mixing and hybridization to 180k CGH arrays (Agilent Technologies, Santa Clara, CA) for 24 hours in a rotating 65°C oven. The median overall probe spacing in the array is 13 kbp. All microarray slides were scanned using an Agilent 2565C DNA scanner, and the images were analyzed with Agilent Feature Extraction version 10.7 using default settings. The aCGH data were assessed with a series of QC metrics and subsequently analyzed using Agilent Genomic Workbench v.7.0 software with the aberration detection algorithm ADM2.¹⁷

RESULTS

Clinical Characteristics

Case 1 was a female patient who presented with stage IIIB disease at the age of 72. A 7×9×10 cm tumor mass was detected by magnetic resonance imaging in the medial right hip, and the staging computed tomography scan revealed additional cervical, abdominal, and thoracic lymphadenopathy. There was no bone marrow infiltration. DLBCL was diagnosed from an axillary lymph node biopsy. The patient received 6 cycles of R-CHOP chemotherapy, followed by 2 cycles of rituximab and achieved complete remission. There was no evidence of disease recurrence 6 years after treatment, and the patient is still alive.

Case 2 was a male patient who presented with stage IVA disease with splenomegaly and bone marrow involvement at the age of 63. Computed tomography scan revealed generalized lymphadenopathy, and a cervical 4.4×4.2×3 cm tumor mass was biopsied. The case was classified as a B-cell lymphoma with features intermediate between DLBCL and MCL. The patient received high-dose chemotherapy with autologous stem cell support consisting of 3 alternating cycles of R-CHOP and R-DHAP, followed by BEAM. The patient achieved complete remission and is still alive 1 year and 7 months after diagnosis.

Morphology and Immunophenotype

In case 1, the lymph node architecture was effaced by medium-sized to large-sized blastoid B cells with brisk mitotic activity (Fig. 1A). There were > 10% centroblasts intermingled with immunoblasts. In case 2, the lymph node showed diffuse effacement by a monotonous infiltrate of small centroblastoid cells intermingled with phagocytosing histiocytes and scattered hyalinized microvessels (Fig. 2A) and brisk mitotic activity. Cyclin D1 showed strong nuclear staining in both cases, that is, 80% and 100% of tumor cells, respectively (Figs. 1B, 2B). Tumor cells displayed a non-GCB phenotype (CD10⁻, GCET⁻, FOXP1⁺, MUM1⁺) in both cases. BCL6 was positive in case 1 but negative in case 2. Both neoplasms expressed CD20 in all tumor cells and p27 in 10% (case 1) and 60% (case 2) of tumor cells, respectively, but no expression of CD5 and SOX11 was detected (Figs. 1C, D and 2C, D). The proliferation fraction evaluated by MIB1 expression was 80% and 85%, respectively. Both cases

were negative for CD138 and for EBER. The complete immunophenotypes of both lymphomas are summarized in Table 1.

Translocation Detection by FISH and PCR

In case 1, t(11;14)(q13;q32) was detected by both applied *CCND1* FISH probes (Figs. 1E, F). In case 2, the break-apart probe for *CCND1* showed split signals in the tumor cells (Fig. 2E), but the *CCND1/IGH* probe failed to detect gene fusions. Chromosome analysis using spectral karyotyping on the cells from the bone marrow biopsy of case 2 revealed a complex translocation t(4;11;14)(q22;q13;q32) (Fig. 3A), and metaphase-FISH showed that a major fragment of chromosome 14 bearing the *IgH* locus is translocated to the long arm of chromosome 4 (Fig. 3B), masking the translocation for conventional interphase-FISH. *MYC* and *BCL2* were not rearranged in either case. Translocations in both cases were confirmed by a multiplex PCR assay, which yielded fusion products between the MCL-specific major translocation cluster upstream to the *CCND1* gene on chromosome 11 and the J segment of *IGH* of 232 and 256 bp in cases 1 and 2, respectively (data not shown).

aCGH Analysis

Genetic aberrations were detected in both cases, as summarized in Figure 4. In case 1, three chromosomes had genetic imbalances affecting 605 protein-coding genes. Heterozygous deletions of 1p36.11-p34.2, 3p21.31-p13, and 6p21.33-21.32 were found, and 1 copy gain of 6p21.32-p21.2 was detected. Of particular interest are the aberrations in chromosome 6, wherein a highly gene-rich region was disturbed, that is, a major part of the *HLA* (human leukocyte antigen) gene locus was affected, showing loss of heterozygosity in 2 members of HLA class I (*HLA-B* and *HLA-C*) and additional copies of HLA class II genes. Moreover, the 6p21.32-p21.2 region contains genes that have previously been reported to be cancer relevant, including *CDKN1A*, *HMGAI*, *MAPK13*, and *MAPK14*.¹⁸⁻²²

In case 2, six chromosomes showed genetic imbalances affecting 2742 protein-coding genes. The majority of these aberrations were heterozygous deletions varying in size from several megabases to the heterozygous loss of the complete arm of a chromosome. The regions affected by losses included 1p22.2-p12, 8p23.3-p11.1, 8q11.1-q13.3, 9p24.3-p11.2, 9q21.11-q31.2, 10q26.11-q26.2, 14q32.33, and 17p13.3-p11.2. Notably, 1 homozygous deletion was detected that spanned ~350 kb region at 9p21.3 and included the 2 protein-coding genes *CDKN2A* and *CDKN2B* as well as 1 recently discovered noncoding RNA, designated as ANRIL (*CDKN2BAS*). The homozygous deletion of the region was also confirmed by FISH analysis (Fig. 2F). *CDKN2A* and *CDKN2B* code for 2 well-known inhibitors of the cell cycle, p16INK4a and p15INK4b, respectively, and are frequently deleted in various neoplasms, including DLBCL and MCL. Notably, in the case 2 tumor, we also detected loss of 1 copy of *TP53* located on the short arm of chromosome 17. The only gain of genetic material occurred in 9q31.2-q34.3.

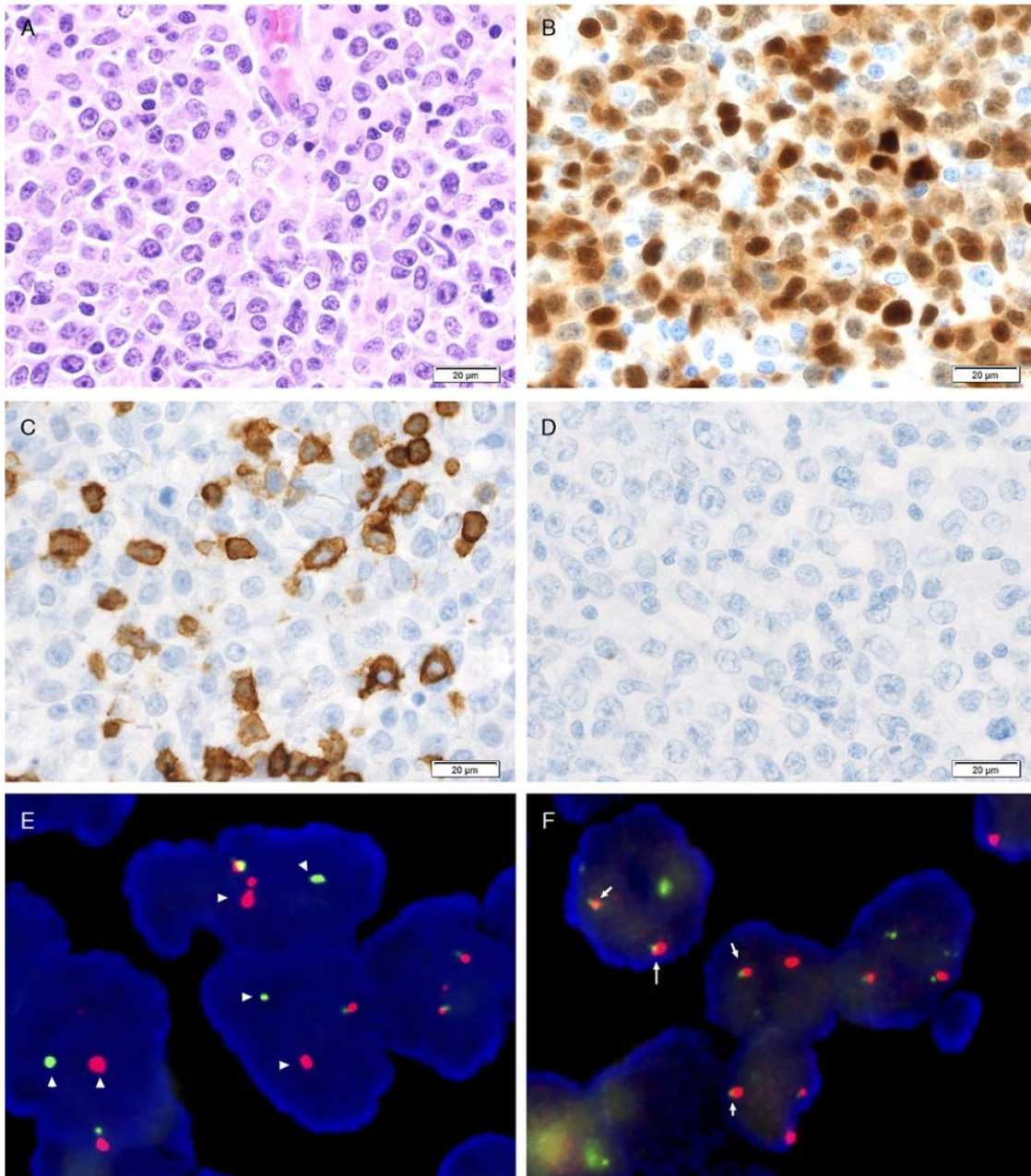


FIGURE 1. Cyclin D1-positive DLBCL, case 1. A, H&E staining showing diffuse lymph node effacement by medium-sized to large-sized blastoid B cells. More than 10% centroblasts are intermingled with immunoblasts. B, The majority of lymphoma cells express cyclin D1. The tumor cells are negative for CD5 (C) and SOX11 (D). The tumor cells bear t(11,14). FISH probes for *CCND1* show split signals with the break-apart probe (white triangles, D) and merged signals with the *CCND1-IGH* fusion probe (white arrows, E). H&E indicates hematoxylin and eosin.

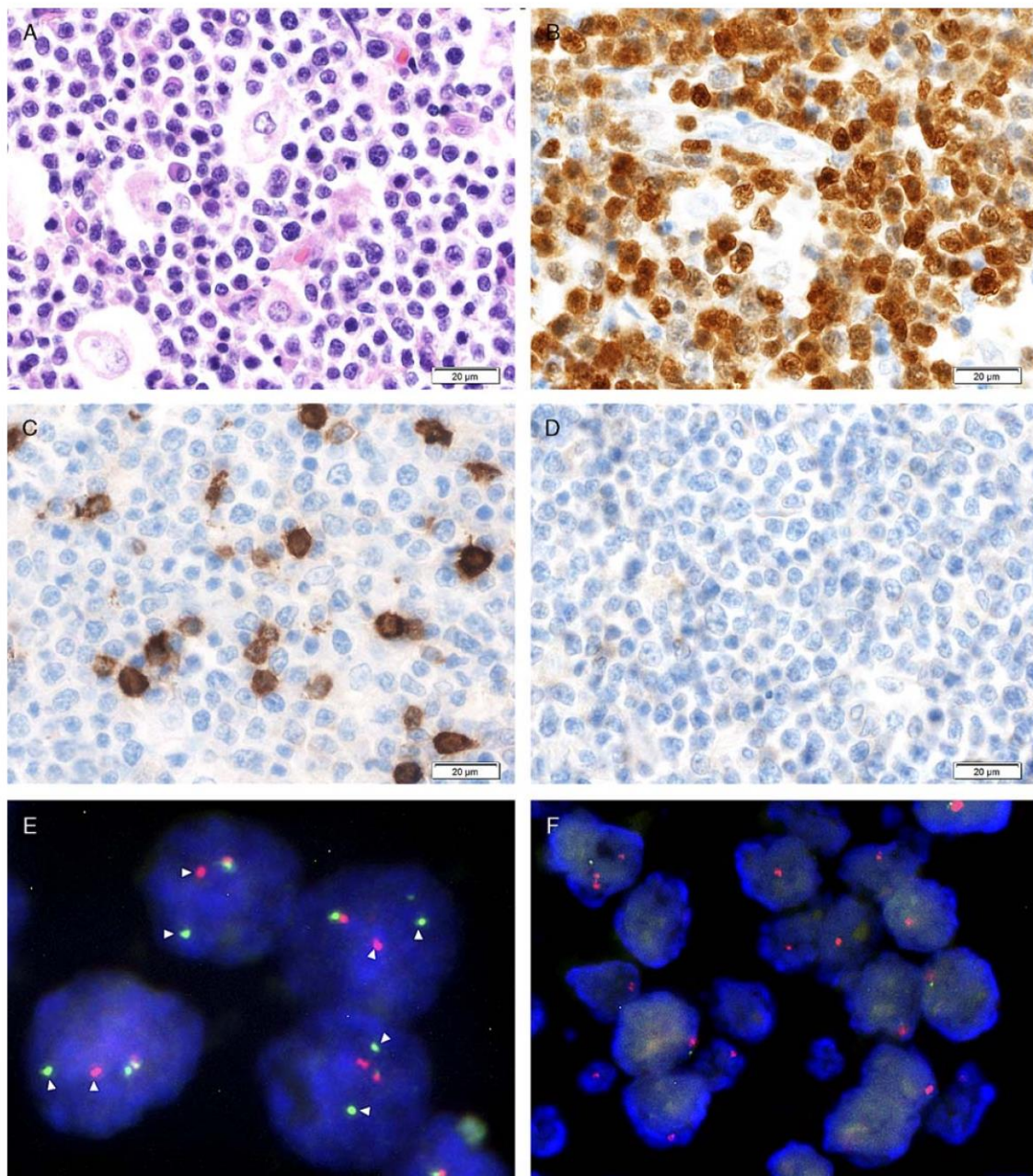


FIGURE 2. Cyclin D1-positive blastoid B-cell lymphoma, case 2. A, H&E staining showing diffuse lymph node effacement by a monotonous infiltrate of small centroblastoid cells intermingled with phagocytosing histiocytes and scattered microvessels. B, Almost 100% of lymphoma cells express cyclin D1. The tumor cells are negative for CD5 (C) and SOX11 (D). E, FISH with the *CCND1* break-apart probe, showing split signals in the majority of tumor cells (white triangles). *CCND1-IGH* fusion result was negative (not shown). F, In situ hybridization with the *CDKN2A* gene probe showing homozygous deletion 9p21.3 (lack of green signals) and only 1 copy of chromosome 9 (red centromere signals) in the majority of tumor cells. H&E indicates hematoxylin and eosin.

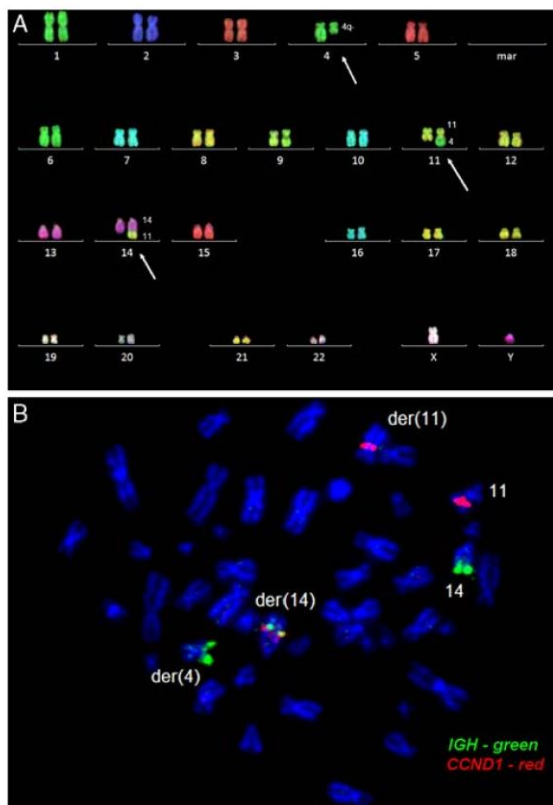


FIGURE 3. A, Complex $t(4;11;14)(q22;q13;q32)$ translocation identified by spectral karyotyping of metaphase chromosomes. A part of the long arm of chromosome 11 is translocated to the long arm of chromosome 14, whereas a part of the long arm of chromosome 4 is attached to chromosome 11. This is a balanced translocation without any loss of genetic material as evident from further genetic copy number analysis. White arrows mark the affected chromosomes. B, Metaphase-FISH showing fusion of the *CCND1* and *IGH* genes on the derivative chromosome 14. Chromosome 4 is also involved in the complex translocation with a part of chromosome 14 attached to its long arm. The figures were kindly provided by Prof. Torsten Haferlach from MLL Munich Leukemia Laboratory, Munich, Germany. Adaptations are themselves works protected by copyright. So in order to publish this adaptation, authorization must be obtained both from the owner of the copyright in the original work and from the owner of copyright in the translation or adaptation.

Interestingly, no copy number aberrations were detected in the chromosomes involved in the translocations $t(11;14)$ and $t(4;11;14)$ in either case, indicating that these translocations were essentially balanced.

DISCUSSION

Cyclin D1 protein expression in DLBCL has been documented, and all cyclin D1-positive DLBCL cases reported thus far were negative for the canonical

$t(11;14)(q13;q32)$ translocation.^{14,23–26} Overexpression of the protein was attributed to either the increased copy number of the *CCND1* gene or alterations in genes controlling its transcriptional activity (eg, *MYC*) or post-translational modification (eg, in AKT/GSK3 β -signaling pathway, GSK3 has been shown to phosphorylate cyclin D1 on a site that promotes its degradation in the proteasome²⁷). Structural aberrations of the *CCND1* locus other than $t(11;14)$ were also found in at least 2 studies.^{12,25} These findings led to the assumption that discovery of $t(11;14)(q13;q32)$ in doubtful cases with cyclin D1 expression precludes the diagnosis of DLBCL.

In this study, we report 2 cases of cyclin D1-positive blastoid B-cell lymphomas that displayed translocations affecting the *CCND1* gene on chromosome 11 and could not be classified as MCL. On the basis of their morphologic and immunophenotypic features, as well as copy number aberrations, they fall into the diagnostic category of DLBCL (case 1) and into a “gray zone” between blastoid MCL and cyclin D1-positive DLBCL (case 2). Yet, such a “gray zone” has not been recognized by the current World Health Organization classification. Currently, only 2 borderline diagnostic categories of B-cell lymphoma exist: “B-cell lymphoma, unclassifiable, with features intermediate between DLBCL and classical Hodgkin lymphoma” and “B-cell lymphoma, unclassifiable, with features intermediate between DLBCL and Burkitt lymphoma.”⁹ However, the second case in this study did not completely fulfill the proposed criteria for these 2 borderline categories given the lack of *BCL2* and *MYC* rearrangements, existing *CCND1* translocation, and aCGH profile featuring copy number aberrations common for both DLBCL and MCL. Therefore, we posit that our observation points toward the existence of a possible exceptional and diagnostically challenging “gray zone” of DLBCL to MCL that should be considered in future classifications.

Consistent with previous reports, the 2 cases investigated in the present study displayed focal centroblastic morphology. Both showed non-GCB phenotypes by the Tally algorithm,²⁸ which is a point against the diagnosis of MCL because MCL is believed to originate from a naive pre-germinal center B cell.²⁹ Our 2 cases were also negative for CD5, further reducing the likelihood of MCL, as the majority of MCL are CD5⁺.⁹ In addition, both cases showed strong positivity for the applied markers of activated-germinal center/post-germinal center B cells, MUM1 and FOXP1, and case 2 in particular expressed p27 in a considerable proportion of tumor cells, making the diagnosis of blastoid or pleomorphic variant of MCL highly unlikely.^{30–32} Finally, as SOX11 was shown to be a useful marker in differentiating cyclin D1-positive DLBCL from MCL, being expressed in 89% (19/22) of MCL and negative in all DLBCL (0/98), including 4 cases showing cyclin D1 positivity,¹³ we investigated whether our 2 cases expressed SOX11 and found that they did not.

In contrast to previous studies on DLBCL wherein only weak or moderate expression of cyclin D1 was detected, cyclin D1 was highly expressed in both cases discussed in this report. This difference might be due to translocations

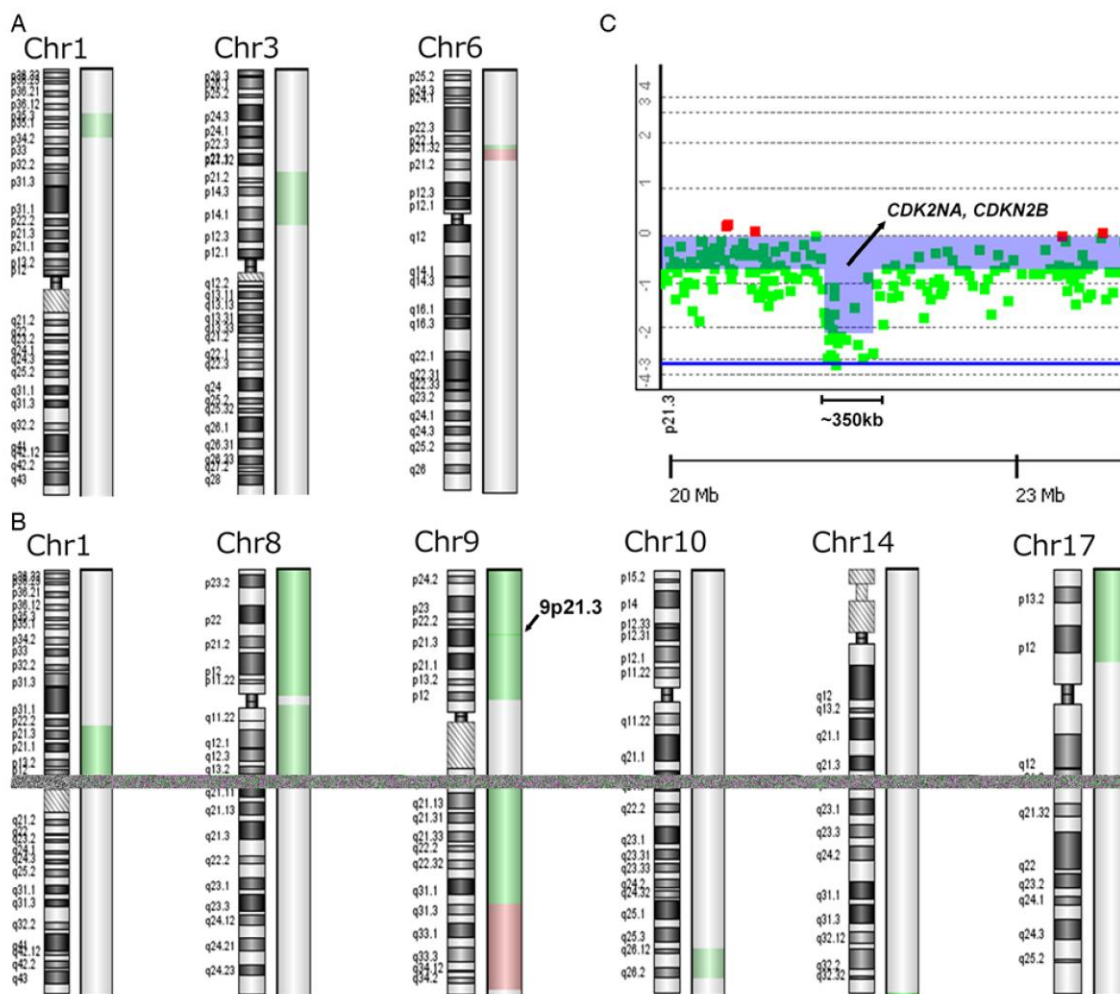


FIGURE 4. Copy number aberration summary of case 1 (A) and case 2 (B). Affected chromosome ideograms are shown; regions with genetic losses are displayed in green, genetic gains in red. C, aCGH probe-view of the 9p21 region magnifying the region of the homozygous deletion *CDKN2A* gene. In the context of heterozygous deletion of the short arm of chromosome 9 (the log ratio value of neighboring probes is -1), multiple probes show homozygous deletion with log ratios between -2 and -3 . Green or red squares represent a single probe in this illustration.

involving the *CCND1* gene, which, as recurrently observed in MCL, most probably drove overexpression in our patients. Interestingly, case 1 with the canonical t(11;14) (q13;q32) translocation had lower cyclin D1 expression (85%) compared with case 2, which had a complex translocation t(4;11;14)(q22;q13;q32) involving 3 chromosomes (100%). However, strong cyclin D1 expression is not necessarily due to chromosomal translocations. In the study by Vela-Chavez et al,¹⁴ 2 cases of Richter transformations expressed cyclin D1 in 70% to 80% of tumor cells without any evidence of structural aberrations involving the *CCND1* gene. Translocations involving chromosomes 11 and 14 are also observed in plasma cell neoplasms, but the breakpoints detected are different from those typical to MCL because of

different mechanisms involved.^{33–35} Translocations of *CCND1* into the *IGH* locus in MCL predominantly occur during recombination activation gene complex-mediated V(D)J-rearrangement so that double-strand breaks occur in the V gene segments. In plasma cell neoplasms, the translocations are thought to be generated by abnormal class switch recombination events mediated by activation-induced cytidine deaminase and, therefore, double-strand breaks occur in the constant *IGH* gene segments. Thus, by performing a multiplex PCR assay designed to detect t(11;14) translocations with MCL-specific breakpoints and yielding fusion products in both studied cases, we ruled out the possibility of plasma cell neoplasm-typical *CCND1* rearrangements.

To resolve the issue of whether our cases showed copy number alterations typical for MCL or DLBCL at the molecular level, we performed aCGH and found that 2 of 3 chromosomal regions affected by genetic imbalances in case 1 overlapped with those reported to be recurrently aberrant in DLBCL. The heterozygous deletion of 3p21.31-p13 affects the tumor suppressor fragile histidine triad (*FHIT*) gene in 3p14.2, which is deleted in about 30% of DLBCLs. Gain of copy in 6p21.32-p21.2 overlaps with the recurrently amplified region 6p21.1-p25.3 in DLBCL, a region that contains the *CDKN1A* gene coding for the tumor suppressor p21, which is reportedly amplified in 33% of DLBCLs.³⁶ Moreover, deletion of 6p21.33-21.32 affecting the locus coding *HLA* genes and contributing to loss of HLA class II and I expression is a well-known feature in DLBCL of the central nervous system.^{37,38} Importantly, none of the 3 regions found to be aberrant in case 1 were reported in genomic studies of MCL,³⁹ and only losses of 1p36.11-p34.2 spanning a 1p35.2 region are observable in about 15% of plasma cell neoplasms.⁴⁰

The genomic profile of case 2 is more ambiguous. Although it had some copy number aberrations common for DLBCL (losses of 9p24.3-p11.2, 9p21.3, 10q26.11-q26.2; gain of 9q31.2-q34.3),^{36,41} some regions of genomic imbalances at least partially overlapped with those reported in MCL (losses of 1p22.2-p12, 9p24.3-p11.2, 9q21.11-q31.2, 17p13.3-p11.2)³⁹ and plasma cell neoplasms (losses of 1p22.2-p12, 8p23.3-p11.1, 10q26.11-q26.2, 17p13.3-p11.2; gain of 9q31.2-q34.3).^{40,42} This can be best illustrated by the homozygous deletion 9p21.3 affecting the locus, which codes for the well-known tumor suppressors p16^{INK4a}, p14^{ARF}, and p15^{INK4b}. Detected in case 2 in the present study, this specific aberration is rarely ever detected in plasma cell neoplasms but found in about 30% of activated B cell-type DLBCL, wherein it predicts adverse survival⁴³ and might be involved in chemoresistance.⁴⁴ In contrast, 9p21.3 is heterozygously or homozygously deleted in 18% to 30% of MCL patients, and such losses are also associated with an aggressive disease course.⁴⁵ Summarizing our aCGH findings, case 1 had aberrations exclusively detectable in DLBCL and not in MCL nor in plasma cell neoplasms, whereas case 2 was equivocal, bearing aberrations recurrently detectable in all 3 entities.

From the clinical perspective, the course of the first patient does not favor a diagnosis of MCL. This elderly patient achieved complete remission after R-CHOP treatment and is still alive without evidence of recurrence 6 years after diagnosis. The disease course of the second patient is somewhat different in that he was diagnosed with a more widespread lymphoma involving the bone marrow, but he is in complete remission 1 year and 9 months after high-dose chemotherapy with autologous stem cell support.

In conclusion, we report 2 patients with blastoid B-cell lymphomas expressing cyclin D1 and bearing translocations affecting the *CCND1* gene. In case 1, the clinical course, morphologic appearance, and immunophenotypic

characteristics, supplemented by the information on genetic imbalances, lead us to diagnose cyclin D1-positive DLBCL. Therefore, detection of the structural genomic signature of MCL, that is, t(11;14)(q13;q32), should not preclude the diagnosis of cyclin D1-positive DLBCL in cases in which all other findings suggest this diagnosis. The second case, in our opinion, cannot be classified unambiguously because of equivocal morphology, genetic profile, and clinical characteristics, and despite the phenotypic profile in support of DLBCL, we tend to assign it into an as yet unrecognized “gray zone” between blastoid MCL and cyclin D1-positive DLBCL that could be considered in future classifications.

ACKNOWLEDGMENTS

The authors are grateful for Prof. Torsten Haferlach and MLL Munich Leukemia Laboratory, for their contribution to the paper.

REFERENCES

- Baldin V, Lukas J, Marcote MJ, et al. Cyclin D1 is a nuclear protein required for cell cycle progression in G1. *Genes Dev.* 1993;7:812–821.
- Quelle DE, Ashmun RA, Shurtleff SA, et al. Overexpression of mouse D-type cyclins accelerates G1 phase in rodent fibroblasts. *Genes Dev.* 1993;7:1559–1571.
- de Boer CJ, van Krieken JH, Kluijn-Nelemans HC, et al. Cyclin D1 messenger RNA overexpression as a marker for mantle cell lymphoma. *Oncogene.* 1995;10:1833–1840.
- Troussard X, Avet-Loiseau H, Macro M, et al. Cyclin D1 expression in patients with multiple myeloma. *Hematol J.* 2000;1:181–185.
- Bosch F, Campo E, Jares P, et al. Increased expression of the PRAD-1/CCND1 gene in hairy cell leukaemia. *Br J Haematol.* 1995;91:1025–1030.
- de Boer CJ, Kluijn-Nelemans JC, Dreef E, et al. Involvement of the CCND1 gene in hairy cell leukemia. *Ann Oncol.* 1996;7:251–256.
- Raffeld M, Jaffe ES. BI-1, t(11;14), and mantle cell-derived lymphomas. *Blood.* 1991;78:259–263.
- D'Amico M, Hulit J, Amanatullah DF, et al. The integrin-linked kinase regulates the cyclin D1 gene through glycogen synthase kinase 3beta and cAMP-responsive element-binding protein-dependent pathways. *J Biol Chem.* 2000;275:32649–32657.
- Swerdlow SH, Campo E, Harris NL, et al. *WHO Classification of Tumours of Haematopoietic and Lymphoid Tissues.* 4th ed. Lyon: IARC press; 2008.
- Harada S, Suzuki R, Uehira K, et al. Molecular and immunological dissection of diffuse large B cell lymphoma: CD5+, and CD5- with CD10+ groups may constitute clinically relevant subtypes. *Leukemia.* 1999;13:1441–1447.
- Zukerberg LR, Yang WI, Arnold A, et al. Cyclin D1 expression in non-Hodgkin's lymphomas. Detection by immunohistochemistry. *Am J Clin Pathol.* 1995;103:756–760.
- Ehinger M, Linderth J, Christensson B, et al. A subset of CD5-diffuse large B-cell lymphomas expresses nuclear cyclin D1 with aberrations at the CCND1 locus. *Am J Clin Pathol.* 2008;129:630–638.
- Hsiao SC, Cortada IR, Colomo L, et al. SOX11 is useful in differentiating cyclin D1-positive diffuse large B-cell lymphoma from mantle cell lymphoma. *Histopathology.* 2012;61:685–693.
- Vela-Chavez T, Adam P, Kremer M, et al. Cyclin D1 positive diffuse large B-cell lymphoma is a post-germinal center-type lymphoma without alterations in the CCND1 gene locus. *Leuk Lymphoma.* 2011;52:458–466.
- Sambrook J, Fritsch EF, Maniatis T. *Molecular Cloning: A Laboratory Manual.* New York: Cold Spring Harbor Laboratory; 1989.
- Meier VS, Ruffe A, Gudat F. Simultaneous evaluation of T- and B-cell clonality, t(11;14) and t(14;18), in a single reaction by a four-color multiplex polymerase chain reaction assay and automated high-resolution fragment analysis. *Am J Pathol.* 2001;159:2031–2043.

17. Lipson D, Aumann Y, Ben-Dor A, et al. Efficient calculation of interval scores for DNA copy number data analysis. *J Comput Biol.* 2006;13:215–228.
18. Shah SN, Cope L, Poh W, et al. HMGA1: a master regulator of tumor progression in triple-negative breast cancer cells. *PLoS One.* 2013;8:e63419.
19. Eckert RL, Efimova T, Balasubramanian S, et al. p38 Mitogen-Activated Protein Kinases on the Body Surface - A Function for p38[delta]. *J Invest Dermatol.* 2003;120:823–828.
20. Li G, Liu Z, Sturgis EM, et al. Genetic polymorphisms of p21 are associated with risk of squamous cell carcinoma of the head and neck. *Carcinogenesis.* 2005;26:1596–1602.
21. Soto Martinez JL, Cabrera Morales CM, Serrano Ortega S, et al. Mutation and homozygous deletion analyses of genes that control the G1/S transition of the cell cycle in skin melanoma: p53, p21, p16 and p15. *Clin Transl Oncol.* 2005;7:156–164.
22. Watanabe M, Nakahata S, Hamasaki M, et al. Downregulation of CDKN1A in adult T-cell leukemia/lymphoma despite overexpression of CDKN1A in human T-lymphotropic virus 1-infected cell lines. *J Virol.* 2010;84:6966–6977.
23. Izquierdo F, Suarez D. CD5(-) diffuse large B-cell lymphoma with peculiar cyclin D1+ phenotype. Pathologic and molecular characterization of a single case. *Hum Pathol.* 2012;43:1344–1345.
24. Lucioni M, Novara F, Riboni R, et al. CD5(-) diffuse large B-cell lymphoma with peculiar cyclin D1+ phenotype. Pathologic and molecular characterization of a single case. *Hum Pathol.* 2011;42:1204–1208.
25. Rodriguez-Justo M, Huang Y, Ye H, et al. Cyclin D1-positive diffuse large B-cell lymphoma. *Histopathology.* 2008;52:900–903.
26. Schneider A, Meyer P, DiMaio D, et al. Diffuse large B-cell lymphoma with both CD5 and cyclin D1 expression—a case report and review of the literature. *J Hematopathol.* 2010;3:145–148.
27. Nicholson KM, Anderson NG. The protein kinase B/Akt signalling pathway in human malignancy. *Cell Signal.* 2002;14:381–395.
28. Meyer PN, Fu K, Greiner TC, et al. Immunohistochemical methods for predicting cell of origin and survival in patients with diffuse large B-cell lymphoma treated with rituximab. *J Clin Oncol.* 2011;29:200–207.
29. Campo E, Raffeld M, Jaffe ES. Mantle-cell lymphoma. *Semin Hematol.* 1999;36:115–127.
30. Capello D, Vitolo U, Pasqualucci L, et al. Distribution and pattern of BCL-6 mutations throughout the spectrum of B-cell neoplasia. *Blood.* 2000;95:651–659.
31. Tsuboi K, Iida S, Inagaki H, et al. MUM1/IRF4 expression as a frequent event in mature lymphoid malignancies. *Leukemia.* 2000;14:449–456.
32. Quintanilla-Martinez L, Thieblemont C, Fend F, et al. Mantle cell lymphomas lack expression of p27Kip1, a cyclin-dependent kinase inhibitor. *Am J Pathol.* 1998;153:175–182.
33. Jares P, Colomer D, Campo E. Molecular pathogenesis of mantle cell lymphoma. *J Clin Invest.* 2012;122:3416–3423.
34. Walker BA, Wardell CP, Johnson DC, et al. Characterization of IGH locus breakpoints in multiple myeloma indicates a subset of translocations appear to occur in pregerminal center B cells. *Blood.* 2013;121:3413–3419.
35. Gonzalez D, van der Burg M, Garcia-Sanz R, et al. Immunoglobulin gene rearrangements and the pathogenesis of multiple myeloma. *Blood.* 2007;110:3112–3121.
36. Tagawa H, Tsuzuki S, Suzuki R, et al. Genome-wide array-based comparative genomic hybridization of diffuse large B-cell lymphoma: comparison between CD5-positive and CD5-negative cases. *Cancer Res.* 2004;64:5948–5955.
37. Booman M, Douwes J, Glas AM, et al. Mechanisms and effects of loss of human leukocyte antigen class II expression in immune-privileged site-associated B-cell lymphoma. *Clin Cancer Res.* 2006;12:2698–2705.
38. Riemersma SA, Jordanova ES, Schop RF, et al. Extensive genetic alterations of the HLA region, including homozygous deletions of HLA class II genes in B-cell lymphomas arising in immune-privileged sites. *Blood.* 2000;96:3569–3577.
39. Jares P, Colomer D, Campo E. Genetic and molecular pathogenesis of mantle cell lymphoma: perspectives for new targeted therapeutics. *Nat Rev Cancer.* 2007;7:750–762.
40. Carrasco DR, Tonon G, Huang Y, et al. High-resolution genomic profiles define distinct clinico-pathogenetic subgroups of multiple myeloma patients. *Cancer Cell.* 2006;9:313–325.
41. Tirado CA, Chen W, Garcia R, et al. Genomic profiling using array comparative genomic hybridization define distinct subtypes of diffuse large B-cell lymphoma: a review of the literature. *J Hematol Oncol.* 2012;5:54.
42. Largo C, Saez B, Alvarez S, et al. Multiple myeloma primary cells show a highly rearranged unbalanced genome with amplifications and homozygous deletions irrespective of the presence of immunoglobulin-related chromosome translocations. *Haematologica.* 2007;92:795–802.
43. Lenz G, Wright GW, Emre NC, et al. Molecular subtypes of diffuse large B-cell lymphoma arise by distinct genetic pathways. *Proc Natl Acad Sci USA.* 2008;105:13520–13525.
44. Kreisel F, Kulkarni S, Kerns RT, et al. High resolution array comparative genomic hybridization identifies copy number alterations in diffuse large B-cell lymphoma that predict response to immuno-chemotherapy. *Cancer Genet.* 2011;204:129–137.
45. Pinyol M, Hernandez L, Cazorla M, et al. Deletions and loss of expression of p16INK4a and p21Waf1 genes are associated with aggressive variants of mantle cell lymphomas. *Blood.* 1997;89:272–280.

3.5 Array CGH-based analysis of post-transplant plasmacytic hyperplasia reveals 'intact genomes' arguing against categorizing it as part of the post-transplant lymphoproliferative disease spectrum.

Menter, T, **Juskevicius D.**, Tzankov A.

-Letter to the editor-
Published in *Transplant International*, 2014

Contribution: I performed plasma cell enrichment, aCGH of sorted populations and analysis of genetic data

LETTER TO THE EDITORS

Array CGH-based analysis of post-transplant plasmacytic hyperplasia reveals 'intact genomes' arguing against categorizing it as part of the post-transplant lymphoproliferative disease spectrum

doi:10.1111/tri.12400

Dear Sirs,

Post-transplant lymphoproliferative disorders (PTLD) are defined as lymphoid proliferations arising after solid organ or hematopoietic stem cell transplantation [1]. The majority of them are associated with Epstein–Barr virus (EBV) infection facilitated by the continuous immunosuppression of the patients. PTLD are categorized by the World Health

Organization (WHO) into four categories. They range from early lesions (ePTLD) to overt lymphomas. ePTLD are further subdivided into plasmacytic hyperplasia (PH) and infectious mononucleosis-like lesions [1]. ePTLD are known to be polyclonal [2]. In 2007, Vakiani *et al.* [3] proposed a third entity of ePTLD described as follicular hyperplasia, which showed cytogenetic abnormalities using

Table 1. Patients' characteristics.

	Patient 1	Patient 2	Patient 3	Patient 4	Patient 5
Age at transplantation (years)	40.4	17.4	57.5	57.5	5.3
Age at diagnosis of ePTLD (years)	52.3	28.0	61.9	64.6	10.3
Type of organ transplant	Kidney	Heart	Heart	Kidney	Kidney
Time from transplantation to detection of ePTLD (months)	143.3	126.6	52.4	85.9	60.4
Site of ePTLD	Tonsil	Tonsil	Paracolic lymph node	Inguinal lymph node	Tonsil
Serological EBV-status at transplantation	Positive	Positive	No serological information available	Positive	Positive
Presence of EBV in the ePTLD specimen	Negative	Positive in 1–2% of cells	Positive in 1–2% of cells	Negative	Negative
Treatment of ePTLD	No specific treatment	No specific treatment	No specific treatment	No specific treatment	Reduction of immunosuppression
Development of other forms of PTLD	No	No	No	No	No
Recurrence of ePTLD	No	No	No	No	No
Follow-up	Squamous carcinoma of the tongue 2 years prior to the development of ePTLD. Several recurrences of squamous carcinoma afterwards	Alive with good transplant function 5 years after diagnosis of ePTLD	Death because of colon carcinoma 4 years after diagnosis of ePTLD	Death because of cardiac failure 2 years after diagnosis of ePTLD	Transplant loss 6 years after diagnosis of ePTLD
Duration of follow-up (years)	4.9	4.5	4.2	2.1	6.9

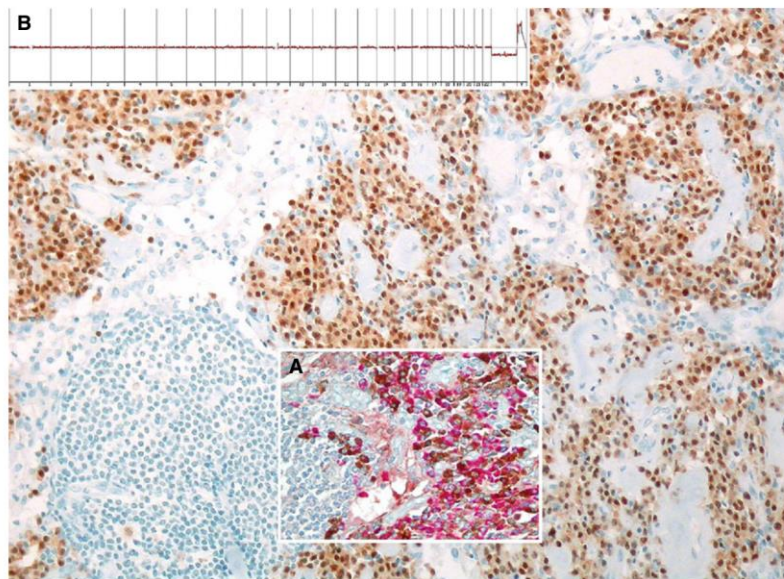


Figure 1 MUM1-staining highlighting abundance of plasma cells in the parafollicular areas of a lymph node. (A) Double immunostaining for kappa and lambda light chains showing an equal (polyclonal) distribution. (B) Array CGH genome overview plot showing no copy number imbalances in the chromosomes of isolated MUM1-positive plasma cell nuclei of PH-ePTLD. The shown male sample was hybridized to female reference genomic DNA, thus a single copy of chromosome X and a gain of chromosome Y are visible.

Giemsa banding and spectral karyotype analysis. Most ePTLD arise in the adenoids or lymph nodes; however, there are also rare case reports on ePTLD arising in the transplanted organs as well [4].

The absence of clonality does not exclude malignancy and cytogenetic abnormalities have been documented in ePTLD previously [3]. Therefore, we aimed to look for genomic aberrations in PH at higher resolution. We selected five PH-ePTLD cases with available formalin-fixed paraffin-embedded (FFPE) material from the archive of our institution (for patients' characteristics see Table 1). Applying our recently developed technique ([5], see also Supplementary material) we processed FFPE tissue sections to specifically extract intact and immunogenic cell nuclei. Using a monoclonal antibody reactive against the nuclear protein multiple myeloma oncogene 1 (MUM1), plasma cell nuclei of PH were labeled and then isolated by flow-sorting. Purity of the sorts was evaluated by subsequent morphologic examination and was estimated to be higher than 85% in all cases. Genomic DNA from the sorted plasma cell nuclei was extracted and used for array-comparative genomic hybridization (aCGH) on the Agilent SurePrint G3 CGH 180k arrays following the procedures described previously [6]. Microarray slides were scanned and then data was analyzed using AGILENT GENOMIC WORKBENCH v.7.0 software with the aberration detection algorithm ADM2 [7].

We did not find any genetic copy number aberrations detectable by aCGH in our cohort (Fig. 1). None of the

patients developed another form of PTLD or a relapse of the ePTLD in the follow-up (mean: 4.5 years; range: 2.1–6.9 years). Only two of the five cases showed *in situ* single detectable EBV-RNA-positive cells. However, four patients had been EBV-seropositive at the time of transplantation. After the diagnosis of ePTLD, immunosuppression was reduced in one of the five patients, while in the others no adjustments of the immunosuppressive regimens were done (Table 1).

We could thus confirm on purified cellular populations that beyond being not clonal, PH-ePTLD do not yield genomic aberrations assessable by aCGH. Since the classification of PTLD in the late 1980s by Nalesnik *et al.* [8] there is a debate whether PH should be included into the spectrum of PTLD. Our findings might add momentum to the hypothesis that events other than those occurring within PH-ePTLD are necessary to develop a neoplastic lymphoproliferation leading to more aggressive forms of PTLD. Thus, PH categorization as PTLD might rather be reconsidered both because of the indolent clinical course and based on these genetic findings.

Thomas Menter, Darius Juskevicius
and Alexandar Tzankov
*Institute of Pathology, University Hospital Basel,
Basel, Switzerland
e-mail: alexandar.tzankov@usb.ch*

Conflicts of interest

The authors have no conflict of interest to declare.

Funding

Krebsliga beider Basel 03-2012.

Acknowledgements

The authors would like to thank Prof. Dr. M. Dickenmann and Dr. O. Pfister for helping to obtain the clinical data of the patients.

Supporting information

Additional Supporting Information may be found in the online version of this article:

Isolation of plasma cell nuclei from the FFPE tissues

References

1. Swerdlow SH, Webber SA, Chadburn A, Ferry JA. Post-transplant lymphoproliferative disorders. In: Swerdlow SH, Campo E, Harris NL, *et al.*, eds. *WHO Classification of Tumours of Haematopoietic and Lymphoid Tissues*. Lyon, France: IARC, 2008: 343–349.
2. Nelson BP, Wolniak KL, Evens A, Chenn A, Maddalozzo J, Proytcheva M. Early posttransplant lymphoproliferative disease: clinicopathologic features and correlation with mTOR signaling pathway activation. *Am J Clin Pathol* 2012; **138**: 568.
3. Vakiani E, Nandula SV, Subramaniam S, *et al.* Cytogenetic analysis of B-cell posttransplant lymphoproliferations validates the World Health Organization classification and suggests inclusion of florid follicular hyperplasia as a precursor lesion. *Hum Pathol* 2007; **38**: 315.
4. Harada H, Miura M, Shimoda N, *et al.* A case of plasmacytic hyperplasia arising in a kidney allograft salvaged with immunosuppression reduction alone. *Clin Transplant* 2004; **18** (Suppl. 11): 50.
5. Juskevicius D, Dietsche T, Lorber T, *et al.* Extracavitary primary effusion lymphoma: clinical, morphological, phenotypic and cytogenetic characterization using nuclei enrichment technique. *Histopathology* 2014; DOI: 10.1111/his.12478.
6. Juskevicius D, Ruiz C, Dirnhofer S, Tzankov A. Clinical, morphologic, phenotypic, and genetic evidence of cyclin D1-positive diffuse large B-cell lymphomas with CYCLIN D1 gene rearrangements. *Am J Surg Pathol* 2014; **38**: 719.
7. Lipson D, Aumann Y, Ben-Dor A, Linial N, Yakhini Z. Efficient calculation of interval scores for DNA copy number data analysis. *J Comput Biol* 2006; **13**: 215.
8. Nalesnik MA, Jaffe R, Starzl TE, *et al.* The pathology of post-transplant lymphoproliferative disorders occurring in the setting of cyclosporine a-prednisone immunosuppression. *Am J Pathol* 1988; **133**: 173.

3.6 Comprehensive phenotypic characterization of PTLD reveals potential reliance on EBV or NF- κ B signaling instead of B-cell receptor signaling

Menter T., Dickenmann D., **Juskevicius D.**, Steiger J., Dirnhofer S., Tzankov A.

-Research article-

Published in *Hematological Oncology*, 2016

Contribution: I performed clustering analysis of immunohistochemical data, wrote the respective section in materials and methods and produced figure 1.

Original Research Article

Comprehensive phenotypic characterization of PTLD reveals potential reliance on EBV or NF- κ B signalling instead of B-cell receptor signalling

Thomas Menter¹, Michael Dickenmann², Darius Juskevicius¹, Juerg Steiger², Stephan Dimhofer¹ and Alexandar Tzankov^{1*}

¹Institute of Pathology, University Hospital Basel, Basel, Switzerland

²Clinic for Transplantation Immunology and Nephrology, University Hospital Basel, Basel Switzerland

*Correspondence to: Prof. Dr. Alexandar Tzankov, Institute of Pathology, University Hospital Basel, Schönbeinstrasse 40, 4031 Basel, Switzerland.
E-mail: alexandartzankov@usb.ch

Abstract

Post-transplant lymphoproliferative disorders (PTLD) are a major problem in transplant medicine. So far, the insights into pathogenesis and potentially druggable pathways in PTLD remain scarce. We investigated a cohort of PTLD patients, consisting of both polymorphic ($n=3$) and monomorphic ($n=19$) B-cell lymphoproliferations. Several signalling pathways, cell of origin of PTLD and their relation to viruses were analysed by immunohistochemistry and *in situ* hybridization. Most PTLD were of activated B-cell origin. Two-thirds of cases showed an Epstein–Barr virus (EBV) infection of the neoplastic cells. NF- κ B signalling components were present in the majority of cases, except for EBV-infected cases with latency type III lacking CD19 and upstream B-cell signalling constituents. Proteins involved in B-cell receptor signalling like Bruton tyrosine kinase were only present in a minority of cases. Phosphoinositide 3-kinase (PI3K) was expressed in 94% of cases and the druggable PI3K class 1 catalytic subunit p110 in 76%, while proteins of other signalling transduction pathways were expressed only in single cases. Unsupervised cluster analysis revealed three distinct subgroups: (i) related to EBV infection, mainly latency type III and mostly lacking CD19, upstream B-cell signalling and NF- κ B constituents; (ii) mostly related to EBV infection with expression of the alternative NF- κ B pathway compound RelB, CD10, and FOXP1 or MUM1; and finally, (iii) mostly unrelated to virus infection with expression of the classic NF- κ B pathway compound p65. EBV and NF- κ B are important drivers in PTLD in contrast to B-cell receptor signalling. The main signal transduction pathway is related to PI3K. This links PTLD to other subgroups of EBV-related lymphomas, highlighting also new potential treatment approaches. Copyright © 2016 John Wiley & Sons, Ltd.

Keywords: PTLD; DLBCL; NF- κ B; B-cell receptor signalling; PI3K; EBV

Received 25 September 2015

Revised 1 December 2015

Accepted 15 December 2015

Introduction

Post-transplant lymphoproliferative disorders (PTLD) are a major problem in transplantation medicine, occurring in about 5% of solid organ transplant patients and in 1% of hematopoietic stem cell transplant patients [1]. PTLD are heterogeneous, ranging from early lesions such as plasmacytic hyperplasias and infectious mononucleosis-like disorders to overt lymphomas [1]. Most clinically relevant forms of PTLD are B-cell lymphomas, mainly diffuse large B-cell lymphomas (DLBCL). Compared with DLBCL arising in non-immunocompromised hosts (hereafter referred to and specified as conventional DLBCL), DLBCL-PTLD have a poorer prognosis and higher mortality rates [2].

Information about conventional DLBCL pathogenesis and identification of prognostic and predictive markers have rapidly increased in the last few years, but knowledge regarding the various subtypes such as DLBCL-PTLD remains scarce [3]. Targeted therapy has now become the focus of research as a potential new way of lymphoma treatment [4]. Examples for such an approach in conventional DLBCL are the NF- κ B pathway modulation using bortezomib [5] and the inhibition of the Bruton tyrosine kinase (BTK) using ibrutinib [6]. Recently, the use of idelalisib, a phosphoinositide 3-kinase-delta (PI3K δ) inhibitor, was approved in chronic lymphocytic leukaemia and follicular lymphoma [7]. BTK is a direct B-cell receptor downstream target that activates multiple transcription factors such as NF- κ B and survival signalling cascades involving the PI3K-activated or mitogen-activated protein

kinases (MAPK)/extracellular signal-regulated kinases (ERK) pathways [8]. Data on the dependence of PTLD on B-cell receptor signalling and activating mutations of proteins involved in this pathway are lacking.

Besides these novel opportunities, new prognostic biomarkers in conventional DLBCL have been established. Inactivating mutations of *TP53* correlate with a worse outcome [9], as do rearrangements of the *MYC* and *BCL2* genes [10]. In addition, overexpression of c-myc and bcl2 at the protein level detected by immunohistochemistry can serve as a prognostic factor, too [11], thus opening the door to a more widespread use of these markers. However, little is known about infrequent lymphoma entities such as PTLD concerning these topics, primarily because of the scarcity of cases and the resultant difficulties in performing large-scale studies.

We aimed to comprehensively characterize PTLD regarding potentially targetable intracellular signalling pathways (mainly the B-cell receptor pathway and the NF- κ B pathway) and signalling proteins as alluded to earlier as well as their relation to viruses.

Methods

Patients and clinical data

Patients diagnosed with PTLD between 1988 and 2014 were identified from the pathology archives of the University Hospital Basel in collaboration with the Clinic for Transplantation, Immunology and Nephrology of the University Hospital Basel. Criteria for inclusion in the study were documented solid organ transplantation, available clinical history, documented diagnosis of a PTLD and sufficient formalin-fixed paraffin-embedded material of a PTLD for further investigations. Altogether, 22 patients could be enclosed in this study. Five patients with early forms of PTLD were analysed in a separate study [12]. Patients' characteristics are summarized in Table 1. The study was approved by the local ethics committee (EKNZ 2014-252).

Tissue microarray

The tissue microarray (TMA) was constructed as described elsewhere [13]. Two cores from each sample were included.

Immunohistochemistry and fluorescence *in situ* hybridization analysis

The antibodies and conditions of the immunohistochemical stainings are listed in Table 2. Phosphorylated and, thus, activated forms of proteins belonging to signalling cascades [e.g. signal transducer and activator of transcription (STAT) isoforms, PI3K isoforms and MAPK isoforms]

were investigated. For each protein, the cellular sublocalization of the activated protein was specifically considered (e.g. nuclear expression for STAT-proteins or c-myc). For markers showing an unexpected staining pattern (e.g. only positive cases or very few or no positive cases), additional control tissues like tonsils and colon carcinomas and/or further TMA slides were stained in order to verify the reliability of the staining. The relative proportion (percentage) of positively stained tumour cells and not the staining intensity was considered. Cut-offs were determined as described in previous publications [14]. Briefly, for markers of potential discriminatory power related to outcome or clinico-pathological parameters, a statistically calculated relevant cut-off score has been tried to be chosen, but because this did not apply to the markers of this cohort, the median was considered, occasionally leading to cut-off scores $>0\%$, that is, expression of the respective marker in any cell. Yet, considering such markers with low cut-off scores, the respective protein was always detectable in at least 15% of the tumour cells in positive cases. For formal correctness, these cut-offs are listed in Table 3 as 'any expression'. For c-myc and bcl2, cut-off scores $>70\%$ and $>40\%$, respectively, as suggested by Johnson *et al.*, were considered [11]. Cut-offs for determining the DLBCL cell of origin (COO) were according to Meyer *et al.* [15]. Interphase fluorescence *in situ* hybridization analysis for *BCL2*, *C-MYC* and *TP53* was performed as published previously [9,16].

Statistical analyses

All statistical analyses were performed using the Statistical Package of Social Sciences (IBM SPSS version 22.0, Chicago, IL, USA) for Windows and reported applying the Reporting Recommendations for Tumor Marker Prognostic Studies guidelines [17]. The Spearman rank correlation was used to analyse relationships between biomarkers and clinical and laboratory parameters; only correlations showing a coefficient (ρ) $> \pm 0.3$ were further considered and reported. The Mann–Whitney *U* and Kruskal–Wallis tests were applied, where appropriate, to identify quantitative differences between groups. Relapse-free survival (RFS) was measured from the time of diagnosis to last follow-up or relapse. RFS probabilities were determined using the Kaplan–Meier method, and differences were compared using the log-rank test. $p < 0.01$ was considered statistically significant.

Cluster analysis

Cluster analysis was used to organize cases according to their similarities or dissimilarities and illustrated in a dendrogram. We stick to recommendations used for

Comprehensive phenotypic characterization of PTLD

Table 1. Patients' characteristics

Characteristics, <i>far</i>	Numbers/time
Sex (male/female)	16/6
Lymphoma type	DLBCL Plasmablastic lymphoma Lymphomatoid granulomatosis Polymorphous PTLD
Transplanted organ	Kidney Heart Liver
Age at transplantations (years)	6–60 (mean 36)
Age at diagnosis of PTLD (years)	12–79 (mean 43)
Time between transplantation and diagnosis of PTLD (days)	49–7024 (mean 2375)
Positive EBV serostatus at transplantation	12/12
Follow-up of the transplanted organ	Good function Loss of function
Death of disease	6
Remission of the PTLD	5/22
Relapse of the PTLD	17/22
Late-onset PTLD	4/22 18/22

DLBCL, diffuse large B-cell lymphomas; EBV, Epstein–Barr virus; PTLD, post-transplant lymphoproliferative disorders.

employing clustering techniques for immunohistochemical expression data derived from TMA experiments [18]. Immunohistochemical data were converted to binary format defining positivity or negativity for every individual marker as described above. Calculations and graphical representation were performed with the statistical software R (<http://www.r-project.org/>). Distance matrix was calculated according to Jaccard's distance measure [19], and Ward's method [20] was used for unsupervised clustering. The following proteins were excluded from the cluster analysis as they were expressed in no (FoxP3, human herpes virus 8, IDH1, mammalian target of rapamycin, p-Jnk, pSTAT1 and pSTAT5) or in every case (p16).

Results

Clinical characteristics

Patients with kidney ($n=17$), liver ($n=3$) and heart ($n=2$) transplants were included in our study. The mean follow-up time was 156 months (range, 4.4–303 months; median, 110 months). All patients with available serological records at the time of transplantation ($n=14$) demonstrated Epstein–Barr virus (EBV) seropositivity. Four patients developed a PTLD within the first 12 months after transplantation (all EBV+), but most developed late-onset PTLD ($n=18$; mean 78.1 months; range 12.8–230.9 months; median 110 months; 13 EBV+). All patients with monomorphic PTLD had been treated with chemotherapy. After diagnosis of PTLD, immunosuppression was reduced in 12 out of 19 patients with monomorphic PTLD. None of the polymorphic PTLD was treated with chemotherapy, while immunosuppression was reduced in two of three cases, the third did not receive any specific PTLD-related

treatment, and none of the two former relapsed, while the third died of infection with still detectable disease. A remission of PTLD after therapy was observed in 17 of 21 patients. Four patients experienced a relapse of PTLD after a median period of 27 months (see also in the paragraph describing the cluster analysis and in Figure 1). Altogether, four patients died of their monomorphic PTLD, three after having achieved a complete remission and one rapidly died with still detectable polymorphic PTLD. Six transplanted organs were lost because of chronic rejection during follow-up; function of the other organs was retained until the end of the follow-up.

Most DLBCL-PTLD are of activated B-cell origin

Fifteen DLBCL-PTLD were analysable for COO. Eight of 15 DLBCL-PTLD were of the activated B-cell (ABC) COO as suggested by the Tally algorithm [15], and in three additional patients, the COO was considered the most probable ABC because, yet lacking MUM1, they did not express either CD10 or GCET and one was FOXP1 positive. All relapses occurred in ABC-DLBCL patients. Three of these relapses did not show any relation to EBV. Expression of *c-myc* correlated negatively with the ABC-COO ($\rho=-0.843$, $p<0.001$). There was no statistically significant difference in the clinical outcome between the two COO groups.

B-cell lineage markers are expressed in PTLD, while infiltrating regulatory T cells are almost lacking

All but one DLBCL-PTLD case were positive for CD20; all cases expressed CD79a. CD38 and MUM1 could be detected in three DLBCL cases each (Figure 1 and Table 3).

Table 2. Antibodies for immunohistochemistry/*in situ* hybridization

	Source	Dilution/incubation	Retrieval	Detection
AKT	Dako M3628	1:20	Tec 98 °C/30 min microwave	DAB
BCL2	Ventana 790-4464	Prediluted	CCI mild (Benchmark XT)	DAB
BTK	Thermo MA5-15337	1:20 000	CCI 24 min (Benchmark XT)	DAB
CD10	Ventana 760-2705	Prediluted	CCI mild (Benchmark XT)	DAB
CD19	Dako IR656	Prediluted	CCI mild (Benchmark XT)	DAB
CD20	Dako IR604	Prediluted, A/B Block	CCI mild (Benchmark XT)	DAB
CD21	Ventana 760-4245	Prediluted	CCI mild (Benchmark XT)	DAB
CD23	Ventana 790-4408	Prediluted	CCI mild (Benchmark XT)	DAB
CD3	Ventana 790-4341	Prediluted	CCI (Benchmark XT)	DAB
CD30	Ventana 790-2926	Prediluted	CCI mild (Benchmark XT)	DAB
CD38	Ventana 760-4785	Prediluted	CCI 16 min (Benchmark XT)	DAB
CD44s	Ventana 790-4537	1:100 overnight 4 °C	CCI 8 min (Benchmark XT)	DAB
CD5	Ventana 790-445140	Prediluted, A/B Block	CCI mild (Benchmark XT)	DAB
CD79a	Ventana 790-4432	Prediluted	CCI mild (Benchmark XT)	DAB
c-myc	Ventana 790-4628	Prediluted	CCI (Benchmark XT)	DAB
C-Rel	Abcam ab108299	1:50	CCI (Benchmark XT)	DAB
CXCR4	Abcam ab2074	1:50	CCI (Benchmark XT)	DAB
EBER	Ventana 800-2842	Prediluted	ISH Protease 3 4 min	DAB
EBNA2	LeicaNCL-EBV-PE2	1:25	CCI (Benchmark XT)	DAB
EBV LMP	Ventana 760-2640	Prediluted	CCI (Benchmark XT)	DAB
FOXP1	Abcam ab32010	1:12 000	Citrate 98 °C/30 min microwave	DAB
FOXP3	Abcam ab20034	1:50	CCI 40 min (Benchmark XT)	DAB
GCET1	Abcam ab68889	1:400 overnight 4 °C	Citrate 98 °C/30 min microwave	DAB
HHV8	Ventana 760-4260	Prediluted	CCI mild (Benchmark XT)	DAB
Id3	CalBioagents M101	1:50	CCI 32 min	DAB
IDH mut	Dianova IDH1R132H	1:10	CCI (Benchmark XT)	DAB
IRAK	Abcam ab63484	1:50	CCI 24 min	DAB
IRAK4	Abcam ab32511	1:200	CCI 24 min	DAB
JAK2	Cell Signaling 3230	1:20 overnight 4 °C	Citrate 98 °C/30 min microwave	DAB
LMO2	Ventana 790-4368	prediluted	CCI (Benchmark XT)	DAB
MCL1	Abcam ab32087	1:40	CCI mild	DAB
Mib1	Dako IR626	Prediluted	CCI mild (Benchmark XT)	DAB
mTOR	Cell Signaling 29765	1:100	CCI std	DAB
MUM1	Cellmarque 358 M-18	Prediluted	CCI mild (Benchmark XT)	DAB
p16	Ventana 705-4713	Prediluted	CCI 16 min (Benchmark XT)	DAB
p44/42	Cell Signaling 9101S	20	CCI 16 min (Benchmark XT)	DAB
p50	Abcam ab31410	1:50	CCI (Benchmark XT)	DAB
p52	Abcam ab31409	1:50	CCI (Benchmark XT)	DAB
p65	Abcam ab31481	1:20	CCI (Benchmark XT)	DAB
pCXCR4	Abcam ab74012	1:20	CCI (Benchmark XT)	DAB
PD1	Ventana 760-4448	Prediluted	CCI 24 min (Benchmark XT)	DAB
PDL1	Cell Signaling 13684	1:50	CCI 24 min (Benchmark XT)	DAB
PI3K	BD Laboratories 610046	1:50	CCI 16 min (Benchmark XT)	DAB
PI3K p110	Abcam ab200372	1:50	CCI 24 min (Benchmark XT)	DAB
pSTAT1	Cell Signaling 9167S	1:50 overnight 4 °C	Citrate 98 °C/30 min microwave	DAB
pSTAT3	Cell Signaling 9145	1:50 overnight 4 °C	Citrate 98 °C/30 min microwave	DAB
pSTAT5	Cell Signaling 9359	1:50 overnight 4 °C	Citrate 98 °C/15 min microwave	DAB
pSTAT6	Abcam ab28829	1:20 overnight 4 °C	Tec 98 °C/30 min microwave	AEC
Rel-B	Abcam ab33917	1:50	CCI (Benchmark XT)	DAB
TRAF1	Thermo MA5-15043	1:50	CCI 24 min (Benchmark XT)	DAB

One polymorphic PTLD also showed expression of CD38. Fifty per cent of all (6/12) evaluable DLBCL-PTLD had a proliferation rate >50%. EBV-infected cases with latency type III lacked CD19.

Only very few FoxP3-positive regulatory T cells could be detected. To verify these findings obtained on the

TMA, we also stained whole mount sections of five PTLD cases of our cohort for FoxP3, which confirmed the result.

PD1 and PDL1 expressions by tumour cells was observed in three and five cases, respectively; the reliability of this staining was also suggested by a positive correlation of these proteins ($\rho=0.717$, $p=0.001$).

Comprehensive phenotypic characterization of PTLD

Table 3. Results of the immunohistochemical stainings

	Number of positive cases (%)				Cut-off (%)
	Polymorphic PTLD		Monomorphic PTLD		
pAKT	1/3	33	0/18	0	Any expression ^a
BCL2	1/3	33	2/18	11	70
BTK	2/3	67	3/14	21	30
CD10	1/3	33	6/14	43	Any expression
CD19	3/3	100	10/17	59	Any expression
CD20	3/3	100	17/19	89	Any expression
CD30	1/3	33	0/17	0	Any expression
CD38	1/3	33	3/16	19	Any expression
CD44s	3/3	100	10/16	63	90
CD79a	3/3	100	17/17	100	Any expression
c-myc	0/3	0	5/16	31	Any expression
c-Rel	3/3	100	14/15	93	Any expression
CXCR4	2/3	67%	10/13	77	5
EBER	1/3	33	11/19	58	Any expression
EBNA2	0/3	0	5/18	28	Any expression
EBV LMP	1/3	33	7/19	37	Any expression
FOXP1	1/3	33	3/19	16	80
FOXP3	0/3	0	0/18	0	Any expression
GCET1	0/3	0	1/13	8	80
HHV8	0/3	0	0/19	0	Any expression
Id3	1/3	33	5/15	33	30
IDH mut	0/3	0	0/19	0	10
IRAK1	1/3	33	1/14	7	30
IRAK4	2/3	67	2/14	14	30
JNK	0/3	0	0/18	0	100
LMO2	1/3	33	6/15	40	30
MCL1	3/3	100	7/14	50	30
Mib1	0/3	0	6/13	46	30
mTOR	0/3	0	0/15	0	Any expression
MUM1	0/3	0	3/17	18	80
p16	3/3	100	14/14	100	Any expression
p44/42 MAPK	0/3	0	2/14	14	Any expression
p50	2/3	67	11/15	73	Any expression
p52	2/3	67	5/14	36	5
p65	2/3	67	8/15	53	Any expression
pCXCR4	3/3	100	12/19	63	30
PD1	1/3	33	2/15	13	Any expression
PDL1	2/3	67	3/15	20	Any expression
PI3K	2/3	67	14/15	93	30
PI3K p110	2/3	67	10/13	77	30
pSTAT1	0/3	0	0/18	0	50
pSTAT3	1/3	33	2/16	13	Any expression
pSTAT5	0/3	0	0/19	0	30
pSTAT6	0/3	0	5/19	26	Any expression
RelB	2/3	67	1/15	7	Any expression
TRAF1	2/3	67	2/14	14	Any expression

^aAs stated in the Methods section, the median percentage of positively stained tumour cells for most markers was chosen as the cut-off value for determining positive and negative cases, because this was the most appropriate method in the setting of our cohort and the median for most of these markers was 0, that is, 'any expression'. Yet, in almost all instances in positive cases, the expression of the respective markers was in 15% to 100% of cells.

PI3K but not MAPK/ERK and STAT are expressed in PTLD

Phosphoinositide 3-kinase expression was strong and diffuse in all but one PTLD (Figure 2). Looking at the more specific p110 subunit of PI3K, an expression

could be observed in 77% of monomorphic PTLD and two out of three polymorphic PTLD; the expression of this subunit also showed a positive correlation with CD19 as expected from the literature [21] ($\rho=0.667$, $p=0.005$).

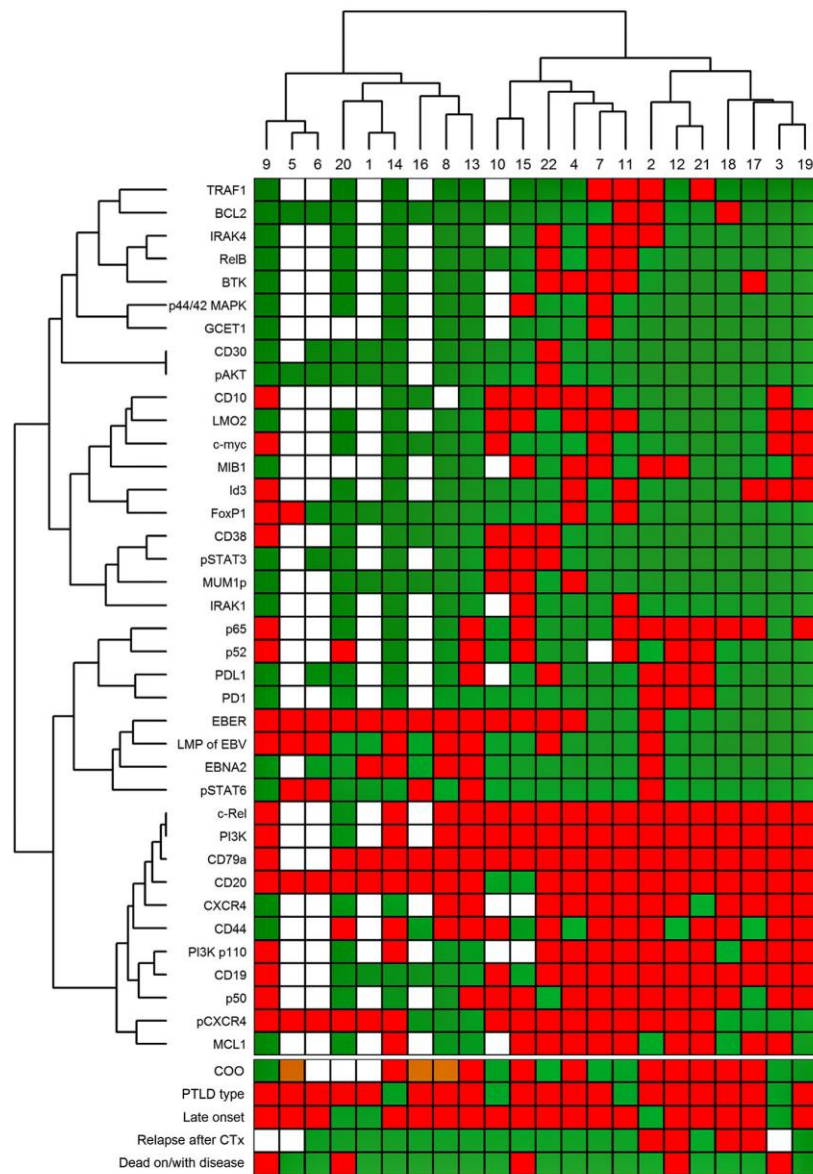


Figure 1. Cluster analysis illustrating three different phenotypic subgroups of post-transplant lymphoproliferative disorders (PTLD). The upper dendrogram shows the patients split into three clusters. For the immunohistochemically investigated markers, red indicates expression and green indicates no expression. Empty spots depict markers that were not analysable in the respective cases. Regarding clinical data, colours indicate the following: PTLD type—red, monomorphic PTLD; green, polymorphic PTLD. Late onset—red, late onset; green, early onset. Relapse after chemotherapy (CTx)—red, relapses; green, ongoing remission; empty spots apply to polymorphic PTLD cases and patients who did not achieve remission after primary CTx or for whom the respective information was missing. Dead on/with disease—red, lethality; green, patient still alive at last contact

Nuclear pSTAT3 was seen in only two DLBCL-PTLD cases, while nuclear pSTAT6 expression was detected in isolated tumour cells of five cases. pSTAT1 and pSTAT5 were not detectable in any case. Expression of p44/42 MAPK/ERK component was only detected in two of 14 evaluable cases.

NF-κB pathway components are highly active in PTLD

The two NF-κB signalling pathways were investigated assessing nuclear expression of p50, p65 and c-Rel for the canonical pathway and p52 and RelB for the non-canonical

Comprehensive phenotypic characterization of PTLD

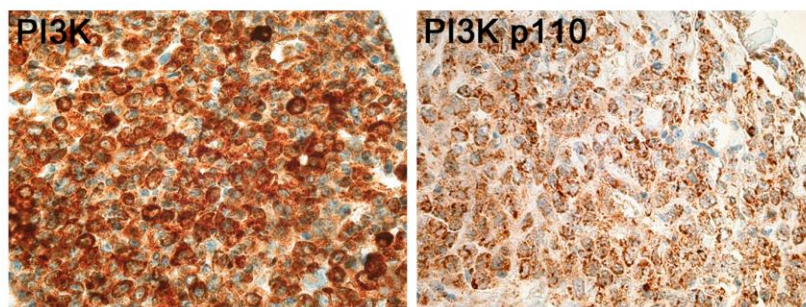


Figure 2. Expression of phosphoinositide 3-kinase (PI3K) and the druggable PI3K p110 component in a post-transplant lymphoproliferative disorder diffuse large B-cell lymphomas case (400 \times)

pathway. In six DLBCL-PTLD cases (mostly EBV negative), only proteins of the canonical pathway were present; in one case, only proteins of the non-canonical pathway were present. Five cases showed expression of proteins of both signalling pathways. Only two DLBCL-PTLD (both EBV associated with latency type III) did not show any expression of NF- κ B signalling-related proteins.

B-cell receptor signalling components are expressed in a minority of PTLD

This pathway was analysed by evaluation of the expression of BTK (Figure 3), interleukin-1 receptor-associated

kinases 1 and 4 (IRAK1 and IRAK4) and tumour necrosis factor α receptor-associated factor 1 (TRAF1). As expected, IRAK4 expression and TRAF1 expression correlated positively with each other ($\rho=0.673$, $p=0.003$). Two of three polymorphic PTLD expressed these proteins, one case even all four. Only three out of 14 DLBCL-PTLD expressed BTK: one of them in combination with IRAK4 and TRAF1, another case showed expression of both IRAK4 and TRAF1 and one single case was positive for IRAK1 without expression of other proteins of this signalling cascade. A positive correlation was observed between these proteins and the non-canonical NF- κ B signalling (IRAK4-p65: $\rho=0.835$, $p<0.001$; BTK-RelB: $\rho=0.717$,

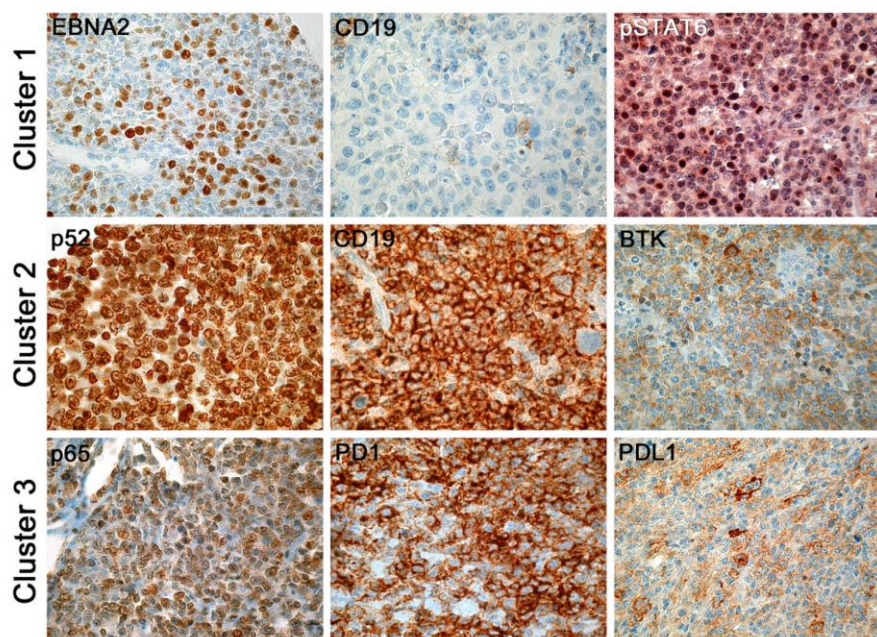


Figure 3. Immunohistochemical stainings of various markers, which were differently expressed in the three phenotypic clusters. First row (from left to right): cases of cluster 1 showing expression of EBV nuclear antigen 2 (EBNA2) (360 \times), lacking expression of CD19 (non-neoplastic lymphocytes serving as positive internal control; 400 \times), and expressing pSTAT6 (360 \times). Second row (from left to right): cases of cluster 2 showing expression of p52 (400 \times), CD19 (400 \times) and Bruton tyrosine kinase (BTK) (360 \times). Third row (from left to right): cases of cluster 3 showing expression of p65, PD1 and PDL1 (all 360 \times)

$p=0.001$). IRAK1 correlated negatively with expression of CD20 ($\rho=-0.685$, $p=0.002$).

The majority of PTLD is EBV associated

Epstein–Barr virus latency status was assessed by investigating the expression of EBV nuclear antigen 2 (EBNA2), EBV latent membrane protein 1 (LMP1) and EBV-encoded small RNA (EBER). Expression of CD19 was negatively correlated to EBER ($\rho=-0.599$, $p=0.005$) and, as mentioned, was completely absent in EBNA2-positive cases. Four DLBCL-PTLD each were of latency type I, II and III, respectively. In eight cases, neither EBV-RNA nor EBV-associated proteins were detected; all of these were late-onset PTLD. As expected, the case of lymphomatoid granulomatosis displayed latency type I. One case of the polymorphic PTLD was of latency type I, and the others were not EBV associated.

Human herpes virus 8 staining was negative in all cases.

Fluorescence *in situ* hybridization analysis

Rearrangements of the *BCL2* and *C-MYC* and deletions of the *TP53*-loci could not be found in any case.

Cluster analysis

Unsupervised hierarchical clustering revealed segregation of our cases into three different groups (Figure 1): cluster 1, related to EBV infection, mainly latency type III (EBNA2+) and mostly lacking CD19, upstream B-cell signalling and NF- κ B constituents; cluster 2, mostly related to EBV infection with expression of the alternative NF- κ B pathway compound RelB and CD10, as well as either FOXP1 or MUM1p; and cluster 3, mostly unrelated to virus infection with expression of the classic NF- κ B pathway compound p65 and containing the three cases with checkpoint (PD1/PDL1) component coexpression. Clusters 2 and 3 were closely related to each other than to cluster 1. Follow-up analysis revealed a statistically significant negative impact of cluster 3 on RFS (Figure 4); no other factor had an impact on survival (RFS, overall survival or disease-specific survival; data not shown).

Discussion

Here, we present a comprehensive phenotypical analysis of a clinically well-characterized cohort of PTLD patients. We show that PI3K and NF- κ B signalling and EBV activation seem to be of central importance for both monomorphic (DLBCL) and polymorphic cases. In addition, we identify a phenotypic cluster unrelated to virus infection with

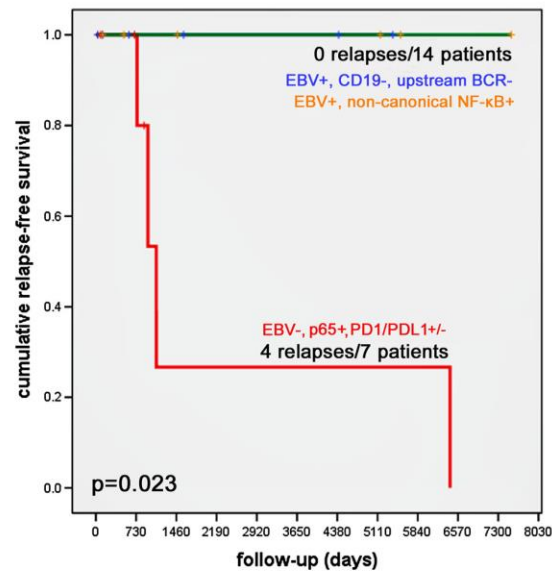


Figure 4. Relapse-free survival curves related to the different clusters showing a worse relapse-free survival for patients of cluster 3 (red line). Both clusters related to Epstein–Barr virus (EBV) are summarized in the green line as none of these patients relapsed. As one patient died shortly after the initial diagnosis of his post-transplant lymphoproliferative disorders, he was excluded from the relapse-free survival analysis that included 21 patients

potentially druggable checkpoint (PD1/PDL1) component expression of possible prognostic importance.

Comprehensive immunohistochemical analysis of all five NF- κ B sub-compounds has been performed in only few studies so far [14,22,23]. The importance of NF- κ B signalling in relation to the EBV status has been analysed in a study of similar size on DLBCL-PTLD [24], yet that study only focused on p50 and p52. Our observed link between EBV infection in cluster 2 (mainly EBV latency type I and II cases) and compounds of the non-canonical NF- κ B pathway has been reported: in the provisional entity of another immunodysregulation-related DLBCL, ‘EBV-positive DLBCL of the elderly’, an activity of the NF- κ B pathway has been shown [25,26] and validated *in vitro* [27]. A particular novel finding of ours is that EBV-associated cases with latency type III infection (with productive virus replication) show lower presence of nuclear NF- κ B compounds, thus probably being less dependent on that pathway’s activity.

B-cell receptor signalling has emerged as a new therapeutic target in DLBCL, mainly by inhibiting BTK, particularly in ABC-DLBCL [28]. Our study is the first assessing the expression of BTK in a large cohort of PTLD using immunohistochemistry. Fernández-Vega *et al.* could show that 86% of DLBCL showed a predominantly weak or moderate positivity for BTK [29]. In contrast to these findings, BTK expression was only detected in a minority

Comprehensive phenotypic characterization of PTLD

of patients in our cohort. Thus, B-cell receptor signalling might not be as important for PTLD as for lymphomas in non-immunocompromised patients. In confirmation of this theory, the study on EBV-related DLBCL, alluded to previously, showed that activating mutations of genes encoding proteins involved in B-cell receptor signalling (*CD79B*, *CARD11*, *MYD88*) are scarce in EBV-related lymphomas [26]. These findings, together with our observed lack of typical chromosomal aberrations of conventional DLBCL like rearrangements of *BCL2* and *C-MYC* and deletions of *TP53* in PTLD, corroborate the hypothesis that signalling related to EBV may act as a substitute for B-cell receptor signalling in the respective virus-infected lymphomas. This is in concordance with studies by others [30–32].

Several intracellular signalling pathways—PI3K, STATs and MAPK/ERK—were investigated in our study. So far, most knowledge on these pathways in PTLD has been derived from *in vitro* cell line experiments [33–35]. We demonstrate that PTLD probably more heavily relies on PI3K than on STAT and MAPK signalling. The strong expression of PI3K was confirmed on another TMA containing DLBCL cases of non-immunocompromised patients (data not shown). High expression levels of PI3K are a frequent finding in DLBCL [36], which has now also raised interest as a potential point of action in targeted therapy [7]. By analysing the p110 subunit of PI3K, which can be specifically targeted by idelalisib [37], we detected substantial expression in a high proportion of PTLD cases, thus identifying a new intriguing therapeutic target. The positive clustering of the p110 PI3K subunit with CD19 and its inverse clustering with EBV indicates that especially PTLD not related to EBV (the more aggressive subgroup in our cohort) might be candidates for idelalisib.

Cluster analysis has so far mainly been applied for gene expression analyses, yet several groups have paved the way for introducing this method into phenotypical immunohistochemical analysis, mainly in various carcinoma subtypes [18,38,39]. By unsupervised clustering, we identified reasonable PTLD subgroups with logical interrelations, which also make sense regarding the biology of the investigated proteins. The observed tripartition of PTLD might have important implications for more tailored PTLD treatment, for example, by showing not only the potential negative prognostic impact of cluster 3 but also the more abundant presence of targetable checkpoint compounds (PD1/PDL1) in it.

Investigations of the microenvironment of PTLD showed absence of FoxP3 regulatory T cells. This finding is in concordance with previous studies investigating the microenvironment of PTLD [40,41]. Interestingly, it has recently been shown that a large number of FoxP3 regulatory T cells in the microenvironment of DLBCL predict a better response to rituximab-based chemotherapy [42], and this might be one of the several reasons that PTLD respond worse to R-CHOP than lymphomas in

immunocompetent patients. PD1 and PDL1 are also postulated to have a modulatory effect on the microenvironment in lymphomas [43]. The infrequent expression of these proteins in our cohort, except for the EBV-negative cluster 3, is another argument supporting the hypothesis that the microenvironment does not play a major role in EBV-related PTLD.

One of the shortcomings of this study is the relatively small amount of cases; yet all cases included had a well-documented detailed clinical history. As several findings like the virtual absence of FoxP3 regulatory cells and some of the observed relations between markers have been confirmed in larger cohorts, our results seem to reflect the pathophysiology of PTLD. However, further studies will be needed, especially regarding the role of the identified phenotypic clusters prior to clinical translation.

In this study, we comprehensively characterized PTLD, focusing on potentially targetable intracellular pathways as well as important proteins regarding lymphomagenesis. Cluster analysis showed three distinct subgroups of PTLD. Signalling cascades involving PI3K are active in the majority of PTLD, while those related to B-cell receptor, MAPK/ERK, pSTAT and p-Jnk signalling are not.

Conflict of interest

All authors declare to have no conflict of interest.

Acknowledgements

The authors would like to thank Mrs Petra Hirschmann for the immunohistochemical stainings.

Thomas Menter thanks the Nuovo-Soldati Cancer Research Foundation, Vaduz, Liechtenstein, for the support of the ongoing studies on PTLD.

References

1. Swerdlow SH, Webber SA, Chadburn A, Ferry JA. Post-transplant lymphoproliferative disorders. In WHO Classification of Tumours of Haematopoietic and Lymphoid Tissues (4th edn). Swerdlow SH, Campo E, Harris NL, *et al.* (eds). Internat. Agency for Research on Cancer: Lyon, 2008; 343–349.
2. Parker A, Bowles K, Bradley JA, *et al.* Diagnosis of post-transplant lymphoproliferative disorder in solid organ transplant recipients—BCSH and BTS Guidelines. *Br J Haematol* 2010; **149**: 675–692.
3. Carbone A, Ghoghini A, Kwong Y, Younes A. Diffuse large B cell lymphoma: using pathologic and molecular biomarkers to define subgroups for novel therapy. *Ann Hematol* 2014; **93**: 1263–1277.
4. Wilson WH. Treatment strategies for aggressive lymphomas: what works? *Hematology Am Soc Hematol Educ Program* 2013; **2013**: 584–590.
5. Davis RE, Ngo VN, Lenz G, *et al.* Chronic active B-cell-receptor signalling in diffuse large B-cell lymphoma. *Nature* 2010; **463**: 88–92.

6. Dasmahapatra G, Patel H, Dent P, Fisher RI, Friedberg J, Grant S. The Bruton tyrosine kinase (BTK) inhibitor PCI-32765 synergistically increases proteasome inhibitor activity in diffuse large-B cell lymphoma (DLBCL) and mantle cell lymphoma (MCL) cells sensitive or resistant to bortezomib. *Br J Haematol* 2013; **161**: 43–56.
7. Yang Q, Modi P, Newcomb T, Quéva C, Gandhi V. Idelalisib: first-in-class PI3K delta inhibitor for the treatment of chronic lymphocytic leukemia, small lymphocytic leukemia, and follicular lymphoma. *Clin Cancer Res* 2015; **21**: 1537–1542.
8. Mohamed AJ, Yu L, Bäckesjö C, et al. Bruton's tyrosine kinase (BTK): function, regulation, and transformation with special emphasis on the PH domain. *Immunol Rev* 2009; **228**: 58–73.
9. Xu-Monette ZY, Wu L, Visco C, et al. Mutational profile and prognostic significance of TP53 in diffuse large B-cell lymphoma patients treated with R-CHOP: report from an International DLBCL Rituximab-CHOP Consortium Program Study. *Blood* 2012; **120**: 3986–3996.
10. Horn H, Ziepert M, Becher C, et al. MYC status in concert with BCL2 and BCL6 expression predicts outcome in diffuse large B-cell lymphoma. *Blood* 2013; **121**: 2253–2263.
11. Johnson NA, Slack GW, Savage KJ, et al. Concurrent expression of MYC and BCL2 in diffuse large B-cell lymphoma treated with rituximab plus cyclophosphamide, doxorubicin, vincristine, and prednisone. *J Clin Oncol* 2012; **30**: 3452–3459.
12. Menter T, Juskevicius D, Tzankov A. Array CGH-based analysis of post-transplant plasmacytic hyperplasia reveals 'intact genomes' arguing against categorizing it as part of the post-transplant lymphoproliferative disease spectrum. *Transpl Int* 2015; **28**: 120–122.
13. Tzankov A, Went P, Zimpfer A, Dirnhofer S. Tissue microarray technology: principles, pitfalls and perspectives—lessons learned from hematological malignancies. *Exp Gerontol* 2005; **40**: 737–744.
14. Menter T, Ernst M, Drachneris J, et al. Phenotype profiling of primary testicular diffuse large B-cell lymphomas. *Hematol Oncol* 2014; **32**: 72–81.
15. Meyer PN, Fu K, Greiner TC, et al. Immunohistochemical methods for predicting cell of origin and survival in patients with diffuse large B-cell lymphoma treated with rituximab. *J Clin Oncol* 2011; **29**: 200–207.
16. Tzankov A, Xu-Monette ZY, Gerhard M, et al. Rearrangements of MYC gene facilitate risk stratification in diffuse large B-cell lymphoma patients treated with rituximab-CHOP. *Mod Pathol* 2014; **27**: 958–971.
17. McShane LM, Altman DG, Sauerbrei W, Taube SE, Gion M, Clark GM. REporting recommendations for tumor MARKer prognostic studies (REMARK). *Nat Clin Pract Oncol* 2005; **2**: 416–422.
18. Makretsov NA, Huntsman DG, Nielsen TO, et al. Hierarchical clustering analysis of tissue microarray immunostaining data identifies prognostically significant groups of breast carcinoma. *Clin Cancer Res* 2004; **10**: 6143–6151.
19. Sneath PH. Some thoughts on bacterial classification. *J Gen Microbiol* 1957; **17**: 184–200.
20. Ward J. Hierarchical grouping to optimize an objective function. *J Am Stat Assoc* 1963; **58**: 236–244.
21. Hobeika E, Levit-Zerdoun E, Anastasopoulou V, et al. CD19 and BAFF-R can signal to promote B-cell survival in the absence of Syk. *EMBO J* 2015; **34**: 925–939.
22. Odqvist L, Montes-Moreno S, Sánchez-Pacheco RE, et al. NFκB expression is a feature of both activated B-cell-like and germinal center B-cell-like subtypes of diffuse large B-cell lymphoma. *Mod Pathol* 2014; **27**: 1331–1337.
23. Ok CY, Xu-Monette ZY, Li L, et al. Evaluation of NF-κB subunit expression and signaling pathway activation demonstrates that p52 expression confers better outcome in germinal center B-cell-like diffuse large B-cell lymphoma in association with CD30 and BCL2 functions. *Mod Pathol* 2015; **28**: 1202–1213.
24. Proust A, Rincé P, Creidy R, et al. p52 activation in monomorphic B-cell posttransplant lymphoproliferative disorder/diffuse large B-cell lymphoma without BAFF-R expression. *Am J Pathol* 2011; **179**: 1630–1637.
25. Montes-Moreno S, Odqvist L, Diaz-Perez JA, et al. EBV-positive diffuse large B-cell lymphoma of the elderly is an aggressive post-germinal center B-cell neoplasm characterized by prominent nuclear factor-κB activation. *Mod Pathol* 2012; **25**: 968–982.
26. Gebauer N, Gebauer J, Hardel TT, et al. Prevalence of targetable oncogenic mutations and genomic alterations in Epstein-Barr virus-associated diffuse large B-cell lymphoma of the elderly. *Leuk Lymphoma* 2015; **56**: 1100–1106.
27. Mohr CF, Kalmer M, Gross C, et al. The tumor marker Fascin is induced by the Epstein-Barr virus-encoded oncoprotein LMP1 via NF-κB in lymphocytes and contributes to their invasive migration. *Cell Commun Signal: CCS* 2014; **12**: 46.
28. Yang Y, Shaffer AL, Emre NCT, et al. Exploiting synthetic lethality for the therapy of ABC diffuse large B cell lymphoma. *Cancer Cell* 2012; **21**: 723–737.
29. Fernández-Vega I, Quirós LM, Santos-Juanes J, Pane-Foix M, Marafioti T. Bruton's tyrosine kinase (BTK) is a useful marker for Hodgkin and B cell non-Hodgkin lymphoma. *Virchows Arch* 2015; **466**: 229–235.
30. Mancao C, Altmann M, Jungnickel B, Hammerschmidt W. Rescue of "crippled" germinal center B cells from apoptosis by Epstein-Barr virus. *Blood* 2005; **106**: 4339–4344.
31. Bräuninger A, Spieker T, Mottok A, Baur AS, Küppers R, Hansmann M. Epstein-Barr virus (EBV)-positive lymphoproliferations in post-transplant patients show immunoglobulin V gene mutation patterns suggesting interference of EBV with normal B cell differentiation processes. *Eur J Immunol* 2003; **33**: 1593–1602.
32. Capello D, Cerri M, Muti G, et al. Analysis of immunoglobulin heavy and light chain variable genes in post-transplant lymphoproliferative disorders. *Hematol Oncol* 2006; **24**: 212–219.
33. Hatton O, Phillips LK, Vaysberg M, Hurwich J, Krams SM, Martinez OM. Syk activation of phosphatidylinositol 3-kinase/Akt prevents HtrA2-dependent loss of X-linked inhibitor of apoptosis protein (XIAP) to promote survival of Epstein-Barr virus+ (EBV+) B cell lymphomas. *J Biol Chem* 2011; **286**: 37368–37378.
34. Vaysberg M, Lambert SL, Krams SM, Martinez OM. Activation of the JAK/STAT pathway in Epstein-Barr virus+ associated posttransplant lymphoproliferative disease: role of interferon-gamma. *Am J Transplant* 2009; **9**: 2292–2302.
35. Furukawa S, Wei L, Krams SM, Esquivel CO, Martinez OM. PI3K inhibition augments the efficacy of rapamycin in suppressing proliferation of Epstein-Barr virus (EBV)+ B cell lymphomas. *Am J Transplant* 2013; **13**: 2035–2043.
36. Uddin S, Hussain AR, Siraj AK, et al. Role of phosphatidylinositol 3'-kinase/AKT pathway in diffuse large B-cell lymphoma survival. *Blood* 2006; **108**: 4178–4186.
37. Maffei R, Fiorcari S, Martinelli S, Potenza L, Luppi M, Marasca R. Targeting neoplastic B cells and harnessing microenvironment: the "double face" of ibrutinib and idelalisib. *J Hematol Oncol* 2015; **8**: 60.
38. Muñoz-Repeto I, García MJ, Kamieniak M, et al. Phenotypic characterization of hereditary epithelial ovarian cancer based on a tissue microarray study. *Histol Histopathol* 2013; **28**: 133–144.
39. Hammer SH, Prall F. Close relation of large cell carcinoma to adenocarcinoma by hierarchical cluster analysis: implications for histologic

Comprehensive phenotypic characterization of PTLD

- typing of lung cancer on biopsies. *Appl Immunohistochem Mol Morphol* 2015; **23**: 550–557.
40. Berglund D, Kinch A, Edman E, *et al.* Expression of intratumoral forkhead box protein 3 in posttransplant lymphoproliferative disorders: clinical features and survival outcomes. *Transplantation* 2015; **99**: 1036–1042.
 41. Richendollar BG, Tsao RE, Elson P, *et al.* Predictors of outcome in post-transplant lymphoproliferative disorder: an evaluation of tumor infiltrating lymphocytes in the context of clinical factors. *Leuk Lymphoma* 2009; **50**: 2005–2012.
 42. Coutinho R, Clear AJ, Mazzola E, *et al.* Revisiting the immune microenvironment of diffuse large B-cell lymphoma using a tissue microarray and immunohistochemistry: robust semi-automated analysis reveals CD3 and FoxP3 as potential predictors of response to R-CHOP. *Haematologica* 2015; **100**: 363–369.
 43. Berghoff AS, Ricken G, Widhalm G, *et al.* PD1 (CD279) and PD-L1 (CD274, B7H1) expression in primary central nervous system lymphomas (PCNSL). *Clin Neuropathol* 2014; **33**: 42–49.

3.7 Lenalidomide monotherapy leads to a complete remission in refractory B-cell post-transplant lymphoproliferative disorder

Läubli H., Tzankov A., **Juskevicius D.**, Degen L., Rochlitz, L., Stenner-Liewen F.

-Letter to the editor-
Published in *Leukemia & Lymphoma*, 2015

Contribution: I performed genetic characterization of the investigated case and composed part B of the Figure 1.

LETTER TO THE EDITOR

Lenalidomide monotherapy leads to a complete remission in refractory B-cell post-transplant lymphoproliferative disorder

Heinz Läubli^{1,2}, Alexander Tzankov³, Darius Juskevicius³, Lukas Degen⁴, Christoph Rochlitz¹ & Frank Stenner-Liewen^{1,2}

¹Department of Internal Medicine, Division of Medical Oncology, University Hospital Basel, Switzerland, ²Department of Biomedicine, Cancer Immunology Laboratory, University Hospital Basel, Switzerland, ³Institute of Pathology, University Hospital Basel, Switzerland, and ⁴Division of Gastroenterology and Hepatology, University Hospital Basel, Switzerland

Post-transplant lymphoproliferative disorders (PTLD) are serious complications after solid organ- and allogeneic hematopoietic stem cell transplantation [1]. While EBV-associated polymorphic PTLD cases can often be treated with reduction of immunosuppression, monomorphic PTLD are usually treated with immuno-chemotherapy. Despite therapy, prognosis is often poor and treatment options are limited [1]. The choice of chemotherapy is determined by the type of lymphoma and the type of graft [1]. Treatment of EBV-associated PTLD with EBV-specific T cells is another promising treatment approach [2]. We report here a case of a patient who developed a refractory B-cell PTLD after liver transplantation with an impressive response to monotherapy with lenalidomide that was started after several lines of immunotherapy and chemotherapy.

A 41-year-old female patient developed an EBV-associated B-cell PTLD (diffuse large B-cell lymphoma, DLBCL) three years after liver transplantation for a cirrhosis due to primary sclerosing cholangitis associated with colitis ulcerosa. At diagnosis the patient was under immunosuppression with tacrolimus. Presenting symptoms were abdominal discomfort and a computed tomography of the abdomen revealed enlarged mediastinal lymph nodes. An FDG-PET/CT demonstrated that no other lymph node regions or organs were involved. Biopsy of a mediastinal lymph node revealed a DLBCL. Polymerase chain reaction (PCR) for EBV in the peripheral blood and also *in situ* hybridization for EBV (EBER) were positive [Fig. 1A, right panel]. Initially, immunosuppression with tacrolimus and azathioprine was stopped. Six cycles of immuno-chemotherapy with rituximab, cyclophosphamide, doxorubicin, vincristine and prednisone

(R-CHOP) and two additional cycles of rituximab led to a complete remission shown by subsequent FDG-PET/CT. The liver graft remained functional throughout the therapy.

Immunosuppression with tacrolimus was re-initiated after completion of therapy. Three relapse-free years later, she presented again with abdominal symptoms. CT of the abdomen revealed thickening of a part of the jejunum that was interpreted as suggestive of a PTLD relapse. Laboratory abnormalities included a mild anemia (10 g/dL) and an increased C-reactive protein (CRP, 111.2 mg/L). Endoscopic biopsy confirmed an intestinal affection with DLBCL. At this point, however, *in situ* hybridization for EBV was negative [Fig. 1A, left panel] and EBV DNA in the peripheral blood was undetectable. These findings raised the suspicion of a secondary DLBCL PTLD rather than a relapse of the primary DLBCL. Indeed, array-comparative genomic hybridization (aCGH) and immunoglobulin heavy gene (*IGH*) fragment length and sequencing analyses confirmed an independent malignant B-cell clone. In addition, while the first DLBCL showed a germinal cell B-cell (GCB) phenotype, the second occurrence was of the activated B-cell type (ABC) as determined by immunohistochemistry exactly applying published protocols [3]. It also harbored distinct *IGH* gene rearrangements, both at the PCR product length- and at the DNA sequence level. Moreover, primary and relapse DLBCL had a modest number of DNA copy number aberrations, but none of them were shared between both tumors [Fig. 1B]. Immunosuppression was changed from tacrolimus to sirolimus and lowered over time (from 2 to 1 mg). Due to her poor and declining

Correspondence: Heinz Läubli,  Division of Medical Oncology and Cancer Immunology Laboratory, University Hospital Basel, Petersgraben 4, 4031 Basel, Switzerland. Tel: +41 61 265 5074. Fax: +41 61 265 5316.  heinz.laebli@usb.ch

(Received 12 May 2015; revised 30 June 2015; accepted 11 August 2015)

© 2015 Taylor & Francis


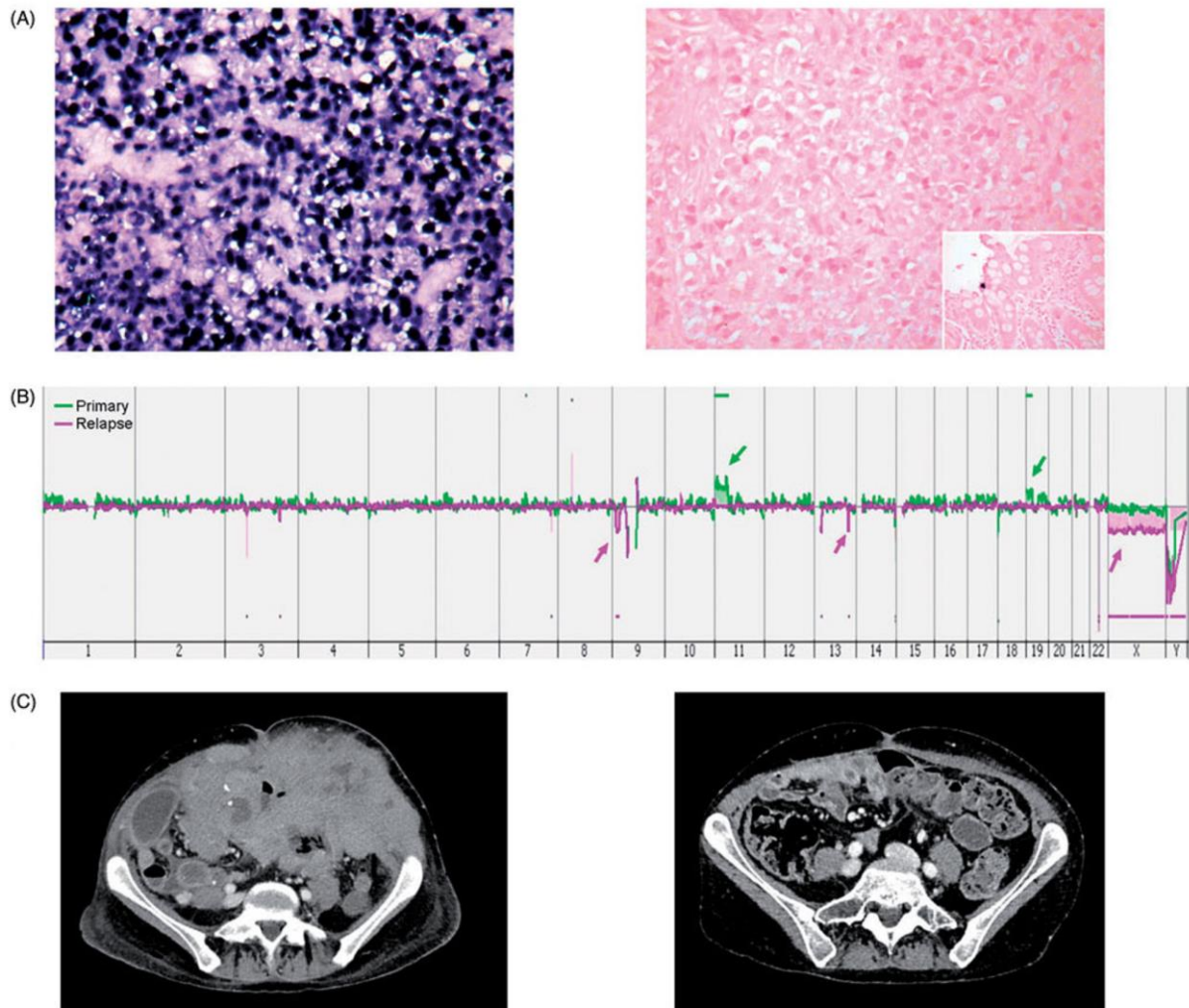
2  H. LÄUBLI ET AL.

Figure 1. (A) EBV status of both lymphoma occurrences. EBER-stain in primary (left) and relapsed DLBCL, (original magnification $\times 360$). Note that the EBER-stain is negative in the intestinal DLBCL “relapse” despite EBV-positive bowel epithelial cells are present as internal positive controls in the stained slide (insert). (B) Genome overview plots show relatively small number of chromosomal copy number aberrations occurring in the primary and relapse tumors. None of the aberrations are shared, which supports lack of clonal relationship between both occurrences. For genomic hybridization, genomic DNA was extracted from formalin-fixed paraffin-embedded tissues with $>70\%$ tumor content and was used for aCGH on the Agilent SurePrint 180k oligonucleotide microarrays. (C) Treatment with lenalidomide monotherapy leads to a major response. Computed tomography scans before the initiation with lenalidomide (left) and after 2 months of treatment (right).

performance status, rituximab monotherapy was initiated. These interventions resulted in a clinical stabilization and allowed resection of the affected jejunum. After four cycles of rituximab, however, signs of a mechanical bowel obstruction developed and a CT scan showed diffuse thickening of the small intestine. Treatment with the glyco-engineered anti-CD20 antibody obinutuzumab (GA101) proved to be ineffective in this situation. Rescue chemotherapy with carboplatin and etoposide was initiated. During this therapy the patient’s status deteriorated with a rapid weight loss. Her BMI decreased from $20.5\text{--}16.3\text{ kg/m}^2$, and lymphoma

progression manifested as a large tumor mass within the abdominal wall. Chemotherapy was stopped after two cycles and palliative irradiation with 14 Gy of the abdominal wall was initiated in order to reduce local pain. Radiotherapy was well tolerated, but the lesion in the abdominal wall progressed further. Confronted with a rapidly progressing PTLD [Fig. 1C, left panel] in a young patient with a severely impaired performance status (ECOG 3), we initiated a monotherapy with lenalidomide in accordance with a previous case report of a T-cell PTLD [4] and reports that ABC type DLBCL seem to be sensitive to treatment with

immunomodulatory drugs such as lenalidomide [5,6]. Lenalidomide was started with 15 mg on days 1 through 21 of repeated 28 day cycles. For the further cycles the lenalidomide dose could be increased to 20 mg daily. After two cycles the patient experienced improvement of her intestinal symptoms, her BMI increased to 18.0 kg/m² and her pain regressed. A CT scan showed a major response of the abdominal lesions and the intestinal thickening to lenalidomide monotherapy [Fig. 1C, right panel]. After another cycle, the patient achieved a complete radiological response. Four months after lenalidomide therapy was initiated, an intestinal bowel obstruction developed, which was treated by surgical adhesiolysis and resection of a segment of the small intestine. Microscopic analysis of the resected segment showed no evidence of malignancy, although the segment was within the tumor bulk before installation of lenalidomide therapy. This was interpreted as complete pathological remission under the therapy as well. Thus, the degree of remission achieved with this therapy allowed redefining of the therapeutic strategy and opened new perspectives, including high dose chemotherapy with autologous stem cell support. At this time, according to the patient's preference, she is still on lenalidomide maintenance therapy.

Lenalidomide is approved for multiple myeloma, 5q- myelodysplastic syndrome and relapsed or refractory mantle cell lymphoma [5,6]. Furthermore, lenalidomide has activity in other types of lymphoma including Hodgkin lymphoma, peripheral T-cell lymphoma and DLBCL [5–10]. The biological activity of lenalidomide can be divided into direct effects towards tumor cells and effects on the tumor microenvironment including the tumor immunosurveillance [5,6]. Previously described effects on lymphoma cells are interference with the NF- κ B pathway, which is an oncogenic driver pathway in ABC type DLBCL [5,6]. Effects on the microenvironment comprise of anti-angiogenic and immunomodulatory properties [5,6]. Lenalidomide has been shown to increase antibody-dependent cellular cytotoxicity of NK-cells, influence T-cell activation and inhibit the proliferation of regulatory T-cells (Tregs) in the tumor microenvironment [5,6]. The role of Tregs in GCB and ABC type DLBCL seems to differ. While in GCB type DLBCL a high number of FOXP3 positive Tregs are associated with an improved survival, in ABC type DLBCL the presence of Tregs are associated with poorer prognosis [11]. Taken together, all these data suggest that lenalidomide might have augmented activity in ABC type DLBCL through multiple pathways and could also explain the significant effect that we observed in our B-cell PTLT patient.

Lenalidomide was studied in relapsed DLBCL in several phase II trials [5,6,12], showing response rates in combination with rituximab of 33–35% [8,10]. Lenalidomide is also active as monotherapy in relapsed or refractory DLBCL with overall response rates of 19–28% [9,13]. In support of an enhanced activity of lenalidomide in patients with ABC type DLBCL, a recent analysis found a complete response rate of 23.5% in ABC DLBCL versus 4.3% in GCB DLBCL and a progression-free survival of 6.2 versus 1.7 months [14]. Combination strategies of lenalidomide with immunochemotherapy as first line regimen were tested in different trials and the addition of lenalidomide to R-CHOP was shown to overcome the worse prognosis of non-GCB DLBCL compared to GCB-DLBCL [6,15]. For our patient, lenalidomide has led to a major, near-complete response after less than 8 weeks of treatment and to a pathologically proven complete response after 4 months. Moreover, it was well tolerated in her severely reduced nutritional and performance status. The significant response to lenalidomide treatment was observable in her second PTLT DLBCL occurrence, which was of ABC cellular origin and EBV-negative, being in accordance with the current evidence of an increased lenalidomide activity in ABC type DLBCL [6]. Noteworthy, the immune-stimulatory effect of lenalidomide had no effect on graft function in our patient.

To our knowledge, this is the first description of a significant response induced by lenalidomide in a B-cell PTLT. Our report and a previous case that describes a response of T-cell PTLT to lenalidomide [4] suggest that lenalidomide may be an effective and safe option for PTLT. No other cases of PTLT treated with lenalidomide are reported and therefore further studies are warranted to address the question if B-cell PTLT manifesting as ABC type DLBCL are a more responsive to lenalidomide and if the EBV-status could have an impact as well.

Consent

Written informed consent was obtained from the patient for publication of this case report and any accompanying images. A copy of the written consent is available for review by the Editor-in-Chief of this journal.

Acknowledgements

We thank the patient and her family for letting us publish her case in this report.

Potential conflict of interest: Disclosure forms provided by the authors are available with the full text of this article at www.informahealthcare.com/lal.

References

- [1] Parker A, Bowles K, Bradley JA, et al. Management of post-transplant lymphoproliferative disorder in adult solid organ transplant recipients – BCSH and BTS Guidelines. *Br J Haematol* 2010; 149: 693–705.
- [2] Heslop HE. How I treat EBV lymphoproliferation. *Blood* 2009; 114: 4002–4008.
- [3] Meyer PN, Fu K, Greiner TC, et al. Immunohistochemical methods for predicting cell of origin and survival in patients with diffuse large B-cell lymphoma treated with rituximab. *J Clin Oncol* 2011; 29: 200–207.
- [4] Portell C, Nand S. Single agent lenalidomide induces a response in refractory T-cell posttransplantation lymphoproliferative disorder. *Blood* 2008; 111: 4416–4417.
- [5] Kritharis A, Coyle M, Sharma J, et al. Lenalidomide in non-Hodgkin lymphoma: biological perspectives and therapeutic opportunities. *Blood* 2015; 125: 2471–2476.
- [6] Thieblemont C, Delfau-Larue MH, Coiffier B. Lenalidomide in diffuse large B-cell lymphoma. *Adv Hematol* 2012; 2012: 861060.
- [7] Hitz F, Fischer N, Pabst T, et al. Rituximab, bendamustine, and lenalidomide in patients with aggressive B cell lymphoma not eligible for high-dose chemotherapy or anthracycline-based therapy: phase I results of the SAKK 38/08 trial. *Ann Hematol* 2013; 92: 1033–1040.
- [8] Wang M, Fowler N, Wagner-Bartak N, et al. Oral lenalidomide with rituximab in relapsed or refractory diffuse large cell, follicular and transformed lymphoma: a phase II clinical trial. *Leukemia* 2013; 27: 1902–1909.
- [9] Wiernik PH, Lossos IS, Tuscano JM, et al. Lenalidomide monotherapy in relapsed or refractory aggressive non-Hodgkin's lymphoma. *J Clin Oncol* 2008; 26: 4952–4957.
- [10] Zinzani PL, Pellegrini C, Gandolfi L, et al. Combination of lenalidomide and rituximab in elderly patients with relapsed or refractory diffuse large B-cell lymphoma: a phase 2 trial. *Clin Lymphoma Myeloma Leuk* 2011; 11: 462–466.
- [11] Tzankov A, Meier C, Hirschmann P, et al. Correlation of high numbers of intratumoral FOXP3+ regulatory T cells with improved survival in germinal center-like diffuse large B-cell lymphoma, follicular lymphoma and classical Hodgkin's lymphoma. *Haematologica* 2008; 93: 193–200.
- [12] Witzig TE, Nowakowski GS, Habermann TM, et al. A comprehensive review of lenalidomide therapy for B-cell non-Hodgkin lymphoma. *Ann Oncol* 2015; 26: 1667–1677.
- [13] Witzig TE, Vose JM, Zinzani PL, et al. An international phase II trial of single-agent lenalidomide for relapsed or refractory aggressive B-cell non-Hodgkin's lymphoma. *Ann Oncol* 2011; 22: 1622–1627.
- [14] Hernandez-Ilizaliturri FJ, Deeb G, Zinzani PL, et al. Higher response to lenalidomide in relapsed/refractory diffuse large B-cell lymphoma in nongerminal center B-cell-like than in germinal center B-cell-like phenotype. *Cancer* 2011; 117: 5058–5066.
- [15] Nowakowski GS, LaPlant B, Macon WR, et al. Lenalidomide combined with R-CHOP overcomes negative prognostic impact of non-germinal center B-cell phenotype in newly diagnosed diffuse large B-Cell lymphoma: a phase II study. *J Clin Oncol* 2015; 33: 251–257.

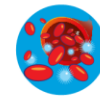
3.8 Multiparameter analysis of homogeneously R-CHOP-treated diffuse large B cell lymphomas identifies CD5 and FOXP1 as relevant prognostic biomarkers: report of the prospective SAKK 38/07

Tzankov A., Leu N., Muenst S., **Juskevicius D.**, Klingbiel D., Mamot C., Dirnhover S.

-Research article-

Published in *Journal of hematology & oncology*, 2015

Contribution: I performed aCGH analysis of CD5-positive DLBCL cases, produced Figure 3 and formatted the manuscript



RESEARCH ARTICLE

Open Access



Multiparameter analysis of homogeneously R-CHOP-treated diffuse large B cell lymphomas identifies CD5 and FOXP1 as relevant prognostic biomarkers: report of the prospective SAKK 38/07 study

Alexandar Tzankov^{1*}, Nora Leu¹, Simone Muenst¹, Darius Juskevicius¹, Dirk Klingbiel², Christoph Mamot³ and Stephan Dirnhofer¹

Abstract

Background: The prognostic role of tumor-related parameters in diffuse large B cell lymphoma (DLBCL) is a matter of controversy.

Methods: We investigated the prognostic value of phenotypic and genotypic profiles in DLBCL in clinical trial (NCT00544219) patients homogeneously treated with six cycles of rituximab, cyclophosphamide, hydroxydaunorubicin, vincristine, prednisone (R-CHOP), followed by two cycles of R (R-CHOP-14). The primary endpoint was event-free survival at 2 years (EFS). Secondary endpoints were progression-free (PFS) and overall survival (OS). Immunohistochemical (bcl2, bcl6, CD5, CD10, CD20, CD95, CD168, cyclin E, FOXP1, GCET, Ki-67, LMO2, MUM1p, pSTAT3) and in situ hybridization analyses (*BCL2* break apart probe, *C-MYC* break apart probe and *C-MYC/IGH* double-fusion probe, and Epstein-Barr virus probe) were performed and correlated with the endpoints.

Results: One hundred twenty-three patients (median age 58 years) were evaluable. Immunohistochemical assessment succeeded in all cases. Fluorescence in situ hybridization was successful in 82 instances. According to the Tally algorithm, 81 cases (66 %) were classified as non-germinal center (GC) DLBCL, while 42 cases (34 %) were GC DLBCL. *BCL2* gene breaks were observed in 7/82 cases (9 %) and *C-MYC* breaks in 6/82 cases (8 %). "Double-hit" cases with *BCL2* and *C-MYC* rearrangements were not observed. Within the median follow-up of 53 months, there were 51 events, including 16 lethal events and 12 relapses. Factors able to predict worse EFS in univariable models were failure to achieve response according to international criteria, failure to achieve positron emission tomography response ($p < 0.005$), expression of CD5 ($p = 0.02$), and higher stage ($p = 0.021$). Factors predicting inferior PFS were failure to achieve response according to international criteria ($p < 0.005$), higher stage ($p = 0.005$), higher International Prognostic Index (IPI; $p = 0.006$), and presence of either *C-MYC* or *BCL2* gene rearrangements ($p = 0.033$). Factors predicting inferior OS were failure to achieve response according to international criteria and expression of FOXP1 ($p < 0.005$), cyclin E, CD5, bcl2, CD95, and pSTAT3 ($p = 0.005, 0.007, 0.016, \text{ and } 0.025$, respectively). Multivariable analyses revealed that expression of CD5 ($p = 0.044$) and FOXP1 ($p = 0.004$) are independent prognostic factors for EFS and OS, respectively.

Conclusion: Phenotypic studies with carefully selected biomarkers like CD5 and FOXP1 are able to prognosticate DLBCL course at diagnosis, independent of stage and IPI and independent of response to R-CHOP.

Keywords: DLBCL, Prognosis, Phenotype, FISH, Prospective trial, CD5, FOXP1

* Correspondence: alexandar.tzankov@usb.ch

¹Institute of Pathology, University Hospital Basel, Schoenbeinstrasse 40, CH-4031 Basel, Switzerland

Full list of author information is available at the end of the article



© 2015 Tzankov et al. This is an Open Access article distributed under the terms of the Creative Commons Attribution License (<http://creativecommons.org/licenses/by/4.0/>), which permits unrestricted use, distribution, and reproduction in any medium, provided the original work is properly credited. The Creative Commons Public Domain Dedication waiver (<http://creativecommons.org/publicdomain/zero/1.0/>) applies to the data made available in this article, unless otherwise stated.

Background

Diffuse large B cell lymphoma (DLBCL) is the most common nodal lymphoid malignancy, comprising approximately 30 % of all adult lymphomas, with a rapidly rising incidence [1, 2]. DLBCL demonstrates an aggressive clinical course, but potentially 60–70 % of patients can be cured with the established rituximab, cyclophosphamide, hydroxydaunorubicin, vincristine, prednisone (R-CHOP) treatment standard [3]. Prediction of survival and stratification of patients for risk-adjusted therapy is based on the International Prognostic Index (IPI) [4]. R-CHOP has not only led to a marked improvement of survival in DLBCL but has also called into question the significance of the IPI [5], leading to introduction of the revised IPI (R-IPI) [6]. Recent data suggests that IPI and R-IPI no longer reliably identify DLBCL risk groups with a <50 % chance of survival, despite about 30–40 % of patients will still die of/with disease. Thus, there is a need for additional, particularly tumor-related, prognostic (and predictive) factors in DLBCL [7].

To date, only a limited number of tumor-related prognostic parameters exist for DLBCL like presence of *C-MYC* rearrangements or co-expression of *bcl2* and *c-myc*. The morphological heterogeneity of DLBCL is reflected by significant molecular diversity at the genotypic, gene expression, and phenotypic levels [8, 9]. Gene expression profiling data convincingly showed that DLBCLs are derived from germinal center B cells (GCB) or activated B cells (ABC) [9–11]. Although the scientific evidence is robust and prognostically relevant, its translation into daily practice remains impractical because of the required high standard of tissue preservation, procedure duration, and costs. This problem prompted the search for molecular prognostic markers applicable to routine biopsies from patients with DLBCL. As a result, a large body of surrogate (phenotypic) models and algorithms to identify GCB and non-GCB DLBCL have been proposed and linked to outcomes [12]. Unfortunately, reliability and reproducibility of these models is often poor, impeding their translation into standard practice to predict survival and stratify patients for risk-adjusted therapy [12–14]. Technical issues, poor study designs, lack of standardization of evaluation procedures, and, particularly, lack of prospective trials all prevent an efficient clinical translation. A PubMed search for “DLBCL,” “R-CHOP,” “prognostic,” “marker,” and “prospective” identifies only a few prospective studies, in which biomarkers have been considered (e.g., [15–24]). Thus, there is an unmet requirement for further marker validation in prospective trials.

The translational study of the clinical trial “SAKK 38/07 Prospective evaluation of the prognostic value of positron emission tomography (PET) in patients with diffuse large B-cell-lymphoma under R-CHOP-14. A multicenter study” offered a unique opportunity to

prospectively analyze the prognostic and predictive value of phenotypic and genotypic biomarkers suggested to play a prognostic role in DLBCL on a well-documented and homogeneously treated clinical trial collective.

Materials and methods

Patient recruitment, selection, and treatment

The recruitment of patients for the SAKK 38/07 study started in November 2007 and finished in June 2010. Evaluation of the prognostic value of metabolic responses, as assessed by early PET after two cycles of R-CHOP-14, to identify a poor outcome patient subgroup was the main objective. PET was performed before, after two cycles of therapy, and at the end of treatment and was evaluated according to a 5-point scoring system with a cutoff determining positivity being set at 4 points (moderately increased uptake compared with the liver) [25]. The primary endpoint was event-free survival (EFS) at 2 years, and the secondary endpoints were progression-free (PFS) and overall survival (OS) after 2 and 5 years as well as the objective responses according to international criteria [26]. In accordance with the statistical advice for reaching sufficient power to address the two endpoints, recruitment of 154 patients was aimed. Because of concurrent registrations on the last recruitment day, 156 instead of 154 patients were recruited. Inclusion criteria were histologically proven diagnosis of CD20-positive DLBCL (no pretreatment revision of the slides by an expert hematopathologist was planned) including all Ann Arbor stages, tumor size >14 mm on CT or MRI (because lymph nodes ≥15 mm are considered “pathologic” on computerized imaging), PET positivity of the tumors (documented 2 weeks to 4 days prior to registration), performance status 0–2 on the ECOG scale, age >17, as well as no evidence of symptomatic central nervous system (CNS) disease, HIV, and/or hepatitis infection [27]. The study treatment consisted of R-CHOP given for six cycles followed by additional two applications of rituximab every 2 weeks (R-CHOP-14). Additionally, G-CSF support was given. The patients were asked to provide informed consent for the study and, separately, for the translational research. The primary pathology institutions were asked to send representative paraffin blocks for translational research after accomplishing the in-house diagnostic procedures to the Institute of Pathology at the University Hospital Basel. The study was approved by the Ethics Committee Beider Basel. Details of the SAKK 38/07 study are reported elsewhere [28].

In situ biomarker analysis

Immunohistochemical (*bcl2*, *bcl6*, *c-myc*, CD5, CD10, CD95, CD168, cyclin E, FOXP1, GCET, LMO2, MUM1p, pSTAT3) and in situ hybridization analyses [*BCL2*

break apart probe (BAP), *C-MYC* BAP and *C-MYC/IGH* double-fusion probe (DFP), and Epstein–Barr virus probe (EBER)] were performed and correlated with clinicopathological parameters and clinical endpoints. Cell of origin (COO) was determined according to the Tally algorithm [29]. Additionally, selected cases were stained for CD23, CD30, cyclin D1, D2, D3, Ki-67, p27, p63, and SOX11 for specification of diagnosis. Reagent sources, pretreatment and incubation conditions, and cutoff scores are listed in Table 1. Immunohistochemical markers were assessed by microscopic counting of positive cells/tumor cells and were recorded in 5 % increments in the primary statistical table. All cases were scored after training by at least two observers (either AT, SM, or SD), and only markers for which Cronbach's alpha analysis suggested good agreement between observers (alpha >0.75) were considered for prognostic evaluation. Relevant cutoff scores were either taken from the literature [29, 30] or calculated applying receiver operating characteristic (ROC) analysis [12]. Discrepancies in the results for evaluated markers, which were almost exclusively due to differential assessment of weak staining signals, were discussed at a double-headed microscope and the concordant result was considered. Fluorescence in situ hybridization (FISH) was performed exactly as described elsewhere [31]. All cases were FISH-scored twice (NL and AT) with an excellent agreement (alpha = 1) between both observers.

Statistics

All statistical analyses were performed using the Statistical Package of Social Sciences (IBM SPSS version 19.0, Chicago, IL, USA) for Windows and reported applying the REMARK guidelines [32]. The inter-observer agreement was assessed using the Cronbach's alpha reliability analysis; an alpha value of >0.75 indicates very good agreement. The Spearman rank correlation was used to analyze relationships between biomarkers and clinical and laboratory parameters; only correlations with a $\rho \geq \pm 0.300$ were considered. The Mann–Whitney *U* and Kruskal–Wallis tests were applied, where appropriate, to identify quantitative differences between groups. The prognostic performance of variables and determination of optimal cutoff values (except those extracted from the most recent literature) was assessed by ROC curve plotting sensitivity versus 1-specificity with special consideration of the respective area under the ROC (AUROC). The optimal cutoff point was calculated using Youden's index (*Y*), denoting $Y = \text{sensitivity} + \text{specificity} - 1$, since this method can be applied to find the optimal unbiased cutoff value with the highest sensitivity and specificity [12]. OS was measured from registration to death or last follow-up, PFS from registration to relapse, death of any cause, or to last follow-up, and EFS from registration to relapse or death of any cause, initiation of any non-protocol anticancer treatment because of lymphoma symptoms or need of concomitant radiotherapy or to

Table 1 Applied biomarker panel

Marker	Source/clone	Pretreatment	Dilution	Incubation	Other	Cutoff (AUROC or reference)
bcl2	Ventana/Roche 790-4604	CC1 16'	RTU	12'		70 % [34, 46]
bcl6	Ventana/Roche 760-4241	CC1 32'	RTU	28'		30 % [30]
c-myc	Ventana/Roche 790-4628	CC1 92'	RTU	16', 37 °C		40 % [34, 46]
CD5	Ventana/Roche 790-4451	CC1 24'	RTU	12'		20 % (0.542)
CD10	Ventana/Roche 790-4506	CC1 24'	RTU	16'		20 % [29]
CD95	Leica NCL-FAS-310	PC 120 °C, 3', citrate buffer pH 6	1:400	60', 20 °C		1 % (0.613)
CD168	Leica NCL-CD168	CC1 extended 92'	1:200	32'	Biotin blocker Amplification	10 % (0.536)
Cyclin E	Thermo MS-1060-S	MW 98 °C, 30', citrate buffer pH 6	1:20	Overnight, 4 °C		12 % (0.669)
FOXP1	Ventana/Roche 760-4611	CC1 16'	RTU	12'		50 % [45]
GCET	Abcam Ab68889	CC1 32'	1:25	20'		60 % [29]
LMO2	Ventana/Roche 790-4368	CC1 32'	RTU	16'		30 % [29]
MUM1p	Ventana/Roche 760-4529	CC1 24'	RTU	16'		70 % [29]
pSTAT3	Cell Signaling 9145	MW 98 °C, 30', TEC buffer pH 8	1:50	Overnight, 4 °C	Biotin blocker	17 % (0.602)
<i>BCL2</i> BAP	Abbott/Vysis 07 J75-001	Exactly as described [31]				>3 % [31]
<i>C-MYC</i> BAP	Abbott/Vysis 05 J91-001					>4 % [31]
<i>MYC/IGH</i> DFP	Abbott/Vysis 05 J75-001					>6.5 % [31]
EBER	Ventana/Roche 760-1209	According to the manufacturer's protocol				10 %

For diagnostic purposes and to "subtract" CD3-positive T cells in CD5-positive DLBCL, CD3 and CD20 stainings were also performed, but these were not considered biomarkers *sensu stricto*

last follow-up. The probabilities of survival were determined using the Kaplan–Meier method, and differences were compared using the log-rank test. All biomarkers of prognostic significance in univariable models underwent multivariable analysis using the Cox proportional hazards model in a two-step manner since only that response criterion (either according to international criteria or PET or combined PET/CT response) with the highest relevance in an independent first step Cox model, run without biomarkers, was considered and compared to the biomarkers in the second step. All *p* values were two-sided and considered statistically significant if <0.05. No adjustment for multiple testing was applied for secondary analyses because they were considered hypothesis generating and exploratory.

Results

Patients, case review, and clinico-pathologic characteristics

Nineteen patients refused a participation in the translational research part of the project. In 11 cases, no material for translational research was present. Thus, 126 cases were further studied: DLBCL diagnosis could not be confirmed in three of these cases by conventional morphology and additional immunohistochemical evaluation (the final diagnosis of marginal zone lymphoma was established in two cases and one turned to be a blastoid mantle cell lymphoma). Thus, the analysis was finally performed on 123 cases. Patient characteristics are given in Table 2. Survival data were complete for 116 patients.

Eighty-nine lymphomas were primary nodal or of lymphoid tissue (including the mediastinum, the spleen, and Waldeyer's ring), while 34 were extranodal (most commonly soft tissue, gastrointestinal tract, and bones). Based on integrative analysis, 100 cases were shown to be centroblastic DLBCL, five were immunoblastic DLBCL, three were anaplastic DLBCL, six were unclassifiable, six were primary mediastinal large B cell lymphomas (PMBL); thereof, two were nodal DLBCL with morphologic and phenotypic features of PMBL, two were T cell- and histiocyte-rich B cell lymphomas (THRBCL), and one was a lymphomatoid granulomatosis (LG) grade 3.

The study material consisted of 66 (54 %) lymphadenectomy specimens that were studied on tissue microarrays (TMA) and 57 (46 %) cases with only small core needle biopsy material available, which were considered non-arrayable and were studied on conventional serial sections. Arrayable cases were brought into a TMA format applying the 1-mm core needle as described [33].

In situ biomarkers

Immunohistochemistry was evaluable in all cases, while FISH was successful in 82 (67 %) instances (Table 3, Fig. 1a–d); importantly, cases in which FISH failed were evenly distributed among arrayable lymphadenectomy

Table 2 Basic patient characteristics

Age, median (range)		58 (18–81)
Gender, <i>N</i> (%)	F	68 (55)
	M	55 (45)
Stage, <i>N</i> (%)	I	12 (10)
	II	41 (34)
	III	30 (24)
	IV	39 (32)
	Missing	1
IPI, <i>N</i> (%)	0	23 (19)
	1	36 (29)
	2	27 (22)
	3	20 (16)
	4	13 (11)
	5	4 (3)
Treatment response according to international criteria, <i>N</i> (%)	CR	102 (83)
	PR	18 (15)
	SD	2 (2)
	PD	0 (0)
	Missing	1
Combined metabolic and morphologic responses, <i>N</i> (%)	Complete metabolic and morphologic response	68 (59)
	Complete metabolic response with residual mass	24 (21)
	Partial metabolic response with residual mass	23 (20)
	Missing	8
Collecting institutions, <i>N</i> (%)	University hospitals	33 (27)
	Other hospitals	90 (73)

specimens and small core needle biopsy specimens but were more commonly observed in tissues from certain primary pathology institutions. Taking into consideration the Tally algorithm, 81 cases (66 %) were classified as non-GCB DLBCL, while 42 cases (34 %) were GCB DLBCL; after excluding the PMBL, THRBCL, and LG, there were 39 GCB and 75 non-GCB cases. *BCL2* gene breaks were observed in 7/82 cases (9 %); 6 of the 7 (86 %) rearranged cases were of the GCB type. Two cases (all of the non-GCB type) showed *BCL2* amplifications. *C-MYC* breaks were observed in 6/82 cases (8 %); 4 were of the GCB type. Of the *C-MYC* rearranged cases, only 2 displayed *C-MYC/IGH* fusions, detectable by both DFP and BAP and corresponding to *t*(8;14), while *C-MYC* rearrangements were detectable only by BAP in the other 4 cases and were thus assumed to have occurred with alternative non-*IGH C-MYC* rearrangement partners. “Genetic double-hit” cases with *BCL2* and *C-MYC* rearrangements were not observed.

Table 3 Immunohistochemical staining results

	COO	bcl2	c-myc	CD5	CD95	CD168	Cyclin E	FOXP1	pSTAT3	EBER
Evaluable cases	123	123	123	123	123	123	123	123	123	123
Mean % of stained cells \pm SD	na	34 \pm 38	32 \pm 26	2 \pm 14	32 \pm 42	4 \pm 9	8 \pm 13	31 \pm 38	19 \pm 27	na
N (%) above cutoff	na	34 (28)	44 (36)	4 (3)	60 (48)	38 (31)	30 (24)	44 (36)	44 (36)	2 (1.5)
Mean % of stained cells \pm SD in positive cases	na	94 \pm 10	61 \pm 20	72 \pm 27	65 \pm 38	13 \pm 13	26 \pm 13	79 \pm 17	49 \pm 26	33 \pm 25
Germinal center B cell (GCB) like, N (%)	42 (34)	11 (32) ^a	16 (36) ^a	1 (25) ^a	22 (37) ^a	18 (47) ^a	11 (37) ^a	8 (18) ^a	17 (39) ^a	1 (50) ^a

Except for FOXP1, which was of prognostic significance as an isolated marker, all other relevant proteins for cell of origin (COO) classification according to the Tally algorithm are summarized within the COO column

na not applicable

^aGCB out of the positive cases

The presence of *BCL2* breaks correlated with expression of *bcl2* ($\rho = 0.355$, $p = 0.001$), *CD10* ($\rho = 0.388$, $p < 0.005$), and *GCB* ($\rho = 0.302$, $p = 0.006$). As expected, expression of *GCET*, *bcl6*, *CD10*, and *LMO2* correlated with each other (*GCB COO*). *pSTAT3* correlated with *MUM1p*, *FOXP1*, *bcl6*, and *CD168* ($\rho = 0.301$ – 0.473 , $p = 0.01$ – 0.0001). *FOXP1* correlated with *bcl2*, *MUM1p*, and *c-myc* ($\rho = 0.429$, 0.438 , and 0.319 , respectively, $p < 0.001$). Expression of *CD5* did not correlate with any of the examined single variables but showed a weak correlation with the so-called phenotypic *bcl2/c-myc* double hits ($\rho = 0.24$, $p = 0.02$). Phenotypic *bcl2/c-myc* double hits [34] correlated with expression of *FOXP1* ($\rho = 0.379$, $p = 0.0002$) and *BCL2* rearrangements ($\rho = 0.319$, $p = 0.005$).

Outcome analysis

The primary study endpoint, i.e., EFS at 2 years, correlated with failure to achieve response according to international criteria and failure to achieve complete combined metabolic and morphologic response or metabolic response (ρ values for all >0.470 , p values for all $<1e-5$). The median follow-up period was 53 months (95 % CI 45–51). There were 48 events, including 16 lethal events and 12 relapses 3 months after achievement of CR, of which 6 occurred >12 months after initial diagnosis. The 16 lethal events encompassed 9 deaths with/of disease and 7 deaths unrelated to cancer. Mean OS was 68 months (95 % CI 64–71), mean PFS was 59 months (95 % CI 53–65), and mean EFS was 46 months (95 % CI 40–52); median OS, PFS, and EFS for the whole collective were not reached.

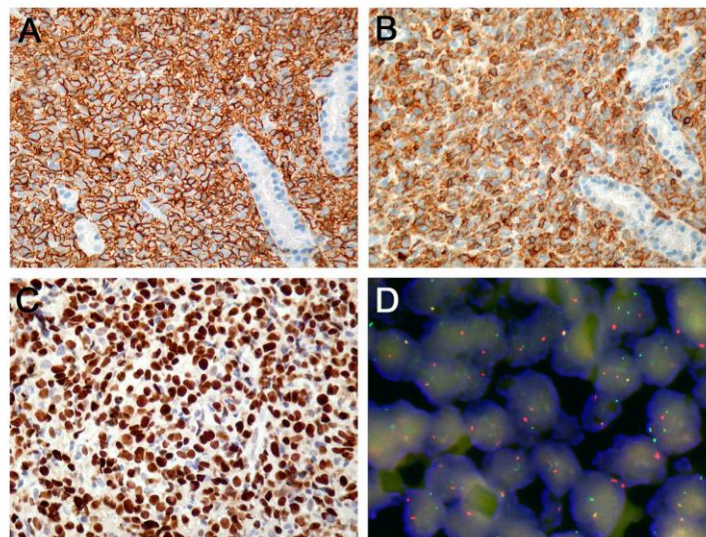


Fig. 1 Microphotographs of selected cases. Co-expression of *CD20* (a) and *CD5* (b) in an extranodal (intestinal) *CD5*-positive diffuse large B cell lymphoma. Microphotographs have been taken from consecutive sections; note deeper sections in **b** of the same glandular structures from **a**. Original magnification $\times 320$. **c** Expression of *FOXP1* in a positive case. Original magnification $\times 400$. **d** Split red and green signals corresponding to a *BCL2* gene rearrangement (translocation). Fused yellow signals corresponding to the non-translocated allele. Original magnification $\times 800$

All biomarkers were assessed for their prognostic importance after rational dichotomization (cutoffs listed in Table 1). Factors able to predict worse EFS in univariate Kaplan–Meier models were failure to achieve response according to international criteria, failure to achieve complete combined metabolic and morphologic response or metabolic response (p values for all <0.005), expression of CD5 ($p = 0.02$; Fig. 2a), and higher stage ($p = 0.021$). Factors predicting inferior PFS were failure to achieve response according to international criteria, failure to achieve complete combined metabolic and morphologic (but not only metabolic) response ($p < 0.005$), higher IPI ($p = 0.006$), higher stage ($p = 0.005$), presence of either *C-MYC* or *BCL2* gene rearrangements ($p = 0.033$; Fig. 2b), and expression of cyclin E in $>12\%$ of tumor cells ($p = 0.046$; Fig. 2c). Finally, factors predicting inferior OS were failure to achieve response according to international criteria, failure to achieve complete combined metabolic and morphologic (but not only metabolic) response (p values for all <0.005), expression of FOXP1 in $>50\%$ of tumor cells ($p < 0.005$; Fig. 2d), expression of cyclin E in $>12\%$ of tumor cells ($p = 0.005$), expression of CD5 ($p = 0.007$), expression of *bcl2* in $>70\%$ of tumor cells ($p = 0.016$), expression of CD95 in any tumor cell ($p = 0.018$), and expression of pSTAT3 in $>17\%$ of tumor cells ($p = 0.025$). All other clinico-pathological and phenotypic variables were not of prognostic significance respecting EFS, PFS, and OS. The multivariable analyses' results for EFS, PFS, and OS are shown in Table 4. Subgroup analysis limited to the DLBCL, not otherwise specified (NOS) cohort

(omitting PMBL, THRBCL, and LG because of their more specific biology) revealed that expression of CD5 ($p = 0.044$) retained its independent prognostic significance with respect to EFS (more sensitive for early events) and expression of FOXP1 ($p = 0.004$) with respect to OS (later events), while all other biomarkers failed to add prognostic information. In the case of CD5 because of the only weak correlation of CD5 with phenotypic *bcl2/c-myc* double hits, the limited number of CD5-positive cases, and the lacking prognostic significance of phenotypic *bcl2/c-myc* double hits in that series, multivariable analysis was not adjusted for phenotypic *bcl2/c-myc* double hits. Adjustment for phenotypic *bcl2/c-myc* double-hit scores in the case of FOXP1 showed that it retained its prognostic significance in those DLBCL, NOS cases scored 0 and 1 (and outperformed failure to achieve combined metabolic and morphologic remission in cases scored 0), but neither expression of FOXP1 nor failure to achieve complete combined metabolic and morphologic remission were of prognostic significance with respect to OS in phenotypic *bcl2/c-myc* double-hit score 2 DLBCL, NOS cases (data not shown in detail).

Since CD5 expression appeared to be of significant relevance, we thoroughly revised the four CD5-positive cases and evaluated multiple immunohistochemical markers to exclude blastoid mantle cell lymphomas (shown above). The four CD5-positive DLBCL were negative for cyclin D1 and SOX11 and expressed p27. These cases stained positively for CD5 in 50 to 100 % of tumor cells did not show an intravascular component and were negative for

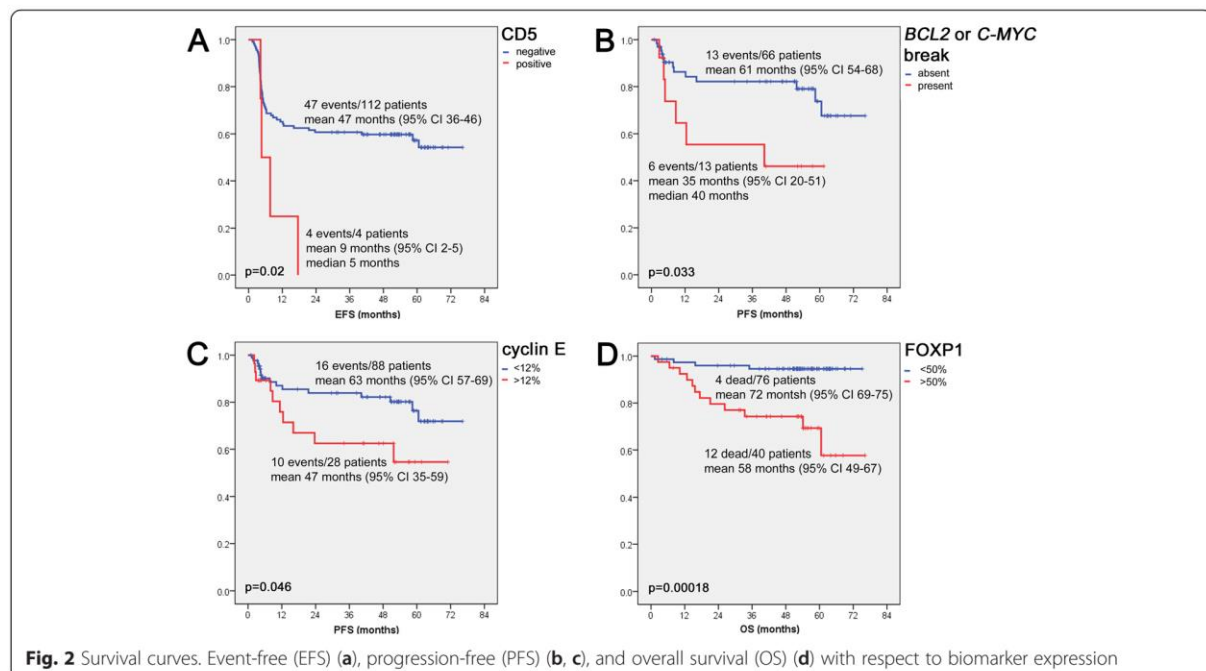


Table 4 Multivariable analysis

Survival	Parameter	Hazard ratio	95 % CI	p value
Event-free	Lack of complete combined metabolic and morphologic remission	2.54	1.84–3.51	<0.005
	Expression of CD5	2.99	1.02–9.13	0.047
Progression-free	Lack of complete remission according to international criteria	16.39	4.57–58.82	<0.005
Overall	Expression of FOXP1	5.61	1.34–23.4	0.018
	Lack of complete combined metabolic and morphologic remission	1.93	1.04–3.58	0.038

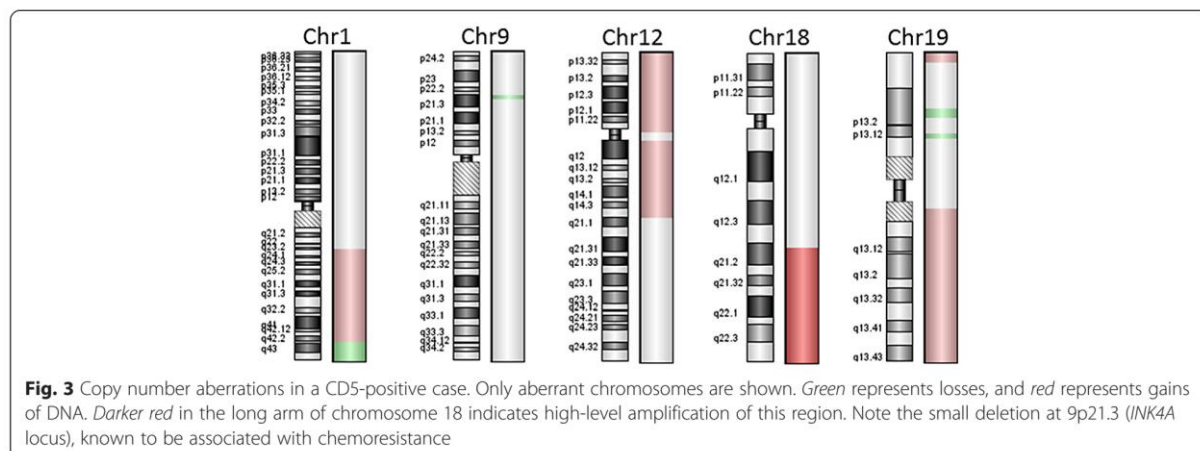
Only significant results are shown

EBER; three were classified as non-GCB, while one was GCB; and three showed centroblastic morphology, while one was classified as centroblastic with increased immunoblasts. None of these four CD5-positive cases showed presence of either *C-MYC* or *BCL2* gene rearrangements; however, two patients fulfilled phenotypic criteria for double-hit lymphoma, expressing *bcl2* or *c-myc* above the respective cutoff scores. Two patients were male; two suffered from nodal lymphomas; two were Ann Arbor stage II, while the other two were stage I and III, respectively; and two patients had an IPI of 1 and two an IPI of 2. The mean age of the CD5-positive patients was 64 ± 13 years, while that of the CD5-negative was 58 ± 13 (difference not of statistical significance). Two of the four patients failed to achieve remission (one of these two patients died of/with lymphoma) and in the other two DLBCL relapsed after 8 and 38 months, respectively. Finally, DNA of the four CD5-positive cases was extracted and subjected to array comparative genomic hybridization (aCGH) analysis (Fig. 3) exactly as described elsewhere [35]. The analysis was successful in two cases and showed recurrent gains of 19q and losses of 1q43 [36], thus further corroborating the diagnosis of DLBCL. One of the cases showed specific loss of 9p21 (*INK4A* locus, also known as p16) known to be associated with DLBCL resistance to R-CHOP [37].

Discussion

Within this prospective study, we identified potential biomarkers (expression of CD5 for EFS and expression of FOXP1 for OS) that were able to predict the course of DLBCL at diagnosis, independent of stage and IPI. As expected ([38] and literature therein), dynamic parameters, such as response to therapy and especially failure to achieve complete remission, which are not obtainable at diagnosis, seem to be the most reliable outcome indicators in DLBCL, yet expression of CD5 and FOXP1 added information independent of these disease dynamic parameters.

Concerning the central aim of our study, i.e., to detect in situ biomarkers that reliably help predicting the outcome of DLBCL in a prospective, homogeneously treated collective of patients, our phenotypic and genotypic analyses show that carefully selected indicators such as CD5 might identify small yet prognostically relevant subgroups with adverse outcomes under R-CHOP. CD5 as biomarker has a special sensitivity towards early adverse events, which might not be the case for some of the currently propagated biomarkers of prognostic relevance such as *c-myc* expression/*C-MYC* gene status. Furthermore, our data reappraise the prognostic role of FOXP1 with respect to OS. Several other previously studied biomarkers with suspected prognostic potential



like COO, expression of *bcl2*, or phenotypic double-hit score appeared to be less potent in the studied collective. This might in part be due to the small size of our study, in part to genuine properties of these markers, and in part to the fact that some of these markers, while being applicable to CHOP-treated DLBCL patients, are not applicable to cases treated with R-CHOP [39]. Considering our study size, there are obvious and inevitable limitations. Yet, because of the other characteristics of our collective (123 uniformly treated patients with a median follow-up period of 53 months and altogether 51 adverse events), our data solidifies understanding of the prognostic importance of in situ biomarkers in DLBCL and the 2-year EFS analysis delivers important results. Respecting the genuine properties of some markers, especially those used as surrogates to determine COO, our results as well as observations of others [14] seriously challenge their reliability to identify prognostically and/or biologically meaningful groups among DLBCL.

Our observed prognostic role of CD5 and FOXP1 and possible prognostic role of *bcl2* as well as structural genetic aberrations of (either) *BCL2* or *C-MYC* are supported by other reports ([31, 40–46] and literature therein). While a considerable number of recent papers focused on the role of *bcl2* and *c-myc* in DLBCL [34, 46, 47], it seems that CD5 merits special attention for several reasons: (a) it can be very easily detected in DLBCL by standard application of CD5 (instead of CD3) immunohistochemistry in the primary diagnostic panel with subsequent application of CD3 in CD5-positive cases (to subtract the “true” T cells), as well as CD23, cyclin D1, and SOX11 (to exclude transformed small lymphocytic B cell lymphomas and blastoid mantle cell lymphomas); (b) the respective cases express CD5 in a high proportion of tumor cells (>50–100 %) with a moderate to strong staining intensity, and thus, its evaluation is unequivocal without the need for subjective and error-prone cutoff scores; and (c) because there is an increasing body of literature suggesting that CD5-positive DLBCL might represent a distinct biologic entity, being more prone to intravascular spread and extranodal location (particularly CNS), affecting individuals from the Far East and displaying a more aggressive behavior probably requiring alternative treatment approaches [40]. CD5-positive DLBCL are typically ABC [42, 48], show recurrent gains of 16p and losses of 1p and of 9q21 [36, 49], the latter being involved in chemoresistance [37], and display downregulation of extracellular matrix-related genes and upregulation of neurological function-related genes [48]. Addition of rituximab to CHOP improved the survival of CD5-positive DLBCL patients [50]; however, similarly to our results, the outcome of these patients is still significantly poorer compared to CD5-negative DLBCL patients [51], and the rate of CNS involvement seems not to be lowered by rituximab [52]. A recent very large

retrospective report on 879 R-CHOP-treated DLBCL cases convincingly showed CD5 to be an IPI (and *bcl2* and pSTAT3)-independent prognosticator in DLBCL as well [53] and pointed out distinct clinico-pathological peculiarities of such patients such as increased age, bone marrow spread, poor performance status, and B symptoms. Considering the possible direct biological effect of CD5 on B cells, namely its role as a negative regulator of B cell signaling, its influence on the ERK, PI3K, and calcineurin pathways as well as survival stimulation through autocrine IL10-related loops and the predominant expression of integrin beta-1 on the tumor cells, CD5 seems to be of probable functional and therapeutic importance for targeted approaches [40, 54–56]. In addition, CD5-positive cases seem to overexpress *bcl2*, *CARD11*, *CCND2*, and *FOXP1* at the protein and mRNA level and to be more rich in *c-Rel*, *p65*, and pSTAT3 [53], all known to identify DLBCL patients at risk; this study [53] also confirmed [48] downregulation of cellular adhesion genes in such instances. Taken together, previous data and our observations might justify a separation of CD5-positive DLBCL out of the group of DLBCL, NOS, as a distinct clinico-pathological entity in need of R-CHOP treatment alternatives and, probably, CNS prophylaxis.

The prognostic role of FOXP1 in DLBCL was well established in the “pre-rituximab” era ([45] and references therein), while less attention has been paid to it in R-CHOP-treated cases. Importantly, prognostically relevant COO algorithms pay special attention towards expression of FOXP1 to classify non-GCB-like DLBCL and >90 % concordance with GEP was only achievable by consideration of FOXP1 in these algorithms (e.g., [29, 44]). In line with these results, the recent report on the very poor prognosis of DLBCL reciprocally expressing the endocytic protein Huntingtin-interacting protein 1-related (*HIP1R*) and FOXP1 (the latter being a direct repressor of the *HIP1R* gene), i.e., FOXP1(hi)/*HIP1R*(lo) patients [57], and our prospective study findings suggest a more substantial relevance of FOXP1 in DLBCL. Importantly, FOXP1 belongs to the most reproducibly assessable markers in DLBCL as shown in an international inter- and intra-institutional and inter- and intra-observer study [58], further calling for its regular evaluation.

Unexpectedly, a significant (33 % for FISH and 50 % for aCGH) dropout of cases for genotypic studies was noted. Detailed analysis of these cases revealed that pre-analytic conditions like inappropriate application of un-buffered formalin, fixation duration, surrounding temperature, and exact dehydration procedures were probably more relevant for lack of analytic success than the exact amount of examined tissue. Indeed, these failures were evenly distributed between core needle biopsies and lymphadenectomy specimens but were more commonly observed among tissues from a few centers. As expected, diagnostic tissue

obtained by core needle biopsy procedures (usually 14–18G needles) was not arrayable and was rapidly exhausted for purposes of the study, precluding further analyses. Since cohorts of prospective clinical trials are characterized by meticulous documentation and uniform treatment of patients (the latter, if not uniform, can more substantially affect disease prognosis than many biomarkers), biomarker analyses should desirably be performed on cases collected within such studies. Therefore, the amount and the pre-analytical handling of tissue required for study inclusion must be considered also under the aspect of biomarker analyses. This particularly implies that physicians obtaining and handling the respective biopsies as well as the pathology laboratories must take responsibility for error-free and safe pre-analytic conduits, guaranteeing optimal tissue fixation and dehydration, which are indispensable for an accurate morphologic, phenotypic, and genetic analysis. For practical purposes, the protocol for probe handling from the laboratory, which provided probes with least dropout on molecular testing, is given in Additional file 1: Table S1.

Conclusions

In summary, distinct biomarkers like CD5 and FOXP1 are able to prognosticate DLBCL course at diagnosis, independent of stage and IPI and independent of initial therapy response. For the design of prospective DLBCL studies, issues like review of the slides by a central pathology, pre-analytic factors such as time to and time of fixation, choice of fixative, and dehydration as well as handling of biological entities and sub-entities in the spectrum of aggressive large B cell lymphomas should be properly discussed and promptly addressed.

Additional file

Additional file 1: Table S1. Summary of pre-analytics in the lab, submitting probes with least number of molecular testing dropouts.

Abbreviations

ABC: Activated B cell; aCGH: Array comparative genomic hybridization; AUROC: Area under the ROC curve; BAP: Break-apart probe; CNS: Central nervous system; COO: Cell of origin; DFP: Double-fusion probe; DLBCL: Diffuse large B cell lymphoma; ECOG: Eastern Cooperative Oncology Group; EFS: Event-free survival; FISH: Fluorescence in situ hybridization; GCB: Germinal center B cell; G-CSF: Granulocyte colony-stimulating factor; GEP: Gene expression profiling; HIV: Human immunodeficiency virus; IPI: International Prognostic Index; LG: Lymphomatoid granulomatosis; MRI: Magnetic resonance imaging; NOS: Not otherwise specified; OS: Overall survival; PET: Positron emission tomography; PSF: Progression-free survival; PMBL: Primary mediastinal B cell lymphoma; R-CHOP: Rituximab, cyclophosphamide, hydroxydaunorubicin, vincristine, prednisone; R-IPI: Revised International Prognostic Index; ROC: Receiver operating characteristic; THRBCL: T cell- and histiocyte-rich B cell lymphomas; TMA: Tissue microarray.

Competing interests

The authors declare that they have no competing interests.

Authors' contributions

AT wrote the manuscript. AT, DK, CM, and SD designed the study. AT, NL, and SM performed immunohistochemical and FISH analyses. AT and DK performed statistical analyses. DJ performed aCGH analyses and formatted the manuscript. All authors read and approved the final manuscript.

Acknowledgements

This study was supported by the Oncosuisse grant OCS 02072-04-2007.

Author details

¹Institute of Pathology, University Hospital Basel, Schoenbeinstrasse 40, CH-4031 Basel, Switzerland. ²Swiss Group for Clinical Cancer Research (SAKK), Effingerstrasse 40, CD-3008 Bern, Switzerland. ³Division of Hematology and Oncology, Cantonal Hospital Aarau, Tellstrasse house Nr. 40, CH-5001 Aarau, Switzerland.

Received: 20 April 2015 Accepted: 5 June 2015

Published online: 14 June 2015

References

- Stein H, Warnke RA, Chan WC, Jaffe ES. Diffuse large B-cell lymphoma, not otherwise specified. In: Swerdlow SH, Campo E, Harris NL, Jaffe ES, Pileri SA, Stein H, Thiele J, Vardiman JW, editors. WHO classification of tumours of haematopoietic and lymphoid tissues. 4th ed. Lyon: WHO Press; 2008. p. 233–7.
- Cultrera JL, Dalia SM. Diffuse large B-cell lymphoma: current strategies and future directions. *Cancer Control*. 2012;19:204–13.
- Nastoupil LJ, Rose AC, Flowers CR. Diffuse large B-cell lymphoma: current treatment approaches. *Oncology*. 2012;26:488–95.
- Anonymous. A predictive model for aggressive non-Hodgkin's lymphoma. The International Non-Hodgkin's Lymphoma Prognostic Factors Project. *N Engl J Med*. 1993; 329:987–94.
- Sehn LH, Berry B, Chhanabhai M, Fitzgerald C, Gill K, Hoskins P, et al. The revised International Prognostic Index (R-IPI) is a better predictor of outcome than the standard IPI for patients with diffuse large B-cell lymphoma treated with R-CHOP. *Blood*. 2007;109:1857–61.
- Zhou Z, Sehn LH, Rademaker AW, Gordon LI, Lacasce AS, Crosby-Thompson A, et al. An enhanced International Prognostic Index (NCCN-IPI) for patients with diffuse large B-cell lymphoma treated in the rituximab era. *Blood*. 2014;123:837–42.
- Sehn LH. Paramount prognostic factors that guide therapeutic strategies in diffuse large B-cell lymphoma. *Hematology Am Soc Hematol Educ Program*. 2012;2012:402–9.
- Said JW. Aggressive B-cell lymphomas: how many categories do we need? *Mod Pathol*. 2013;26 Suppl 1:S42–56.
- Pasqualucci L. The genetic basis of diffuse large B-cell lymphoma. *Curr Opin Hematol*. 2013;20:336–44.
- Alizadeh AA, Eisen MB, Davis RE, Ma C, Lossos IS, Rosenwald A, et al. Distinct types of diffuse large B-cell lymphoma identified by gene expression profiling. *Nature*. 2000;403:503–11.
- Shipp MA, Ross KN, Tamayo P, Weng AP, Kutok JL, Aguiar RC, et al. Diffuse large B-cell lymphoma outcome prediction by gene-expression profiling and supervised machine learning. *Nat Med*. 2002;8:68–74.
- Tzankov A, Zlobec I, Went P, Robl H, Hoeller S, Dirnhofer S. Prognostic immunophenotypic biomarker studies in diffuse large B cell lymphoma with special emphasis on rational determination of cut-off scores. *Leuk Lymphoma*. 2010;51:199–212.
- De Jong D, Rosenwald A, Chhanabhai M, Gaulard P, Klapper W, Lee A, et al. Immunohistochemical prognostic markers in diffuse large B-cell lymphoma: validation of tissue microarray as a prerequisite for broad clinical applications—a study from the Lunenburg Lymphoma Biomarker Consortium. *J Clin Oncol*. 2007;25:805–12.
- Gutierrez-Garcia G, Cardesa-Salzmann T, Climent F, Gonzalez-Barca E, Mercadal S, Mate JL, et al. Gene-expression profiling and not immunophenotypic algorithms predicts prognosis in patients with diffuse large B-cell lymphoma treated with immunochemotherapy. *Blood*. 2011;117:4836–43.
- Winter JN, Weller EA, Horning SJ, Krajewska M, Variakojis D, Habermann TM, et al. Prognostic significance of Bcl-6 protein expression in DLBCL treated with CHOP or R-CHOP: a prospective correlative study. *Blood*. 2006;107:4207–13.
- Hara T, Tsurumi H, Goto N, Kanemura N, Yoshikawa T, Kasahara S, et al. Serum soluble Fas level determines clinical outcome of patients with diffuse

- large B-cell lymphoma treated with CHOP and R-CHOP. *J Cancer Res Clin Oncol.* 2009;135:1421–8.
17. Shustik J, Han G, Farinha P, Johnson NA, Ben Neriah S, Connors JM, et al. Correlations between BCL6 rearrangement and outcome in patients with diffuse large B-cell lymphoma treated with CHOP or R-CHOP. *Haematologica.* 2010;95:96–101.
 18. Evens AM, Sehn LH, Farinha P, Nelson BP, Raji A, Lu Y, et al. Hypoxia-inducible factor-1 (alpha) expression predicts superior survival in patients with diffuse large B-cell lymphoma treated with R-CHOP. *J Clin Oncol.* 2010;28:1017–24.
 19. Ott G, Ziepert M, Klapper W, Horn H, Szczepanowski M, Bernd HW, et al. Immunoblastic morphology but not the immunohistochemical GCB/nonGCB classifier predicts outcome in diffuse large B-cell lymphoma in the RICOVER-60 trial of the DSHNHL. *Blood.* 2010;116:4916–25.
 20. Tomita N, Sakai R, Fujisawa S, Fujimaki K, Taguchi J, Hashimoto C, et al. SIL index, comprising stage, soluble interleukin-2 receptor, and lactate dehydrogenase, is a useful prognostic predictor in diffuse large B-cell lymphoma. *Cancer Sci.* 2012;103:1518–23.
 21. Perry AM, Cardesa-Salzmann TM, Meyer PN, Colomo L, Smith LM, Fu K, et al. A new biologic prognostic model based on immunohistochemistry predicts survival in patients with diffuse large B-cell lymphoma. *Blood.* 2012;120:2290–6.
 22. Hong J, Park S, Park J, Jang SJ, Ahn HK, Sym SJ, et al. CD99 expression and newly diagnosed diffuse large B-cell lymphoma treated with rituximab-CHOP immunochemotherapy. *Ann Hematol.* 2012;91:1897–906.
 23. Horn H, Ziepert M, Becher C, Barth TF, Bernd HW, Feller AC, et al. MYC status in concert with BCL2 and BCL6 expression predicts outcome in diffuse large B-cell lymphoma. *Blood.* 2013;121:2253–63.
 24. Winter JN, Li S, Aurora V, Variakojis D, Nelson B, Krajewska M, et al. Expression of p21 protein predicts clinical outcome in DLBCL patients older than 60 years treated with R-CHOP but not CHOP: a prospective ECOG and Southwest Oncology Group correlative study on E4494. *Clin Cancer Res.* 2010;16:2435–42.
 25. Meignan M, Gallamini A, Haioun C. Report on the first international workshop on interim-PET-scan in lymphoma. *Leuk Lymphoma.* 2009;50:1257–60.
 26. Cheson BD, Pfistner B, Juweid ME, Gascoyne RD, Specht L, Horning SJ, et al. Revised response criteria for malignant lymphoma. *J Clin Oncol.* 2007;25:579–86.
 27. PET scans in patients with diffuse large B-cell lymphoma receiving rituximab, cyclophosphamide, doxorubicin, vincristine, and prednisone. <http://clinicaltrials.gov/show/NCT00544219>.
 28. Mamot C, Klingbiel D, Hitz F, Renner C, Pabst T, Driessen C, et al. Final results of a prospective evaluation of the predictive value of interim PET in patients with DLBCL treated with R-CHOP-14 (SAKK 38/07). *J Clin Oncol.* 2015. [in press].
 29. Meyer PN, Fu K, Greiner TC, Smith LM, Delabie J, Gascoyne RD, et al. Immunohistochemical methods for predicting cell of origin and survival in patients with diffuse large B-cell lymphoma treated with rituximab. *J Clin Oncol.* 2011;29:200–7.
 30. Visco C, Li Y, Xu-Monette ZY, Miranda RN, Green TM, Li Y, et al. Comprehensive gene expression profiling and immunohistochemical studies support application of immunophenotypic algorithm for molecular subtype classification in diffuse large B-cell lymphoma: a report from the International DLBCL Rituximab-CHOP Consortium. *Leukemia.* 2012;2103–2113.
 31. Tzankov A, Xu-Monette ZY, Gerhard M, Visco C, Dirnhofer S, Gisin N, et al. Rearrangements of MYC gene facilitate risk stratification in diffuse large B-cell lymphoma patients treated with rituximab-CHOP. *Mod Pathol.* 2014;27:958–71.
 32. McShane LM, Altman DG, Sauerbrei W, Taube SE, Gion M, Clark GM. Reporting recommendations for tumour MARKer prognostic studies (REMARK). *Eur J Cancer.* 2005;41:1690–6.
 33. Nagel S, Hirschmann P, Dirnhofer S, Gunther U, Tzankov A. Coexpression of CD44 variant isoforms and receptor for hyaluronic acid-mediated motility (RHAMM, CD168) is an International Prognostic Index and C-MYC gene status-independent predictor of poor outcome in diffuse large B-cell lymphomas. *Exp Hematol.* 2010;38:38–45.
 34. Green TM, Young KH, Visco C, Xu-Monette ZY, Orazi A, Go RS, et al. Immunohistochemical double-hit score is a strong predictor of outcome in patients with diffuse large B-cell lymphoma treated with rituximab plus cyclophosphamide, doxorubicin, vincristine, and prednisone. *J Clin Oncol.* 2012;30:3460–7.
 35. Juskevicius D, Ruiz C, Dirnhofer S, Tzankov A. Clinical, morphologic, phenotypic, and genetic evidence of cyclin D1-positive diffuse large B-cell lymphomas with CYCLIN D1 gene rearrangements. *Am J Surg Pathol.* 2014;38:719–27.
 36. Tagawa H, Tsuzuki S, Suzuki R, Karnan S, Ota A, Kameoka Y, et al. Genome-wide array-based comparative genomic hybridization of diffuse large B-cell lymphoma: comparison between CD5-positive and CD5-negative cases. *Cancer Res.* 2004;64:5948–55.
 37. Kreisel F, Kulkarni S, Kerns RT, Hassan A, Deshmukh H, Nagarajan R, et al. High resolution array comparative genomic hybridization identifies copy number alterations in diffuse large B-cell lymphoma that predict response to immuno-chemotherapy. *Cancer Genet.* 2011;204:129–37.
 38. Benjamin JE, Chen GL, Cao TM, Cao PD, Wong RM, Sheehan K, et al. Long-term follow-up of patients with diffuse large B-cell non-Hodgkin's lymphoma receiving purged autografts after induction failure. *Bone Marrow Transpl.* 2010;45:303–9.
 39. Frei E, Visco C, Xu-Monette ZY, Dirnhofer S, Dybkaer K, Orazi A, et al. Addition of rituximab to chemotherapy overcomes the negative prognostic impact of cyclin E expression in diffuse large B-cell lymphoma. *J Clin Pathol.* 2013;66:956–61.
 40. Jain P, Fayad LE, Rosenwald A, Young KH, O'Brien S. Recent advances in de novo CD5+ diffuse large B cell lymphoma. *Am J Hematol.* 2013;88:798–802.
 41. Salles G, de Jong D, Xie W, Rosenwald A, Chhanabhai M, Gaulard P, et al. Prognostic significance of immunohistochemical biomarkers in diffuse large B-cell lymphoma: a study from the Lunenburg Lymphoma Biomarker Consortium. *Blood.* 2011;117:7070–8.
 42. Yamaguchi M, Nakamura N, Suzuki R, Kagami Y, Okamoto M, Ichinohasama R, et al. De novo CD5+ diffuse large B-cell lymphoma: results of a detailed clinicopathological review in 120 patients. *Haematologica.* 2008;93:1195–202.
 43. Ennishi D, Takeuchi K, Yokoyama M, Asai H, Mishima Y, Terui Y, et al. CD5 expression is potentially predictive of poor outcome among biomarkers in patients with diffuse large B-cell lymphoma receiving rituximab plus CHOP therapy. *Ann Oncol.* 2008;19:1921–6.
 44. Visco C, Tzankov A, Xu-Monette ZY, Miranda RN, Tai YC, Li Y, et al. Patients with diffuse large B-cell lymphoma of germinal center origin with BCL2 translocations have poor outcome, irrespective of MYC status: a report from an International DLBCL rituximab-CHOP Consortium Program Study. *Haematologica.* 2013;98:255–63.
 45. Hoeller S, Schneider A, Haralambiava E, Dirnhofer S, Tzankov A. FOXP1 protein overexpression is associated with inferior outcome in nodal diffuse large B-cell lymphomas with non-germinal centre phenotype, independent of gains and structural aberrations at 3p14.1. *Histopathology.* 2010;57:73–80.
 46. Johnson NA, Slack GW, Savage KJ, Connors JM, Ben-Neriah S, Rogic S, et al. Concurrent expression of MYC and BCL2 in diffuse large B-cell lymphoma treated with rituximab plus cyclophosphamide, doxorubicin, vincristine, and prednisone. *J Clin Oncol.* 2012;30:3452–9.
 47. Hu S, Xu-Monette ZY, Tzankov A, Green T, Wu L, Balasubramanyam A, et al. MYC/BCL2 protein coexpression contributes to the inferior survival of activated B-cell subtype of diffuse large B-cell lymphoma and demonstrates high-risk gene expression signatures: a report from The International DLBCL Rituximab-CHOP Consortium Program. *Blood.* 2013;121:4021–31. quiz 4250.
 48. Suguro M, Tagawa H, Kagami Y, Okamoto M, Ohshima K, Shiku H, et al. Expression profiling analysis of the CD5+ diffuse large B-cell lymphoma subgroup: development of a CD5 signature. *Cancer Sci.* 2006;97:868–74.
 49. Yoshioka T, Miura I, Kume M, Takahashi N, Okamoto M, Ichinohasama R, et al. Cytogenetic features of de novo CD5-positive diffuse large B-cell lymphoma: chromosome aberrations affecting 8p21 and 11q13 constitute major subgroups with different overall survival. *Genes Chromosom Cancer.* 2005;42:149–57.
 50. Niitsu N, Okamoto M, Tamaru JI, Yoshino T, Nakamura N, Nakamura S, et al. Clinicopathologic characteristics and treatment outcome of the addition of rituximab to chemotherapy for CD5-positive in comparison with CD5-negative diffuse large B-cell lymphoma. *Ann Oncol.* 2010;21:2069–74.
 51. Hyo R, Tomita N, Takeuchi K, Aoshima T, Fujita A, Kuwabara H, et al. The therapeutic effect of rituximab on CD5-positive and CD5-negative diffuse large B-cell lymphoma. *Hematol Oncol.* 2010;28:27–32.
 52. Miyazaki K, Yamaguchi M, Suzuki R, Kobayashi Y, Maeshima AM, Niitsu N, et al. CD5-positive diffuse large B-cell lymphoma: a retrospective study in 337 patients treated by chemotherapy with or without rituximab. *Ann Oncol.* 2011;22:1601–7.
 53. Xu-Monette ZY, Tu M, Jabbar KJ, Cao X, Tzankov A, Visco C, et al. Clinical and biological significance of de novo CD5+ diffuse large B-cell lymphoma in Western countries. *Oncotarget.* 2015;6:5615–33.
 54. Kobayashi T, Yamaguchi M, Kim S, Morikawa J, Ogawa S, Ueno S, et al. Microarray reveals differences in both tumors and vascular specific gene

- expression in de novo CD5+ and CD5- diffuse large B-cell lymphomas. *Cancer Res.* 2003;63:60–6.
55. Gary-Gouy H, Sainz-Perez A, Marteau JB, Marfaing-Koka A, Delic J, Merle-Beral H, et al. Natural phosphorylation of CD5 in chronic lymphocytic leukemia B cells and analysis of CD5-regulated genes in a B cell line suggest a role for CD5 in malignant phenotype. *J Immunol.* 2007;179:4335–44.
 56. Gary-Gouy H, Harriague J, Bismuth G, Platzer C, Schmitt C, Dalloul AH. Human CD5 promotes B-cell survival through stimulation of autocrine IL-10 production. *Blood.* 2002;100:4537–43.
 57. Wong KK, Gascoyne DM, Brown PJ, Soilleux EJ, Snell C, Chen H, et al. Reciprocal expression of the endocytic protein HIP1R and its repressor FOXP1 predicts outcome in R-CHOP-treated diffuse large B-cell lymphoma patients. *Leukemia.* 2014;28:362–72.
 58. Lawrie CH, Ballabio E, Soilleux E, Sington J, Hatton CS, Dirnhofer S, et al. Inter- and intra-observational variability in immunohistochemistry: a multicentre analysis of diffuse large B-cell lymphoma staining. *Histopathology.* 2012;61:18–25.

**Submit your next manuscript to BioMed Central
and take full advantage of:**

- Convenient online submission
- Thorough peer review
- No space constraints or color figure charges
- Immediate publication on acceptance
- Inclusion in PubMed, CAS, Scopus and Google Scholar
- Research which is freely available for redistribution

Submit your manuscript at
www.biomedcentral.com/submit



4. DISCUSSION

4.1 Clonally-unrelated relapses of DLBCL

Clonally-unrelated lymphoma relapses have been already documented. This was entirely based on investigation of *IG* heavy and light chain rearrangement or detection of common translocation breakpoints or both. Generally, *V(D)J* rearrangements take place early in B-cell development and represent a robust clonality marker. However, it was shown in CLL that tumor-initiating genetic lesions can occur prior to *IG* rearrangement²⁰¹. Such events might represent earliest markers of clonal origin and can be overlooked by *IG* rearrangement analysis. Moreover, such analysis provides no information about differences in the general genetic constitution between primary and relapsed tumors. Finally, many clonality studies of primary-relapse pairs focused on detection of clonal relationship rather than lack of it, therefore many of described allegedly clonally-unrelated cases in DLBCL are not sufficiently documented^{175,182,202}. This, taken together with relatively low percentage of clonally-unrelated relapses, led to discouragement of clonality testing in routine of lymphoma diagnostics¹⁸⁴.

To my best knowledge, our study is the most comprehensive demonstration of clonally-unrelated DLBCL recurrence so far. In addition to standard clonality analysis by multiplex PCR and sequencing, which showed clear usage of different *IG* gene segments for the productive *VDJ* rearrangements in 2 out of 3 detected clonally-unrelated cases (out of the studied collective of 20 DLBCL pairs 3, i.e. 15%, displayed clonally unrelated relapses), we also contrasted copy number and mutational profiles between the investigated two tumor episodes of the same patient. This analysis unequivocally demonstrated different genetic constitution of primary and relapses. Moreover, it advantageously clarified clonal relationship in one other case, where *V(D)J* rearrangement could not be amplified. Despite complex genomes in multiple cases, the clonally unrelated tumors had no shared genetic lesions. Instead each tumor showed a very individual profile of genome-wide chromosomal imbalances and nucleotide-level variations suggesting separate clonal origin and independent genomic evolution.

Such unequivocal demonstration demands attention to the clinical aspects of clonally-unrelated relapses as previously explained (see introduction). This need is especially highlighted by exceptional clinical courses of two patients in our cohort. In one patient clonally-unrelated DLBCL recurrence did not respond to rituximab and rescue chemotherapy but was treated successfully with lenalidomide monotherapy. The tumor was eradicated and the patient still enjoys a long-lasting clinical remission²⁰³. Another patient suffered from primary testicular

DLBCL followed by clonally-unrelated DLBCL of the central nervous system. The CNS tumor was successfully treated with high-dose chemotherapy. In both cases such favorable outcomes would bona fide not be expected if patients had clonally-related, treatment-resistant DLBCL relapses.

4.2 DLBCL relapses occur via two distinct genetic evolution patterns

Until recently, before the recognition of a substantial genetic heterogeneity in cancer, tumor evolution was understood as a linear, step-wise process, during which accumulation of genetic lesions leads to an uncontrolled cell growth and malignancy. According to this model evolution occurs in one direction i.e. from the intact germline genome towards an aberrant cancer genome, with numbers of lesions increasing in the later. Likewise, until recently lymphoma relapses, even after a prolonged period of remission, were regarded as direct outgrowths of the primary tumor, assuming that all genetic alterations that were present in it are directly passed to the relapse. Therefore a relapse was considered to be a more evolutionary advanced stage of the primary tumor. This was supported by a stable detection of some selected genetic aberrations (e.g. classical drivers of lymphomagenesis such as *BCL2* or *CYCLIN D1* translocations) throughout the whole history of the individual disease. The lack of ability to investigate the entirety of tumor's genetic landscape prevented from looking deeper into this issue.

The detection of at least two different genetic evolution patterns of clonally-related DLBCL relapse in this work, namely 1) early-divergent/branching evolution and 2) late-divergent evolution by aCGH and targeted sequencing, contradicts the linear scenario of lymphoma development. Rather, it points towards a model of clonal growth and selection, which seems to be nearly universal in cancer^{204,205}. Similar evolutionary patterns were detected in a paired DLBCL cohort by deep-sequencing of *IGH* gene somatic hypermutations¹⁷⁵. Moreover, non-linear evolution and the phenomenon of early and late divergence were documented by various approaches in other lymphoid neoplasms such as follicular lymphoma^{179,180,200,206–209}, multiple myeloma²¹⁰, mantle cell lymphoma²¹¹ as well as in investigations of genetic differences between primary tumor and metastasis in carcinomas^{212–214}.

Early-divergent/branching evolution pattern (Figure 10a) is characterized by high genetic dissimilarity between primary and relapsed tumors. Primary tumors in our study had private genetic alterations, most importantly homo- or heterozygous deletions, which are not detectable at relapse, even at the very low frequency. However, despite this dissimilarity paired samples always have a variant number of shared identical somatic genetic alterations proving their clonal origin.

Late-divergent evolution pattern (Figure 10b) most closely resembles the linear mode of tumor evolution, as most of genetic aberrations are shared between primary and relapse. However, also in this mode the majority of diagnostic samples show low number of variant somatic mutations, detected by targeted NGS, which are not detectable in relapses suggesting a limited degree of independent evolution.

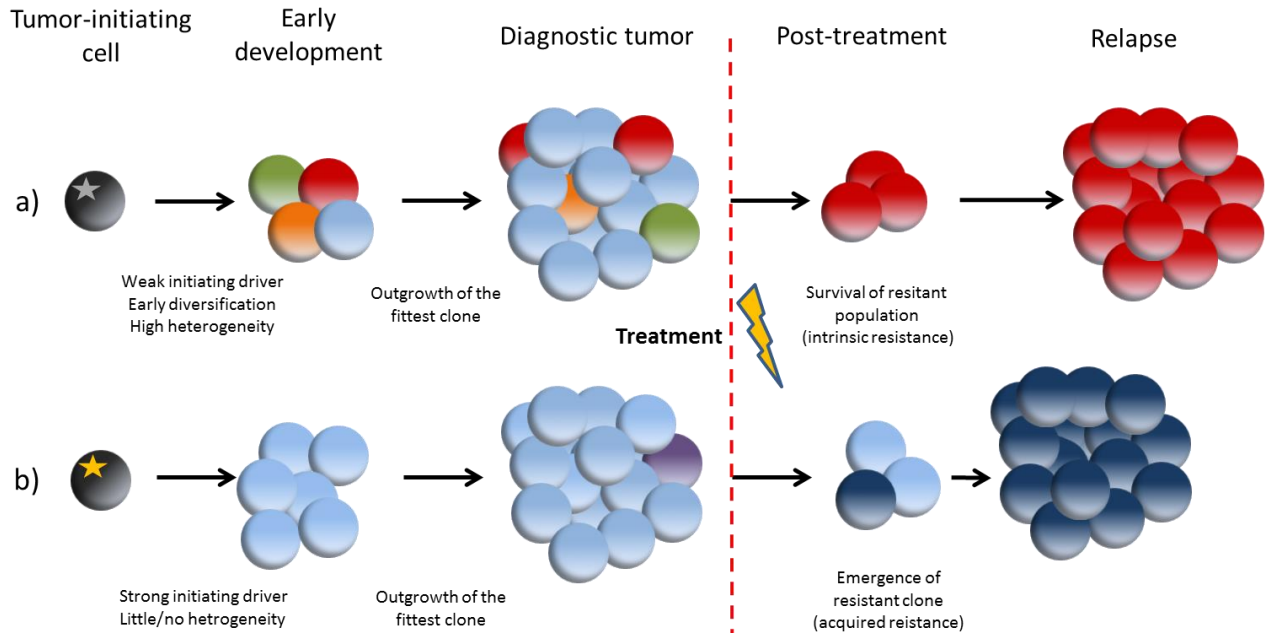


Figure 10. Schematic representation of two proposed patterns of genetic evolution in relapsing DLBCL. Different colors represent genetically distinct clones that possess private genetic alterations due to independent genome evolution. **A.** In the early-divergent/branching scenario, the divergence occurs early in tumor development. The majority of subpopulations stagnate but one clone eventually acquires the effective combination of drivers, expands and gives rise to a heterogeneous primary tumor. The dominant population is exterminated by the treatment, however an intrinsically resistant clone exists and gives rise to a DLBCL relapse. **B.** In the late-divergent/linear evolution scenario, DLBCL initially possesses a strong driver combination (e.g. *BCL2* and *C-MYC* “double hit”). Therefore neoplastic cells grow fast and unrestricted, giving rise to a homogeneous primary tumor. Such a tumor is almost exterminated by the treatment but an acquired resistance emerges. The resistant subclone already has drivers of effective growth and proliferation and rapidly replenishes the tumor mass giving rise to a DLBCL relapse.

In our study 6/20 (35%) of cases evolved from an early common progenitor and showed a branching evolution pattern. The frequency distribution between early- and late-divergent patterns of genetic evolution varies greatly in different studies (Table 2). This variation can be attributed to small collective sizes, heterogeneous criteria for inclusion, different methodologies as well as inherent differences in relapse/progression profiles between different types of lymphoid neoplasms.

Table 2. Frequencies of evolutionary patterns detected in other studies of relapsing lymphoma

Study	Year	Early-divergent	Late-divergent	Neoplasm	Methods used
Okosun et al. ¹⁷⁹	2014	4(12.5%)	28(87.5%)	FL	WES, Targeted NGS
Pasqualucci et al. ¹⁸⁰	2014	10(83.3%)	2(16.6%)	FL	WES, Targeted NGS
Jiang et al. ¹⁷⁵	2014	6(46.1%)	7(53.8%)	DLBCL	WES, SHM seq (NGS)
Bea et al. ²¹⁵	2013	2(33.3%)	4(66.7%)	MCL	WES
Carlotti et al. ²⁰⁷	2009	12(66.7%)	6(33.3%)	FL	SHM seq
Green et al. ²¹⁶	2013	1(50%)	1(50%)	FL	WES
Ruminy et al. ²⁰⁸	2008	0(0%)	6(100%)	FL	SHM seq
Magrangeas et al. ²¹⁷	2012	8(33,3%)	16(66,6%)	MM	aCGH
Eide et al. ²⁰⁰	2010	29(80,5%)	7(19,5%)	FL	aCGH

aCGH – array-comparative genomic hybridization; DLBCL – diffuse large B-cell lymphoma; FL – follicular lymphoma; MCL – mantle cell lymphoma; MM – multiple myeloma; NGS – next generation sequencing; SHM seq – sequencing of somatic hypermutations in *IG* genes; WES – whole exome sequencing

Methodological considerations

We have chosen a strategy of genomic profiling at three different levels, namely *IGH* rearrangement analysis, genome-wide assaying of chromosomal copy number aberrations and targeted detection of mutations in the frequently affected genes in lymphomas. It proved advantageous for robust identification of evolutionary patterns. Analysis of each of the datasets separately showed that important evolutionary and biological aspects of relapse development could be missed. For example, DNA copy number analysis alone would have overlooked late-divergence in many cases and misclassified them as examples of relapse via either linear genetic evolution or no genetic progression. This potential oversimplification is prevalent in other comparable studies, where aCGH was the only method utilized^{200,210}. This shortcoming of aCGH is explained by the fact that chromosomal aberrations represent large-scale genomic alterations occurring seldom compared to single nucleotide mutations and thus providing only a crude resolution for the analysis of evolutionary relationships. On the other hand, targeted sequencing alone queries functionally important, but structurally negligibly small portion of the genome and thus can overlook important events happening outside of the pre-defined regions.

The lack of patient-matched germline controls in this study represented an important challenge in sequencing data analysis. It is known that mutations in coding regions of cancer-relevant genes can be a part of patient-specific germline variation. On the other hand, mutations, which are generally classified as germline variations in genetic databases, may be of somatic origin in a

particular patient²¹⁸. Therefore, specific attention has to be paid to the process of somatic mutation detection in tumor-only samples. False-positives and false-negatives can hamper the correct interpretation of the evolutionary relationship. To mitigate this risk we used several strategies to exclude germline variants in our study. First, since bulk tumors were sequenced, they invariably had a fraction of infiltrating non-malignant cells. Therefore, all mutations shared between primary and relapse, which had variant allelic frequency (VAF) indicative of perfect hetero- or homozygosity, ~50% and ~100%, respectively, were excluded. Copy number of the mutation-affected region was also included in this consideration. Second, we excluded variants that are listed in dbSNP database but not included in other databases of somatic variants in cancer (e.g. COSMIC). Third, in evolutionary analysis, a case was allocated to one or another evolutionary pattern based on the overall results of all three profiling approaches. Therefore the potential risk of false-positive or false-negative mutations influencing classification was minimized

Implications of distinct genetic patterns of DLBCL relapse

The discovery of two distinct evolution patterns at relapse raises additional questions and offers basis for new hypothesis generation about various aspects of lymphoma biology. Such topics include considerations regarding tumor heterogeneity, timing of tumor growth, mechanisms of resistance and potential for improved therapy design.

Relapse pattern as marker for genetic heterogeneity of the primary tumor

It has been suggested, that relapse pattern can potentially correlate with the degree of intratumoral heterogeneity of a pre-diagnostic or diagnostic tumor^{211,219}. Primary tumors that relapse via the late-divergent mode of evolution would expectedly be more homogenous and composed of one dominant clone. In contrast, primary tumors of cases where relapse occurred via late-divergent/branching evolution could have a more complex subclonal structure with a dominant clone accompanied by minor clones that are the product of branching tumor evolution in early tumor development. Intratumoral heterogeneity is shown on individual cases in DLBCL²²⁰ and we have also detected evidence of it in multiple samples of our cohort (Figure S3 in section 3.1). It has been shown in CLL that the presence of subclonal populations at presentation is an independent risk factor of disease progression²²¹. However, this issue was not addressed in DLBCL and needs additional dedicated studies to uncover the true significance of this phenomenon.

Implications to mechanisms of therapy resistance

It is also possible that two different evolutionary patterns represent two distinct mechanisms of resistance. Late-divergence can represent a spontaneous effort of a tumor to survive under the selective pressure of treatment. In this scenario, resistance is not pre-existing, but rather (rapidly) acquired at the time of necessity. Mutagenic agents included in chemotherapy regimen might provide genetic instability that is required for evolution to occur and to acquire resistance mutations guaranteeing clone's survival. Already having all characteristics required for rapid tumor formation, such survivor clones would replenish tumor mass that was lost due to cytotoxic effects of the treatment and form an earlier relapse. In contrast, early-divergence is obviously not occurring due to therapy pressure, but rather due to limitations imposed by internal organism processes such as immune response, lack of nutrients, oxygen, etc. Additionally, genuine tumor properties such as higher degree of genomic instability due to defects in DNA repair, increased SHM or aberrant mitosis can contribute to early divergence. The resistance to treatment would therefore occur as a purely stochastic product of clonal divergence. Genetic lesions that grant tumor cell resistance to treatment are not beneficial to clone, which is unexposed to therapeutic pressure. They can be even disadvantageous²²². Therefore such clones proliferate slowly or stagnate while others, more efficient ones, thrive and lead to initial lymphoma manifestation. Despite small contribution to mass and volume, such populations would confer to lymphoma an intrinsic resistance to therapy. Once treatment is applied and the dominant clone is destroyed, resistant subpopulation would survive, increase its growth potential by acquiring additional DNA lesions and gradually develop relapse tumor.

Potential implications to treatment

If the above model is feasible and indeed late-divergent and early-divergent relapses can correlate with acquired and pre-existing (intrinsic) resistance, respectively, correct identification of relapse pattern can have important implications to treatment, especially in the coming era of targeted treatment approaches¹⁴⁰. It has been shown that intrinsic and acquired resistances occur via principally distinct cellular mechanisms related to specific types of selective pressures that are applied to developing tumor populations. Acquired resistance primarily occurs due to mutations in the very same molecule that is targeted. In such scenario initial response to treatment is usually observed, until resistance-granting mutations are accumulated. Effects of such mutations can be variable and include: 1) increased target's expression (through inactivation of negative regulation loops or gene amplifications); 2) compromised binding of drug to a target (specific mutations in drug binding sites); 3) changes modulating target's activity

(mutations in target's functional domains)²²³. In contrast, intrinsic resistance to targeted treatment is characterized by alterations that are initially present upstream or downstream of target's signaling pathway. Therefore target's inhibition is not effective as the tumor has a pre-developed mechanism of circumventing target's function and delivering important tumorigenic signals via alternative pathways. In such scenario, the resistant cell population (possibly a minor clone in the context of whole tumor, as discussed earlier) is unaffected by the therapy.

Both intrinsic and acquired resistance can contribute to relapses. For example, one study reported two types of mutations responsible for the acquired resistance to the BTK inhibitor Ibrutinib in CLL: 1) mutations in *BTK* itself that change Ibrutinib-mediated BTK inactivation from irreversible to reversible and 2) gain-of-function mutations in phospholipase gamma 2 (*PLCγ2*), which is a downstream phosphorylation target of BTK²²⁴. Although not directly stated by the authors, *BTK* mutations most obviously represent acquired resistance, while *PLCγ2* mutations are related to pre-existing resistance in small subpopulation. This hypothesis is strongly supported by detection of *PLCγ2* mutation in the diagnostic CLL sample at a very low frequency in one patient. It is known that intrinsic resistance to Ibrutinib in DLBCL occurs due to the presence of L265P mutation in MYD88. Mechanisms of acquired resistance to Ibrutinib in DLBCL are still unknown²²⁵. In conclusion, early-divergent and late-divergent patterns of genetic evolution at relapse can provide valuable information about which type of treatment resistance is potentially present in the recurrence and can consequently help to design better targeted treatment approaches.

Early-divergent tumors are related to later relapses

We found that DLBCL relapses, which followed the early-divergent/branching mode of evolution, took significantly longer time to occur as compared to late-divergent/linear relapses. This is in contrast to the results of another study, which didn't find this association¹⁷⁵. Importantly, this trend of later relapses was also reported in some studies on follicular lymphoma transformation¹⁷⁹. There are several probable explanations to the delayed relapses seen in cases that diverged early. First, the relapse-initiating clones are most likely very small in size; this is supported by the fact that relapse-specific mutations are rarely detected in the primary tumor and if they are detected, they often have a very small allelic frequency^{178,221,226}. Second, such subclones need time to acquire additional genetic aberrations that would allow them to increase their capacity to proliferate. This argument is supported by data showing that putative common progenitors in early-divergent/branching mode of evolution have a small number of genetic

lesions, while lymphoma clones, which are “successful” and give rise to detectable tumors are often characterized by profound genomic complexity^{227,228}.

Poor correlation between evolution time and tumor genome complexity

Also of interest is the fact early-divergent/branching relapses generally have equal amount or less DNA lesions compared to their corresponding primary tumors, despite having had much more time to develop (median time to relapse 52 months). This suggests that: 1) tumor populations can maintain relatively stable genomes for a long period of time; 2) length of genetic evolution does not necessarily lead to increased genetic complexity. It also shows that at least in DLBCL, relapses are not associated with large-scale genome rearrangements and catastrophic events (genome doubling, chromothripsis, chromoplexy, etc.) as seen in other types of tumors^{229–232}.

Considerations regarding the speed of tumor formation

It is currently unknown how long does it take on average from the first cancer-initiating mutation to clinically-detectable tumor to develop. Some studies suggest that it can be a decade-long process, while others demonstrate a very fast and aggressive tumor growth. In a speculative spirit one could hypothesize that tumors, which have early-divergent/branching pattern of evolution take longer to grow and manifest compared to those, which are late-divergent and thus more homogenous at the early stages. The very fact of early divergence points towards limiting factors that restrain the growth of a pre-malignant clone, which have to evolve and diversify in order to overcome these constraints. The stochastic search of the proper combination of powerful driver mutations can be a very long process and thus it can take decades until the clinically detectable tumor is formed. On the other hand, homogeneity in early lymphomagenesis (characterized by late-divergent evolution) can represent fast and effective growth of lymphoma from the very outset of the malignant process. Such pace can be mediated by very early acquisition of powerful driver lesions, which give cells a strong competitive advantage. It has been shown, that even if two tumors have identical somatic mutations at diagnosis, the order of their acquisition can greatly influence the vast majority of tumor features including morphology, aggressiveness and importantly – speed of growth²¹⁶.

4.3 Identification of genetic drivers of DLBCL relapse

Based on what is known about tumor biology it is reasonable to hypothesize that DLBCL relapses occur as a consequence of genetic evolution. Therefore it is conceivable that

investigation of exact changes that occur during this evolution should result in identification of genetic drivers of the process as well as prognostic, predictive markers and, hopefully, “genetic vulnerabilities”, which could be targeted to improve currently available treatments. In our study we pursued this strategy by two related lines of action: first, we aimed to identify possible genetic events that lead to DLBCL recurrence by investigating matched primary and relapsed tumors; second, we acquired genetic profiles of a cohort of primary non-relapsing DLBCL (relapse-free for at least 6 years) and compared them to the ones of primaries of DLBCL that relapsed. In this way we sought to identify genetic alterations that could predict disease course at the time of its detection.

Due to the lack of matched primary DLBCL samples other comparable studies mostly investigated relapsed/refractory tumors only. Although by this approach potentially larger cohorts can be collected, it has a significant drawback in that it is nearly impossible to accurately differentiate between mutations that have been present in the primary stage and the ones that are relapse-specific. This problem can be illustrated by the ambiguous status of *MYD88* L265P mutations in DLBCL. In our study this mutation was detected exceptionally as heterozygous early driver lesion present in both primary and relapsed tumors of the same patient. In contrast, an earlier DLBCL genome sequencing study by Morin et al. reported that classic driver events such as mutations of *MYD88*, *CD79A/B* and *EZH2* can also be sub-clonally present within primary DLBCL. Therefore *MYD88* mutation can be both an early and a late event in DLBCL development but this discrimination is highly problematic in cases where only relapsed tumor samples are examined. Additionally, the existence of a significant share (~15%) of clonally-unrelated relapses in DLBCL, as shown in our and other studies, represent a risk that genetic lesions in *de novo* DLBCL, which are only clinically present as “relapses” but indeed represent a second independent disease of the same diagnostic category in the same patient, could be misclassified as relapse-specific. The above mentioned shortcomings can partially explain why there is only limited overlap between 4 genomic studies of DLBCL relapses so far (Table 3). This modest overlap can also be attributed to the intrinsic high heterogeneity of DLBCL that small-scale genetic studies fail to encompass entirely.

It has recently been demonstrated that in addition to genetic mechanisms, changes of the epigenetic landscape can also play a role in DLBCL relapse. Pan et al. found that relapses have significantly decreased intra-tumoral methylation heterogeneity²³³. Further they showed that higher intra-tumoral methylation heterogeneity in a primary tumor correlate with its tendency to relapse after treatment. Unsurprisingly for a genome-wide study, multiple recurrently hypo- or

hypermethylated genes were identified. The functional significances of these are unclear as they were not implicated in cancerogenesis before thus they remain a topic for further investigation.

Table 3. Overview of findings in four studies on the genetic background of DLBCL relapse

	Jiang et al. ¹⁷⁵	Mareschal et al. ¹⁷⁷	Morin et al. ¹⁷⁸	Juskevicius et al.
Study design	WES of 7 matched primary-relapse pairs and matched germline samples. Mutations confirmed by targeted sequencing	WES of 14 rrDLBCL and their germline controls. Mutation frequencies compared to published DLBCL exome data	WES of 38 rrDLBCL and their germline controls. Targeted sequencing of 12 matched diagnostic samples. Mutations frequencies compared to 138 diagnostic DLBCL	aCGH and targeted NGS of 20 matched primary-relapse pairs and 11 primary non-relapsing DLBCL
Genes mutations, implicated in early lymphomagenesis	<i>KMT2D</i> , <i>EP300</i>	NA	NA	<i>KMT2D</i> , <i>MYD88</i> , <i>CD79B</i> , <i>PIM1</i>
Gene mutations implicated in DLBCL relapse	<i>CD58</i> , <i>B2M</i> , <i>ARHGEF7</i> , <i>PLCB2</i> , <i>IL9R</i>	<u>ABC</u> : <i>MYD88</i> , <i>CD58</i> , <i>TBLIXR1</i> , <i>IRF4</i> . <u>GCB</u> : <i>BCL2</i> , <i>MEF2B</i> , <i>DUSP2</i> , <i>NFKBIA</i> , <i>PIM1</i> , <i>KMT2D</i> , <i>GNA13</i> . <u>PMBCL</u> : <i>SOCS1</i> , <i>STAT6</i> , <i>TNAIFP3</i> ; <i>B2M</i> , <i>ITPKB</i> , <i>NFKBIE</i>	<i>TP53</i> , <i>FOXO1</i> , <i>MLL3</i> , <i>NFKBIZ</i> , <i>STAT6</i> , <i>MYC</i> , <i>MLL3</i> , <i>MPEG1</i> , <i>CCND3</i> , <i>MYD88</i> , <i>FOXO1</i> , <i>TNFRSF14</i> , <i>CARD11</i> , <i>B2M</i> , <i>MEF2B</i> , <i>ARID1A</i> , <i>TBLIXR1</i> , <i>NFKBIE</i> , <i>SOCS1</i> , <i>CD79B</i> , <i>BCL2</i>	<i>KMT2D</i> , <i>MEF2B</i> , gain chr10p15.3-13(<i>GATA3</i> , <i>PRKCQ</i>)
GO and pathways associated with relapses.	Apoptosis; transmembrane receptor tyrosine kinases; calcium channel activity; p53 binding	NF-κB signaling, sucrose degradation, tryptophan degradation, JAK-STAT signaling, meiosis; epigenetic regulation; S1P2 signaling pathway	JAK-STAT signaling	NA
Non-relapsing DLBCL-specific lesions	NA	NA	NA	Mutations: <i>SOCS1</i> , <i>RELN</i> . Deletions: <i>CYP7B1</i> . Multiple gains: <i>REL</i> and other (see Table 2 in section 3.1)

GO – gene ontology term; NA – not accessed; rrDLBCL – relapse/refractory DLBCL; WES- whole exome sequencing. Genes that were found mutated in at least two different studies within the same category are marked in bold.

All combined, it appears that we are now just at the beginning of understanding the genetic and epigenetic mechanisms of DLBCL relapse. Since there is a lack of suitable specimens to conduct large-scale comprehensive studies on human samples, it could be worthwhile to pursue alternative strategies. One potential opportunity would be to conduct the most comprehensive studies of selected single cases at multiple currently accessible levels (i.e. genome, epigenome, transcriptome, proteome, metabolome), attempting to develop a state-of-the-art individual tumor (tumor pair) profile that would reveal at great depth the inner workings and vulnerabilities of it. Another, complementary strategy could be DLBCL relapse simulation in currently available or newly established animal models^{124,139}. In this way potential relapse-causing events could be isolated, functionally tested and then screened by focused assays on human sample cohorts. In

addition, potential relapse-causing DNA lesions identified in human DLBCL tumors could be functionally tested in advanced modelling systems.

4.4 Branching evolution and hematopoietic plasticity of follicular lymphoma relapse and its transformation to histiocytic sarcoma

In a single case study we investigated the clonal relationship and genomic evolution of a follicular lymphoma (FL) and its transformation to histiocytic sarcoma. Four samples of one patient (primary FL, two relapses at different timepoints and a histiocytic sarcoma) were available for comprehensive characterization by histological, clonality, translocation and DNA copy number analysis. It is the most comprehensive investigation of such clinical setting so far, providing several important insights about the evolutionary development of two distinct hematolymphoid neoplasms in the same patient.

First, our study confirmed multiple previous observations that dendritic/histiocytic neoplasms and a preceding indolent lymphomas are clonally related²³⁴⁻²³⁶. Tumors of both cancer types derived from the same B-cell precursor as evident by shared *IGH* rearrangement and identical t(14;18) translocation breakpoints. It is an important finding since histiocytes belong to a distinct hematopoietic lineage and “spontaneous” histiocytic sarcomas usually lack clonal *IG* gene rearrangements and/or common translocations observed in lymphomas²³⁷.

Secondly, our report challenged the most favored hypothesis that attempts to explain the arousal of histiocytic sarcomas in the context of indolent lymphomas, namely a transdifferentiation of a lymphoma B-cells to a histiocyte. The genetic data acquired from both tumor types was incompatible with this hypothesis. The FL of our patient had an aberrant and relatively complex genome with multiple gains and deletions of genetic material. In contrast, the subsequent histiocytic sarcoma had a completely intact genome, at least from the perspective of unbalanced copy number changes. Moreover, mutational analysis by targeted sequencing of the most frequent cancer genes yielded no significant somatic alterations that could be reliably related to sarcoma development. This suggests a branching evolution of FL and histiocytic sarcoma. The divergence from a common progenitor should have taken place after the pre-B-cell stage of B-cell development, when *IGH* rearrangements and chromosomal translocations, particularly t(14;18) occurred, but before the acquisition of any chromosomal imbalances by the prospect FL clone. It is known that the majority of FL arise from t(14;18)-bearing GC centroblasts that acquired this translocation at the early B-cell developmental stage due to aberrant functions of the *IGH* rearrangement machinery, and many of their genetic defects are related to aberrant SHM

and CSR. Therefore it is intriguing to think that some abnormal, probably t(14;18)-driven divisions of the very early progenitor B-cell resulted in some daughter cells changing their lineage and converting into histiocyte-like cells.

Such scenario is not entirely compatible with the classical dichotomous model of hematopoiesis, which states that commitment to lymphoid and myeloid lineages occur in early stages of hematopoiesis and that common lymphocyte progenitors (CLP) as well as common myeloid progenitors (CMP) possess a high level of lineage fidelity^{238–240}. Instead, it fits well with a postulated alternative myeloid-based model, which argues that later lymphocyte developmental stages retain plasticity and capability to differentiate into cells of the myeloid lineage²⁴¹. Indeed it is known that early T-cell progenitors retain myeloid differentiation potential in mice²⁴². Moreover, it has been shown *in vitro* that in the absence of Pax5, murine pre-B-1 cells, already bearing *D-J* rearranged *IGH* genes, could differentiate into various hematopoietic cell types, including macrophages²⁴³. Suppression of *PAX5* is thought to be crucial for early B-cell plasticity⁷. Interestingly, the FL cells in our case expressed *PAX5* while the histiocytic sarcoma was *PAX5*-negative. Unfortunately, we didn't have the opportunity to look for mutations in the coding part of *PAX5* gene and its regulators at the time of the project so the role of this B-cell fate controller in our case remains unclear.

In most of the studies, early B-cell plasticity has been demonstrated on animal models in laboratory conditions. Our case is one of the few proofs of such plasticity in humans. It is most likely that this plasticity is physiologically constrained, but can be reactivated as a part of aberrant cell processes during tumorigenesis.

In agreement with other FL studies and also with our DLBCL study discussed earlier, FL relapses in this single case developed from a common progenitor following an early-divergent/branching evolution scenario. Exceptionally high quality aCGH data acquired from this patient samples allowed us to identify at least two subpopulations in the primary tumor with approximate frequencies of 70% and 30%. Analysis of chromosomal copy numbers in two recurrences at two distinct time points suggested that relapses evolved from the less frequent subpopulation. The more frequent clone was probably made extinct by the initial treatment. This data suggests an intrinsically present treatment resistance in a subpopulation of the primary tumor leading to an outgrowth after therapy. Interestingly, despite more than two-year period between the second and third relapse, no private chromosomal imbalances were observed in the former, indicating that after a bottleneck, imposed by treatment-induced selection of a resistant subclone, FL relapses tend to be more homogenous.

4.5. Sorting of FFPE-tissue derived tumor nuclei enables genetic investigation of rare cancer cell populations

The majority of human tumors almost entirely consist of proliferating malignant cancer cells, which are admixed with smaller percentages of normal tumor-infiltrating immune cells and stromal cells. However some tumors have this morphological feature reversed i.e. malignant cancer cells constitute only a small percentage of all tumor cells. In such cases individual cancer cells are scattered throughout the affected tissue and are surrounded by tumor-infiltrating cells. In extreme cases the frequency of malignant cancer cells can be as little as 0.5%. Within the group of hematolymphoid neoplasms, this morphological feature is mostly characteristic to classical Hodgkin lymphoma (cHL) and T-cell/histiocyte-rich B-cell lymphoma, but it can also be encountered in other cancer types in individual cases⁷².

Genetic investigation of such tumors requires a prior enrichment of malignant cells because otherwise tumor-specific genetic features are masked by the genome readout of normal cells and are undetectable. Laser-capture microdissection (LCM), fluorescence-assisted flow sorting (FACS), antibody-conjugated magnetic beads and other methods are used for enrichment in such instances. However, the choice of methods is extremely limited when cells need to be enriched from FFPE tissues. In most such cases LCM is applied since the majority of antibody-based approaches are designed for fresh cells and do not function with fixed archival material. The main drawback of LCM is that laser energy applied to cells during microdissection further fragments the already-fragmented DNA from FFPE tissues, rendering it unsuitable for many downstream applications²⁴⁴. Further it is a low-throughput method, making cell enrichment very labor- and time-intensive.

The above mentioned reasons motivated us to develop protocols for rare cell extraction from archival tissues by FACS. We took advantage of available monoclonal antibodies that are used in routine immunohistochemical diagnostics and which were optimized to bind epitopes on FFPE tissues. We focused our efforts on establishing FACS enrichment based on nuclear and cytoplasmic markers such as MUM1, CD30, PAX5 and the HHV-8 viral nuclear protein LANA1, which are commonly expressed by lymphoid neoplasms having low tumor cell frequencies.

Protocols for nuclei extraction using enzymatic digestion were previously published and used mainly for determination of tumor DNA content by staining cell nuclei with propidium iodide or DAPI^{245–248}. We modified these protocols to enable staining with specific antibodies. Importantly, we avoided the usage of broad-specificity proteases such as pepsin and trypsin but rather used more specific ones such as collagenase, dispase and hyaluronidase to avoid over-

digestion and cleavage of the epitopes of interest. Immunohistochemical staining of nuclear suspensions proved that the epitopes were conserved during the extraction process, retained their antigenicity and are recognized by specific monoclonal antibodies (Figure 11).

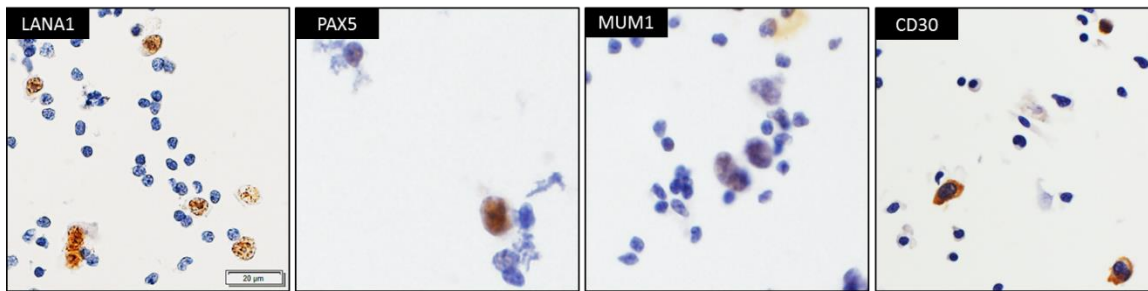


Figure 11. Confirmation of specific primary antibody binding to nuclei extracted from FFPE tissues by immunohistochemical staining in cases of HHV8+ solid forms of primary effusion lymphomas and Hodgkin lymphomas.

Marker-based sorting of FFPE-derived nuclei has previously been performed for carcinoma cell enrichment making use of their specific (compared to the intermingled non-neoplastic stroma cells) cytokeratin expression^{245,249}. In lymphomas successful staining of cells with antibodies against CD79A, CD3 and CD20 has been demonstrated²⁵⁰. Using staining for the HHV-8 viral LANA1 protein we sorted HHV-8-positive tumor cells of solid variants of primary effusion lymphomas²⁵¹. Staining for MUM1 allowed us to enrich plasma cells in 5 samples of post-transplant plasmacytic hyperplasia that only partially affected tonsils and lymph nodes²⁵². In both studies at least 10 000 cells-of-interest per case could be collected, allowing robust analysis of clonality and copy number aberrations in each of them. This enabled us to answer disease-specific clinical and biological questions, which could otherwise not be addressed.

We have also demonstrated the potential of this technique to enrich Hodgkin and Reed-Sternberg (HRS) nuclei of cHL from FFPE tissues²⁵³. Until now only cell lines and limited cohorts of fresh or fresh-frozen tissues from this neoplasm could be genetically analyzed^{254–257}. High-throughput enrichment of HRS cells from FFPE tissue will open opportunities for investigation of much larger, well-described collections of archived cHL cases. This will without doubt lead to better characterization and improved understanding of the genetic basis of this disease.

GENERAL CONCLUSION

Investigation of the genetic background and evolution of DLBCL relapses

Investigating matched primary-relapse sample pairs by genome-wide copy number, targeted mutational and clonality analysis we unequivocally demonstrated the existence of clonally-unrelated recurrences in diffuse large B-cell lymphoma (DLBCL). Such unrelated DLBCL occurrences arise independently one from another, possibly under the influence of potential predisposing factors such as immunosuppression and presence of somatic mutations in the healthy hemato-lymphopoiesis.

Clonally-related DLBCL relapses consistently share some common DNA lesions but follow at least two distinct evolutionary scenarios. The early-divergent/branching pattern is characterized by a small number of shared genetic alterations, which represent early events in lymphomagenesis and large number of stage-specific DNA lesions. Consequently, the genetic distance between the postulated common progenitor and the respective primary tumor is large. The late-divergent/linear relapse pattern is characterized by a large number of shared genetic alterations between the primary and relapse tumors. The primary tumors in this pattern have none or very limited numbers of private DNA lesions and therefore the genetic distance to the common progenitor is small.

Based on the observations above it is likely that primary DLBCL tumors, which relapse via the early-divergent/branching pattern, have an intrinsic resistance to therapy. In contrast, primary DLBCL, which relapse via the late-divergent genetic evolution pattern, acquire resistance after treatment is administered.

Detailed analysis of genetic data from paired tumor samples also revealed recurrently shared mutations representing early drivers of lymphomagenesis and recurrent group-specific genetic alterations. These events were characteristic to non-relapsing and relapsing primary DLBCL and might be linked to treatment susceptibility and the emergence of recurrences, respectively.

Studying transformation of follicular lymphoma (FL) into histiocytic sarcoma: indications for a common neoplastic progenitor

In this one case study we genetically characterized a histiocytic sarcoma occurring in the background of follicular lymphoma. My results confirm previous paradoxical observations that both FL and histiocytic sarcoma share identical immunoglobulin gene rearrangements and t(14;18) translocation, proving their clonal origin. Moreover, distinct copy number aberration

patterns allowed us to approximately estimate the divergence time of lymphoma- and sarcoma-initiating clones. This led to a rare demonstration in humans that B-cells maintain the potential to revert their lineage commitment and differentiate into histiocyte-like cells until as late as a pre-B developmental stage.

Enabling enrichment and genetic analysis of rare tumor cell populations from archival formalin-fixed paraffin-embedded (FFPE) tissues

We developed and optimized protocols that enable reliable high-throughput marker-based enrichment of rare lymphoid tumor cells from FFPE material. Archival tissue cell suspensions can be prepared, specifically labelled according to their expression of distinct cellular markers and enriched by flow-sorting. This technique enabled us to genetically analyze cases of solid variants of primary effusion lymphomas and post-transplant plasmacytic hyperplasias answering relevant research questions in each of these two diseases. Moreover, this enrichment method can be further refined and applied to enable genetic investigations of other tumor cell-scarce lymphoid neoplasms such as classical Hodgkin lymphoma and T-cell/histiocyte rich B-cell lymphoma.

REFERENCES

1. Kindt TJ, Goldsby RA, Osborne BA. *Kuby Immunology*. 2013.
2. Nagasawa T. Microenvironmental niches in the bone marrow required for B-cell development. *Nat. Rev. Immunol.* 2006;6(2):107–116.
3. Allman D, Li J, Hardy RR. Commitment to the B Lymphoid Lineage Occurs before DH-JH Recombination. *J. Exp. Med.* 1999;189(4):735–740.
4. Vilagos B, Hoffmann M, Souabni A, et al. Essential role of EBF1 in the generation and function of distinct mature B cell types. *J. Exp. Med.* 2012;209(4):775–92.
5. Revilla-i-Domingo R, Bilic I, Vilagos B, et al. The B-cell identity factor Pax5 regulates distinct transcriptional programmes in early and late B lymphopoiesis. *EMBO J.* 2012;31(14):3130–3146.
6. Fuxa M, Skok J, Souabni A, et al. Pax5 induces V-to-DJ rearrangements and locus contraction of the immunoglobulin heavy-chain gene. *Genes Dev.* 2004;18(4):411–22.
7. Nutt SL, Heavey B, Rolink AG, Busslinger M. Commitment to the B-lymphoid lineage depends on the transcription factor Pax5. *Nature.* 1999;401(6753):556–62.
8. Delogu A, Schebesta A, Sun Q, et al. Gene repression by Pax5 in B cells is essential for blood cell homeostasis and is reversed in plasma cells. *Immunity.* 2006;24(March):269–281.
9. Bräuninger a, Goossens T, Rajewsky K, Küppers R. Regulation of immunoglobulin light chain gene rearrangements during early B cell development in the human. *Eur. J. Immunol.* 2001;31(12):3631–7.
10. Pieper K, Grimbacher B, Eibel H. B-cell biology and development. *J. Allergy Clin. Immunol.* 2013;131(4):959–971.
11. Mihalcik S a, Huddlestone PM, Wu X, Jelinek DF. The structure of the TNFRSF13C promoter enables differential expression of BAFF-R during B cell ontogeny and terminal differentiation. *J. Immunol.* 2010;185(2):1045–54.
12. Rauch M, Tussiwand R, Bosco N, Rolink AG. Crucial role for BAFF-BAFF-R signaling in the survival and maintenance of mature B cells. *PLoS One.* 2009;4(5):e5456.
13. Batten M, Groom J, Cachero TG, et al. BAFF mediates survival of peripheral immature B lymphocytes. *J. Exp. Med.* 2000;192(10):1453–1466.
14. Sasaki Y, Casola S, Kutok JL, Rajewsky K, Schmidt-Supprian M. TNF family member B cell-activating factor (BAFF) receptor-dependent and -independent roles for BAFF in B cell physiology. *J. Immunol.* 2004;173(4):2245–52.
15. Abbas Abul K., Lichtman; AH, Pillai S. *Cellular and Molecular Immunology*. Philadelphia: 2015.
16. Jung D, Giallourakis C, Mostoslavsky R, Alt FW. Mechanism and control of V(D)J recombination at the immunoglobulin heavy chain locus. *Annu. Rev. Immunol.* 2006;24(D):541–570.
17. Davis MM, Calame K, Early PW, et al. An immunoglobulin heavy-chain gene is formed by at least two recombination events. *Nature.* 1980;283(21):733–739.
18. Oettinger MA, Schatz DG, Gorka C, Baltimore D. RAG-1 and RAG-2, adjacent genes that synergistically activate V(D)J recombination. *Science.* 1990;248(4962):1517–1523.
19. Nieuwenhuis P, Opstelten D. Functional anatomy of germinal centers. *Am. J. Anat.* 1984;170(3):421–35.
20. Pereira JP, Kelly LM, Jason JGC. Finding the right niche: B-cell migration in the early phases of T-dependent antibody responses. *Int. Immunol.* 2010;22(6):413–419.
21. Harwood NE, Batista FD. Early Events in B Cell Activation. *Annu. Rev. Immunol.* 2010;28(1):185–210.
22. MacLennan IC. Germinal centers. *Annu. Rev. Immunol.* 1994;12:117–39.
23. Han S, Hathcock K, Zheng B, et al. Cellular interaction in germinal centers. Roles of CD40 ligand and B7-2 in established germinal centers. *J. Immunol.* 1995;155(2):556–567.
24. Elgueta R, Benson MJ, de Vries VC, et al. Molecular mechanism and function of CD40/CD40L engagement in the immune system. *Immunol. Rev.* 2009;229(1):152–72.
25. de Villartay J-P, Fischer A, Durandy A. The mechanisms of immune diversification and their disorders. *Nat. Rev. Immunol.* 2003;3(12):962–72.
26. DiSanto JP, Bonnefoy JY, Gauchat JF, Fischer A, de Saint Basile G. CD40 ligand mutations in x-linked immunodeficiency with hyper-IgM. *Nature.* 1993;361(6412):541–543.

27. Ferrari S, Giliani S, Insalaco A, et al. Mutations of CD40 gene cause an autosomal recessive form of immunodeficiency with hyper IgM. *Proc. Natl. Acad. Sci. U. S. A.* 2001;98(22):12614–9.
28. Victora GD, Nussenzweig MC. Germinal Centers. *Annu. Rev. Immunol.* 2012;30(1):null.
29. Janeway C a. The discovery of T cell help for B cell antibody formation: a perspective from the 30th anniversary of this discovery. *Immunol. Cell Biol.* 1999;77(2):177–9.
30. Bortnick A, Chernova I, Quinn WJ, et al. Long-lived bone marrow plasma cells are induced early in response to T cell-independent or T cell-dependent antigens. *J. Immunol.* 2012;188(11):5389–96.
31. Stevenson F, Sahota S, Zhu D, et al. Insight into the origin and clonal history of B-cell tumors as revealed by analysis of immunoglobulin variable region genes. *Immunol. Rev.* 1998;162:247–59.
32. Zhang J, MacLennan IC, Liu YJ, Lane PJ. Is rapid proliferation in B centroblasts linked to somatic mutation in memory B cell clones? *Immunol Lett.* 1988;18(4):297–299.
33. Allen CDC, Ansel KM, Low C, et al. Germinal center dark and light zone organization is mediated by CXCR4 and CXCR5. *Nat. Immunol.* 2004;5(9):943–952.
34. Klein U, Dalla-Favera R. Germinal centres: role in B-cell physiology and malignancy. *Nat Rev Immunol.* 2008;8(1):22–33.
35. Muramatsu M, Kinoshita K, Fagarasan S, et al. Class switch recombination and hypermutation require activation-induced cytidine deaminase (AID), a potential RNA editing enzyme. *Cell.* 2000;102(5):553–63.
36. Di Noia JM, Neuberger MS. Molecular mechanisms of antibody somatic hypermutation. *Annu. Rev. Biochem.* 2007;76(1):1–22.
37. Rada C, Williams GT, Nilsen H, et al. Immunoglobulin isotype switching is inhibited and somatic hypermutation perturbed in UNG-deficient mice. *Curr. Biol.* 2002;12(20):1748–55.
38. Wilson TM, Vaisman A, Martomo SA, et al. MSH2-MSH6 stimulates DNA polymerase eta, suggesting a role for A:T mutations in antibody genes. *J. Exp. Med.* 2005;201(4):637–45.
39. Wagner SD, Neuberger MS. Somatic hypermutation of immunoglobulin genes. *Annu. Rev. Immunol.* 1996;14(1):441–57.
40. Goossens T, Klein U, Küppers R. Frequent occurrence of deletions and duplications during somatic hypermutation: implications for oncogene translocations and heavy chain disease. *Proc. Natl. Acad. Sci. U. S. A.* 1998;95(5):2463–2468.
41. Victora GD, Schwickert TA, Fooksman DR, et al. Germinal center dynamics revealed by multiphoton microscopy with a photoactivatable fluorescent reporter. *Cell.* 2010;143(4):592–605.
42. Allen CDC, Okada T, Cyster JG. Germinal-Center Organization and Cellular Dynamics. *Immunity.* 2007;27(2):190–202.
43. Depoil D, Zaru R, Guiraud M, et al. Immunological synapses are versatile structures enabling selective T cell polarization. *Immunity.* 2005;22(2):185–194.
44. Reinhardt RL, Liang H-E, Locksley RM. Cytokine-secreting follicular T cells shape the antibody repertoire. *Nat. Immunol.* 2009;10(4):385–93.
45. Kepler TB, Perelson a S. Cyclic re-entry of germinal center B cells and the efficiency of affinity maturation. *Immunol. Today.* 1993;14(8):412–415.
46. Ta V-T, Nagaoka H, Catalan N, et al. AID mutant analyses indicate requirement for class-switch-specific cofactors. *Nat. Immunol.* 2003;4(9):843–848.
47. Rooney S, Chaudhuri J, Alt FW. The role of the non-homologous end-joining pathway in lymphocyte development. *Immunol. Rev.* 2004;200:115–131.
48. Foy TM, Aruffo a, Bajorath J, Buhlmann JE, Noelle RJ. Immune regulation by CD40 and its ligand GP39. *Annu. Rev. Immunol.* 1996;14:591–617.
49. McAdam AJ, Greenwald RJ, Levin MA, et al. ICOS is critical for CD40-mediated antibody class switching. *Nature.* 2001;409(6816):102–5.
50. Castigli E, Wilson S a, Scott S, et al. TACI and BAFF-R mediate isotype switching in B cells. *J. Exp. Med.* 2005;201(1):35–39.
51. Basso K, Dalla-Favera R. Germinal centres and B cell lymphomagenesis. *Nat. Rev. Immunol.* 2015;15(3):172–184.
52. Recaldin T, Fear DJ. Transcription factors regulating B cell fate in the germinal centre. *Clin. Exp. Immunol.* 2015;
53. Pasqualucci L, Migliazza A, Basso K, et al. Mutations of the BCL6 proto-oncogene disrupt its negative autoregulation in diffuse large B-cell lymphoma. *Blood.* 2003;101(8):2914–23.

54. Phan RT, Dalla-Favera R. The BCL6 proto-oncogene suppresses p53 expression in germinal-centre B cells. *Nature*. 2004;432(7017):635–639.
55. Phan R, Saito M, Basso K, Niu H, Dalla-Favera R. BCL6 interacts with the transcription factor Miz-1 to suppress the cyclin-dependent kinase inhibitor {...}. *Nat. Immunol.* 2005;
56. Niu H, Cattoretti G, Dalla-Favera R. BCL6 controls the expression of the B7-1/CD80 costimulatory receptor in germinal center B cells. *J. Exp. Med.* 2003;198(2):211–21.
57. Shaffer A., Yu X, He Y, et al. BCL-6 Represses Genes that Function in Lymphocyte Differentiation, Inflammation, and Cell Cycle Control. *Immunity*. 2000;13(2):199–212.
58. Basso K, Saito M, Sumazin P, et al. Integrated biochemical and computational approach identifies BCL6 direct target genes controlling multiple pathways in normal germinal center B cells. *Blood*. 2010;115:975–984.
59. Tunyaplin C, Shaffer a L, Angelin-Duclos CD, et al. Direct repression of prdm1 by Bcl-6 inhibits plasmacytic differentiation. *J. Immunol.* 2004;173(2):1158–65.
60. Teng G, Hakimpour P, Landgraf P, et al. MicroRNA-155 is a negative regulator of activation-induced cytidine deaminase. *Immunity*. 2008;28(5):621–9.
61. Basso K, Dalla-Favera R. Roles of BCL6 in normal and transformed germinal center B cells. *Immunol. Rev.* 2012;247(1):172–83.
62. Baumjohann D, Okada T, Ansel KM. Cutting Edge: Distinct waves of BCL6 expression during T follicular helper cell development. *J. Immunol.* 2011;187(5):2089–92.
63. Lee CH, Melchers M, Wang H, et al. Regulation of the germinal center gene program by interferon (IFN) regulatory factor 8/IFN consensus sequence-binding protein. *J. Exp. Med.* 2006;203(1):63–72.
64. Willis SN, Good-Jacobson KL, Curtis J, et al. Transcription factor IRF4 regulates germinal center cell formation through a B cell-intrinsic mechanism. *J. Immunol.* 2014;192(7):3200–6.
65. Dominguez-Sola D, Victora GD, Ying CY, et al. The cell-cycle regulator c-Myc is essential for the formation and maintenance of germinal centers. *Nat. Immunol.* 2012;13(11):1092–1100.
66. Conacci-Sorrell M, McFerrin L, Eisenman RN. An overview of MYC and its interactome. *Cold Spring Harb Perspect Med.* 2014;4(1):a014357.
67. Chu Y, Vahl JC, Kumar D, et al. B cells lacking the tumor suppressor TNFAIP3/A20 display impaired differentiation and hyperactivation and cause inflammation and autoimmunity in aged mice. *Blood*. 2011;117(7):2227–36.
68. Lin K-I, Angelin-Duclos C, Kuo TC, Calame K. Blimp-1-dependent repression of Pax-5 is required for differentiation of B cells to immunoglobulin M-secreting plasma cells. *Mol. Cell. Biol.* 2002;22:4771–4780.
69. Taubenheim N, Tarlinton DM, Crawford S, et al. High rate of antibody secretion is not integral to plasma cell differentiation as revealed by XBP-1 deficiency. *J. Immunol.* 2012;189(7):3328–38.
70. Lenz G, Staudt LM. Aggressive lymphomas. *N Engl J Med.* 2010;362(15):1417–1429.
71. Project TN-HLC. A clinical evaluation of the International Lymphoma Study Group classification of non-Hodgkin's lymphoma. The Non-Hodgkin's Lymphoma Classification Project. *Blood*. 1997;89(11):3909–18.
72. Swerdlow Campo, E., Harris, N.L., Jaffe, E.S., Pileri, S.A., Stein, H., Thiele, J., Vardiman, J.W SH. WHO Classification of Tumours of Haematopoietic and Lymphoid Tissues, Fourth Edition. *IARC Press. Lyon.* 2008;
73. Alizadeh AA, Eisen MB, Davis RE, et al. Distinct types of diffuse large B-cell lymphoma identified by gene expression profiling. *Nature*. 2000;403(6769):503–511.
74. Wright G, Tan B, Rosenwald A, et al. A gene expression-based method to diagnose clinically distinct subgroups of diffuse large B cell lymphoma. *Proc. Natl. Acad. Sci. U. S. A.* 2003;100(17):9991–9996.
75. Rosenwald A, Wright G, Leroy K, et al. Molecular diagnosis of primary mediastinal B cell lymphoma identifies a clinically favorable subgroup of diffuse large B cell lymphoma related to Hodgkin lymphoma. *J. Exp. Med.* 2003;198(6):851–862.
76. Shaffer AL, Young RM, Staudt LM. Pathogenesis of human B cell lymphomas. *Annu. Rev. Immunol.* 2012;30:565–610.
77. Tsujimoto Y, Louie E, Bashir MM, Croce CM. The reciprocal partners of both the t(14; 18) and the t(11; 14) translocations involved in B-cell neoplasms are rearranged by the same mechanism. *Oncogene*. 1988;2(4):347–351.
78. Lenz G, Nagel I, Siebert R, et al. Aberrant immunoglobulin class switch recombination and switch translocations in activated B cell-like diffuse large B cell lymphoma. *J. Exp. Med.* 2007;204(3):633–43.

79. Ruminy P, Etancelin P, Couronné L, et al. The isotype of the BCR as a surrogate for the GCB and ABC molecular subtypes in diffuse large B-cell lymphoma. *Leukemia*. 2011;25(4):681–8.
80. Monti S, Savage KJ, Kutok JL, et al. Molecular profiling of diffuse large B-cell lymphoma identifies robust subtypes including one characterized by host inflammatory response. *Blood*. 2005;105(5):1851–1861.
81. Scott DW, Mottok A, Ennishi D, et al. Prognostic Significance of Diffuse Large B-Cell Lymphoma Cell of Origin Determined by Digital Gene Expression in Formalin-Fixed Paraffin-Embedded Tissue Biopsies. *J. Clin. Oncol.* 2015;33(26):2848–56.
82. Meyer PN, Fu K, Greiner TC, et al. Immunohistochemical methods for predicting cell of origin and survival in patients with diffuse large B-cell lymphoma treated with rituximab. *J Clin Oncol.* 2011;29:200–207.
83. Scott DW, Wright GW, Williams PM, et al. Determining cell-of-origin subtypes of diffuse large B-cell lymphoma using gene expression in formalin-fixed paraffin embedded tissue. *Blood*. 2014;1214–1217.
84. Lenz G, Wright G, Dave SS, et al. Stromal gene signatures in large-B-cell lymphomas. *N. Engl. J. Med.* 2008;359(22):2313–23.
85. Thieblemont C, Briere J, Mounier N, et al. The germinal center/activated B-cell subclassification has a prognostic impact for response to salvage therapy in relapsed/refractory diffuse large B-cell lymphoma: A bio-CORAL study. *J. Clin. Oncol.* 2011;29(31):4079–4087.
86. Dunleavy K, Pittaluga S, Czuczman MS, et al. Differential efficacy of bortezomib plus chemotherapy within molecular subtypes of diffuse large B-cell lymphoma. *Blood*. 2009;113(24):6069–6076.
87. Pasqualucci L, Neumeister P, Goossens T, et al. Hypermutation of multiple proto-oncogenes in B-cell diffuse large-cell lymphomas. *Nature*. 2001;412(6844):341–346.
88. Küppers R, Dalla-Favera R. Mechanisms of chromosomal translocations in B cell lymphomas. *Oncogene*. 2001;20(40):5580–94.
89. Khodabakhshi AH, Morin RD, Fejes AP, et al. Recurrent targets of aberrant somatic hypermutation in lymphoma. *Oncotarget*. 2012;3(11):1308–19.
90. Morin RD, Mendez-Lago M, Mungall AJ, et al. Frequent mutation of histone-modifying genes in non-Hodgkin lymphoma. *Nature*. 2011;476(7360):298–303.
91. Pasqualucci L, Trifonov V, Fabbri G, et al. Analysis of the coding genome of diffuse large B-cell lymphoma. *Nat. Genet.* 2011;43(9):830–7.
92. Zhang J, Grubor V, Love CL, et al. Genetic heterogeneity of diffuse large B-cell lymphoma. *Proc. Natl. Acad. Sci. U. S. A.* 2013;110(4):1398–403.
93. Lohr JG, Stojanov P, Lawrence MS, et al. Discovery and prioritization of somatic mutations in diffuse large B-cell lymphoma (DLBCL) by whole-exome sequencing. *Proc Natl Acad Sci U S A.* 2012;
94. Pasqualucci L, Dalla-Favera R. The genetic landscape of diffuse large B-cell lymphoma. *Semin. Hematol.* 2015;52(2):67–76.
95. Pasqualucci L, Dominguez-Sola D, Chiarenza A, et al. Inactivating mutations of acetyltransferase genes in B-cell lymphoma. *Nature*. 2011;471(7337):189–195.
96. Goodman RH, Smolik S. CBP/p300 in cell growth, transformation, and development. *Genes Dev.* 2000;14(13):1553–77.
97. Zhang J, Dominguez-Sola D, Hussein S, et al. Disruption of KMT2D perturbs germinal center B cell development and promotes lymphomagenesis. *Nat. Med.* 2015;21(10):1190–8.
98. Cattoretti G, Pasqualucci L, Ballon G, et al. Dereglated BCL6 expression recapitulates the pathogenesis of human diffuse large B cell lymphomas in mice. *Cancer Cell*. 2005;7(5):445–55.
99. Ichinohasama R, Miura I, Funato T, et al. A recurrent nonrandom translocation (3;7)(q27;p12) associated with BCL-6 gene rearrangement in B-cell diffuse large cell lymphoma. *Cancer Genet. Cytogenet.* 1998;104(1):19–27.
100. Saito M, Gao J, Basso K, et al. A Signaling Pathway Mediating Downregulation of BCL6 in Germinal Center B Cells Is Blocked by BCL6 Gene Alterations in B Cell Lymphoma. *Cancer Cell*. 2007;12(3):280–292.
101. Challa-Malladi M, Lieu YK, Califano O, et al. Combined genetic inactivation of β 2-Microglobulin and CD58 reveals frequent escape from immune recognition in diffuse large B cell lymphoma. *Cancer Cell*. 2011;20(6):728–40.
102. Trinh DL, Scott DW, Morin RD, et al. Analysis of FOXO1 mutations in diffuse large B-cell lymphoma. *Blood*. 2013;121(18):3666–3674.
103. Monti S, Chapuy B, Takeyama K, et al. Integrative analysis reveals an outcome-associated and targetable

- pattern of p53 and cell cycle deregulation in diffuse large B cell lymphoma. *Cancer Cell*. 2012;22(3):359–72.
104. Dominguez-Sola D, Victora GD, Ying CY, et al. The proto-oncogene MYC is required for selection in the germinal center and cyclic reentry. *Nat. Immunol*. 2012;13(11):1083–91.
 105. Saito M, Novak U, Piovan E, et al. BCL6 suppression of BCL2 via Miz1 and its disruption in diffuse large B cell lymphoma. *Proc. Natl. Acad. Sci. U. S. A.* 2009;106(27):11294–11299.
 106. Morin RD, Johnson NA, Severson TM, et al. Somatic mutations altering EZH2 (Tyr641) in follicular and diffuse large B-cell lymphomas of germinal-center origin. *Nat. Genet*. 2010;42(2):181–5.
 107. Sneeringer CJ, Scott MP, Kuntz KW, et al. Coordinated activities of wild-type plus mutant EZH2 drive tumor-associated hypertrimethylation of lysine 27 on histone H3 (H3K27) in human B-cell lymphomas. *Proc. Natl. Acad. Sci. U. S. A.* 2010;107(49):20980–5.
 108. Beguelin W, Popovic R, Teater M, et al. EZH2 is required for germinal center formation and somatic EZH2 mutations promote lymphoid transformation. *Cancer Cell*. 2013;23(5):677–692.
 109. Green J a, Suzuki K, Cho B, et al. The sphingosine 1-phosphate receptor S1P(2) maintains the homeostasis of germinal center B cells and promotes niche confinement. *Nat. Immunol*. 2011;12(7):672–80.
 110. Muppidi JR, Schmitz R, Green J a., et al. Loss of signalling via Gα13 in germinal centre B-cell-derived lymphoma. *Nature*. 2014;
 111. Lenz G, Wright GW, Emre NC, et al. Molecular subtypes of diffuse large B-cell lymphoma arise by distinct genetic pathways. *Proc Natl Acad Sci U S A*. 2008;105(36):13520–13525.
 112. Woods K, Thomson JM, Hammond SM. Direct regulation of an oncogenic micro-RNA cluster by E2F transcription factors. *J. Biol. Chem*. 2007;282(4):2130–2134.
 113. Yan HL, Xue G, Mei Q, et al. Repression of the miR-17-92 cluster by p53 has an important function in hypoxia-induced apoptosis. *EMBO J*. 2009;28(18):2719–2732.
 114. Hong L, Lai M, Chen M, et al. The miR-17-92 cluster of microRNAs confers tumorigenicity by inhibiting oncogene-induced senescence. *Cancer Res*. 2010;70(21):8547–8557.
 115. Inomata M, Tagawa H, Guo Y-M, et al. MicroRNA-17-92 down-regulates expression of distinct targets in different B-cell lymphoma subtypes. *Blood*. 2009;113(2):396–402.
 116. Xiao C, Srinivasan L, Calado DP, et al. Lymphoproliferative disease and autoimmunity in mice with increased miR-17-92 expression in lymphocytes. *Nat. Immunol*. 2008;9(4):405–14.
 117. Pfeifer M, Grau M, Lenze D, et al. PTEN loss defines a PI3K/AKT pathway-dependent germinal center subtype of diffuse large B-cell lymphoma. *Proc. Natl. Acad. Sci. U. S. A.* 2013;110(30):12420–5.
 118. Liu W, Meckel T, Tolar P, Sohn HW, Pierce SK. Intrinsic properties of immunoglobulin IgG1 isotype-switched B cell receptors promote microclustering and the initiation of signaling. *Immunity*. 2010;32(6):778–89.
 119. Dogan I, Bertocci B, Vilmont V, et al. Multiple layers of B cell memory with different effector functions. *Nat. Immunol*. 2009;10(12):1292–9.
 120. Nagel D, Vincendeau M, Eitelhuber a C, Krappmann D. Mechanisms and consequences of constitutive NF-κB activation in B-cell lymphoid malignancies. *Oncogene*. 2014;33(50):5655–65.
 121. Vallabhapurapu S, Karin M. Regulation and function of NF-kappaB transcription factors in the immune system. *Annu. Rev. Immunol*. 2009;27:693–733.
 122. Hinz M, Krappmann D, Eichten a, et al. NF-kappaB function in growth control: regulation of cyclin D1 expression and G0/G1-to-S-phase transition. *Mol. Cell. Biol*. 1999;19(4):2690–2698.
 123. Toth CR, Hostutler RF, Baldwin Jr. AS, Bender TP. Members of the nuclear factor kappa B family transactivate the murine c-myc gene. *J Biol Chem*. 1995;270(13):7661–7671.
 124. Calado DP, Zhang B, Srinivasan L, et al. Constitutive canonical NF-κB activation cooperates with disruption of BLIMP1 in the pathogenesis of activated B cell-like diffuse large cell lymphoma. *Cancer Cell*. 2010;18(6):580–9.
 125. Davis RE, Brown KD, Siebenlist U, Staudt LM. Constitutive nuclear factor kappaB activity is required for survival of activated B cell-like diffuse large B cell lymphoma cells. *J. Exp. Med*. 2001;194(12):1861–74.
 126. Clark MR, Tanaka A, Powers SE, Veselits M. Receptors, subcellular compartments and the regulation of peripheral B cell responses: the illuminating state of anergy. *Mol. Immunol*. 2011;48(11):1281–6.
 127. Kraus M, Alimzhanov MB, Rajewsky N, Rajewsky K. Survival of resting mature B lymphocytes depends on BCR signaling via the Igalpha/beta heterodimer. *Cell*. 2004;117(6):787–800.
 128. Young RM, Wu T, Schmitz R, et al. Survival of human lymphoma cells requires B-cell receptor engagement

- by self-antigens. *Proc. Natl. Acad. Sci. U. S. A.* 2015;112(44):13447–54.
129. Davis RE, Ngo VN, Lenz G, et al. Chronic active B-cell-receptor signalling in diffuse large B-cell lymphoma. *Nature.* 2010;463(7277):88–92.
 130. Smedby KE, Foo JN, Skibola CF, et al. GWAS of follicular lymphoma reveals allelic heterogeneity at 6p21.32 and suggests shared genetic susceptibility with diffuse large B-cell lymphoma. *PLoS Genet.* 2011;7(4):e1001378.
 131. Ngo VN, Davis RE, Lamy L, et al. A loss-of-function RNA interference screen for molecular targets in cancer. *Nature.* 2006;441(7089):106–110.
 132. Lenz G, Davis RE, Ngo VN, et al. Oncogenic CARD11 Mutations in Human Diffuse Large B Cell Lymphoma. *Science (80-).* 2008;319(5870):1676–1679.
 133. Ngo VN, Young RM, Schmitz R, et al. Oncogenically active MYD88 mutations in human lymphoma. *Nature.* 2011;470(7332):115–119.
 134. Wang JQ, Jeelall YS, Beutler B, Horikawa K, Goodnow CC. Consequences of the recurrent MYD88(L265P) somatic mutation for B cell tolerance. *J Exp Med.* 2014;211(3):413–426.
 135. Kato M, Sanada M, Kato I, et al. Frequent inactivation of A20 in B-cell lymphomas. *Nature.* 2009;459(7247):712–716.
 136. Boone DL, Turer EE, Lee EG, et al. The ubiquitin-modifying enzyme A20 is required for termination of Toll-like receptor responses. *Nat Immunol.* 2004;5(10):1052–1060.
 137. Schmidlin H, Diehl S a., Nagasawa M, et al. Spi-B inhibits human plasma cell differentiation by repressing BLIMP1 and XBP-1 expression. *Blood.* 2008;112(5):1804–1812.
 138. Care M a., Cocco M, Laye JP, et al. SPIB and BATF provide alternate determinants of IRF4 occupancy in diffuse large B-cell lymphoma linked to disease heterogeneity. *Nucleic Acids Res.* 2014;42(12):7591–7610.
 139. Mandelbaum J, Bhagat G, Tang H, et al. BLIMP1 is a tumor suppressor gene frequently disrupted in activated B cell-like diffuse large B cell lymphoma. *Cancer Cell.* 2010;18(6):568–79.
 140. Roschewski M, Staudt LM, Wilson WH. Diffuse large B-cell lymphoma-treatment approaches in the molecular era. *Nat. Rev. Clin. Oncol.* 2014;11(1):12–23.
 141. Coiffier B, Lepage E, Brière J, et al. CHOP Chemotherapy plus Rituximab Compared with CHOP Alone in Elderly Patients with Diffuse Large-B-Cell Lymphoma. *N. Engl. J. Med.* 2002;346(4):235–242.
 142. Pfreundschuh M, Kuhnt E, Trümper L, et al. CHOP-like chemotherapy with or without rituximab in young patients with good-prognosis diffuse large-B-cell lymphoma: 6-year results of an open-label randomised study of the MabThera International Trial (MInT) Group. *Lancet. Oncol.* 2011;12(11):1013–22.
 143. Coiffier B, Thieblemont C, Van Den Neste E, et al. Long-term outcome of patients in the LNH-98.5 trial, the first randomized study comparing rituximab-CHOP to standard CHOP chemotherapy in DLBCL patients: a study by the Groupe d'Etudes des Lymphomes de l'Adulte. *Blood.* 2010;116(12):2040–5.
 144. Gisselbrecht C, Glass B, Mounier N, et al. Salvage regimens with autologous transplantation for relapsed large B-cell lymphoma in the rituximab era. *J. Clin. Oncol.* 2010;28(27):4184–90.
 145. Wilson WH, Jung SH, Porcu P, et al. A cancer and Leukemia Group B multi-center study of DA-EPOCH-rituximab in untreated diffuse large B-cell lymphoma with analysis of outcome by molecular subtype. *Haematologica.* 2012;97(5):758–765.
 146. Yang Y, Shaffer Iii AL, Emre NCT, et al. Exploiting Synthetic Lethality for the Therapy of ABC Diffuse Large B Cell Lymphoma. *Cancer Cell.* 2012;21(6):723–737.
 147. Wilson WH, Young RM, Schmitz R, et al. Targeting B cell receptor signaling with ibrutinib in diffuse large B cell lymphoma. *Nat. Med.* 2015;21(8):922–926.
 148. Chang DH, Liu N, Klimek V, et al. Enhancement of ligand-dependent activation of human natural killer T cells by lenalidomide: therapeutic implications. *Blood.* 2006;108(2):618–21.
 149. Verhelle D, Corral LG, Wong K, et al. Lenalidomide and CC-4047 inhibit the proliferation of malignant B cells while expanding normal CD34+ progenitor cells. *Cancer Res.* 2007;67(2):746–55.
 150. Gandhi AK, Kang J, Naziruddin S, et al. Lenalidomide inhibits proliferation of Namalwa CSN.70 cells and interferes with Gab1 phosphorylation and adaptor protein complex assembly. *Leuk. Res.* 2006;30(7):849–58.
 151. Witzig TE, Nowakowski GS, Habermann TM, et al. A comprehensive review of lenalidomide therapy for B-cell non-Hodgkin lymphoma. *Ann. Oncol.* 2015;26(8):1667–77.
 152. Witzig TE, Vose JM, Zinzani PL, et al. An international phase II trial of single-agent lenalidomide for relapsed or refractory aggressive B-cell non-Hodgkin's lymphoma. *Ann. Oncol.* 2011;22(7):1622–7.
 153. Hernandez-Ilizaliturri FJ, Deeb G, Zinzani PL, et al. Higher response to lenalidomide in relapsed/refractory

- diffuse large B-cell lymphoma in nongermlinal center B-cell-like than in germinal center B-cell-like phenotype. *Cancer*. 2011;117(22):5058–66.
154. A predictive model for aggressive non-Hodgkin's lymphoma. The International Non-Hodgkin's Lymphoma Prognostic Factors Project. *N Engl J Med*. 1993;329:987–994.
155. Sehn LH, Berry B, Chhanabhai M, et al. The revised International Prognostic Index (R-IPI) is a better predictor of outcome than the standard IPI for patients with diffuse large B-cell lymphoma treated with R-CHOP. *Blood*. 2007;109:1857–1861.
156. Zhou Z, Sehn LH, Rademaker AW, et al. An enhanced International Prognostic Index (NCCN-IPI) for patients with diffuse large B-cell lymphoma treated in the rituximab era. *Blood*. 2014;123:837–842.
157. Pfreundschuh M, Ho AD, Cavallin-Stahl E, et al. Prognostic significance of maximum tumour (bulk) diameter in young patients with good-prognosis diffuse large-B-cell lymphoma treated with CHOP-like chemotherapy with or without rituximab: an exploratory analysis of the MabThera International Trial Group. *Lancet. Oncol*. 2008;9(5):435–44.
158. Müller C, Murawski N, Wiesen MHJ, et al. The role of sex and weight on rituximab clearance and serum elimination half-life in elderly patients with DLBCL. *Blood*. 2012;119(14):3276–3284.
159. Sehn LH, Scott DW, Chhanabhai M, et al. Impact of concordant and discordant bone marrow involvement on outcome in diffuse large B-cell lymphoma treated with R-CHOP. *J. Clin. Oncol*. 2011;29(11):1452–1457.
160. Maurer MJ, Micallef INM, Cerhan JR, et al. Elevated serum free light chains are associated with event-free and overall survival in two independent cohorts of patients with diffuse large B-cell lymphoma. *J. Clin. Oncol*. 2011;29(12):1620–6.
161. Johnson NA, Slack GW, Savage KJ, et al. Concurrent expression of MYC and BCL2 in diffuse large B-cell lymphoma treated with rituximab plus cyclophosphamide, doxorubicin, vincristine, and prednisone. *J Clin Oncol*. 2012;30:3452–3459.
162. Sehn LH. Paramount prognostic factors that guide therapeutic strategies in diffuse large B-cell lymphoma. *Hematology Am. Soc. Hematol. Educ. Program*. 2012;2012:402–9.
163. Hoeller S, Schneider A, Haralambieva E, Dirnhofer S, Tzankov A. FOXP1 protein overexpression is associated with inferior outcome in nodal diffuse large B-cell lymphomas with non-germinal centre phenotype, independent of gains and structural aberrations at 3p14.1. *Histopathology*. 2010;57:73–80.
164. Tzankov A, Leu N, Muenst S, et al. Multiparameter analysis of homogeneously R-CHOP-treated diffuse large B cell lymphomas identifies CD5 and FOXP1 as relevant prognostic biomarkers: report of the prospective SAKK 38/07 study. *J. Hematol. Oncol*. 2015;8:70.
165. Salles G, de Jong D, Xie W, et al. Prognostic significance of immunohistochemical biomarkers in diffuse large B-cell lymphoma: a study from the Lunenburg Lymphoma Biomarker Consortium. *Blood*. 2011;117(26):7070–8.
166. Perry AM, Cardesa-Salzman TM, Meyer PN, et al. A new biologic prognostic model based on immunohistochemistry predicts survival in patients with diffuse large B-cell lymphoma. *Blood*. 2012;120:2290–2296.
167. Tzankov A, Zlobec I, Went P, et al. Prognostic immunophenotypic biomarker studies in diffuse large B cell lymphoma with special emphasis on rational determination of cut-off scores. *Leuk Lymphoma*. 2010;51:199–212.
168. De Jong D, Rosenwald A, Chhanabhai M, et al. Immunohistochemical prognostic markers in diffuse large B-cell lymphoma: Validation of tissue microarray as a prerequisite for broad clinical applications - A study from the Lunenburg lymphoma biomarker consortium. *J. Clin. Oncol*. 2007;25(7):805–812.
169. Spaepen K, Stroobants S, Dupont P, et al. Prognostic value of positron emission tomography (PET) with fluorine-18 fluorodeoxyglucose ([18F]FDG) after first-line chemotherapy in non-Hodgkin's lymphoma: is [18F]FDG-PET a valid alternative to conventional diagnostic methods? *J. Clin. Oncol*. 2001;19(2):414–9.
170. Dupuis J, Itti E, Rahmouni A, et al. Response assessment after an inductive CHOP or CHOP-like regimen with or without rituximab in 103 patients with diffuse large B-cell lymphoma: integrating 18fluorodeoxyglucose positron emission tomography to the International Workshop Criteria. *Ann. Oncol*. 2008;20(3):503–507.
171. Vaidya R, Witzig TE. Prognostic factors for diffuse large B-cell lymphoma in the R(X)CHOP era. *Ann. Oncol*. 2014;(X):1–10.
172. Van Den Neste E, Schmitz N, Mounier N, et al. Outcome of patients with relapsed diffuse large B-cell

- lymphoma who fail second-line salvage regimens in the International CORAL study. *Bone Marrow Transplant*. 2015;
173. Gisselbrecht C, Glass B, Mounier N, et al. Salvage regimens with autologous transplantation for relapsed large B-cell lymphoma in the rituximab era. *J. Clin. Oncol.* 2010;28(27):4184–90.
 174. Philip T, Guglielmi C, Hagenbeek A, et al. Autologous bone marrow transplantation as compared with salvage chemotherapy in relapses of chemotherapy-sensitive non-Hodgkin's lymphoma. *N. Engl. J. Med.* 1995;333(23):1540–5.
 175. Jiang Y, Redmond D, Nie K, et al. Deep-sequencing reveals clonal evolution patterns and mutation events associated with relapse in B-cell lymphomas. *Genome Biol.* 2014;15(8):432.
 176. Kreso A, O'Brien CA, van Galen P, et al. Variable clonal repopulation dynamics influence chemotherapy response in colorectal cancer. *Science (80-.)*. 2013;339(6119):543–548.
 177. Mareschal S, Dubois S, Viailly P-J, et al. Whole exome sequencing of relapsed/refractory patients expands the repertoire of somatic mutations in diffuse large B-cell lymphoma. *Genes. Chromosomes Cancer*. 2015;
 178. Morin RD, Assouline SE, Alcaide M, et al. Genetic landscapes of relapsed and refractory diffuse large B cell lymphomas. *Clin. Cancer Res.* 2015;
 179. Okosun J, Bödör C, Wang J, et al. Integrated genomic analysis identifies recurrent mutations and evolution patterns driving the initiation and progression of follicular lymphoma. *Nat. Genet.* 2014;46(2):176–81.
 180. Pasqualucci L, Khiabani H, Fangazio M, et al. Genetics of follicular lymphoma transformation. *Cell Rep.* 2014;6(1):130–140.
 181. Nogai H, Wenzel S-S, Hailfinger S, et al. IκB-ζ controls the constitutive NF-κB target gene network and survival of ABC DLBCL. *Blood.* 2013;122(13):2242–50.
 182. de Jong D, Glas AM, Boerrigter L, et al. Very late relapse in diffuse large B-cell lymphoma represents clonally related disease and is marked by germinal center cell features. *Blood.* 2003;102(1):324–7.
 183. Lossos A, Ashhab Y, Sverdlin E, et al. Late-delayed cerebral involvement in systemic non-hodgkin lymphoma: A second primary tumor or a tardy recurrence? *Cancer.* 2004;101:1843–1849.
 184. Geurts-Giele WRR, Wolvers-Tettero ILM, Dinjens WNM, Lam KH, Langerak AW. Successive B-Cell Lymphomas Mostly Reflect Recurrences Rather Than Unrelated Primary Lymphomas. *Am. J. Clin. Pathol.* 2013;140(1):114–126.
 185. Mao Z, Quintanilla-Martinez L, Raffeld M, et al. IgVH mutational status and clonality analysis of Richter's transformation: diffuse large B-cell lymphoma and Hodgkin lymphoma in association with B-cell chronic lymphocytic leukemia (B-CLL) represent 2 different pathways of disease evolution. *Am. J. Surg. Pathol.* 2007;31(10):1605–14.
 186. Wei Q, Sebastian S, Papavassiliou P, Rehder C, Wang E. Metachronous/concomitant B-cell neoplasms with discordant light-chain or heavy-chain isotype restrictions: evidence of distinct B-cell neoplasms rather than clonal evolutions. *Hum. Pathol.* 2014;45(10):2063–76.
 187. Obermann EC, Mueller N, Rufe A, et al. Clonal relationship of classical hodgkin lymphoma and its recurrences. *Clin Cancer Res.* 2011;17(16):5268–5274.
 188. Obermann EC, Dirnhofer S, Tzankov A. Clonal relationship of relapsing lymphoid neoplasms. *Histol Histopathol.* 2012;27(8):1013–1020.
 189. Steensma DP, Bejar R, Jaiswal S, et al. Clonal hematopoiesis of indeterminate potential and its distinction from myelodysplastic syndromes. *Blood.* 2015;126(1):9–16.
 190. Gazzola A, Mannu C, Rossi M, et al. The evolution of clonality testing in the diagnosis and monitoring of hematological malignancies. *Ther Adv Hematol.* 2014;5(2):35–47.
 191. Boyd SD, Gaëta B a, Jackson KJ, et al. Individual variation in the germline Ig gene repertoire inferred from variable region gene rearrangements. *J. Immunol.* 2010;184(12):6986–6992.
 192. Boyd SD, Marshall EL, Merker JD, et al. Measurement and Clinical Monitoring of Human Lymphocyte Clonality by Massively Parallel V-D-J Pyrosequencing. *Sci. Transl. Med.* 2009;1(12):12ra23–12ra23.
 193. He J, Wu J, Jiao Y, et al. IgH gene rearrangements as plasma biomarkers in Non- Hodgkin's lymphoma patients. *Oncotarget.* 2011;2(3):178–185.
 194. Wu D, Sherwood A, Fromm JR, et al. High-throughput sequencing detects minimal residual disease in acute T lymphoblastic leukemia. *Sci. Transl. Med.* 2012;4(134):134ra63.
 195. Sakr RA, Schizas M, Carniello JVS, et al. Targeted capture massively parallel sequencing analysis of LCIS and invasive lobular cancer: Repertoire of somatic genetic alterations and clonal relationships. *Mol. Oncol.* 2015;

196. Ostrovnya I, Olshen AB, Seshan VE, et al. A metastasis or a second independent cancer? Evaluating the clonal origin of tumors using array copy number data. *Stat. Med.* 2010;29(15):1608–1621.
197. Wang X, Wang M, MacLennan GT, et al. Evidence for common clonal origin of multifocal lung cancers. *J. Natl. Cancer Inst.* 2009;101(8):560–70.
198. Girard N, Ostrovnya I, Lau C, et al. Genomic and mutational profiling to assess clonal relationships between multiple non-small cell lung cancers. *Clin. Cancer Res.* 2009;15(16):5184–90.
199. Siddiqi IN, Ailawadhi S, Huang Q, et al. Deep sequencing reveals lack of a clonal relationship between a metachronous classical hodgkin and diffuse large B-cell lymphoma. *Clin Lymphoma Myeloma Leuk.* 2014;14(3):e87–93.
200. Eide MB, Liestol K, Lingjaerde OC, et al. Genomic alterations reveal potential for higher grade transformation in follicular lymphoma and confirm parallel evolution of tumor cell clones. *Blood.* 2010;116(9):1489–1497.
201. Kikushige Y, Ishikawa F, Miyamoto T, et al. Self-renewing hematopoietic stem cell is the primary target in pathogenesis of human chronic lymphocytic leukemia. *Cancer Cell.* 2011;20(2):246–59.
202. Nishiuchi R, Yoshino T, Teramoto N, et al. Clonal analysis by polymerase chain reaction of B-cell lymphoma with late relapse: a report of five cases. *Cancer.* 1996;77(4):757–62.
203. Läubli H, Tzankov A, Juskevicius D, et al. Lenalidomide monotherapy leads to a complete remission in refractory B-cell post-transplant lymphoproliferative disorder. *Leuk. Lymphoma.* 2015;1–11.
204. Greaves M, Maley CC. Clonal evolution in cancer. *Nature.* 2012;481(7381):306–313.
205. Gerlinger M, McGranahan N, Dewhurst SM, et al. Cancer: Evolution Within a Lifetime. *Annu. Rev. Genet.* 2014;48(1):215–236.
206. Carlotti E, Wrench D, Rosignoli G, et al. High Throughput Sequencing Analysis of the Immunoglobulin Heavy Chain Gene from Flow-Sorted B Cell Sub-Populations Define the Dynamics of Follicular Lymphoma Clonal Evolution. *PLoS One.* 2015;10(9):e0134833.
207. Carlotti E, Wrench D, Matthews J, et al. Transformation of follicular lymphoma to diffuse large B-cell lymphoma may occur by divergent evolution from a common progenitor cell or by direct evolution from the follicular lymphoma clone. *Blood.* 2009;113(15):3553–7.
208. Ruminy P, Jardin F, Picquenot J-M, et al. S mutation patterns suggest different progression pathways in follicular lymphoma: early direct or late from FL progenitor cells. *Blood.* 2008;112(5):1951–1959.
209. Umino A, Nakagawa M, Utsunomiya A, et al. Clonal evolution of adult T-cell leukemia/lymphoma takes place in the lymph nodes. *Blood.* 2011;117(20):5473–5478.
210. Magrangeas F, Avet-Loiseau H, Gouraud W, et al. Minor clone provides a reservoir for relapse in multiple myeloma. *Leukemia.* 2012;27(2):473–81.
211. Beà S, Valdés-Mas R, Navarro A, et al. Landscape of somatic mutations and clonal evolution in mantle cell lymphoma. *Proc. Natl. Acad. Sci. U. S. A.* 2013;110(45):18250–5.
212. Sylvester BE, Vakiani E. Tumor evolution and intratumor heterogeneity in colorectal carcinoma: insights from comparative genomic profiling of primary tumors and matched metastases. *J. Gastrointest. Oncol.* 2015;6(6):668–75.
213. Jiang J-K, Chen Y-J, Lin C-H, Yu I-T, Lin J-K. Genetic changes and clonality relationship between primary colorectal cancers and their pulmonary metastases--an analysis by comparative genomic hybridization. *Genes. Chromosomes Cancer.* 2005;43(1):25–36.
214. Vakiani E, Janakiraman M, Shen R, et al. Comparative genomic analysis of primary versus metastatic colorectal carcinomas. *J. Clin. Oncol.* 2012;30(24):2956–62.
215. Beà S, Valdés-Mas R, Navarro A, et al. Landscape of somatic mutations and clonal evolution in mantle cell lymphoma. *Proc. Natl. Acad. Sci. U. S. A.* 2013;110(45):18250–5.
216. Green MR, Gentles AJ, Nair R V, et al. Hierarchy in somatic mutations arising during genomic evolution and progression of follicular lymphoma. *Blood.* 2013;121(9):1604–1611.
217. Magrangeas F, Avet-Loiseau H, Gouraud W, et al. Minor clone provides a reservoir for relapse in multiple myeloma. *Leukemia.* 2012;(July 2012):473–481.
218. Jones S, Anagnostou V, Lytle K, et al. Personalized genomic analyses for cancer mutation discovery and interpretation. *Sci. Transl. Med.* 2015;7(283):283ra53–283ra53.
219. Guièze R, Wu CJ. Genomic and epigenomic heterogeneity in chronic lymphocytic leukemia. *Blood.* 2015;126(4):445–453.
220. Morin RD, Mungall K, Pleasance E, et al. Mutational and structural analysis of diffuse large B-cell

- lymphoma using whole-genome sequencing. *Blood*. 2013;122(7):1256–1265.
221. Landau D a., Carter SL, Stojanov P, et al. Evolution and impact of subclonal mutations in chronic lymphocytic leukemia. *Cell*. 2013;152(4):714–726.
222. Bozic I, Nowak M a. Timing and heterogeneity of mutations associated with drug resistance in metastatic cancers. *Proc. Natl. Acad. Sci. U. S. A.* 2014;111(45):15964–15968.
223. Asić K. Dominant mechanisms of primary resistance differ from dominant mechanisms of secondary resistance to targeted therapies. *Crit. Rev. Oncol. Hematol.* 2016;97:178–96.
224. Woyach J a, Furman RR, Liu T-M, et al. Resistance mechanisms for the Bruton’s tyrosine kinase inhibitor ibrutinib. *N. Engl. J. Med.* 2014;370(24):2286–94.
225. Zhang SQ, Smith SM, Zhang SY, Lynn Wang Y. Mechanisms of ibrutinib resistance in chronic lymphocytic leukaemia and non-Hodgkin lymphoma. *Br. J. Haematol.* 2015;170(4):445–56.
226. Haffner MC, Mosbrugger T, Esopi DM, et al. Tracking the clonal origin of lethal prostate cancer. *J. Clin. Invest.* 2013;123(11):4918–4922.
227. Vogelstein B, Papadopoulos N, Velculescu VE, et al. Cancer genome landscapes. *Science*. 2013;339(6127):1546–58.
228. Green MR, Kihira S, Liu CL, et al. Mutations in early follicular lymphoma progenitors are associated with suppressed antigen presentation. *Proc. Natl. Acad. Sci. U. S. A.* 2015;112(10):E1116–25.
229. Baca SC, Prandi D, Lawrence MS, et al. Punctuated evolution of prostate cancer genomes. *Cell*. 2013;153(3):666–677.
230. Stephens PJ, Greenman CD, Fu B, et al. Massive genomic rearrangement acquired in a single catastrophic event during cancer development. *Cell*. 2011;144(1):27–40.
231. Nik-Zainal S, Van Loo P, Wedge DC, et al. The life history of 21 breast cancers. *Cell*. 2012;149(5):994–1007.
232. Campbell PJ, Yachida S, Mudie LJ, et al. The patterns and dynamics of genomic instability in metastatic pancreatic cancer. *Nature*. 2010;467(7319):1109–13.
233. Pan H, Jiang Y, Boi M, et al. Epigenomic evolution in diffuse large B-cell lymphomas. *Nat. Commun.* 2015;6:6921.
234. Vos JA, Abbondanzo SL, Barekman CL, et al. Histiocytic sarcoma: a study of five cases including the histiocyte marker CD163. *Mod Pathol.* 2005;18(5):693–704.
235. Feldman AL, Arber DA, Pittaluga S, et al. Clonally related follicular lymphomas and histiocytic/dendritic cell sarcomas: evidence for transdifferentiation of the follicular lymphoma clone. *Blood*. 2008;111(12):5433–5439.
236. Zeng W, Meck J, Cheson BD, Ozdemirli M. Histiocytic sarcoma transdifferentiated from follicular lymphoma presenting as a cutaneous tumor. *J Cutan Pathol.* 2011;38(12):999–1003.
237. Copie-Bergman C, Wotherspoon AC, Norton AJ, Diss TC, Isaacson PG. True histiocytic lymphoma: a morphologic, immunohistochemical, and molecular genetic study of 13 cases. *Am. J. Surg. Pathol.* 1998;22(11):1386–92.
238. Kondo M, Wagers AJ, Manz MG, et al. Biology of hematopoietic stem cells and progenitors: implications for clinical application. *Annu. Rev. Immunol.* 2003;21(1):759–806.
239. Kondo M, Weissman IL, Akashi K. Identification of clonogenic common lymphoid progenitors in mouse bone marrow. *Cell*. 1997;91(5):661–672.
240. Akashi K, Traver D, Miyamoto T, Weissman IL. A clonogenic common myeloid progenitor that gives rise to all myeloid lineages. *Nature*. 2000;404(6774):193–197.
241. Kawamoto H, Wada H, Katsura Y. A revised scheme for developmental pathways of hematopoietic cells: The myeloid-based model. *Int. Immunol.* 2010;22(2):65–70.
242. Bell JJ, Bhandoola A. The earliest thymic progenitors for T cells possess myeloid lineage potential. *Nature*. 2008;452(7188):764–767.
243. Rolink AG. B-cell development and pre-B-1 cell plasticity in vitro. *Methods Mol Biol.* 2004;271:271–281.
244. Vandewoestyne M, Goossens K, Burvenich C, et al. Laser capture microdissection: should an ultraviolet or infrared laser be used? *Anal. Biochem.* 2013;439(2):88–98.
245. Glogovac JK, Porter PL, Banker DE, Rabinovitch PS. Cytokeratin labeling of breast cancer cells extracted from paraffin-embedded tissue for bivariate flow cytometric analysis. *Cytometry*. 1996;24(3):260–7.
246. Jordanova ES, Corver WE, Vonk MJ, et al. Flow cytometric sorting of paraffin-embedded tumor tissues considerably improves molecular genetic analysis. *Am. J. Clin. Pathol.* 2003;120(3):327–34.

247. Holley T, Lenkiewicz E, Evers L, et al. Deep Clonal Profiling of Formalin Fixed Paraffin Embedded Clinical Samples. *PLoS One*. 2012;7(11):e50586.
248. Leers MP, Schutte B, Theunissen PH, Ramaekers FC, Nap M. Heat pretreatment increases resolution in DNA flow cytometry of paraffin-embedded tumor tissue. *Cytometry*. 1999;35(3):260–6.
249. Corver WE, ter Haar NT. High-resolution multiparameter DNA flow cytometry for the detection and sorting of tumor and stromal subpopulations from paraffin-embedded tissues. *Curr Protoc Cytom*. 2009;Chapter 6:Unit 7 37.
250. Leers MP, Theunissen PH, Ramaekers FC, Schutte B, Nap M. Clonality assessment of lymphoproliferative disorders by multiparameter flow cytometry of paraffin-embedded tissue: an additional diagnostic tool in surgical pathology. *Hum. Pathol*. 2000;31(4):422–7.
251. Juskevicius D, Dietsche T, Lorber T, et al. Extracavitary primary effusion lymphoma: clinical, morphological, phenotypic and cytogenetic characterization using nuclei enrichment technique. *Histopathology*. 2014;
252. Menter T, Juskevicius D, Tzankov A. Array CGH-based analysis of post-transplant plasmacytic hyperplasia reveals “intact genomes” arguing against categorizing it as part of the post-transplant lymphoproliferative disease spectrum. *Transpl. Int*. 2014;
253. D. Juskevicius, D. Jucker, T. Dietsche, V. Perrina, C. Ruiz, S. Dirnhofer AT. Genetic profiling of Hodgkin and Reed-Sternberg cells of classical Hodgkin lymphoma enriched from archival formalin-fixed and paraffin-embedded tissues. *Pathologe*. 2015;36(6):628.
254. Steidl C, Diepstra A, Lee T, et al. Gene expression profiling of microdissected Hodgkin Reed-Sternberg cells correlates with treatment outcome in classical Hodgkin lymphoma. *Blood*. 2012;120(17):3530–3540.
255. Liu Y, Razak FR a, Terpstra M, et al. The mutational landscape of Hodgkin lymphoma cell lines determined by whole exome sequencing. *Leukemia*. 2014;1–4.
256. Steidl C, Telenius A, Shah SP, et al. Genome-wide copy number analysis of Hodgkin Reed-Sternberg cells identifies recurrent imbalances with correlations to treatment outcome. *Blood*. 2010;116(3):418–427.
257. Reichel J, Chadburn A, Rubinstein PG, et al. Flow-sorting and exome sequencing reveals the oncogenome of primary Hodgkin and Reed-Sternberg cells. *Blood*. 2014;blood–2014–11–610436.
258. Vermaat JS, Pals ST, Younes A, et al. Precision medicine in diffuse large B-cell lymphoma: hitting the target. *Haematologica*. 2015;100(8):989–93.

LIST OF ABBREVIATIONS

aCGH – array-comparative genome hybridization
ADM2 – aberration detection method
AID – activation-induced deaminase
ARHGEF1 - RHO guanine nucleotide exchange factor 1
ASCT – autologous stem cell transplantation
B2M – beta 2 microglobulin
BAFF – B-cell activator of the TNF- α family
BAFF-R – BAFF receptor
BCL2 – B-cell lymphoma 2
BCR – B-cell receptor
BLIMP – B-lymphocyte-induced maturation protein 1
BRCA2 – breast cancer 2
CARD11 – caspase recruitment domain containing protein 11
CCND3 – cyclin D3
CD – cluster of differentiation
CDR – complementarity-determining region
CSR – class switch recombination
CT – computer tomography
CXCL13 – chemokine (C-X-C Motif) ligand 13
CXCR5 – chemokine (C-X-C Motif) receptor 5
DA-EPOCH-R – dose-adjusted etoposide, prednisolone, oncovin, cyclophosphamide, hydroxydaunorubicin and rituximab
DAPI – 4',6-diamidino-2-phenylindole
DUSP2 – dual specificity phosphatase 2
EBF1 – early B-cell factor 1
EBV – Epstein-Barr virus
EP300 - E1A binding protein p300
EZH2 – enhancer of zeste homolog 2
FACS – fluorescence-assisted cell sorting
FDC – follicular dendritic cells
FLT3 – Fms-like tyrosine kinase 3
FOXO1 – forkhead box protein O1
GATA3 – GATA binding protein 3
GNA13 – guanine nucleotide binding protein alpha 13
HHV-8 – human herpes virus 8
IG – immunoglobulin
IGH – immunoglobulin heavy chain
IGV – immunoglobulin gene variable region
IL – interleukin
INF- γ – interferon gamma
IRF – interferon-regulatory factor

ITPKB – inositol-trisphosphate 3-kinase B
 I κ B – inhibitor of NF- κ B
 JAK – Janus kinase
 LMO2 – LIM domain only 2
 MLL3 – lysine-specific methyltransferase 2C
 MPEG1 – macrophage expressed 1
 MUM1 – see IRF4
 MYD88 – myeloid differentiation primary response protein 88
 NFKBIA – nuclear factor of kappa light polypeptide gene enhancer in B-cells inhibitor alpha
 NFKBIE – nuclear factor of kappa light polypeptide gene enhancer in B-cells inhibitor epsilon
 NFKBIZ – nuclear factor of kappa light polypeptide gene enhancer in B-cells inhibitor zeta
 NF- κ B – nuclear factor kappa B
 NGS – next-generation sequencing
 NOTCH1 – notch homolog 1, translocation-associated
 PAX5 – paired box 5
 PET – positron emission tomography
 PIM1 – Pim-1 proto-oncogene, serine/threonine kinase
 PRDM1 – PR domain zinc finger protein 1
 RAG – recombination activating gene
 R-CHOP – rituximab, cyclophosphamide, hydroxydaunorubicin, oncovin, prednisone
 REL - V-Rel avian reticuloendotheliosis viral oncogene homolog
 HRS – Hodgkin and Reed-Sternberg cells
 RSS – recombination recognition sequence
 S1PR2 – sphingosine-1-phosphate receptor-2
 SHM – somatic hypermutation
 SOCS1 – suppressor of cytokine signaling 1
 STAT6 – signal transducer and activator of transcription 6
 STK11 – serine/threonine kinase 11
 TCR – T-cell receptor
 TdT – terminal deoxynucleotidyl transferase
 TIR – toll/IL-1 receptor domain
 TNF – tumor necrosis factor
 TNFRSF14 – tumor necrosis factor receptor superfamily, member 14
 XBP1 – X-box-binding protein 1

CURRICULUM VITAE

1. General information

1.1. Name: Darius Juškevičius

1.2. Address office: Institute of Pathology
University Hospital
Schoenbeinstrasse 40
4031 Basel / Switzerland
Phone: +41 61 265 27 80 (office)
Fax: +41 61 265 31 94
Email: JuskeviciusD@uhbs.ch



1.4. Date of birth: 30th of September 1986
1.5. Place of birth: Panevėžys/Lithuania
1.6. Citizenship: Lithuanian
1.7. Marital status: married (Reda Juškevičienė)

2. Education

1993-2005: Secondary school No. 5 in Panevezys, Lithuania

2004-2005: Extramural School of Ecology. Vilnius, Lithuania

2005-2009: Vilnius University, Lithuania

25.06.2009: Conferral of bachelor degree in biology (study programme “Molecular Biology”)

Thesis “The assessment of histone deacetylases’ functional significance in the differentiation of human leukemia cells“

2009-2011: Vilnius University, Lithuania

01-06.2010: University of Helsinki, Finland studies via ERASMUS/Socrates programme

22.06.2011. Conferral of a master degree in biology (Magna cum Laude, study programme “Genetics”)

Thesis: “Investigation of Gene IGF2BP3 Methylation in Human Leukemia Cell Lines and in Peripheral Blood B Cells of Chronic Lymphocytic Leukemia Patients“

2012: PhD studies in University of Basel, Medical-Biological Research programme

3. Professional history

2006-2007: Project at the Institute of Experimental and Clinical Medicine, Vilnius, Lithuania.
Supervisor: Dr. A. Pivoriūnas.

2008-2009: Bachelor study project at the Institute of Biochemistry, Vilnius, Lithuania.
Supervisor: Dr. R. Navakauskienė.

2009-2011: Master study project at the Vilnius University Hospital, Santariškių clinics,
Laboratory of Molecular Medicine and Diagnostics. Supervisor: Dr. A. Jakubauskas

2011-2012: Lecturer at “Biotechnology Park Ltd.” A 40-hour introductory course to molecular
methods and diagnostics.

2012: PhD work on the molecular research of lymphoma at the University Hospital Basel,
Institute of Pathology.

4. Publications

1. Jakubauskas A, Vilkeviciene R, **Juskevicius D**, Griskevicius L. Identification of a novel HLA-B allele, B*56:31, by sequence-based typing in a Lithuanian individual. *Tissue Antigens* 2011; 77: 262–3.
2. Jakubauskas A, **Juskevicius D**, Griskevicius L. C*07:185, a novel HLA-C*07 allele identified by sequence-based typing. *Tissue Antigens* 2011; 78: 155–6.
3. **Juskevicius D**, Ruiz C, Dirnhofer S, Tzankov A. Clinical, morphologic, phenotypic, and genetic evidence of cyclin D1-positive diffuse large B-cell lymphomas with CYCLIN D1 gene rearrangements. *Am J Surg Pathol* 2014; 38: 719–27.
4. Brunner P, Rufle A, Dirnhofer S, Lohri A, Willi N, Cathomas G, Krasniqi F, Tzankov A, **Juskevicius D**. Follicular lymphoma transformation into histiocytic sarcoma: indications for a common neoplastic progenitor. *Leukemia* 2014; 28: 1937–40.
5. **Juskevicius D**, Dietsche T, Lorber T, Rufle A, Ruiz C, Mickys U, et al. Extracavitary primary effusion lymphoma: clinical, morphological, phenotypic and cytogenetic characterization using nuclei enrichment technique. *Histopathology* 2014.
6. Menter T, Gasser A, **Juskevicius D**, Dirnhofer S, Tzankov A. Diagnostic Utility of the Germinal Center-associated Markers GCET1, HGAL, and LMO2 in Hematolymphoid Neoplasms. *Appl Immunohistochem Mol Morphol* 2014.
7. Menter T, **Juskevicius D**, Tzankov A. Array CGH-based analysis of post-transplant plasmacytic hyperplasia reveals “intact genomes” arguing against categorizing it as part of the post-transplant lymphoproliferative disease spectrum. *Transpl Int* 2014.
8. Läubli H, Tzankov A, **Juskevicius D**, et al. Lenalidomide monotherapy leads to a complete remission in refractory B-cell post-transplant lymphoproliferative disorder. *Leuk. Lymphoma* 2015:1–11.
9. Tzankov A, Leu N, Muenst S, **Juskevicius D**, et al. Multiparameter analysis of homogeneously R-CHOP-treated diffuse large B cell lymphomas identifies CD5 and FOXP1 as relevant prognostic biomarkers: report of the prospective SAKK 38/07 study. *J. Hematol. Oncol.* 2015;8:70.
10. Menter T, Dickenmann M, **Juskevicius D**, et al. Comprehensive phenotypic characterization of PTLN reveals potential reliance on EBV or NF-κB signalling instead of B-cell receptor signalling. *Hematol. Oncol.* 2016.

5. Language skills

Native language: Lithuanian

Other languages (self-evaluation)

Language	Understanding	Speaking	Writing
<u>English</u>	Excellent	Fluent	Excellent
<u>German</u>	Average	Average	Average
<u>Russian</u>	Average	Basic	Average

6. Non-academic and voluntary experience

2007-2009: Member of Council of Faculty of Nature Sciences, Vilnius University

2007-2008: Chair of Vilnius University Students’ representative office in Faculty of Nature Sciences

2007-2009: Head of organizing committee for International Student Conference of Life Sciences “BioCoin”

2008: Head of organizing committee for students’ open air music festival “GaDi 2008” (Days of Naturalists)

ACKNOWLEDGEMENTS

This work would have not been possible without a contribution from many people to whom I would like to express my heartfelt gratitude. First and foremost, I would like to thank to my supervisor Prof. Dr. Alexandar Tzankov. He put his trust in me and gave me an opportunity to work in a top-quality and stimulating research environment. His leadership, granting me freedom and responsibility, taught me a lot during these years and helped me to grow both as a researcher and as person, greatly boosting my ambitions. He supported and encouraged me in the times of need both in- and outside our projects. I couldn't have even dreamt of a better supervisor.

Next, I would like to thank Prof. Stephan Dirnhofer. He not only helped me to improve my scientific muscles, by critically reviewing my work and giving useful advices, but also strengthened my body and mind by riding long kilometers on the road together as a cycling partner.

I am very grateful to Dr. Christian Ruiz for his support in my research activities, his advice and always positive attitude no matter what problems we faced.

I want to specially thank Tommy Lorber for his priceless contribution to this work in a form of practical advice, exciting scientific discussions and his help in data analysis. I am also very grateful for our friendship, his support and time we spend together both in- and outside work.

I want to thank also thank other lab colleagues, students and other personnel, especially Joël, Cristina, Maarit, Syna, Luca, Mariacarla, Cristina, Valeria, Tanja, Martin, David J., David M., Sebastian, Gabriel, Sara, Sibylle, Sandra, Serenella, Bruno, Diren, Anja, Nadia, Arthur, Petra, Jasmin, Katharina, Alex and others who helped me a lot throughout these years and generated relaxed, helpful and friendly environment in our labs that made my every day useful and enjoyable.

Esu nuoširdžiai dėkingas savo tėvams Aldonai ir Rimui, kurie išugdė man meilę darbui, o taip pat savo parama ir sunkiu darbu suteikė man galimybę lavintis ir siekti užsibrėžtų tikslų. Taip pat dėkoju broliui Kęstučiui už pagalbą ir parodytą gerą pavyzdį.

This work would have not been possible without support from my dear wife Reda. Her presence and love were the most important sources of my motivation and inspiration, and I cannot overstate how grateful I am to her.